



UNIVERSIDAD Nacional Autónoma de México

Facultad DE Ingeniería

A CONTINUOUS Flow EXTRUDER SYSTEM
Design for 3D PRINTED Clay STRUCTURES

T E S I S

QUE PARA OBTENER EL TÍTULO DE:

INGENIERO MECÁNICO

P R E S E N T A :

GIOVANNI ANDRÉ TORRES MARÍN

DIRECTOR DE TESIS

DR. VICENTE BORJA RAMIREZ



CIUDAD UNIVERSITARIA, CDMX, 2024

«Apúntale al sol y llegarás a la luna»

Christian Ancona

Dedicada a mi padre, a mi madre, a mi hermano y a mi abuela, quienes a lo largo de mi vida, no solo estuvieron ahí siempre que lo necesité. sino que también me enseñaron el significado de la palabra "familia". Esto también es de ustedes.

Acknowledgments

Agradezco a mis padres y a mi hermano, por ayudarme a mantenerme calmado ante las pequeñas crisis que tuve, también por ayudarme a resolver problemas, reunir recursos y poder terminar esta Tesis.

Especial agradecimiento al Dr. Borja por haber aceptado ser mi asesor y haberme guiado de la mejor manera para finalizar este trabajo.

A Angelita (Chikis) por soportarme más que nadie y ayudarme en los días que dormía apenas media hora.

A Sara Palma, a Rodrigo Rubio, a Sara Tzintzun por ayudarme a encontrar solución a problemas que tuve durante mi investigación y construcción.

A Montserrat Rodriguez, Ximena Girón, Artuto Brito, Laura Aguilar, Andrea Watty, Leslie Marín, Mauricio Rabay, Brenda Palacios, Martín Chilpa, Christian Juan, Araceli Cortina, Marian Hernández, Julián Sánchez y todos aquellos que contribuyeron a la realización del proyecto en físico.

To Taylor Swift, your music accompanied me through all the nights I stayed awake, all the writing, the angry moments and even the tears, your music was always there for me.

Contents

Acknowledgments	v
1 Abstract	1
2 Introduction	3
3 Problem Definition	5
3.1 Necessity5
3.2 Problem Definition6
3.3 Justification6
3.4 Objectives7
3.5 Scope7
3.6 Solution Approximation8
3.7 Process Flow Diagram8
4 Experimental Process	11
4.1 Background11
4.1.1 Additive Manufacturing11
4.1.2 Context Information12
4.1.3 The AM Types and Applications13
4.1.4 Applications of AM19
4.1.5 Additive manufacturing vs traditional manufacturing21
4.1.6 Current Perspective of Additive Manufacturing23
4.1.7 Historical Overview of AM in The Construction Industry25
4.1.8 AM and New Technologies for the Construction Industry29
4.1.9 Clay and clay additive manufacturing32
4.2 Technical state of the art34
4.2.1 Available technology and designs34
4.2.2 Patent study49
4.3 Requirements and Specifications51
4.3.1 Requirements51
4.3.2 Specifications52
4.4 Solution Options Generation54
4.4.1 Functional Modelling54
4.4.2 Morphological Matrix63

4.4.3	Evaluation and selection68
4.4.4	Preliminary Solutions Designs70
4.4.5	Concepts filtration and evaluation76
4.5	Detailed design81
4.5.1	Extruder detailed design81
4.5.2	Feeder detailed design101
4.5.3	Recycling system detailed design110
4.5.4	Pug mill detailed design125
5	Finite Element Analysis and fabrication Proposal	131
5.1	Finite element analysis131
5.1.1	Blade analysis131
5.1.2	Shaft analysis132
5.1.3	Screw analysis133
5.1.4	Nozzle analysis135
5.1.5	Pinion analysis137
5.2	Fabrication proposal141
5.2.1	Extruder141
5.2.2	Feeder144
5.2.3	Recycling machine145
6	Prototyping	151
6.1	Prototyping151
6.1.1	Extruder prototyping151
6.1.2	Feeder prototyping169
7	Testing	197
7.1	Test of the CWS system197
7.2	Test of the extruder199
8	Conclusions and further studies	207
8.1	Conclusions207
8.2	Recommended improvements and further studies208
9	Appendices	211
9.1	Appendix 1: Derivation of the Navier-Stokes equations211
9.2	Appendix 2: Stepper motor basics219
9.3	Appendix 3: Finite element method223
9.4	Appendix 4: Process for material selection228
9.5	Appendix 5: Fabrication drawings231
9.6	Appendix 6: Data sheets264
	References	290
	References.....	290

List of Figures

3.1	Flow diagram for the process of this thesis. Source: own	9
4.1	Stereolithography. Source: CustomPartNet.....	14
4.2	Sheet Lamination. Source: fabheads.....	15
4.3	Fused Deposition Modelling. Source: (K.-Y. Lee et al., 2015)	15
4.4	Ballistic Particle Manufacturing. Source: (Dehghanhadikolaei et al., 2018) .	16
4.5	Selective Laser Sintering. Source: (Qin et al., 2020).....	17
4.6	Laser Engineered Net Shaping. Source: (Karpagaraj et al., 2020).....	17
4.7	Binder Jet Printing. Source: ELECTROLOOM	18
4.8	Percentage of AM in the Industry: (Vafadar et al., 2021).....	19
4.9	Traditional vs Additive Manufacturing costs. Source: : (Formlabs, n.d.) and (Cherdo,2019).....	23
4.10	Traditional vs Additive Manufacturing costs. Source: (HUBS, 2022)	24
4.11	Key Factors for choosing AM. Source: (HUBS, 2022)	24
4.12	Construction machine with a extruder. Source: (Urschel, 1943).....	27
4.13	Urschel's son design. Source: (R, n.d.)	28
4.14	Contour Crafting. Source: (Khoshnevis, 2004)	28
4.15	Structural Advantage with AM. Source: (Issa et al., 2021).....	29
4.16	Wall-element with integrated tube, additive manufactured by selective cement activation. Source: (Kloft et al., 2021)	30
4.17	Additive manufacturing by extrusion of lightweight concrete and reinforced double-curved wall element, manufactured in shotcrete 3D printing process. Source: (Kloft et al., 2021).....	30
4.18	Components of the digital process image for the development of control con- cepts for the additive production of large scale and reinforced concrete com- ponents. Source: (Kloft et al., 2021).....	31
4.19	Open maker extruder schematic. Source: (Extrusion System for 3D printing ceramics,2021)	35
4.20	Open maker extruder sub systems. Source: (Extrusion System for 3D printing ceramics, 2021)	36
4.21	Open maker tank subsystems. Source: (Extrusion System for 3D printing ceramics, 2021)	37
4.22	CeraStruder configuration. Source: (CeraStruder , n.d.).....	38
4.23	Stone Flower configuration. Source: (Clay 3D printers. Add-ons for clay, porcelain, concrete, suspensions, n.d.)	39

4.24 LUTUM Extruder. (theLUTUM® Eco Clay Extruder , 2020)	39
4.25 3D Potter extruder. Source: (3D Potterbot Scara V4 ceramic 3D clay printer — real clay 3D ceramic printer , n.d.)	40
4.26 Delta Wasp Extruder extruder. Source: (Extruders, n.d.)	40
4.27 Reinforced clay extruder. Source: Reinforced clay printing –, n.d.)	41
4.28 Petter pugger general mechanism. Source: (Peter pugger , n.d.)	42
4.29 venco mini pugmill. Source: (PUG MILLS — venco, n.d.)	43
4.30 NIDEC De-airing pugmill. Source: (NVS-07 , 2019)	44
4.31 Homemade clay pugmill. Source: (Makery, 2020).....	44
4.32 LDM Wasp extruder for concrete. Source (Extruders, n.d.).....	46
4.33 COBOD extruder. Source: (The BOD2 , 2023).....	46
4.34 Cesar’s system fabricated. Source: (Guía et al., 2018)	47
4.35 Extruder for cementitious material. Source: (Jo et al., 2020)	47
4.36 Food extruder. Source: (Carmona Reverte, 2016)	48
4.37 Patent CN211278899U. Source: (JING et al., n.d.)	49
4.38 Patent CN211466777U. Source: (DE’AN, n.d.)	49
4.39 Patent WO2004065707A2. Source: (BEROKH, n.d.).....	49
4.40 Patent CN111929200A. Source: (JIAN et al., n.d.)	50
4.41 Patent CN112476705. Source: (JIQIANG et al., n.d.).....	50
4.42 Patent US20210069789A1. Source: (MATS C, n.d.)	50
4.43 Black Box model. Source: own	54
4.44 Functional Decomposition. Source: own.....	55
4.45 Inputs and outputs for each system. Source: own	56
4.46 Proposed workflow. Source: own	58
4.47 Preliminary solutions for the Recycling System. Source: own	59
4.48 Preliminary solutions for the Pugmill System. Source: own	60
4.49 Preliminary solutions for the Continuous Workflow System System. Source: own	61
4.50 Preliminary solutions for the Feeding System. Source: own	61
4.51 Preliminary solutions for the Extruder shape. Source: own.....	62
4.52 Preliminary solutions for the Extruder internal mechanism. Source: own.....	62
4.53 Preliminary solutions for the Extruder feeding mode. Source: own.....	63
4.54 Morphological matrix. Source: own	64
4.55 Morphological matrix, combination 1. Source: own.....	65
4.56 Morphological matrix, combination 2. Source: own.....	66
4.57 Morphological matrix, combination 3. Source: own.....	67
4.58 Resulting system combinations. Source: own.....	68
4.59 Pugh’s chart. Source: own.....	69
4.60 Extruder first configuration option. Source: own.....	71
4.61 Extruder second configuration option. Source: own	71
4.62 Extruder third configuration option. Source: own	72
4.63 Feeder first configuration option. Source: own	73
4.64 Feeder second configuration option. Source: own	74
4.65 Pugmill first configuration option. Source: own	75
4.66 Recycler first configuration option. Source: own	76

4.67 Extruder final combination decisions. Source: own.....	77
4.68 Extruder final configurations proposal. Source: own.....	78
4.69 Feeder and CWS final configuration proposal. Source: own	79
4.70 Feeder and CWS final configuration. Source: own	80
4.71 Stepper motor scheme. Source (DataSheet4U, n.d.)	81
4.72 Torque curve for the motor nema 17.....	82
4.73 TB660 Driver for controlling stepper motor. Source: https://articulo.mercadolibre.com.mx/83	
4.74 elegoo 2560 R3 ATmega2560. Source: https://www.amazon.com.mx/	83
4.75 Screw parameters. Source: (Parra Rodrigo, 2017).....	84
4.76 Screw extruder zones. Source: own	90
4.77 Apparent viscosity vs Shear rate. Source: (Menchavez et al., 2014).....	92
4.78 Scheme of the flow in the extruder. Source: own	94
4.79 Differential surface area for the screw. Source: own.....	95
4.80 Initial yield stress according to solid concentration. Source: (XianJun et al., 2022).....	97
4.81 Internal pressure on the tube.....	101
4.82 Fully developed flow on the feeder. Source: own	102
4.83 Lead screw used for the feeder	104
4.84 Worm gear geometry. Source. (Mott, 2004).....	106
4.85 Servo motor MG-995 Tower Pro Hi-Speed	108
4.86 Servo motor MG-995 Tower Pro Hi-Speed	109
4.87 Mueller spherical valve. Source: https://www.homedepot.com.mx	110
4.88 Bending strength study. Source: (Afanador García et al., 2012)	111
4.89 Blade geometry proposal. Source: own.....	112
4.90 Motor comparison.....	114
4.91 WEG motor. Source: https://www.weg.net/catalog	115
4.92 Correcting factor for surface. Source: (Norton et al., 2020).....	119
4.93 Concentration factor due to bending stress. Source: (Norton et al., 2020)	120
4.94 Concentration factor due to torsion stress. Source: (Norton et al., 2020)	121
4.95 Physical properties of the blade. Source: own.....	122
4.96 Analysis for the distributed load on the shaft. Source: own.....	123
4.97 Recommended design life for bearings. Source: (Mott, 2004)	124
4.98 Single row ball bearings dimensions and specifications. Source: (Mott, 2004).....	124
4.99 Dimensions drawing for SKF bearing 6000 series. Source: (Mott, 2004).....	125
4.100 Peter pugger pug mill.....	126
4.101 VENCO De airing pug mill	127
4.102 NIDEC NVS07 pug mill.....	128
4.103 Peter pugger pug mill inside 3D model.....	129
5.1 Mesh of the blade in ANSYS. Source: own	132
5.2 Von Misses equivalent stress in ANSYS. Source: own	133
5.3 Stresses near the blade. Source: own	134
5.4 Mesh for the shaft in ANSYS. Source: own	134
5.5 Shaft equivalent Von Misses stress results. Source: own	135
5.6 Screw meshing in ANSYS. Source: own.....	135

5.7	Stress analysis for the screw in ANSYS. Source: own	136
5.8	Screw stress analysis considering 1 MPa of external pressure. Source: own	136
5.9	4 mm nozzle meshing in ANSYS. Source: own	137
5.10	Nozzle 4mm stress analysis in ANSYS. Source: own.....	138
5.11	Nozzle 4mm stress analysis on the tip in ANSYS. Source: own.....	138
5.12	Nozzle 4mm stress analysis for 950 KPa. Source: own.....	139
5.13	Mesh for the pinion in ANSYS. Source: own	139
5.14	Pinion stress analysis. Source: own	139
5.15	gear stress analysis in ANSYS. Source: own	140
5.16	Stainless steel tube for the main vessel. Source (304 stainless steel round tube, n.d.).....	143
5.17	Gearbox 30:1 for nema 23. Source: (http://amazon.com , n.d.).....	145
5.18	"L" aluminium extrusion profile. Source: (Extrusax, n.d.)	145
5.19	Young's modulus vs density graph. Source: (Solá Marcillo, 2009).....	146
5.20	Young's modulus vs Yield strength. Source: (Solá Marcillo, 2009).....	147
6.1	Main body print bottom and top part preview in CURA Ultimaker. Source: own	152
6.2	Inside PVC tube. Source: own.....	153
6.3	Lid print preview in CURA Ultimaker. Source: own.....	154
6.4	Nozzle print test preview on CURA Ultimaker. Source: own	155
6.5	Endless screw print test preview on CURA Ultimaker. Source: own	155
6.6	Drill bit used as a extruder. Source: own.....	156
6.7	Parts for the screw adapter. Source: own.....	157
6.8	Test bank model. Source: own.....	158
6.9	Test bank configuration. Source: own	158
6.10	3D printed lid. Source: own	159
6.11	3D printed nozzle. Source: own	160
6.12	3D printed bottom part. Source: own.....	161
6.13	3D printed top part. Source. own	162
6.14	3D printed motor support. Source: own.....	163
6.15	3D printed screw adapter for the motor. Source: own.....	164
6.16	PVC with the adapted hole. Source. own	165
6.17	Wood bank test. Source: own.....	166
6.18	Pneumatic fitting for hose and screw-nut pair. Source: own.....	167
6.19	Motor and screw assembly. Source: own.....	167
6.20	Final assembly of the prototype. Source: own	168
6.21	Nozzle of the feeder in cura Ultimaker. Source: own.....	169
6.22	Tube-screw adapter to the feeder in cura Ultimaker. Source: own	170
6.23	Feeder lid in cura Ultimaker. Source: own.....	171
6.24	Plunger print preview in CURA Ultimaker. Source: own	172
6.25	Gearbox set preview in CURA Ultimaker. Source: own.....	172
6.26	PVC feeder tube.....	173
6.27	300 mm T8 Lead screw. Source: own	174
6.28	Adapter from gearbox to lead screw. Source: own	175

6.29	Bolts for attaching the gearbox. Source: own	176
6.30	Model of the frame of the feeder. Source: own	177
6.31	Plaque for attaching the nozzle to the frame. Source: own	178
6.32	Clamp for attaching the body to the frame. Source. own	179
6.33	Adapter structure for the motor and the valve. Source: own	179
6.34	Shaft adapter between servo and valve. Source: own	180
6.35	Final look of the feeding system prototype. Source: own	180
6.36	Wooden frame. Source: own	181
6.37	Nozzle with two way fitting. Source: own	182
6.38	Adapter from the tube to the nozzle. Source: own	183
6.39	Printed plunger connected to the lead screw. Source: own	184
6.40	Half of the gearbox with its bearing. Source: own	185
6.41	Other half of the gearbox. Source: own	186
6.42	Crown gear for the worm-gear assembly. Source: own	187
6.43	Worm for the worm-gear assembly. Source: own	188
6.44	Ball bearings to hold the worm. Source: own	189
6.45	Worm-gear gearbox Assembly. Source: own	189
6.46	Final assembly of the worm-gear drive with stepper. Source: own	190
6.47	Top part of the servo and valve adapter. Source: own	191
6.48	Bottom part of the servo and valve adapter. Source: own	192
6.49	Shaft adapter of the servo to the valve. Source: own	193
6.50	Modified valve to fit the shaft adapter. Source: own	194
6.51	Assembly of the CWS system. Source: own	195
6.52	Final assembly prototype. Source: own	196
7.1	Valve opened state. Source: own	199
7.2	Valve closed state. Source: own	199
7.3	Preparation of the clay previous to the extruding. Source: own	200
7.4	Clay inside the feeding tube. Source: own	203
7.5	Truper grease for lubing the worm gear. Source: own	204
7.6	Shape of the clay extrusion in the feeder. Source:own	205
7.7	Measurements for the tests in the extruder. Source: own	206
7.8	Trending curves of the evolution of the clay flow. Source: own	206
9.1	Scheme of the flow in the extruder. Source: own	211
9.2	Significance table. Source: own	213
9.3	Differential surface area for the screw. Source: own	217
9.4	Cross section of a stepper motor. Source: (MPS, 2022)	219
9.5	Two, three and five-phase stators. Source: (MPS, 2022)	220
9.6	Continuous solid vs discretized object. Source: (Hsu, 2018)	223
9.7	Simplex element. Source: (Hsu, 2018)	225
9.8	Example of an use of an Ashby chart given a set limit and a performance index. Source: (Ashby Cebon, 2005)	230

List of Tables

4.1	Typical materials used for the different AM methods. Source (Formlabs, n.d.)	18
4.2	Benefits of materials for the industry. Source: (Castillo-Rodríguez et al., 2022)	21
4.3	Traditional Manufacturing vs Additive Manufacturing. Source: (Toscano, 2023)	22
4.4	Requirements for the extruder system	51
4.5	Metrics for the system	52
4.6	Specifications	53
4.7	Subproblems and possible solutions	57
4.8	Stepper motor characteristics.....	82
4.9	Design parameter for dimensioning the extruder.....	84
4.10	Final dimensions of the screw	89
4.11	Flow rate for wet clay considering the 4 mm nozzle	90
4.12	Flow rate for wet clay considering the 6 mm nozzle	90
4.13	Flow rate for wet clay considering the 8 mm nozzle	91
4.14	Values used to calculate torque	98
4.15	Parameters of the feeders	103
4.16	Lead Screw parameters	104
4.17	Specifications of the servo motor	109
4.18	Motor specifications.....	115
4.19	Properties of AISI 4340 steel. Source. https://matweb.com/	118
4.20	Parameters to select the pugmill	125
6.1	Printing parameters for the body top and bottom parts. Source: own.....	152
6.2	Printing parameters for the Lid. Source: own	153
6.3	Printing parameters for the Screw. Source: own.....	156
6.4	Printing parameters for the Screw. Source: own.....	157
6.5	Printing parameters for the Screw. Source: own.....	171
9.1	Common material indices. Source: (Ashby Cebon, 2005).....	229

1 Abstract

Abstract (English)

Clay is one of the most used materials by humans in the construction industry even to this day. the market value for ceramics alone is projected to grow to USD 219.12 billion by 2028 (Fortune Business Insights, n.d.). This thesis objective is to design a system of clay extrusion that can be used for Additive Manufacturing in several applications. This design was required to be the complete extrusion system, including the pre-processing of the material. Because of that, a shredder machine that works as a recycling machine for used clay was designed, a pugmill that works as a kneading and de-airing system to compact the clay into cylinders ready to go into cartridges was selected. A feeder system was designed, receiving the previous cylinder. The continuous workflow system was conceived to be a series a feeders connected through motorized valves allowing to change between feeders whenever one of them is empty; finally culminating in the extrusion system that consists of an endless screw type of extruder to ensure the complete de-airing of the clay and to have a better control of its flow, retraction and travelling. The resulting system was partially tested as a prototype, to test some of the critical features.

Abstract (Español)

La arcilla es uno de los materiales más usados por la humanidad en la industria de la construcción, incluso hoy en día. El valor actual del mercado solo tomando en cuenta cerámicos está proyectado para crecer hasta USD 219.12 billones en 2028 (Fortune Business Insights, n.d.). El objetivo de esta tesis es diseñar un sistema de extrusión de arcilla que pueda ser usado para manufactura aditiva en varias aplicaciones. Este diseño requería ser el sistema de extrusión completo, incluyendo el pre-procesamiento del material. Por ello, una máquina trituradora que funciona como máquina de reciclado para arcilla usada fue diseñada así como la selección de un molino de arcilla que funcionara como amasador y desecador de la arcilla para transformarla en cilindros compactos listos para ser insertados en cartuchos. Un sistema de alimentación fue diseñado, recibiendo el cilindro previo. El sistema de trabajo continuo fue concebido como una serie de alimentadores conectados mediante válvulas motorizadas que permitieran el cambio entre alimentadores cuando uno de ellos se encuentre vacío; finalmente el sistema de extrusion que consiste de un extrusor de tipo tornillo sin fin para asegurar el completo desecado de la arcilla y para tener un mejor control del flujo, retracción y desplazamientos. El sistema resultado fue parcialmente probado como un prototipo, para probar algunas de las funciones más críticas.

Keywords: Clay, clay extrusion, additive manufacturing, continuous workflow system.

2 Introduction

The increasing necessity of studying additive manufacturing systems, normally known as a technology of rapid prototyping, is very important, since nowadays it is making its way into several industries like automotive, aerospace and industrial machines, But only 3% is destined for the architectural sector (Vafadar, Guzzomi, Rassau, & Hayward, 2021). For this reason, the development of new technologies such as extrusion systems for more viscous fluids, like the ones used in the construction industry, like cement, concrete, cast or clay, take a lot of importance to add to the additive manufacturing industry.

Since additive manufacturing offers a lot of features that traditional manufacturing can not, like saving material, requiring less training to be used, and more importantly, saving money and time, this technique has become very useful for those purposes (Cherdo, 2019). For this reason, the Laboratory of architecture + design and technology experimentation is looking to develop more technology like this.

In order to do some investigation over model structures, clay has been the selected material to 3D print and study throughout several dwelling elements. Clay is a material that is no stranger to the construction industry, and that is why clay structures are very important to study, they not only offer some interesting structural qualities, but also aesthetic and promise to be cheaper, than, for example, concrete.

In this thesis the design of a complete extrusion system is presented. Starting from the recycling system that is a shredder machine that will crush dry clay structures into scraps that can be re claimed into clay slurries to make the clay once again "playable". The next system is a pugmill, which serves two purposes, one is kneading the clay, preparing it to be

in the right consistency for extrusion, and the other is to de-air the clay to avoid bubbles in the following steps of the process.

The previous two systems, were developed only theoretically since it would be very expensive to produce them right now. The other half of the system is the feeding system, which is not only in charge of transporting the clay into the extruder, but also, this system contains the Continuous Workflow System, which is an innovative (since there is virtually no system that achieves continuity this way) system that enables the extruder to receive clay from more than one feeder through an array of valves, making the printing process continuous and not subjected to the amount of clay that the container can have. Finally an extruder was designed with an endless screw system to ensure the complete de-airing of the clay and also offering better control over flow, speed, retraction, and other important parameters.

The studies conducted were from the investigations of the available technology and primary concepts for extruding systems, clay and additive manufacturing in general. Then some concepts and solutions were generated based on the requirements and specifications set for this particular machine and the previous investigation. To finally make a detailed design of the systems from calculations and validate these designs through Finite Element Analysis, to finally end up with a prototype to test some crucial features, however, tests on the actual robotic arm were not conducted in this work.

3 Problem Definition

3.1 Necessity

The Laboratory of Architecture + Design and Technological Experimentation (LATE) is a place that combines investigation, learning, sharing, performance evaluation, and application of the latest available technology, benefiting the creative and productive processes of the UNAM's Architecture School disciplines (*Laboratory of Architecture + Design and Technological Experimentation [LATE], 2023*).

The objectives of the LATE include developing research projects leaned on digital fabrication and visualization, automation, product development that share knowledge, and collaboration with other laboratories in research projects. One of LATE's focus points is fabricating architectural structures using additive manufacturing (AM), testing, and researching new materials such as plastics and ceramics.

The construction sector consumes almost half of the planet's raw materials, significantly impacting the exploitation of nonrenewable resources and greenhouse gas emissions. It is one of the largest economically speaking industries, with almost USD 13 trillion and a 13% increase in the world's GDP by 2018, and it is predicted to grow to USD 14 trillion by 2025 (Abdallah & Estévez, 2021).

As the background check shows, clay is featured in almost every ceramic and refractory product. The industry grew from USD 146.68 billion in 2022 to USD 158.08 billion in 2023 and is expected to grow to USD 207.81 billion in 2027. The International Monetary Fund states that this industry will represent 3.4% of the global GDP by 2021 (*Clay products and*

refractories global market share, key emerging players 2032 , 2023). Because of this, it is natural to leap into the AM picture. Lastly, current systems need a continuous workflow due to the need of developing large components..

3.2 Problem Definition

The LATE has recently found the necessity of having a better clay extrusion system for their 3D printing robotic arm. The problem consists of designing systems to fulfill the requirements of the LATE. As explained before, the increased necessity to study new methods and materials for the AM industry is crucial to the world right now, so it is natural that new applications like construction or architecture are also studied.

The approach of this thesis is to design a complete extrusion system and a new continuous workflow so the clay can be formed, transported, and extruded into a structure of any given size without interrupting the machine's workflow. This problem is split into the clay composition and extrusion and the system's design per se.

3.3 Justification

This work addresses various problems, not only the problem of designing the system but also the ones that specify why studying these systems is essential today. First of all, AM is a fast-growing industry, and the development of new technology is vital for its progress. Not just creating new machines but also investigating new materials, configurations, processes, and workflows that could make AM better.

Another crucial concern nowadays is AM's sustainability (as seen on the background check). AM can lead to fewer carbon emissions, and a proper process could supersede some traditional processes that represent environmental problems. Finally, including AM in the industry can represent lower costs, reduced times, and the capability of testing new ideas in situ. As AM becomes more present in modern manufacturing processes, developing the

technology and advancing it towards better products and more sustainable manufacturing is crucial.

3.4 Objectives

The general objective of this work state as follows:

- Design a continuous extrusion system capable of forming, transporting, and extruding clay to 3D print structures of this material.

The specific objectives state as follows:

- Research the current state of this technology to find room for improvement and innovation.
- Design all the necessary subsystems that the extrusion system needs.
- Create a continuous workflow for the system to operate.
- Perform different analysis with CAM/CAE simulations to validate the parts.
- Build a working prototype and test some of its important features.

3.5 Scope

The results of this thesis shall include:

- A complete design of an extrusion system meeting the requirements of the LATE and based on the investigation made.
- The necessary analysis to validate the design.
- A working prototype of at least one of the subsystems of the whole design.
- Exploration of applications for these systems and new studies to be made in the future.

3.6 Solution Approximation

The solution to this problem will be approximated using the product design method proposed by Ulrich and Eppinger; however, with the objective of being as complete as possible, other methods will be consulted to complement the design. In the same way, this study will be treated like a project for the best organization possible.

3.7 Process Flow Diagram

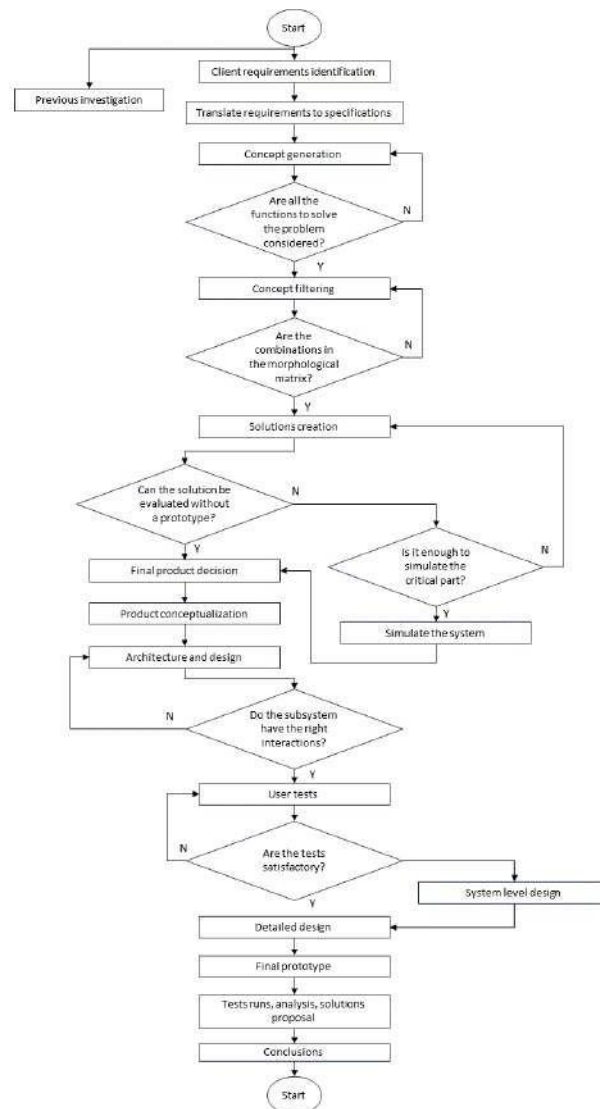


Figure 3.1: Flow diagram for the process of this thesis. Source: own

4 Experimental Process

4.1 Background

4.1.1 Additive Manufacturing

The manufacturing process helps humanity develop and create all the existing ideas and products. It is no coincidence that manufacturing has existed for thousands of years. Nowadays, there are many technologies related to manufacturing, one of them being additive manufacturing (AM), which has recently become one of the most famous due to its benefits.

The ISO/ASTM 52900 defines this method as the creation of physical objects adding layer by layer based on a geometrical representation. Mainly used in engineering, medicine, education, architecture, and others (Standard, 2012).

Additive manufacturing is now what used to be called rapid prototyping and what today colloquially is named 3D printing; according to (Gibson, Rosen, & Stucker, 2010), rapid prototyping is the term that is mainly used to describe a process where a representation or an approximation of a final product can be created. Nevertheless, because of the recent applications developed for this technology, the term “rapid prototyping” is no longer adequate to describe its possibilities. This is why it is decided that this technology is now called additive manufacturing. Now, AM is the manufacturing process that starts from a three-dimensional model (usually following a CAD design) to a physical model without having a previous planning, dimensioning, or preparing process. It works by adding layers of material to build the 3D model using numeric control.

Adding to the previous definition (Jimenez & Galán, 2013) deepens this matter. Considering more traditional manufacturing processes that use a great deal of capacity in order to ensure better and more refined results (since all that is wanted is a product as approximated to the model as possible), these processes all tend to depend on the geometry and quantity that is being manufactured, sometimes even raising the cost of the product. The AM solves the problem of complex geometry since it is a process that adds material, whereas the other processes usually subtract it. (Jimenez & Galán, 2013) clarifies that the process that AM is based on is called dispersion-accumulation.

Other authors, such as (EPMA, 2015), (Díaz, 2016), and (Castillo-Rodríguez et al., 2022), have a very similar position on this matter as the previous two. What could be interesting to point out is that (Castillo-Rodríguez et al., 2022) highlights that the material used for AM can be plastic, ceramic, and even metallic. The point is solidifying a material in a previous form (either liquid, dust, or solid) into single layers, creating cross-sections of the figure inside a confined space. Moreover, the variety of existing technologies is worth knowing, given that each can have a different application and, obviously, different results.

4.1.2 Context Information

Diving more into the history and context of AM, before this technology existed, tests were complex since the resources needed were much more expensive. However, in 1983, the first type of AM was invented. Charles Hull created Stereolithography (SL) in 1983 (Díaz, 2016); by 1987, SL was being developed more massively and started the revolution of AM. SL consists of a process that solidifies thin ultraviolet light-sensitive liquid polymer layers using a laser (Wohlers & Gornet, 2014). The SLA-1 machine was the first one to be on the market. In 1988, the first materials came out of investigation. They were manufactured by 3D systems and Ciba-Geigy, who developed the first SL generation of acrylate resins for commercialization. It was not until 1991 that other AM technologies were commercialized.

In 1991, three more AM techniques were commercialized. Fused Deposition Modelling

(FDM), Solid Ground Curing (SGC) and Laminated Object Manufacturing (LOM). FDM extrudes thermoplastic material in filament form to add them layer by layer. SGC again uses UV-sensitive liquid polymer, but instead of going layer by layer, it solidifies the total layers in one pass. Finally, LOM uses a guided laser to cut sheets of material (Wohlers & Gornet, 2014).

Finally, in 1996, a company called Stratasys released the first form of 3D printing, with a machine named Genisys that used a process like FDM but with a new technology that IBM developed. That same year, 3D Systems sold its first 3D printer (the Actua 2100) that extrudes wax-like material layer by layer. There were a couple of other releases in 1996, and until 2000, many machines and companies released their versions of 3D printing machines and some other technologies. 2000 was a year of several releases of technologies, between 3D printing and SL formed almost all the market that had to do with AM manufacturing (Wohlers & Gornet, 2014). Since that year, there has been non-stop research and development of AM technologies. To this day, AM is now involved in almost every industry and is increasingly being developed. The following section will explain how AM significantly impacts the industry and how more companies are changing to this manufacturing technique.

4.1.3 The AM Types and Applications

AM can be divided into seven different categories (Dehghanhadikolaei, Namdari, Mohammadian, & Fotovvati, 2018), (Group, 2018), (Carbon, n.d.). Also (Castillo-Rodríguez et al., 2022) it can be classified into four main types according to the material used, which is the first thing to be explored. AM can be divided into four main categories according to its source material. The source material can be either liquid, filament or paste, powder, or solid sheet [5]. These four primary materials give birth to the seven AM techniques that exist:

1. Stereolithography (SLA): also known as VAT Photopolymerization, it is one of the most used AM techniques. Basically, the liquid source material is hit by a light (mostly UV or laser) that makes the liquids solidify and this creates the layers. The height of the

layer is controlled by using the properties of the material and the light source so it cannot surpass a specific value. This creates the volume by having a kind of ramp in which the solidified material lies, and every time a layer is solidified, that ramp goes down (as can be seen on the fig. 4.1 down below) and creates the next layer (Dehghanhadikolaie et al., 2018).

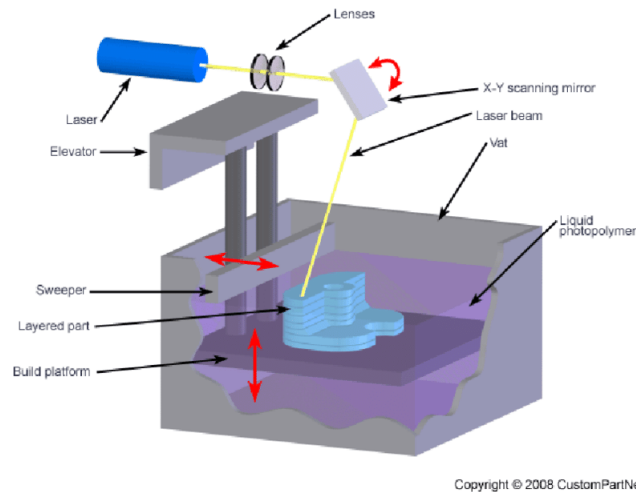


Figure 4.1: Stereolithography. Source: CustomPartNet

2. Sheet Lamination (SL): This AM method is like stereolithography but instead of using photo-sensitive materials, thermoset materials are used. In this case, the source material is also liquid, but a jetting head is the one feeding the material on a surface. For this to become solid there must be a control for the position of the dropped material and a control of the head that feeds adhesive materials to the surface, and finally after heat dissipation the material solidifies. One of the setbacks of this method is the difficulty to control the layer thickness, so oftentimes a milling process is added to the process, and this helps the layer and the result to be very good, but this obviously adds steps to the process. The following image (fig. 4.2) illustrates how this works (Dehghanhadikolaie et al., 2018).

3. Fused deposition modeling (FDM): this method may be the most known of all since it's the method that 3D printers use to work. This process primarily uses a solid source

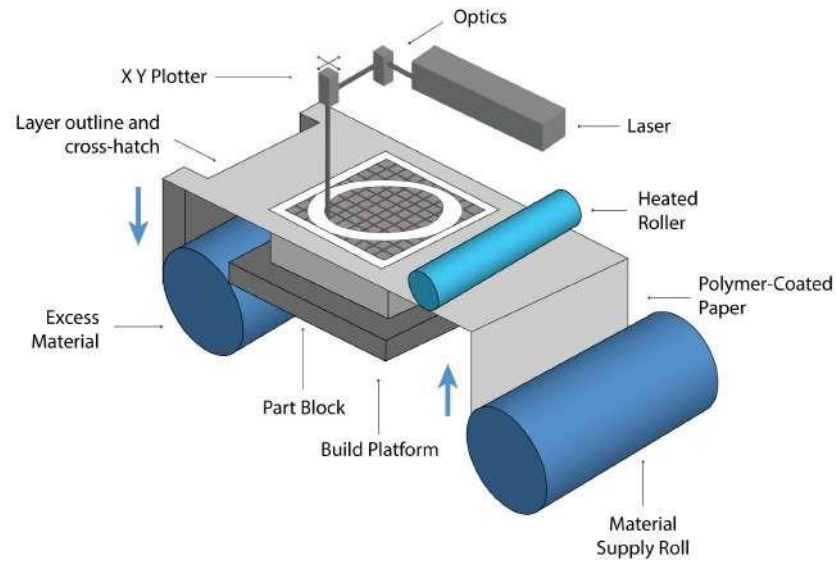


Figure 4.2: Sheet Lamination. Source: fabheads

material (or in filament form) and it consists of a controlled nozzle that deposits the material on a surface. Many variables related to the material exit can be controlled with the nozzle form and size, normally the size of the nozzle diameter relates directly to the precision of the process, and there are other factors such as heat, flow, among others. And, as this is probably the most common process nowadays there are many added benefits, like the capability of having a second nozzle to create composites or the control of temperature so the piece can have a good finish. Another benefit of this process is that it does not need a post-process. The following image (fig. 4.3) can explain how this process is done (Dehghanghadikolaei et al., 2018).

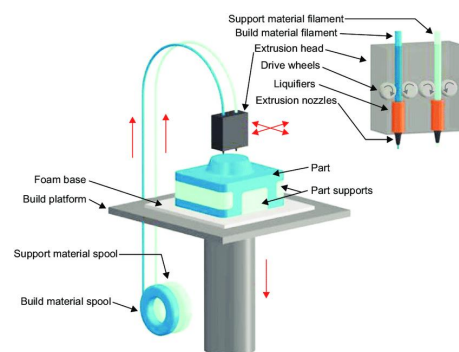


Figure 4.3: Fused Deposition Modelling. Source: (K.-Y. Lee et al., 2015)

4. Ballistic particle manufacturing (BPM): this method also uses a nozzle but, instead of extrusion like in FDM it exits a stream of particles. But also, the material can be fed in the form of droplets. The solidification process depends on a quick change of temperature, as when the material hits the cold substrate it solidifies. This process, also known as material jetting, turns out to be similar to the inkjet printing process (Dehghanghadikolaei et al., 2018).

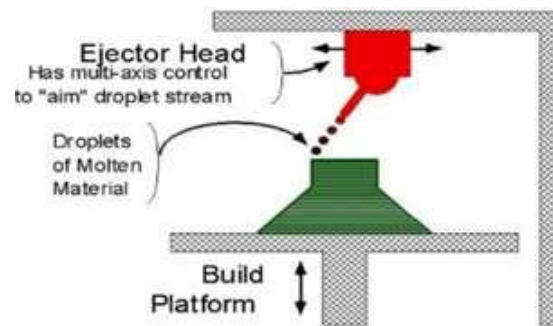


Figure 4.4: Ballistic Particle Manufacturing. Source: (Dehghanghadikolaei et al., 2018)

5. Selective laser sintering (SLM): this technique uses powder as a source material, and in this case, the material is fed by a bed into a roller, or coater, and this takes the powder into the place of fabrication. Similar to other processes above, it uses a laser to solidify the material. As this process is mainly used for metal materials it needs to have very precise and controlled conditions such as vacuum or a controlled atmosphere. One of the most impressive things this method can achieve is that it is able to produce pieces up to 99% of density. This process is also known to be the fastest of the AM methods and that it can create several pieces in one opportunity (Dehghanghadikolaei et al., 2018).

6. Laser Engineered Net Shaping (LENS): like the SLM process this one is also very commonly used in metals, and it is also a very similar process. In this case there is something like a nozzle (see image fig. 4.8) but it feeds powder into a laser beam, which makes the powder in contact with the laser just before it reaches the deposition

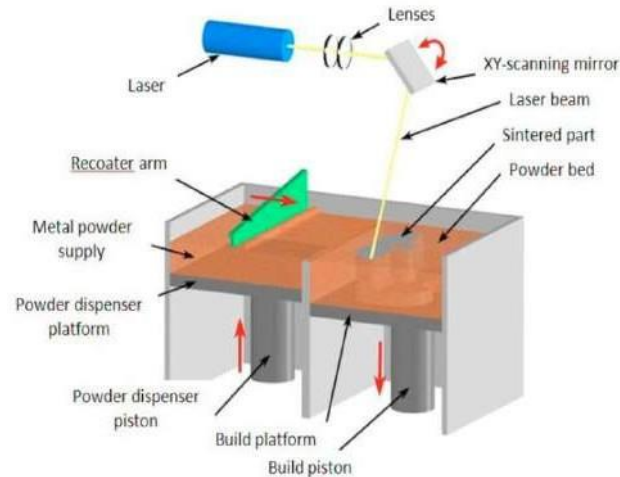


Figure 4.5: Selective Laser Sintering. Source: (Qin et al., 2020)

surface and solidifies it. This process also can achieve 99% density results with mechanical and chemical advantages. The fact that the feeding system works with a flow enables a better cooling of the material and enhanced densities and structure integrity (Dehghanhadikolaei et al., 2018).

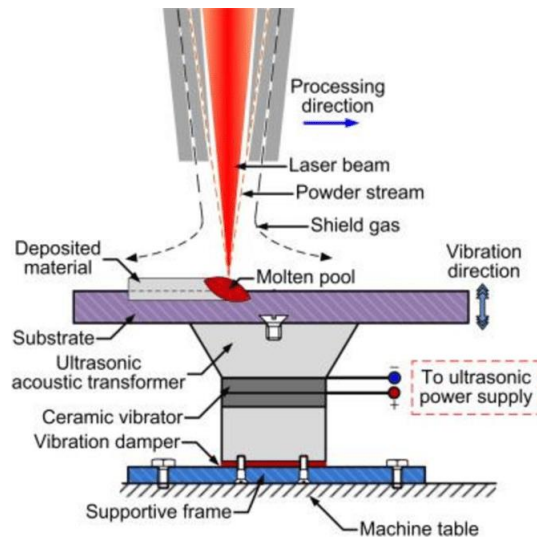


Figure 4.6: Laser Engineered Net Shaping. Source: (Karpagaraj et al., 2020)

7. Binder Jet Printing (BJP): This is another process whose main use is for metals, but it has been known to be used also for ceramic and polymeric materials. The same as the prior two methods, it uses the injection of adhesive materials, and, as the SLM process,

this one also uses a coater that helps the material to have a constant thickness. The main difference with this method in relation to the prior two, is that it does not use a laser, but it uses a head to melt the powder and an adhesive to bind the material. This method, however, needs a further step once the final piece is finished it needs to be cured in a furnace (Dehghanhadikolaie et al., 2018).

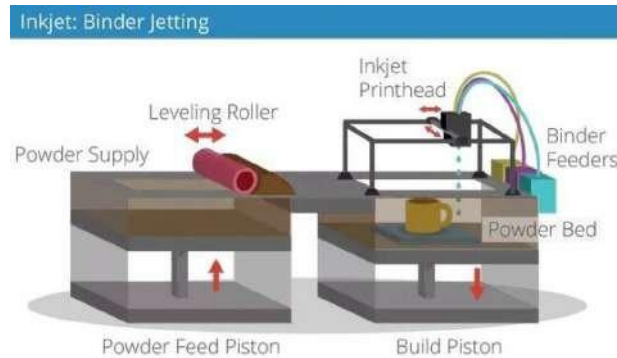


Figure 4.7: Binder Jet Printing. Source: ELECTROLOOM

Something to consider is that every process can be used with different materials. Some are more suitable for polymers, others for metals or ceramics; the following table will show how these different methods are better for some materials. This will come in handy when choosing a method for the problem of this thesis, which is extruding clay.

Table 4.1: Typical materials used for the different AM methods. Source (Formlabs, n.d.)

Method	Material
Stereolithography (SLA)	Varieties of resin (thermoset plastics), high-strength, rigid, flexible, elastic, heat-resistant, castable (wax-like)
Liquid Thermal Polymerization	
Fused Deposition Modelling	Standard thermoplastics, such as ABS, PLA, and their various blends
Ballistic Particle Manufacturing	Soft and hard metals
Selective Laser Sintering	Engineering thermoplastics, such as nylon
Laser Engineered Net Shaping	
Binder Jet Printing	Gypsum (full color), metals

4.1.4 Applications of AM

There are a few sectors in the industry that AM has not touched. Simply listing all the applications and industries that AM had impacted would take much work. Nevertheless, some sectors stand out for being pioneers in its use, and others that, unrelated to AM, can benefit from it. The figure below illustrates the percentage of use of the AM in different industry sectors in 2018 (Khandelwal, 2020). As it can be seen, the industry that uses this technology the most is the automotive and industrial machines, followed closely by the aerospace, and this makes sense given that it is a prevalent need for complex pieces; these three industries alone make up more than 50% of the total adoption of AM technologies.

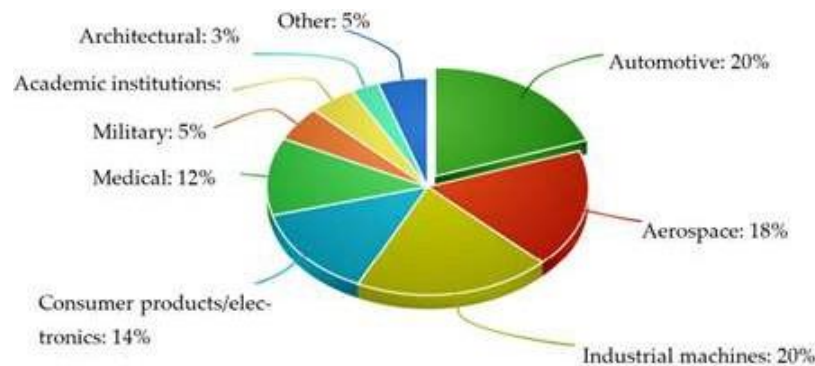


Figure 4.8: Percentage of AM in the Industry: (Vafadar et al., 2021)

The applications can be analyzed by separating, for example, the material that is being used, or the industry sector itself. For instance, different industries use it with different approaches:

Automotive

- It allows for quicker tests and, this can open the gate for innovation and customizable parts (Khandelwal, 2020).
- AM can represent benefit on time and stock. For instance, Ford achieved a manifold test, that would have cost \$500k and 4 months with traditional processes, in just four days and \$3k (Khandelwal, 2020).

- In general, there is a growing tendency to use AM, different techniques and materials are being used to either develop or test different necessities.
- The use of powder bed fusion, electron beam and polymer or metal AM has led the Am to be present in numerous parts of the car such as the interior, suspension, engine, electronics, and the general exterior (Khandelwal, 2020).
- One of the most interesting that AM can represent for the future of automotive industry is the fact that it can play a very important role on the electric transition both in weight reduction and more sustainable components and processes (Charles, Hofer, Elkaseer, & Scholz, 2021).

Aerospace

- AM is also a growing tendency in the aerospace industry and is one of the lead industries that use AM (Chiu, 2020).
- Many companies such as Boeing, Airbus, GE, etcetera have used AM in one way or another. Boeing has been first one to implement AM parts in one of their designs. GE designed the first fuel nozzle and Lockheed made the first ducting system. By 2017 Airbus had its first AM part on one plane (Chiu, 2020).
- Another example is that NASA already has made a 3D printer work in the International Space Station, so astronauts could develop pieces in that moment (Kalender, Kılıç, Ersoy, Bozkurt, & Salman, 2019).
- NASA also developed a rocket metal injector with a nickel-chromium alloy powder (Kalender et al., 2019).

As seen in the paragraph with the different applications in the automotive and aerospace industry and as shown in Table 4.2, there is a little overview on how the AM industry is taking much weight in the global frame. So, the importance of AM and its impact on

Table 4.2: Benefits of materials for the industry. Source: (Castillo-Rodríguez et al., 2022)

Material	Industry	Benefits
Metal	Automotive Aerospatial Medical Building and construction Military	The metal AM processes can offer several benefits to these industries such as the design of complex pieces, multi functional optimization, lighter, stronger, and safer product design. Customization and savings
Polymer and composites	Automotive Aerospatial Biomedics Architecture Sports and toys	Offer cheaper prototypes, saves time and money. Provides better understanding of some products. Some of them even can be end-products, such as some biomedical supports for injuries
Ceramics	Aerospatial Biomedics Chemical	Some of these industries work with materials that need to hold up to reactions or temperature, AM can offer better control of the structure of the pieces
Concrete or similar	Construction and infrastructure	Fast and cheaper processes. Require less labor and can be helpful in hostile environments

today's industry is undeniable. Going back to the tables, it is also noticeable that MANY AM techniques and different materials had made their way into the industry. As such, later in this chapter, how the AM has affected the construction and architectonic industries will be reviewed.

4.1.5 Additive manufacturing vs traditional manufacturing

As the previous paragraph shows, AM has entered the industry and is growing more substantially than many other technologies. However, since this is a technically new technology compared to other traditional techniques like forging or even lathe, it still needs to be discovered how AM compares to other mass production techniques.

As reviewed previously, AM has excellent benefits for the industry, such as the ability to test and experiment with new shapes and complex forms that would be very hard to do with

traditional manufacturing. Also, AM is leading the way in transitioning to more sustainable processes in the industry. However, knowing how and when to use AM is necessary since it is obviously only suitable for replacing some operations. How much cheaper it can be, how much time can be saved, or how it can be used in different scenarios are some of the main questions users generally have when it comes to using AM. Naturally, a comparison between Traditional and Additive Manufacturing must be made.

Table 4.3: Traditional Manufacturing vs Additive Manufacturing. Source: (Toscano, 2023)

Characteristic	Traditional	Additive
Geometry	A single process can't achieve a complex geometry	Achieves complex geometries and gives several options in terms of filling and shape.
Result	Normally requires from several processes to achieve a result	The final shape is the result
Production	Needs to be mass produced so the profits are bigger than the production costs	The production cost is independent on the quantity
Stocking	It is needed since it would be very difficult to produce a piece every time is needed	Since it is a method where pieces can be produced in situ, it is very simple to wait for a spare to be needed
Materials	Depending on the material is the process chosen, e.g., milling is normally used for metals and molding for polymers	It can handle many types of materials, but the method needs to be adapted and the materials must be in a special configuration. Normally, though, the most common materials are polymers
Overall use	<ul style="list-style-type: none"> - Mass production - Final pieces - Specific material property - High repeatability 	<ul style="list-style-type: none"> - Customization - Quick tests Weight optimization - Less source material loss

The Table 4.3 shows that both methods have pros and cons. It all comes down to what the manufacturer needs for the pieces they want to make. However, also, there is the economic factor. Depending on the requirements, there will be a decision in terms of performance and cost. It is worth mentioning that the cost also includes training to use the machines at their maximum capacity. The fig. 4.10 shows the comparison of costs between traditional and Additive Manufacturing.

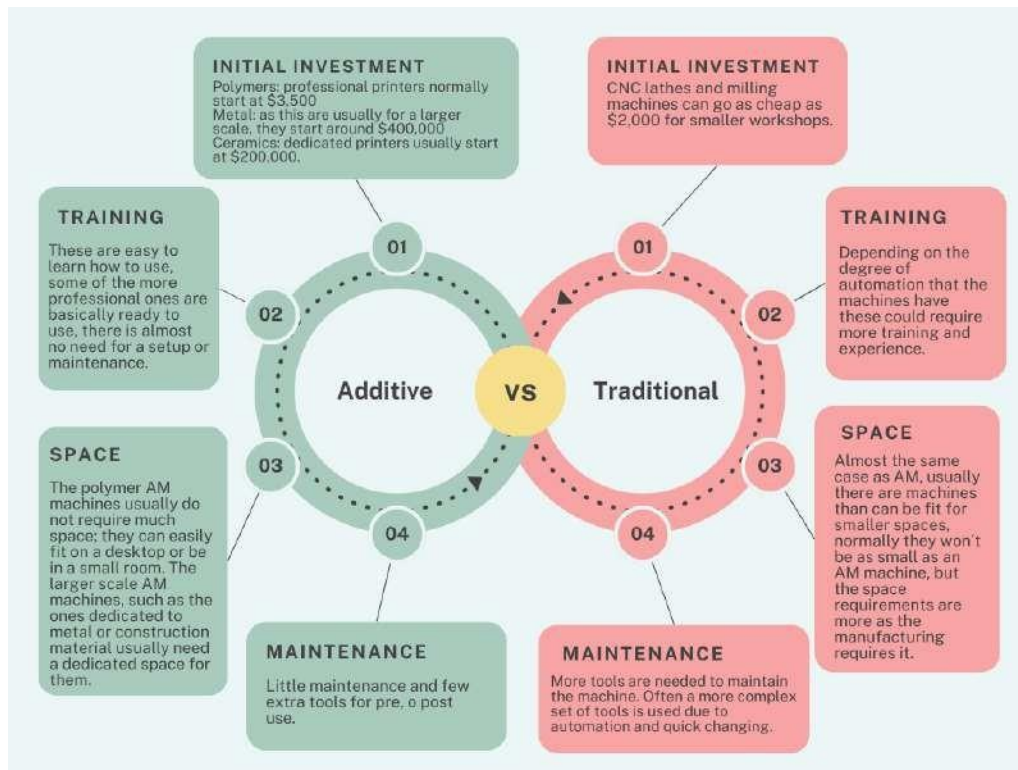


Figure 4.9: Traditional vs Additive Manufacturing costs. Source: : (Formlabs, n.d.) and (Cherdo,2019)

4.1.6 Current Perspective of Additive Manufacturing

As it was said before, AM is growing at a fast rate every year. Wohlers and HUBS (Wohlers & Gornet, 2014), (HUBS, 2022) give great depth on how this industry is evolving and gaining more relevance in many other industries worldwide. In the 2022 Wohler's report, it is said that 3D printing and, generally, AM have a real presence as a technology for end-products. It is predicted that by 2026, the AM market's total value will grow to 44.5 billion dollars. Also, 68% of engineering-related businesses reported using this technology more in 2021 than in 2020. AM has grown exponentially in the past few years in the fig. 4.10.

It can also be observed, there are some trends in the AM market other than the forecasted market value, such as the development of technology or research, that are also expected to grow more in the following years. Research and market are the trends that are expecting a significant leap forward. In 2021, the market value was estimated at 15.1 billion dollars.

This growth represents a 19.8% increase over 2020.

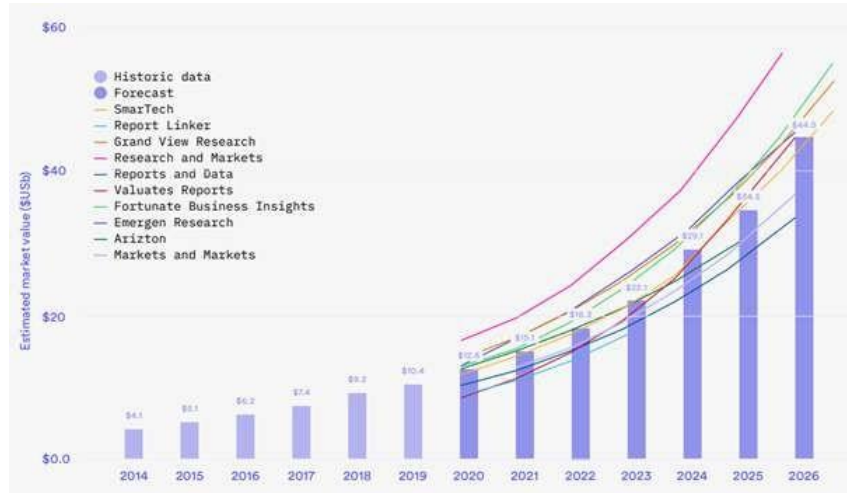


Figure 4.10: Traditional vs Additive Manufacturing costs. Source: (HUBS, 2022)

The following fig. 4.11 also marks some key factors that made companies choose AM technology. The main factor is lead time, given that this technology offers a way to shorten times because of its in-house manufacturing characteristic. Other factors for choosing this technology are obviously the cost reduction in production and materials, the complexity of the geometries that can be achieved, and the easy access to the hardware, among others.

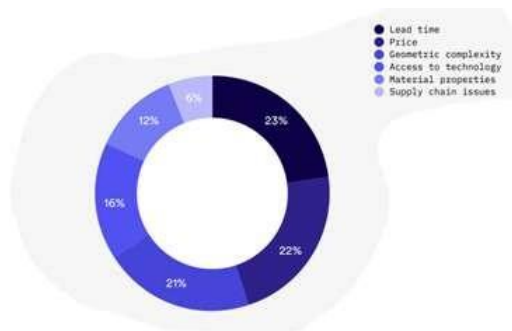


Figure 4.11: Key Factors for choosing AM. Source: (HUBS, 2022)

Other findings on the report that are worth mentioning:

- Even though the AM is past beyond the sole use for rapid prototyping (RP) and starting to gain terrain in end-use parts or spare parts, a 68% of the total use of the technology is still mainly focused on developing prototypes for a faster product development.

- Despite the 68% use for RP, AM is gaining terrain in one-time end-use parts and a little bit less, but not that behind, is repeated orders for end-use parts.
- It is also a common thing to use AM as a support manufacturing process, which combined with other processes makes the workflow easier, faster, or cheaper.
- Something that stands out is that currently the use for this technique is primarily for low volume parts- The main reason being that traditional processes lower the costs a lot when it comes to a high volume of manufactured parts. In many industries, such as motorsport or the aerospace industry, there is the need for very specific parts, which are not required in a high volume.
- Lastly, although it is still focused on low volume production (mostly 1-10 parts), an increase in volume has been reported by companies. 46% of them had said that they are using 3D printing to produce more than just ten parts in 2022, compared to 36% in 2021.

There are also several trends that AM is following, among which are Automation of the process to speed up the process itself; the development of larger formats, for example, the metal 3D printing for air crafts; increasing the reliability and repeatability since there is some inherent error according to the quality of the hardware and the one that this thesis is focused on, the developments of hardware and new materials on the ceramics and composites, which have a vast application on the construction industry.

4.1.7 Historical Overview of AM in The Construction Industry

As reviewed before, AM is a growing technology in almost every single industry, and the construction industry is one of the biggest in the world, economically and socially speaking, since it is the industry that gives people their houses, cities their buildings, and more. Logically, every improvement that can be made will be something to look for. This includes

what AM can do for this industry and how it can lead to savings and a more sustainable future.

One of the first mentions of AM in the context of construction, according to (Issa et al., 2021) citing (Leinster, 1945) mentioned in their thesis, is Murray Leinster's "Things Pass by" - "Thrilling Wonder Stories" v27 n02 [1945-Summer], where a man builds a spaceship layer by layer with a moving arm. It is an interesting take on how AM would work, as it also mentions how pre-scanning shapes do these functions and then reproducing them, which is one of the many processes by which a 3D model can be generated in today's AM.

Another early design and patent came with Urschel (1943) in 1935, where he invented a machine that worked similarly to an AM machine. It is basically a mechanism that looks like today's cylindrical robot would- It is an arm that has a pivot point and can move in the XY plane, goes up in the Z direction, and has a feeder of construction material (see fig. 4.12). This machine's result was a structure like an igloo and more of a spherical structure. This machine also supported varying wall thickness, but obviously, It did not have the automation that machines nowadays have. Despite this, it was a very cleverly designed mechanism.

After this patent, in 1950, E. Shutter (SHUTER, n.d.) invented a machine that had more to do with the shape of the end effector. This is a concern today for printers; the form and how it works are among the main problems that construction-related AM has. This design (fig. 4.12) proposes keeping the walls tighter so they do not expand as much as the concrete is pouring. Then, more inventors came, one of whom was Urschel's son in 1952, who made a machine that worked similarly but for plastics instead of cementitious material (R, n.d.). In 1968, J. Lowes also patented and invented a machine like the first one, but this machine created elliptical structures instead of spherical (J, n.d.). Finally, in 1976 (BRANDT & E, n.d.) and 1988 (T, n.d.) came two more machines that made similar structures but integrated the past techniques in previous patents, the last one using a better power system but still without the automation factor to control the arm or to make other shapes rather than just an ellipse or a sphere.

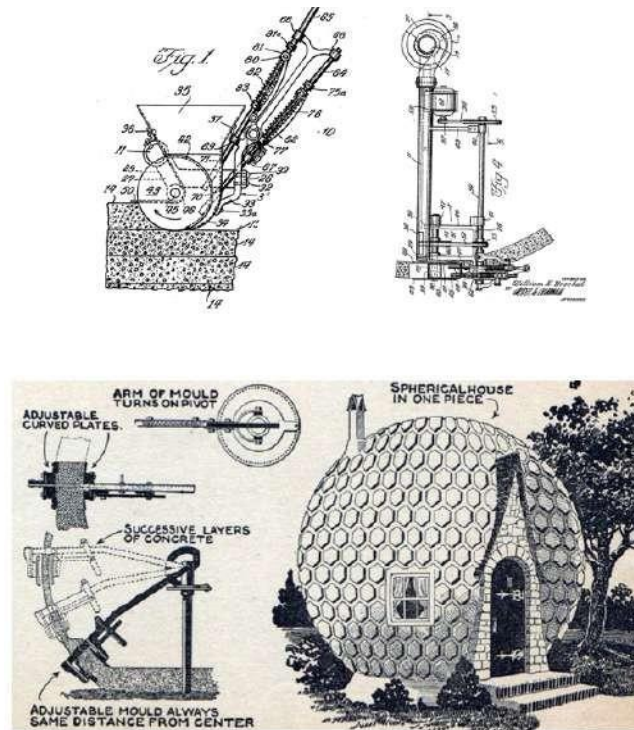


Figure 4.12: Construction machine with an extruder. Source: (Urschel, 1943)

Automation was finally introduced in 1995, the year where the first proper AM machine was introduced. This machine used CAD programs to generate the 3D model in what it was called “solid free form constructions”. It worked by applying what was earlier presented as binder jetting. It used a powder made from sand and cement which was reactive to water vapor and solidifying, this was mentioned on Issa’s thesis (Issa et al., 2021) and in Bedarf et al. paper (Bedarf, Dutto, Zanini, & Dillenburger, 2021).

Khoshnevis (Khoshnevis, 2004) was another designer who made big contributions to the AM picture as it is known today. He designed Contour Crafting (CC). It was an AM technique but with more focus on the surface quality part, speed, and more materials. It used two trowels (like the ones used by construction workers) to smooth the surface while printing it (as seen on fig. 4.14). He also explored some interesting applications that look a lot like the ones that now exist, for instance, he proposed this technique for large scale buildings, also explored 3D printing structures as a frame and then filling it with traditional techniques and also 3D printing the whole structure, showing a better use of material 3D printing all

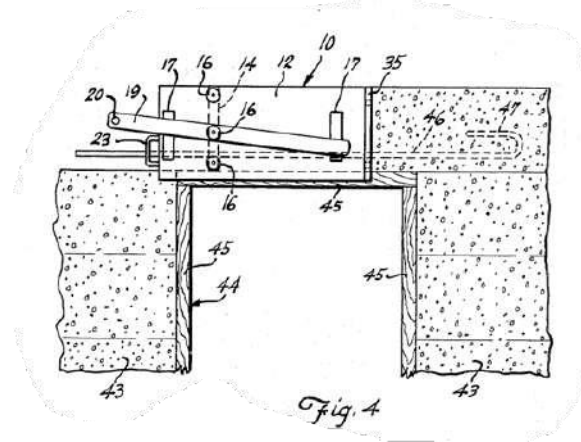


Figure 4.13: Urschel's son design. Source: (R, n.d.)

the structure by using a more efficient filling than just pouring it (fig. 4.15), finally he also proposed applications such as, automated reinforcement, plumbing applications, filling for floors, and even some extraterrestrial applications were considered.

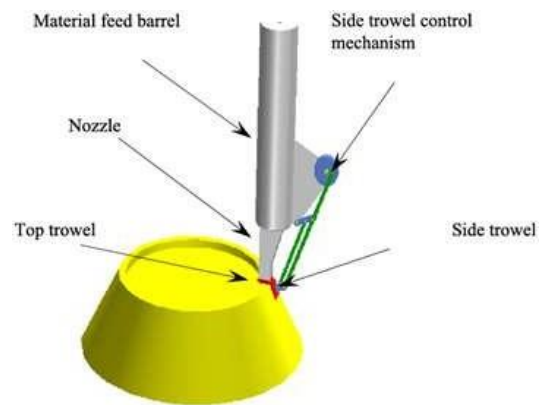


Figure 4.14: Contour Crafting. Source: (Khoshnevis, 2004)

After this technique was created, many more studies were made, and various techniques were implemented to further improve the AM in the construction industry-. Some of these new trends and paths that AM is following will be reviewed in the following paragraphs, as it is very important to understand what is being used today and how, and which one of these systems can help solve this problem.



Figure 4.15: Structural Advantage with AM. Source: (Issa et al., 2021)

4.1.8 AM and New Technologies for the Construction Industry

The TRR 277 is a research center created by the German Research Foundation in 2020 that is dedicated to the research of AM in construction (AMC) and has three focus areas oriented to study some of the major problematics of AMC. The first one is the study of material and processes which is focused on developing materials and processes, not separately, but as one, i.e., looking to what is the best AM technique and process for a certain material or materials, proposing a combination these two and looking how they work together. This has led to identify that the two most likely groups to have an application in AMC are particle-bed based selective solidification and deposition. They have found this solution to be effective in terms of resolution and capacity to develop complex structures. The investigation now has an interesting take on selective cement activation, laser powder bed fusion, and other research projects (Kloft et al., 2021).

The second focus area is computer-aided modelling and process control of the findings in the first area. This is because of the still limited and because of the nonlinear nature of the processes that are being tested, is important to have software capable of simulating and analyzing the several main parameters of AM. This type of investigation leads to a more

accurate understanding and prediction of the final shape, material properties and overall behavior. The third focus area is design and construction, which is more involved in the structural optimization, form optimization and the planning process and new ways to aid the decision-making process to select the most adequate AMC method. The figures below will show some of the projects currently being developed on the TRR 277.



Figure 4.16: Wall-element with integrated tube, additive manufactured by selective cement activation. Source: (Kloft et al., 2021)



Figure 4.17: Additive manufacturing by extrusion of lightweight concrete and reinforced double-curved wall element, manufactured in shotcrete 3D printing process. Source: (Kloft et al., 2021)

Repinskiy, Romaneskul, and Studenkova (2021) delved into the applications and benefits that AM could on the construction industry. Similarly, they found that CC is still being used and developed as one of the main methods to produce AMC and finding that traditional

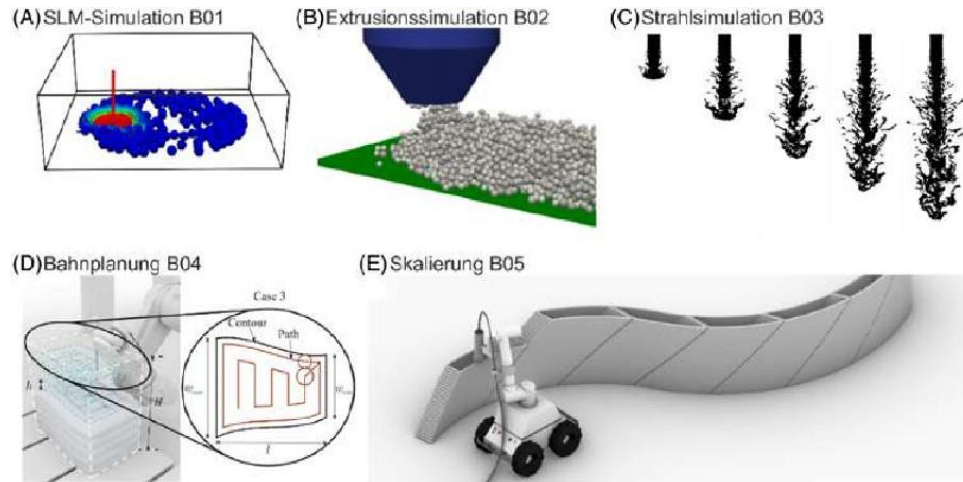


Figure 4.18: Components of the digital process image for the development of control concepts for the additive production of large scale and reinforced concrete components. Source: (Kloft et al., 2021)

methods of construction can produce 3-7 tons of debris and exhaust gases (like vehicles) and when applying the CC methods this contamination becomes minimal. Another exciting application is the capability of building on the moon and mars, saying that most of the material can be obtained mining these two places.

Also, in Shanghai a set of 3D printed houses of 200 square meters has been built. WinSun, a company that specializes in 3D printing using cement, built houses at the amount of just \$4,800 and in just a few hours, and all of these using materials coming from construction and industrial waste. Many benefits are discussed in this paper such as:

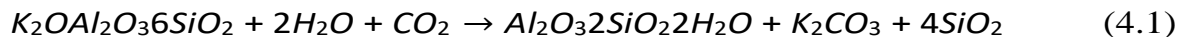
- 1.Reducing time on the construction site.
- 2.Improving quality and repetition of the process.
- 3.Reduction of costs in manufacturing, installation and tooling.
- 4.Improved condition and safety.
- 5.Being a more sustainable industry.

Other authors such as Pacillo, Ranocchiai, Loccarini, and Fagone (2021) explore current solutions in terms of materials and processes as well as commercial solutions on the market,

which will come in handy when talking about a possible method to use with the clay problem. Camacho et al. (2018) discuss many more applications and dive into materials, optimization, repairing, tolerances and more. In the figures down below, it can be seen some of these applications. Paolini, Kollmannsberger, and Rank (2019) and Khajavi et al. (2021) dive a little bit more into the concrete 3D printing, its future and competitiveness. Lastly, Wolf, Rosendahl, and Knaack (2022) explore more about the 3D printing of ceramics in general, which will be very helpful to set a foundation in later chapters-

4.1.9 Clay and clay additive manufacturing

Clay is the chemical wear product of a mineral called feldspar (Ramírez et al., 2021) which is one of the most common minerals on earth. To be formed clay needs the following chemical reaction (Velilla Díaz et al., 2009):



Which is the combination of Feldspar and Caolin.

Clay is very bound to the size of the particles that conforms it. According to (Kumari & Mohan, 2021) the material is soft, freely bound, an the clay particles that conforms it are about 0.005 mm in diameter. This article basically divides the clay into two different classes:

- Residual clay: these are found in the place of origin and formed by surface weathering.
- Transported clay: is the clay that was removed from the place of origin.

(Murali, Sambath, & Mohammed Hashir, 2018) wrote an article about the significance and importance of this material in the engineering industry. For instance civil engineers consider clay as the less than $4\mu\text{m}$ of the soil and are classified as swelling or non-swelling and/or hard or soft.

One of the most important feature for clays are clay minerals, since theses basically form the clay. There are the following (Kumari & Mohan, 2021):

- 1.layer silicates; which include kaolinite, halloysite, smectite, vermiculite, mica, illite and chlorite.
- 2.Chain silicates; which include palygorskite and sepiolite.
- 3.Sesquioxides; which includes metal oxides, metal hydroxides, allophane and imoglite.
- 4.Others; which include carbonate and sulfate.

Even though all of these minerals are clay they all have different properties, like different dry strength, different behaviours when it comes to shrinkage or swelling and different surface areas (Murali et al., 2018).

According to (Kumari & Mohan, 2021) and some very important characteristics of clay are the following:

- 1.Swelling capacity: this is capability of absorbing water, with this comes some changes like volume or density.
- 2.Plasticity: that is the ability clay has to change shape given a certain amount of water.
- 3.Refractoriness: once dried, clay can resist variations on temperature without suffering much on its properties.
- 4.Porosity: the porosity is the property of how material there actually is on the clay.

Other important characteristics that come with experimental studies are such as density, yield stress or viscosity. But these depend a lot on the type of clay, composition and more. Since in this work clay composition is not going to be studied there is no need to delve into that, but it definitely is an option when the study of a certain clay is being performed.

Clay has been a construction material through human history, it is the the material most widely used for bricks and tiles, and also the most common ceramic in the world for pottery (Ramírez et al., 2021). AM has not come short of investigating and experimenting with clay.

The study of (Wolf et al., 2022) presents a very helpful study on how clay is used in AM for construction.

The first thing presented are the different techniques for clay additive manufacturing. The most common being extrusion, which is the simplest process in which a paste goes through a nozzle and gets out by the action of some pressure. There is also photopolymerization which is an adaptation of stereolithography where the final combination of materials gives an extra strength to the printed result. Binder jetting which is a powder based process and sheet lamination, both of which were discussed in the previous section.

Lastly, the paper presents different studies on how clay has been manufactured and tested for different structures, most of these projects have studied architectural structures to test strength, space and also some aesthetic. Along with the information presented in the next section the clay advancement for AM has been a very promising enterprise.

4.2 Technical state of the art

For the state of the art first a review of the available technology will be performed in the form of benchmarking, patent search and some homologues and analogues to further generate concepts and create ideas.

4.2.1 Available technology and designs

For this review similar technology will be highlighted, whether it relates to the systems or that it has a solution that could be used but not necessarily the whole system.

1. Clay extruders

- Open maker clay extruder. (*Extrusion System for 3D printing ceramics*, 2021)

This extrusion system is an open source project that extrudes clay at 18% humidity, with this, they achieve much more stability due to a tougher and drier clay. The schematic of the system can be seen on the following image (see fig. 4.19):

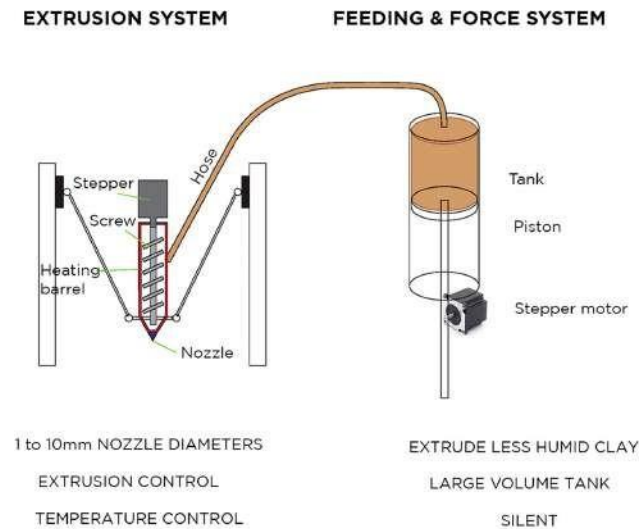


Figure 4.19: Open maker extruder schematic. Source: (Extrusion System for 3D printing ceramics,2021)

The extruder has some characteristics that are relevant to this project, such as a pushing system composed by a Nema 23 stepper motor. An extruding system based on an endless screw, a feeding system connected through a hose to a feeder, a heating system formed by a clamp near the end of the extruder to get a higher flow and a nozzle with an adapted tip to decorate cakes. The fig. 4.20 showcases all these sub systems.

The other part of this system is a feeding tank which has an interior diameter of 15 cm and 80 cm long, This tank has a pushing system with a nema 23 with a high reduction gearbox and a lead screw and the feeding and reduction system, which is the main cylinder and the nozzle connected. This system feeds the extruder and the sub systems can be seen on fig. 4.21.

- CeraStruder open source. (CeraStruder, n.d.)

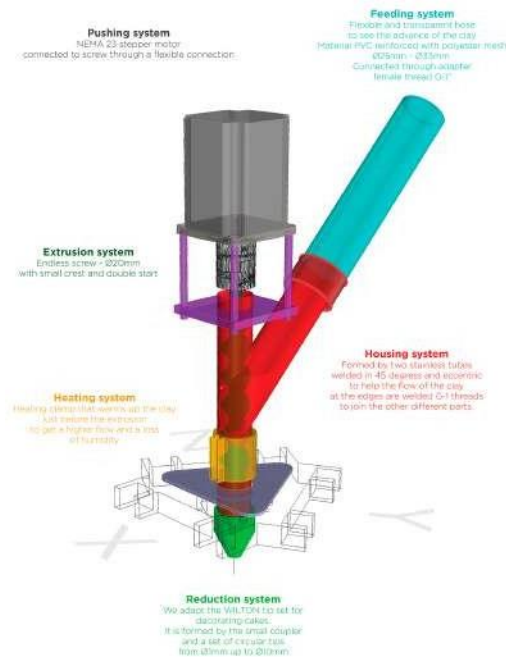


Figure 4.20: Open maker extruder sub systems. Source: (Extrusion System for 3D printing ceramics, 2021)

Another clay extruder open source project is the CeraStruder and it is very similar to the open maker, but with a few extra components. In this case it also consists of an extruding and a feeding system, they both have basically the same configuration than the last one, the extruder system consists of an endless screw, a nozzle and a stepper motor, but in this case the chamber of the extruder is much smaller, and the feeding system is directly connected to the extruder. This feeder is also powered by a motor and a plunger, as it can be seen on fig. 4.22.

The system can also be configured to extrude directly from the feeder or connected to a smaller robotic arm as a static extruder.

- Stone flower opensource project. (*Clay 3D printers. Add-ons for clay, porcelain, concrete, suspensions*, n.d.)

The stone flower project is yet another open source extruding system with very similar characteristics to the other two, it is a print head extruder with an endless screw and

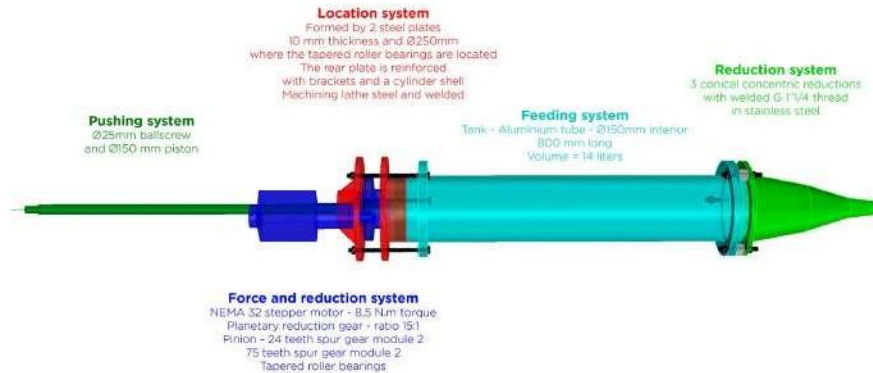


Figure 4.21: Open maker tank subsystems. Source: (Extrusion System for 3D printing ceramics, 2021)

a feeding system powered by a lead screw and a plunger that is connected to the print head. The configurations are very similar, there is a mortar configuration for bigger prints and a smaller one consisting of just the print head and the feeder. There is not a lot of newer components to talk about, so, just to see the configuration similarity turn to fig. 4.23.

- LUTUM Eco Clay commercial extruders and extruders. (*theLUTUM® Eco Clay Extruder*, 2020)

This system is a commercial clay extruder which works with a lot of the same mechanisms of the previous ones, it uses a stepper motor, a power screw, and in this case it uses a much smaller nozzle tip. But, the feeding system uses a system of cartridges to use in succession. The company, LUTUM, not only sells extruders but also complete printer systems used specially for clay. Something different that this system has is that, the cartridge is pushed by suppressed air and then the screw takes the bubbles out (*theLUTUM® Eco Clay Extruder*, 2020).

- 3D Potter commercial extruders and printers. (*3D Potterbot Scara V4 ceramic 3D clay printer — real clay 3D ceramic printer*, n.d.)



Figure 4.22: CeraStruder configuration. Source: (CeraStruder , n.d.)

This extruder is the first that does not use an endless screw, rather it uses a plunger to push the clay down. In this case the clay has to be all previously put into the cylinder before printing something, which gives a limited amount of capacity for printing. A thing in common with previous systems is that this is also powered with a lead screw and a stepper motor (*theLUTUM® Eco Clay Extruder*, 2020).

- Delta Clay Wasp extruder. (*Extruders*, n.d.)

This commercial extruder is very similar to some of the previous models, since it uses an endless screw and a stepper motor. The nozzle is conical and in different sizes (such as some of the others) 4, 6 and 8 mm. Since it is a geared stepper it has the capability to make extrusion of a harder clay mixture. This system has a tank as well, which is pushed by pressured air as well. The system can be seen on (*Extruders*, n.d.).

- Reinforced clay printing. (*Reinforced clay printing* –, n.d.)

This is not exactly a similar system, rather this a system that reinforces FDM prints

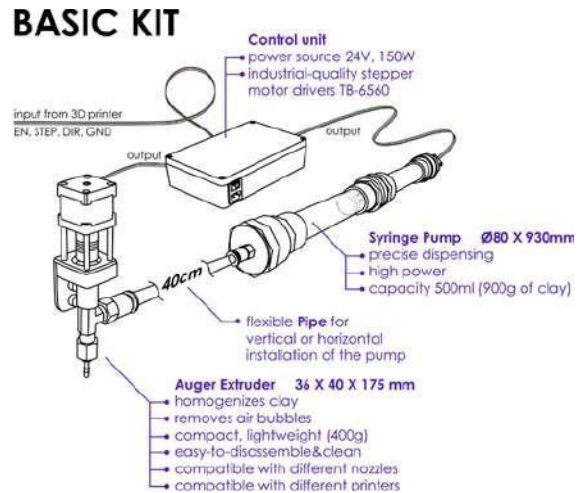


Figure 4.23: Stone Flower configuration. Source: (Clay 3D printers. Add-ons for clay, porcelain, concrete, suspensions, n.d.)



Figure 4.24: LUTUM Extruder. (theLUTUM® Eco Clay Extruder , 2020)

with clay structures. But, still, this design of clay extruder is considered for this purpose. In this case, the extruder works with a solenoid valve to let air pressure in and out. The design is quite basic, with just an acrylic tube and a nozzle, with the clay previously installed on the tube.

Other DIY projects can be found in YouTube for example, such as an extruder system very similar with a printhead extruding with an endless screw and a feeding system that is powered by pressured air. Also a delta adapted robot with a syringe extruder. These are very helpful for this project, one reason is because they show some of the building process and mechanisms that go into the assemblies and, the second reason is because of some learning curve they have had when it comes to the assembly or the



Figure 4.25: 3D Potter extruder. Source: (3D Potterbot Scara V4 ceramic 3D clay printer — real clay 3D ceramic printer , n.d.)



Figure 4.26: Delta Wasp Extruder extruder. Source: (Extruders, n.d.)

actual print.

For instance, (WillysGarageNorway, 2020) discovers some of the importance of the extrusion uniformity and the problem with the limited speed extrusion when it comes to the use of pressured systems. (Lee, 2022) discovers a problem with clay getting stuck in the nozzle and a problem with the rest of the printing needing to stay warm while the printing is being done, but they achieve a fairly smooth finish on the prints.

2. Pugmills, recycling and other ceramic extruders

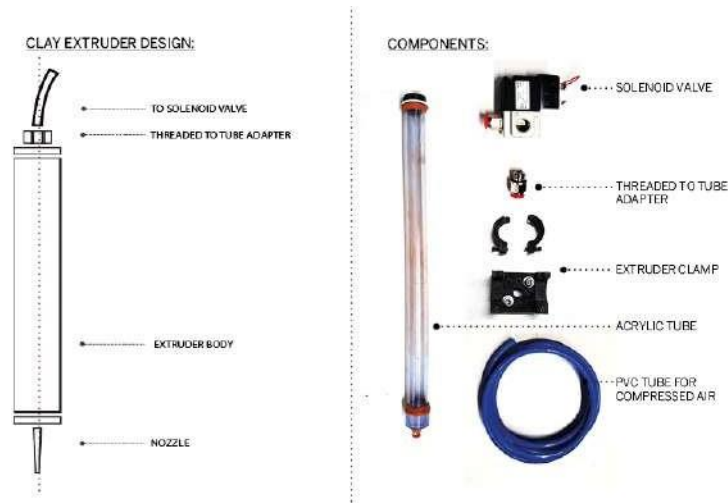


Figure 4.27: Reinforced clay extruder. Source: Reinforced clay printing –, n.d.)

(Ramírez et al., 2021) makes a design for a horizontal clay extruder in which a comprehensive study of the forces and pressures that occur in an endless screw is executed. The purpose of this is to determine if this kind of systems can be made at a low cost and if it can deliver high performance, the screw for this system is still made out of metal, but something that could report an improvement in terms of material cost is the nozzle, because the 3D printed material they used accomplished the objective while being a polymer.

(Velilla Díaz et al., 2009) in this Masters thesis the author investigates how a mathematical model could be developed to analytically approach the process of clay extrusion, specifically for brick extrusion, since there is a lot of these extruders on the market but not a lot of theory as he explains on the thesis overview. To validate this model, a FEA analysis is performed and then an experiment where the resistance of bricks is reviewed, with a very good result giving this model validity.

(Ali, 2019) conducts a similar study to the one mentioned in the paragraph above, only in this study the characteristics and properties that the extrusion material present and how they affect the final product in the extrusion process. (Sánchez & Rivera, 2008) also makes a study on the process and how the mold of the nozzle affects the

resulting bricks.

Regarding AM and other studies that have been conducted, (el Mesbahi, Buj, & el Mesbahi, 2021) study a low cost system for adapting to different open source 3D printing machines. In this case they stride for an innovative system which won't interrupt the printing process by implementing a system of syringes that work simultaneously and every time one is full the other starts to work to make the material flow.

Pugmills are another system very relatable regarding this project, due to the fact that this is probably the most common system to work with clay. They are used mostly for kneading, extruding, mixing and they are used even as a recycling machine. So this is a system that is also worth investigating for this thesis.

- Peter Puger pugmills (*Peter pugger*, n.d.)

Peter pugger is a company that builds clay pugmills, for both potters and industry, they offer a variety of pugmills for different capacities. The one that is probably most related to this work is the De-airing pugmill, which, has all the characteristics of a normal pugmill, this meaning, a screw that is not only for extrusion, but also kneading and avoiding clay sticking (as it can be seen on fig. 4.28).

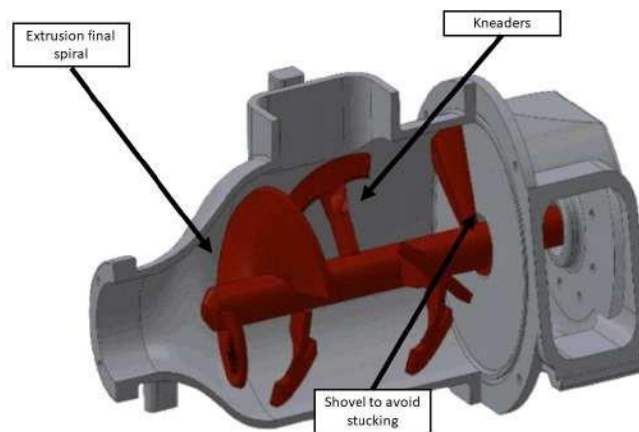


Figure 4.28: Petter pugger general mechanism. Source: (Peter pugger , n.d.)

The De-airing characteristic involves putting a vacuum pump to suck the air of the

exploded bubbles while kneading the clay. This ensures a better extrusion and prevents any defects on the final print, because air bubbles represent a real danger to extruded clay due to the firing process, if there are trapped bubbles the firing process could cause an explosion or can cause cavitation due to the inside pressure. in this case, Peter pugger offers several de-airing pugmills depending of the quantity that needs to be worked.

- Venco pugmills (*PUG MILLS — venco, n.d.*)

VENCO is another company that builds pugmills, these products also have the capability to reclaim scraps and recycle them. This company also offers different pugmills for different applications, such as a mini pugmill, a standard version and a de-airing version. This last version including two different pug mills with different nozzle sizes, which is also something a little odd to see, since the main standard across these machines is a diameter of 3 inches. The mini version of this pugmill can be in fig. 4.29



Figure 4.29: venco mini pugmill. Soruce: (*PUG MILLS — venco, n.d.*)

- NIDEC pugmills (*NVS-07, 2019*)

The NIDEC company offers basically the same two kinds, a de-airing pugmill and a non de-airing. In this particular occasion these pugmills are way more robust that the two previous ones, which makes it capacity a lot higher. Also, both the pugmills they

offer are driven by dual screws and offer a no spiral wedging which is specially useful for potters. Some of the main parts of the de-airing pugmill are shown in fig. 4.30.

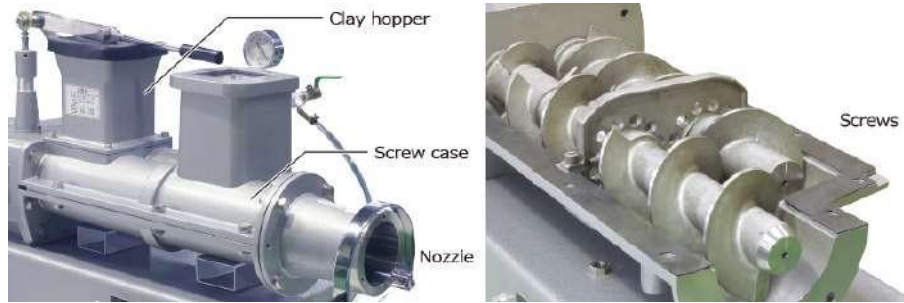


Figure 4.30: NIDEC De-airing pugmill. Source: (NVS-07 , 2019)

Lastly, (Makery, 2020) present some sort of DIY pugmill for clay. It is a very interesting approach, since it shows how it is assembled and then presents the results, with and without a vacuum machine, and the results are way more smooth with the vacuum pump, presenting a little bit of air bubbles, but that is, according to him, because of the time the clay was being mixed. A resulting cylinder of the pugmill is presented on fig. 4.31.



Figure 4.31: Homemade clay pugmill. Source: (Makery, 2020)

- Another clay recycler

In (Muñoz & Cuadros Bedoya, 2019)'s work a design is proposed to recycle clay after this has been dried. For this this design presents a shredder machine to crush ceramics

to the recycle them. This would be very useful for big quantities that need to be crushed into smaller pieces, since a pugmill only can reclaim scraps of clay, the previous process of a shredder would make this very direct and also would save some time as recycled clay from scraps tends to take longer to get ready for using it again.

Another analogue technology

3. Concrete and cement extruders

Another analogue technology of extrusion that has been developing more and more and also being investigated is the 3D printing of concrete and cement for the construction industry as it was discussed on the background section. So in this section some of this examples will be reviewed.

- Delta wasp extruder for concrete. (*Extruders*, n.d.)

Wasp is a company that also produces products for concrete 3D printing. The LDM WASP Extruder XXL (see) is a extruder that has the capacity to extrude very dense materials such as concrete using yet again an endless screw. Only this extruder is way bigger, having a nozzle from 8 mm to 30 mm. Is worth mentioning that this extruder is fed by a continuous feeding system with a mortar and a pump that are constantly mixing concrete and pumping it into the print.

- Other extruders and printers. (*Extruders*, n.d.)

Many of the companies that are dedicated to concrete 3D printing focus more on the whole printer rather than just the extruder, since this can not be easily replaced. But the majority of these system, because of the size of the printer, don't use an endless screw since the size of it makes it no longer viable. Rather, the majority of this nozzles and extruders work on pressure air.

A great example of this is on fig. 4.33, in which not only is shown the size, but also the shape, which tends to be more squared the bigger the printer is.

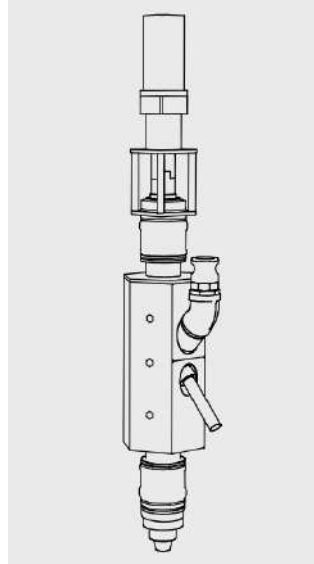


Figure 4.32: LDM Wasp extruder for concrete. Source (Extruders, n.d.)



Figure 4.33: COBOD extruder. Source: (The BOD2 , 2023)

- Design of a extruder for concrete of (Guía et al., 2018)

In this thesis the author designs a extruder for 3D printing concrete, and to adapt it to a frame of a printer. For this case an endless screw also was designed to extrude the concrete, and was tested with several types of concrete. One of the most interesting characteristics of this extruder is the shape of the nozzle, which is squared and also driven by a stepper motor. The model can be seen on fig. 4.34.

- Other studies



Figure 4.34: Cesar's system fabricated. Source: (Guía et al., 2018)

In (Jo, Jo, Cho, & Kim, 2020) there is also another development for a 3D printer of concrete, where they also developed an extruder using an endless screw. The design is very similar to the previous one as it can be seen on the figure below (see fig. 4.35). Only in this case the nozzle is a little bit more pug-nosed.

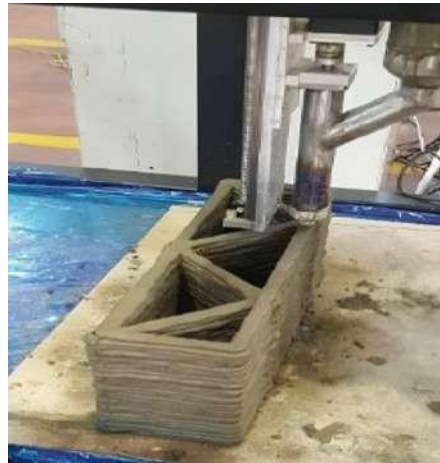


Figure 4.35: Extruder for cementitious material. Source: (Jo et al., 2020)

4.Extruders for food 3D printing

In this case, the study of (Carmona Reverte, 2016) delves into the design of an extruder for 3D printing food (see fig. 4.36), which is very interesting because of the material requirements that it needs for it to be sanitary. Also, whilst they present an

extruder that functions with pressure air, and uses an inside tube to prevent possible contamination and abrasiveness, is very important than in their thesis they propose a system of extrusion with a peristaltic pump, which is probably the only one that has been proposed through the reviewed studies.

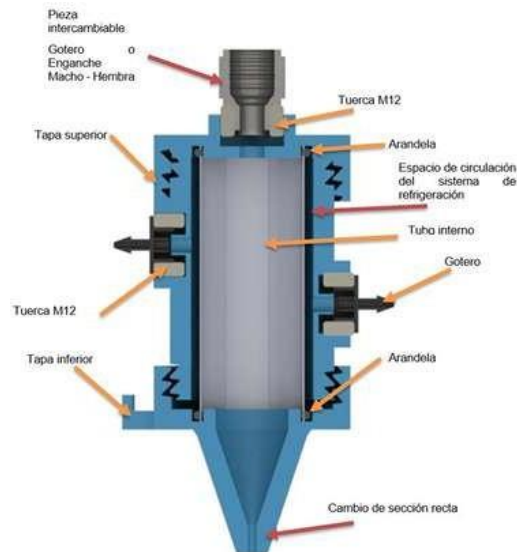


Figure 4.36: Food extruder. Source: (Carmona Reverte, 2016)

4.2.2 Patent study

For the patent study, some patents with interesting approaches are going to be reviewed in order to get some ideas to develop this design.

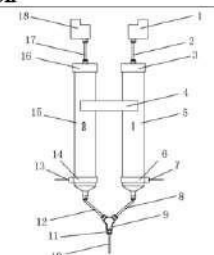
Patent number	Patent description
CN211278899U	
<p>This is a device switches in between feed cylinders connected to the extruder via a valve that changes the pipes of air pressure for keeping the flow of clay</p>	

Figure 4.37: Patent CN211278899U. Source: (JING et al., n.d.)

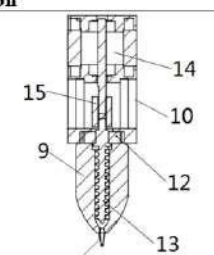
Patent number	Patent description
CN211466777U	
<p>This is a mini clay extruder to ensure a better finishing of the clay. In this case the extruder has two systems that help it extrude better an endless screw and a shaft adjuster.</p>	

Figure 4.38: Patent CN211466777U. Source: (DE'AN, n.d.)

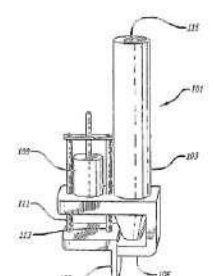
Patent number	Patent description
WO2004065707A2	
<p>This patent is a multi nozzle assembly for extrusion. It has three available nozzle to print from through a control system that switches these nozzles.</p>	

Figure 4.39: Patent WO2004065707A2. Source: (BEROKH, n.d.)

With the previous patents reviewed, now there are some novel ideas and approaches than can be considered to design this system. They mostly have to do with an assembly or set of nozzles, a set of feeders or control systems that help the extrusion process.

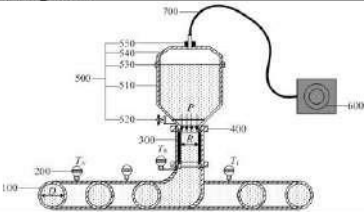
Patent number	Patent description
CN111929200A	
<p>This is a measurement device of the fluidity for concrete. It comprises a spiral pipe, a timer and it is impulse by pressure.</p>	

Figure 4.40: Patent CN111929200A. Source: (JIAN et al., n.d.)

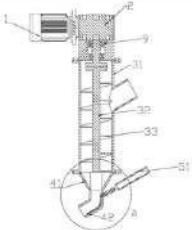
Patent number	Patent description
CN112476705	
<p>This is an extruder that has an interface mechanism to help with the final coagulation of the concrete as it is being extruded.</p>	

Figure 4.41: Patent CN112476705. Source: (JIQIANG et al., n.d.)

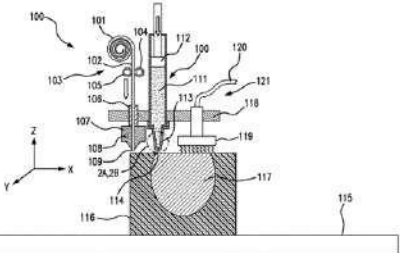
Patent number	Patent description
US 20210069789A1	
<p>This patent is a proposal for a nozzle made out of flexible material, so, for the desired amount of size is the needed amount of pressure to increase the nozzle size.</p>	

Figure 4.42: Patent US20210069789A1. Source: (MATS C, n.d.)

4.3 Requirements and Specifications

4.3.1 Requirements

To start the design process, it is necessary to understand what the client wants from the product. Generally, it is a good idea to put their requests in a table and then “translate” them into specifications (Ulrich, Eppinger, & Yang, 2008), (Ullman, 2003). In this case, it is also a good idea to do research of the current technological state so an idea can be generated on what things can or cannot be reproduced or improved. In table Table 4.4, the requirements the LATE asked, plus some specifications that could be helpful to make the design better.

Table 4.4: Requirements for the extruder system

ID	Part	Req.	Importance
R01	The system	has a continuous workflow	5
R02	The system	admits several types of clay	3
R03	The system	is compatible with the robot	5
R04	The system	allows for different wall sizes	4
R05	The system	recycles material	3
R06	The feeding system	provides a constant supply of material	4
R07	The feeding system	provides clay without bubbles	5
R08	The feeding system	is easy to insert and remove	5
R09	The extruder	controls clay extruded	4
R10	The extruder	has a pressure control	3
R11	The extruder	has retraction	3
R12	The extruder	has variable nozzle sizes	4
R13	The extruder	has removable hoses	4
R14	The clay	maintains constant flow	5

The previous requirements are made out of the conclusions obtained in section 4.2 after a careful and thorough review of the state of the art. Now that all the requirements are known the next step forward is to convert them into specifications so the parameters for design are set. For this, metrics are necessary to establish how the control and the decisions will

be made. Refer to Table 4.6 to see these metrics.

4.3.2 Specifications

Table 4.5: Metrics for the system

No.	Req.	Metric	Imp.	Units
01	R01, R08	Feeders change time	5	[s]
02	R03	Weight of the system	4	[kg]
03	R01, R08, R13	Feeders' pieces to remove	5	pieces
04	R01, R02, R07, R10, R14	Pressure required	4	[Pa]
05	R02, R05, R14	Humidity levels	3	[%]
06	R03, R08, R14	Tolerances	3	[mm]
07	R09, R11, R14	Motor torque	3	[Kgcm]
08	R09, R11, R14	Motor speed	4	[rpm]
09	R07	Torque of the feeding system	4	[Nm]
10	R04, R12	Nozzle size	5	[mm]
11	R05	Crushing force	3	[N]
12	R14	Viscosity levels	5	[Pa s]
13	R14	Flow rate	5	[Kg/h]

All these metrics (see Table 4.6) are going to be translated to specifications giving specific values to each one of the metrics. This is going to set some goals and they are going to work as design parameters to constrain the prototype to the specific case of this work. To set this values to a certain acceptable range values from other products that already exist or from known values that are set from this specific system.

Table 4.6: Specifications

No.	Req.	Metric	Marginal value	Ideal value
01	R01, R08	Feeders change time	300 s	120 s
02	R03	Weight of the system	10 kg	7 kg
03	R01, R08, R13	Feeders' pieces to remove	5	3
04	R01, R02, R07, R10	Pressure required	20 kPa	100 kPa
05	R02, R05, R14	Humidity levels	40%	15%
06	R03, R08, R14	Tolerances	0.6 mm	0.1 mm
07	R09, R11, R14	Motor torque	500 Ncm	20 Ncm
08	R09, R11, R14	Motor speed	30 rpm	10 rpm
09	R07	Torque of the feeder	6 Nm	40 Ncm
10	R04, R12	Nozzle size	4 mm	8 mm
11	R05	Crushing force	3500 N	1500 N
12	R14	Viscosity levels	5 Pa-s	150 Pa-s
13	R14	Flow rate	2 Kg-h	0.5 Kg-h

4.4 Solution Options Generation

4.4.1 Functional Modelling

Black Box Modelling

For this modelling, first the inputs and the outputs need to be understood. A black box model is used to explain this (see fig. 4.43). Three inputs are accounted, new clay; referring to clay or clay components never used before, used clay; referring to clay that is already printed, and electricity/commands; referring to the main source of energy and basic commands for the machine to work.

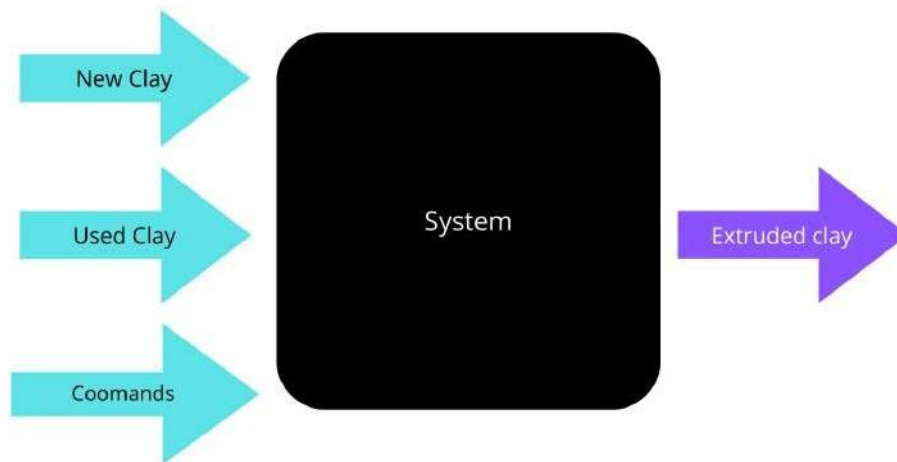


Figure 4.43: Black Box model. Source: own

Functional Decomposition

After the black box model, functional decomposition is a method to identify the main and critical functions of the system in general. This way, it will be easier to model and design by subsystem, rather than design a whole machine. The scheme (see fig. 4.44) will take the same inputs and outputs in the black box, passing through the processes in the functional decomposition.

Basically, there are two possible inputs regarding clay, one is new clay and the other

is used. New clay would not need an extra process and could go directly into the pugmill/kneading system, where clay is kept homogeneous and wet, so fluid properties are not lost. With used clay, a recycling process would be needed, depending on what form is the finished clay, it could have one or several processes before going into the kneading system.

The power and control system must be very straight forward, controlling the flow of the clay and switching between feeders. The continuous workflow system is basically the part of the machine where the clay is pre-extruded and transported into the feeders. Finally the extruder system will perform the main task of printing the layers of clay, this is the most critical because it is going to sense pressure, flow, temperature, etc., and obviously it will control the extrusion flow rate in the nozzle.

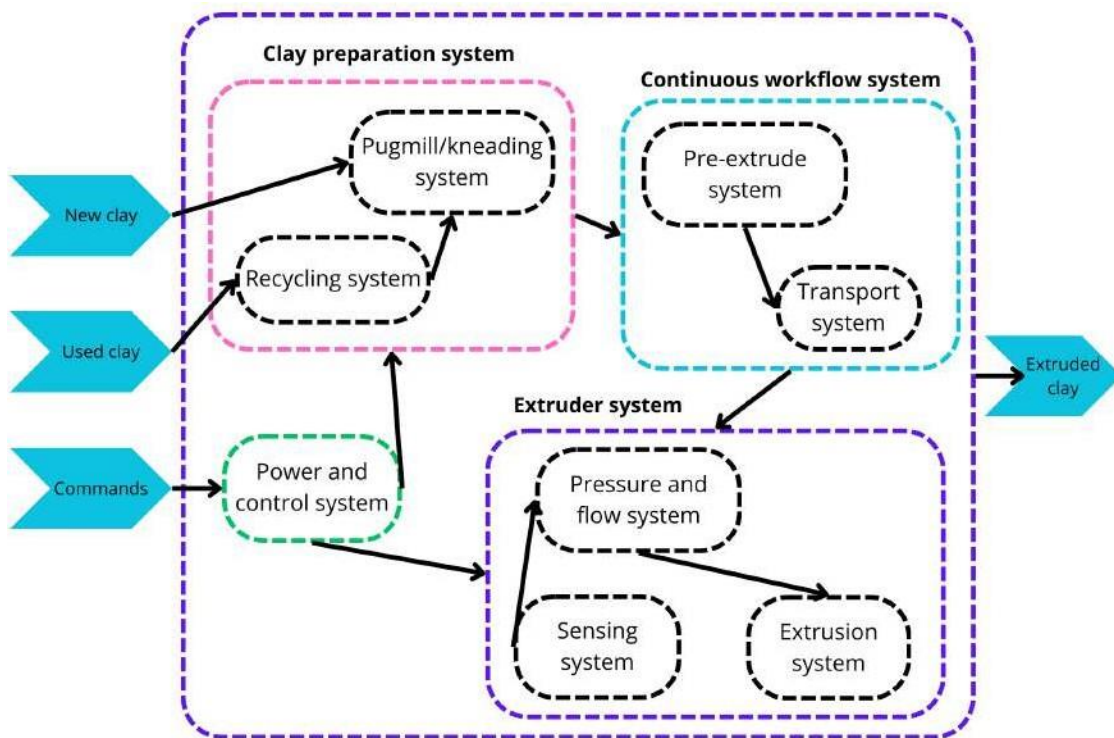


Figure 4.44: Functional Decomposition. Source: own

After this each system must have an input and an output, which will be represented by

the box diagrams, this diagram explains the basic notion for each system (See fig. 4.45). Once this is set, the problem can be divided into sub-problems which can be approached by looking for the solutions for those particular problems and concentrating on the main characteristics and then combining all of those solutions to get a full system, which in this case will be the complete design.

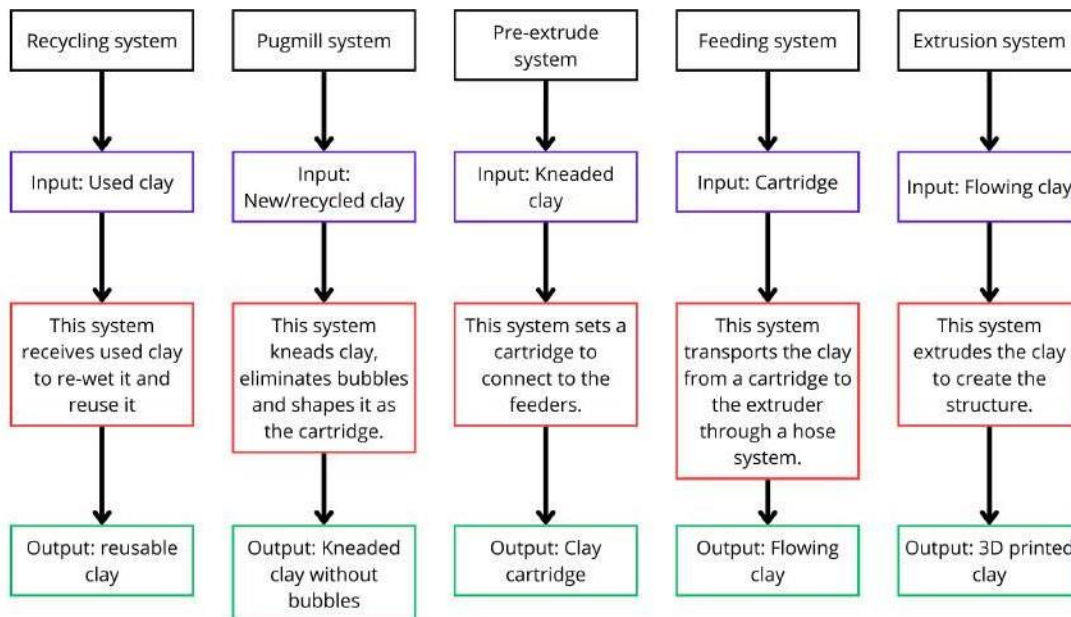


Figure 4.45: Inputs and outputs for each system. Source: own

Then, it is good to identify all the sub problems (shown on the Table 4.7) for which is needed to find a suitable solution. This can be achieved by the revision of the technical state that was revised on a prior paragraph. Now, these sub problems are not necessarily solved separately, for some of them could be covered by the same solution or be solved by result. These will make the morphological matrix easier to identify and combine all of the solutions.

Table 4.7: Subproblems and possible solutions

System	Problem	Parameters or solution
Pugmill system	Clay consistency	Moisture content Particle size Plasticity
	Wear and tear	Clay abrasiveness Material of the blades
	Clogging and blockages	Narrow spaces Sharp corners Cleaning
	Extrusion and pressure	Auger, chamber geometry Pressure control
	Consistency	Ventilation Heating system
Feeder-extruder system	Clay flow	Temperature Composition and additives Viscosity Pressure control
	Extrusion	Extrusion pressure Temperature Nozzle diameter Extrusion speed Extrusion mechanism Heating system Material path Cooling system
3D printing of clay	Properties	Viscosity and thixotropy Particle size, homogeneity Drying, shrinkage
	Adhesion	Adhesion to substrate Layer bonding strenght
	Sintering and firing	Sintering kinetics Firing temperature and time
Controlling the system	Measure flow	Coriolis flow meter Ultrasonic flow meter Magnetic flow meter Differential pressure meter Vortex flow meter
	Temperature control	Heating plaque Thermocouple Thermometer
	Feeding controller	Solenoid valve Motorized valve
	Viscosity monitoring	Vibrational viscometer Calculate with parameters

After reviewing all the sub problems and count the parameters to consider or some possible solutions to investigate. It is important to start generating proposals of the solutions for all the systems. This way a morphological matrix can be proposed and by combing the proposed systems with a preliminary system evaluated according to the most important parameters this system needs to have.

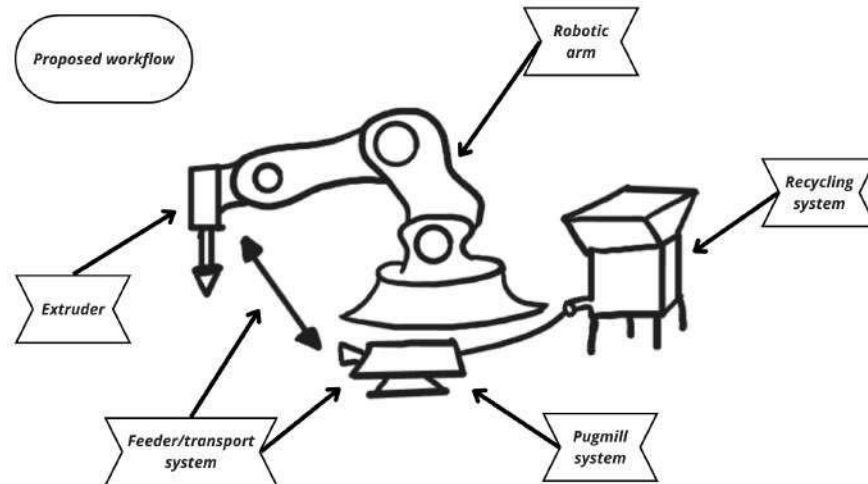


Figure 4.46: Proposed workflow. Source: own

In fig. 4.46 an option for how the workflow should work according to the systems that were proposed in fig. 4.44. First a recycling and storing system is connected to a pugmill, the pug mill main function is to knead the clay enough to eliminate the bubbles and to keep it nice and viscous, which is basically all the previous work that pottery artisans make. After this, the clay will be transported to the extruder in order to be 3D printed. Some drafts on preliminary solutions will be presented next.

Recycling system

The solutions for the recycling system are suggested to be shredders (see fig. 4.47), this is because, how it was seen on the technical state review, it is required that the used clay goes in the form of smaller pieces for it to be easier to re hydrate, so the blades will tear down the clay printed products to a size that can be manageable. After this the process will be somewhat slow, but once the clay is hydrated again, it can be introduced once again into

the pugmill system. The possible shredders that are considered, are a opposing two-bladed shredder, which is probably the most common design for a shredder, then a single bladed shredder with a swing that is stationary that helps give direction to the materials that go into the shredder. The last one is mill-type shredder, where there is a single blade and spikes around it.

The storage system would be underneath the shredder, and it would be very simple, given that after making the clay into pieces it just needs to go into a humid environment for it to recover its properties. So this system will be a container with the right amount of water to generate the necessary conditions, and it must be compatible with the shredder.

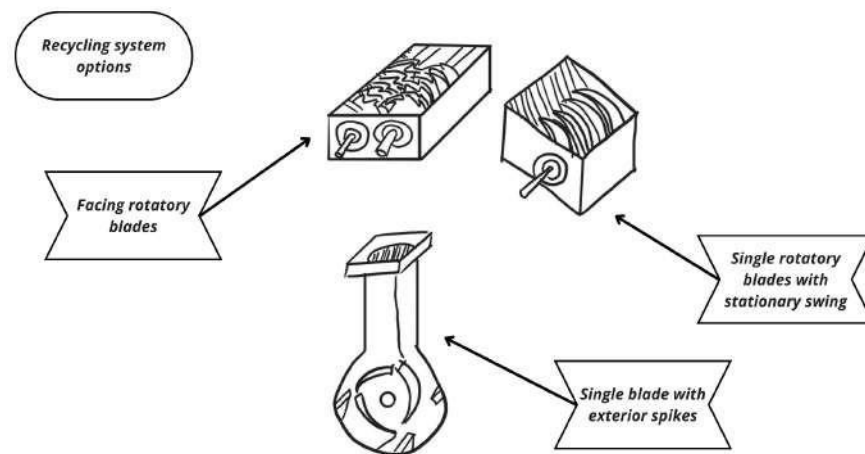


Figure 4.47: Preliminary solutions for the Recycling System. Source: own

Pugmill system

The pugmill's possible solutions are proposed to be two (see fig. 4.48). The first concept from left to right, is a horizontal pugmill with T and spiral shaped mixers. The T shaped mixers would help to knead the clay and the shape is specific for the clay not to get stuck on a blade. Then the spiral mixers would help extrude the clay into the desired shape already without bubbles. The second one, is vertical; the idea behind it is that gravity helps clay to move through the pugmill, the mixers are also T shaped, but at the end a shovel-type mixer has the objective of helping the clay to get unstuck at the bottom. Both proposals must

have the capability to extrude clay.

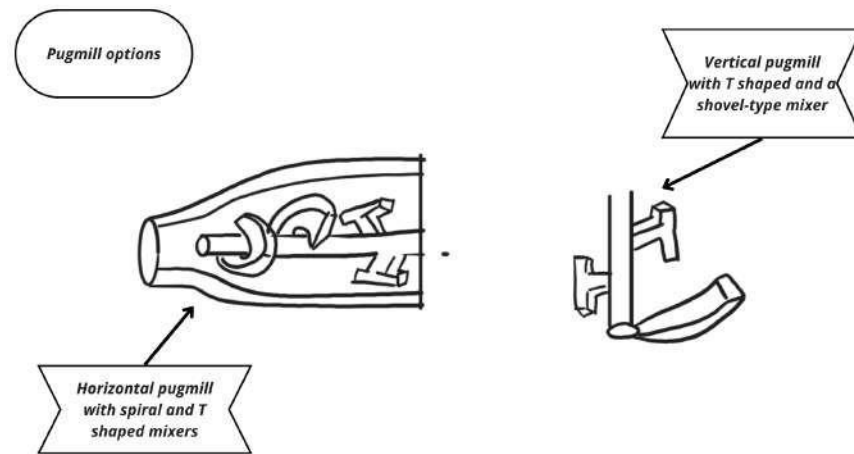


Figure 4.48: Preliminary solutions for the Pugmill System. Source: own

Continuous workflow system

For the continuous workflow system, which is one the most important parts of the complete system, because is the characteristic that we stride to be innovative. The proposition for this system (fig. 4.49) comes in two possibilities, the first one is a hose system (which would also work as the feeding system) with a pump to transport the clay from the pugmill system to the extruder. The second one, would be a system of interchangeable cartridges that connect to the pugmill and to the feeding system which is connected to the extruder trough a much smaller hose.

Feeding system

For the feeding system the proposal depends on the selection of the CWS, because, if the solution selected is the direct connection from the pugmill to the extruder, it would be a hose system with a pump, but, if the option selected is the cartridge one, it will be very important how this system is designed. So in fig. 4.50 a frame is attached to one cartridge and this cartridge comes from the pugmill. For it to be continuous the only thing to do is to add an additional cartridge and frame to be able to fill one whilst the other is being fed by the pugmill, so the continuity does not get interrupted. This would of course require a

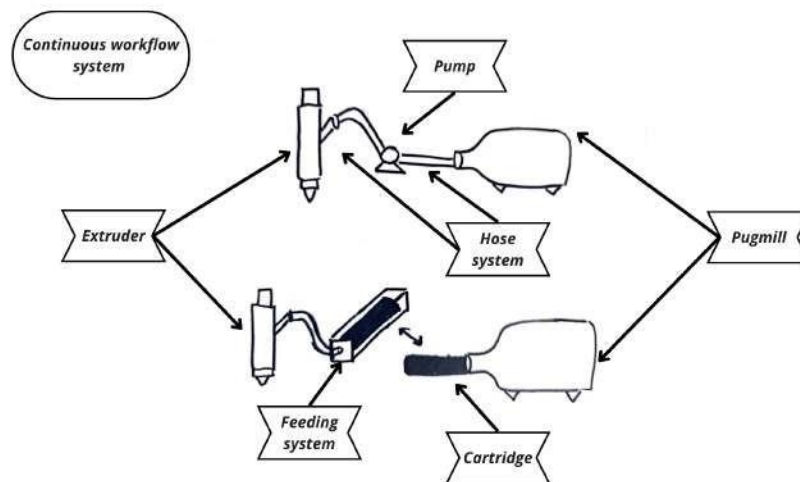


Figure 4.49: Preliminary solutions for the Continuous Workflow System System. Source: own

valve to change in between feeders.

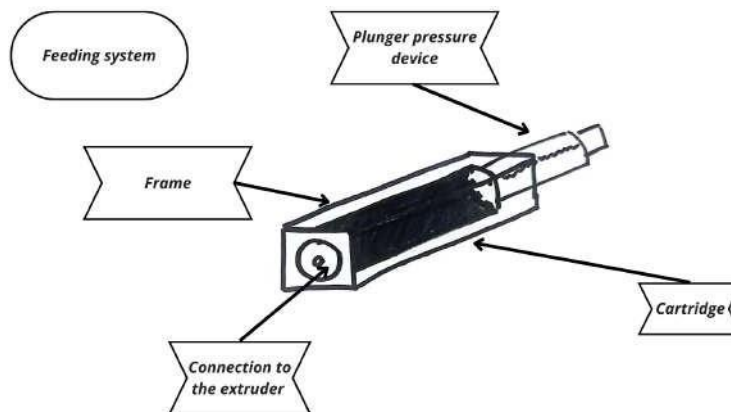


Figure 4.50: Preliminary solutions for the Feeding System. Source: own

Extruder system

The extruder system has some very important features to it, so this is going to be the most detailed design to review. First of all, the extruder can have many shapes and sizes, also the mechanism of extrusion is very important since it will be the main source of control for the clay to changes speed, retract and change flow during a printing process. The first image (fig. 4.51), has to do with the fact that shape, access and size play an important part

on how the inside mechanism could work on the extruder.

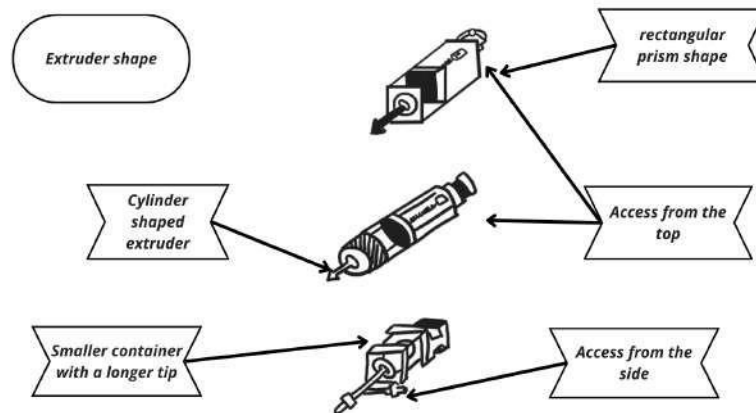


Figure 4.51: Preliminary solutions for the Extruder shape. Source: own

For the extruder internal mechanism there are four main mechanisms proposed fig. 4.52, the first being the most common mechanism for extruders, which is an endless screw type of extruder, then two variations of a peristaltic pump are also considered, which is a very clean mechanism, finally a plunger mechanism, like the one syringes have is also being considered as a possible solution.

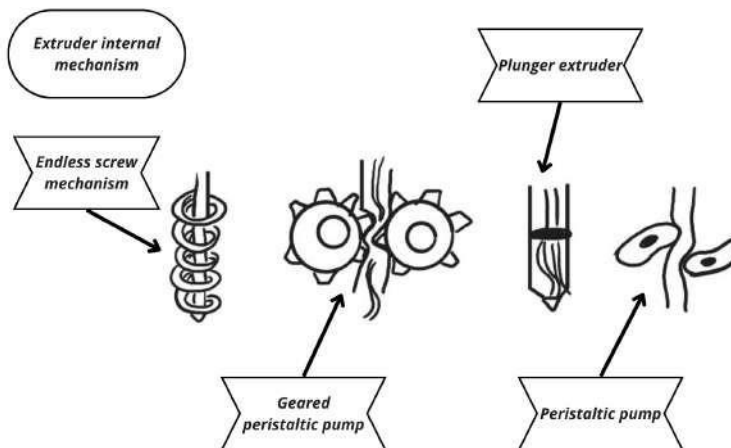


Figure 4.52: Preliminary solutions for the Extruder internal mechanism. Source: own

Finally, other thing to consider is how the extruder is fed (see fig. 4.53), the first row

options are extruder that are fed with an external container connected whether to the feeding system or already full of clay to be extruded. The other option is the extruder connected directly to the feeding system. And by adding a little more to this, the internal vessel has to be considered, despite the mechanism selected.

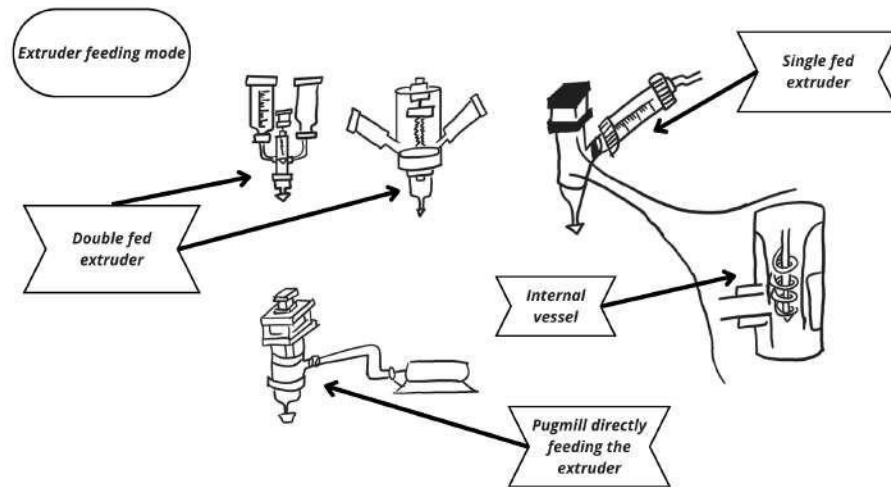


Figure 4.53: Preliminary solutions for the Extruder feeding mode. Source: own

4.4.2 Morphological Matrix

A morphological matrix will help understand how all of the previous solutions approach can be combined into a complete system (Ulrich et al., 2008). This way a more systematic can be taken into how this system is going to look like as a whole. the matrix below (see fig. 4.54) on the first column has all the systems that were identified and have a proposed solution, and also, takes into account some of the sub problems identified in Table 4.7 for a more specific consideration of the system.

Combination 1 fig. 4.55

Combination 2 fig. 4.56

Combination 3 fig. 4.57

Morphological Matrix








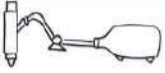

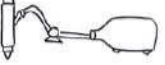





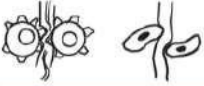




Recycling system			
Storing system			
Pugmill system			
Extrusion pressure	Pressure sensor	Auger chamber geometry	
Consistency on the pugmill	Ventilation and heating system	Humidity levels	Moisture content
CWS			
Control of the continuous workflow system	Motorized valve	Solenoid valve	Pump
Feeding system			
Flow between feeder and extruder	Temperature control	Viscosity control	Pressure control
Extruder shape			
Extruder mechanism			
Temperature control extruder	Heating system	Cooling system	
Nozzle shape			
Flow monitoring	magnetic flow meter	Differential pressure meter	Vortex flow meter

Figure 4.54: Morphological matrix. Source: own

Morphological Matrix

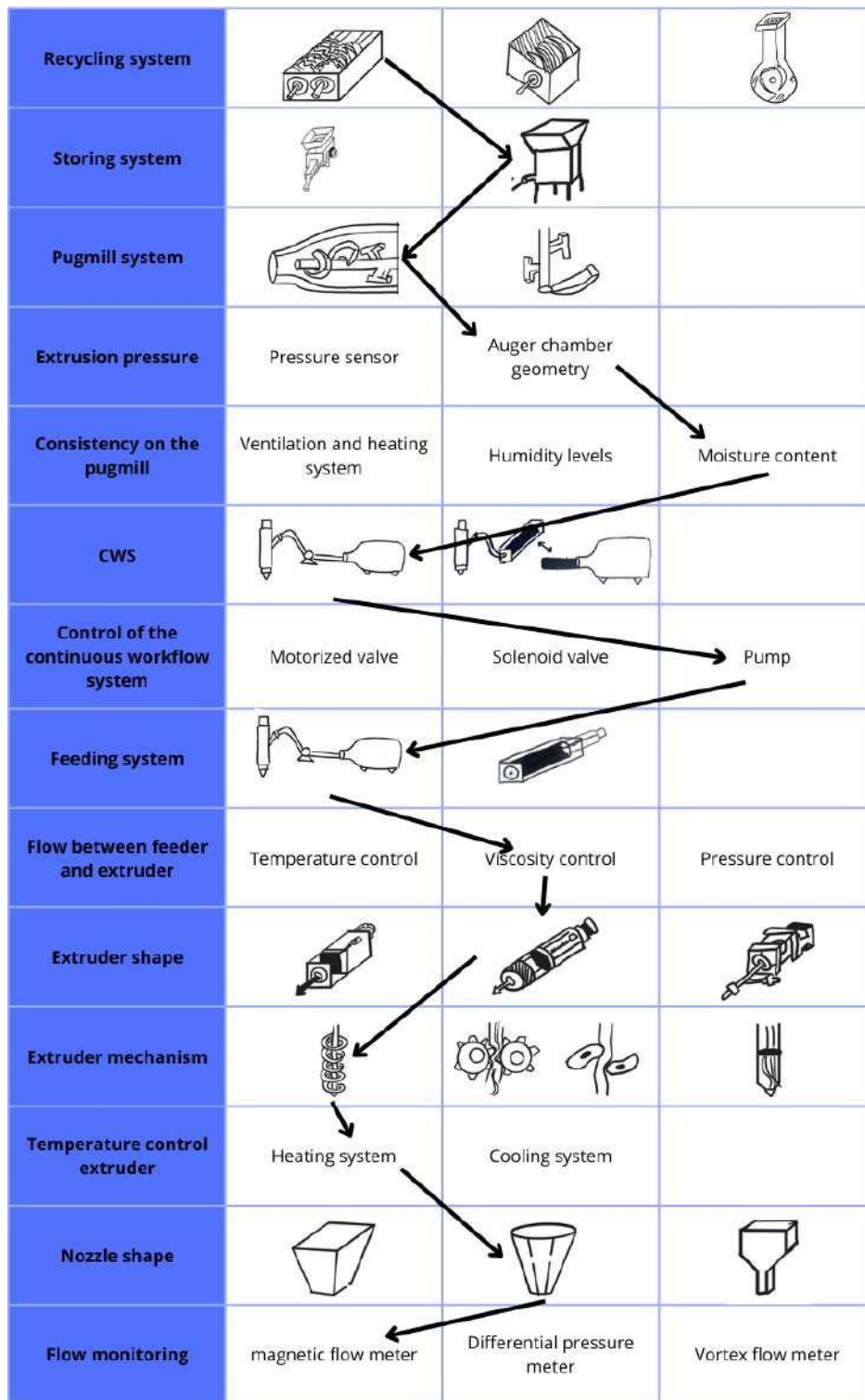


Figure 4.55: Morphological matrix, combination 1. Source: own

Morphological Matrix








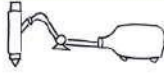

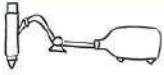





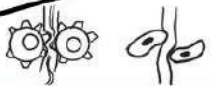




Recycling system			
Storing system			
Pugmill system			
Extrusion pressure	Pressure sensor	Auger chamber geometry	
Consistency on the pugmill	Ventilation and heating system	Humidity levels	Moisture content
CWS			
Control of the continuous workflow system	Motorized valve	Solenoid valve	Pump
Feeding system			
Flow between feeder and extruder	Temperature control	Viscosity control	Pressure control
Extruder shape			
Extruder mechanism			
Temperature control extruder	Heating system	Cooling system	
Nozzle shape			
Flow monitoring	magnetic flow meter	Differential pressure meter	Vortex flow meter

Figure 4.56: Morphological matrix, combination 2. Source: own

Morphological Matrix






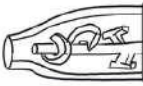



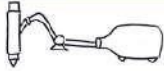





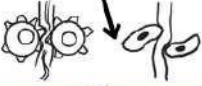




Recycling system			
Storing system			
Pugmill system			
Extrusion pressure	Pressure sensor	Auger chamber geometry	
Consistency on the pugmill	Ventilation and heating system	Humidity levels	Moisture content
CWS			
Control of the continuous workflow system	Motorized valve	Solenoid valve	Pump
Feeding system			
Flow between feeder and extruder	Temperature control	Viscosity control	Pressure control
Extruder shape			
Extruder mechanism			
Temperature control extruder	Heating system	Cooling system	
Nozzle shape			
Flow monitoring	magnetic flow meter	Differential pressure meter	Vortex flow meter

Figure 4.57: Morphological matrix, combination 3. Source: own

The resulting system schematics from the morphological matrix are as shown in fig. 4.58. These are two resulting systems, despite the combinations being three, this is because some of the options that were analyzed were a small part compared to the whole system, nonetheless, they are still being considered for the decision matrices.

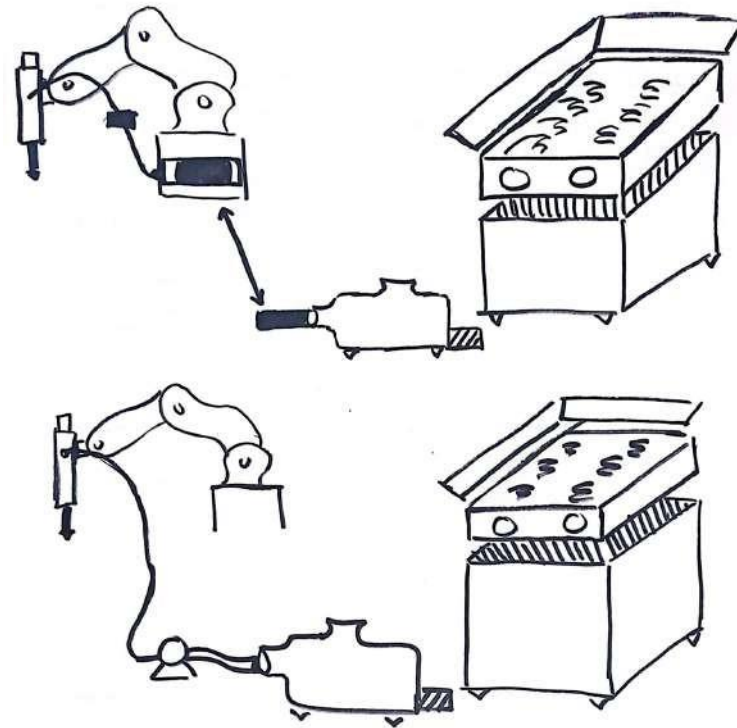


Figure 4.58: Resulting system combinations. Source: own

4.4.3 Evaluation and selection

After making some possible and, of course, logical combinations with the available solutions, it is possible to evaluate them with set design parameters, input them into a decision matrix (Pugh's method (Ullman, 2003)) and weigh the solution so they can be tested in a preliminary design study and then selected for making a detailed design.

The design parameters that will be considered are the following:

- Number of parts

- Cost
- Complexity
- Weight
- Ease of manufacturing
- Material requirement
- Technology availability

The resulting Pugh's chart (see fig. 4.59) evaluated the three proposed systems and according to the parameters that were set, the option that had the highest grade is the one selected for further inspection, however, it is possible that some solutions found on other combinations can be considered if one of the solutions to the sub problems is not suitable or good enough after a detailed design. Some of the more non visible solutions such as electronics, controlling options or internal mechanisms that are not included in the morphological matrix will be evaluated as well in the concepts generation.

	Option 1	Weight	Total	Option 2	Weight	Total	Option 3	Weight	Total
No. of parts	8	0.1	0.8	10	0.1	1	6	0.1	0.6
Cost	8	0.3	2.4	10	0.3	3	6	0.3	1.8
Complexity	10	0.2	2	10	0.2	2	8	0.2	1.6
Weight	9	0.05	0.45	8	0.05	0.4	6	0.05	0.3
Ease of manufacturing	9	0.2	1.8	7	0.2	1.4	5	0.2	1
Material requirement	8	0.05	0.4	8	0.05	0.4	8	0.05	0.4
Technology availability	9	0.1	0.9	10	0.1	1	6	0.1	0.6
Total	-	-	8.75	-	-	9.2	-	-	6.3

Figure 4.59: Pugh's chart. Source: own

4.4.4 Preliminary Solutions Designs

Now that the main problems have a defined suggestion it is necessary to make preliminary concepts so everything is well detailed. In this case, it is not only to propose a system but to clarify what parts could be integrated and also how the unions and mechanisms could be connected with each other. To be more clear, these proposals are going to be called configurations.

Extruder system configurations proposal

The first configuration fig. 4.60 shows a cone shaped nozzle with an endless screw, which will be likely the same through all the concepts, also, there is an internal tube to hold the pressure better and more evenly, the mechanism to attach the lid and nozzle is a screw, which is also in the three concepts, but probably other mechanism will be tested, such as release points or sliders. Depending on the extrusion, the motor might need a gearbox, which is contemplated in the fig. 4.61.

The last test that needs to be run (see fig. 4.62) is the shape of the nozzle, with two possibilities, a cone nozzle, which probably would make extrusion easier, and an abrupt transversal area change nozzle, which would help distribute the pressure more evenly. Lastly, the heating clamp, right at the end of the nozzle, this would favor two things: easing the flow of the clay and generating a sudden temperature change to make the outer weather more aggressive and causing a faster cooling.

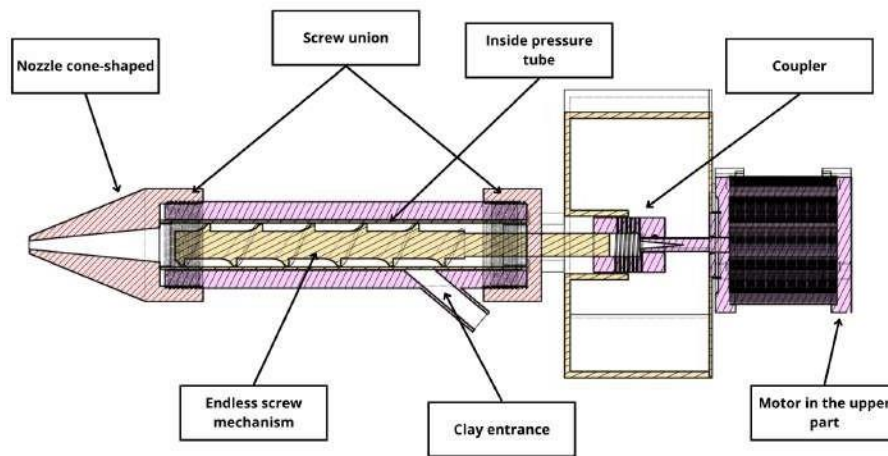


Figure 4.60: Extruder first configuration option. Source: own

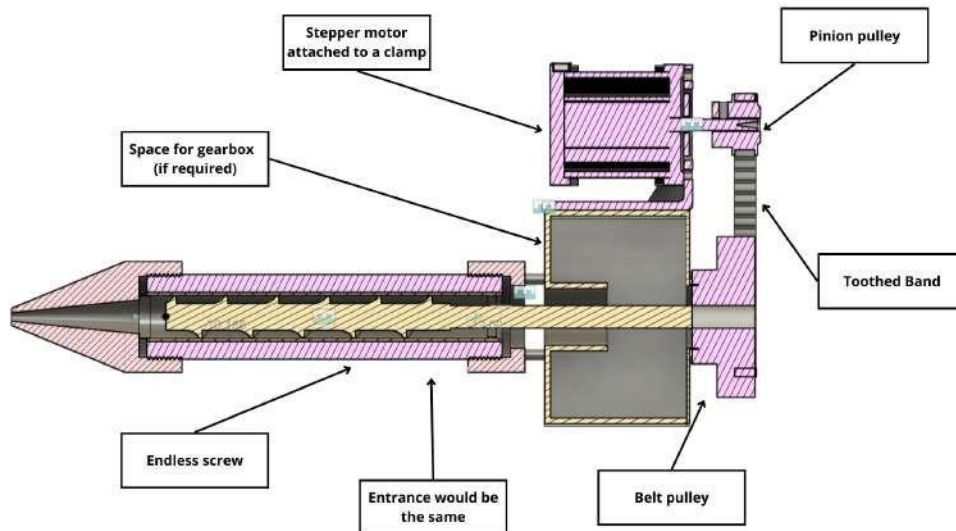


Figure 4.61: Extruder second configuration option. Source: own

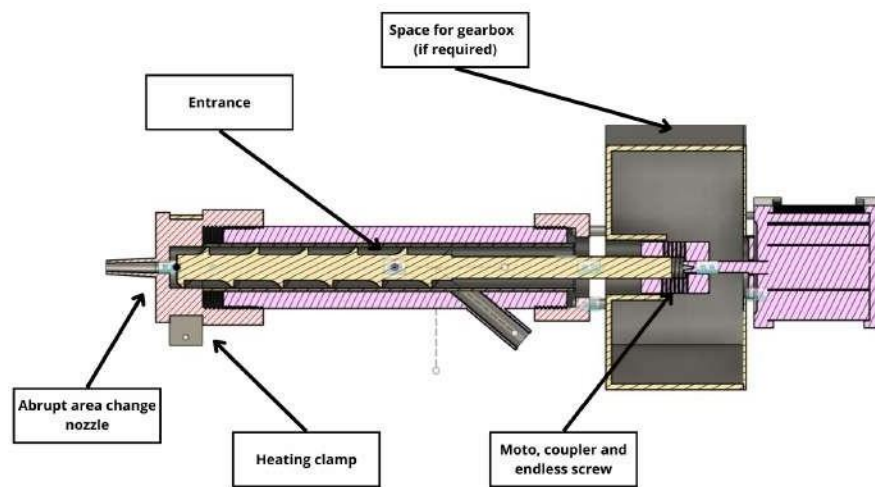


Figure 4.62: Extruder third configuration option. Source: own

Feeding system configurations proposal

After the morphological matrix it was decided that the best way to make this system a continuous one, requires that the feeder would be fixed to some point and have interchangeable cartridges, so that concept really is constant in the next configurations, In fig. 4.63 it is also presented how the system can be continuous, and this is by putting two feeders and controlling which one feeds the extruder with a valve, whether is motorized or a solenoid. The main difference between fig. 4.63 and fig. 4.64 is how the clay is going to be pushed into the pipes, in this case, the first proposal is with compressed air pressure and in the second, with a plunger-like mechanism.

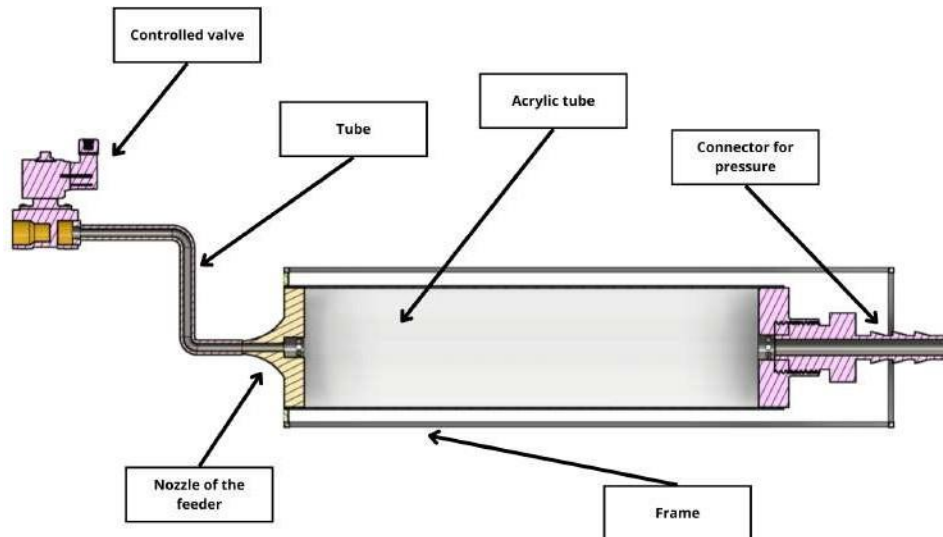


Figure 4.63: Feeder first configuration option. Source: own

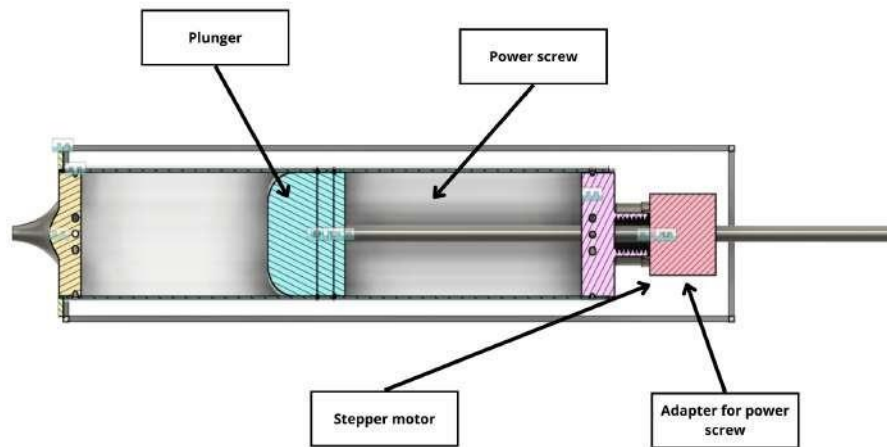


Figure 4.64: Feeder second configuration option. Source: own

Pugmill system configuration proposal

The pugmill is very straight forward, as it can be seen on fig. 4.65, a main container fed in the upper part with clay constantly kneading the clay until it can be extruded into a new cartridge. The only idea that will be tested is the shape of the spiral to be a T instead of a complete spiral to imitate the action of hand actually kneading the clay and eliminating the bubbles. The motor would have an AC motor to have the necessary torque to knead the volume of clay that could go inside the pugmill.

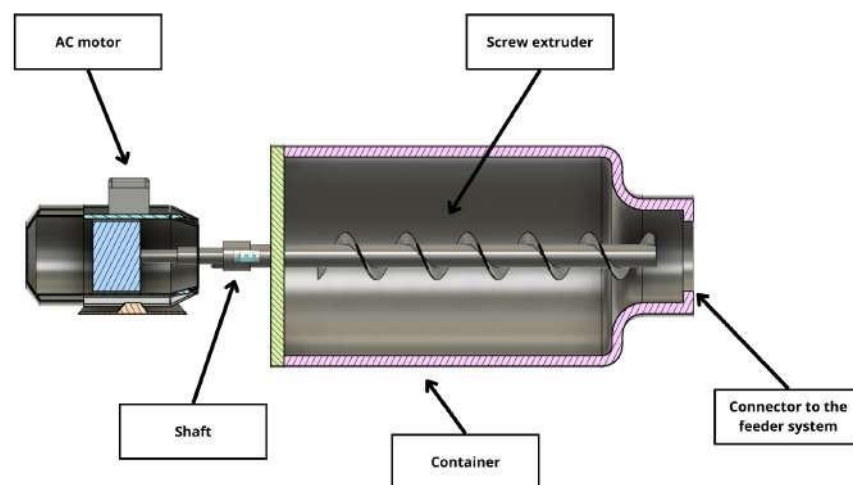


Figure 4.65: Pugmill first configuration option. Source: own

Recycler system configuration proposal

The recycling system is another subsystem design thought with a pretty straight forward solution. Once again, there are a couple of options that are going to be considered, but the general idea and components would only be re arranged for making the second configuration. In fig. 4.66 the system consists of blades with a distance from each other of the same thickness of the blade and also with a twist angle between them. In the first case, there is only one set of blades, the second configuration would be with encountered blades. With a motor to run the system, and below there should be a type of strainer to ensure the size of the pieces that fall to the wet container.

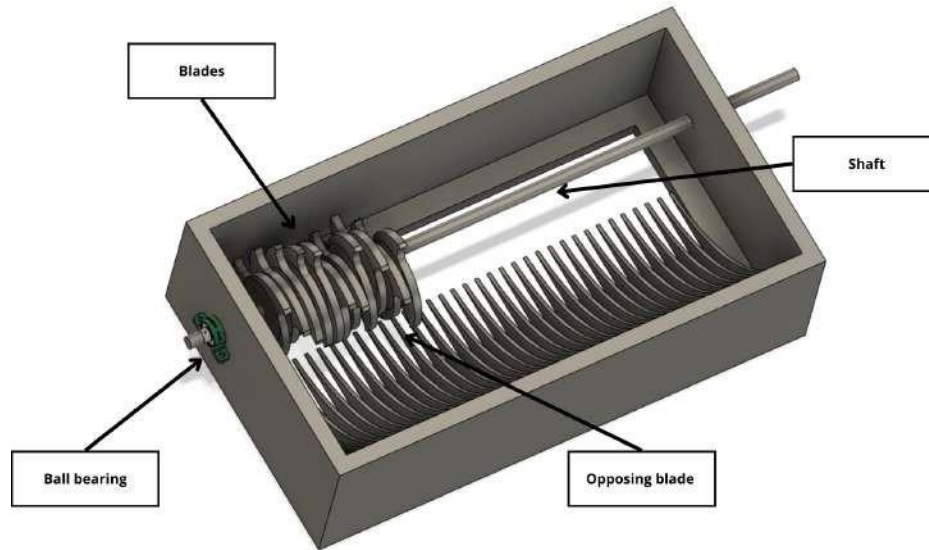


Figure 4.66: Recycler first configuration option. Source: own

4.4.5 Concepts filtration and evaluation

All the configurations generated in the previous sections now will be selected through some evaluation techniques, such as the Pugh's chart that was used in the previous section to select the overall configurations of the whole system, also there will be technological evaluations for the components that are being proposed so availability, complexity and other will be taken into account.

Extruder preliminary design combination

For the extruder, the main question that had to be answered was how the internal mechanism was going to work. The final decision as can be seen on the configurations (fig. 4.60, fig. 4.61 and fig. 4.62) was unanimously to use an endless screw as an extruding mechanism because this would help the possible remaining bubbles to disappear. Almost certainly a gearbox would be necessary, so the second option would cover that space well. A stepper motor would be the best option, it offers easier control of the positions, and since this is exposed as the main option for 3D printers in the market it would be an optimal choice.

Component	Possible combinations							
Gearbox type	Belt pulley		Harmonic or cycloidal drive		Planetary		Arrangement of gears	
Characteristics	<ul style="list-style-type: none"> • Easy to install • Can be bought • Easier to select • Reliable and efficient 	<ul style="list-style-type: none"> • Use of more space • Limited reduction • Additional components 	<ul style="list-style-type: none"> • Better control • More compact • Very efficient • Better reduction ratio • Smooth and silent 	<ul style="list-style-type: none"> • More complex design • More difficult to manufacture 	<ul style="list-style-type: none"> • Compact • Very efficient • Considerable reduction ratio • Efficient 	<ul style="list-style-type: none"> • Complex design • Requires a very precise manufacturing 	<ul style="list-style-type: none"> • Simple to design • Can be arranged to be reducing or increase torque and speed 	<ul style="list-style-type: none"> • Least effective • Loud • Use of more space • Additional components
Continue?	Develop		No		Develop		No	
Nozzle	Cone shape		Sudden area change type					
	<ul style="list-style-type: none"> • Easier flow • Simpler shape 	<ul style="list-style-type: none"> • More complex to pair with the heating clamp • Doesn't offer a consistent pressure 	<ul style="list-style-type: none"> • Easier to pair with the heating clamp • Offers a more consistent extrusion 	<ul style="list-style-type: none"> • More opposition to the flow 				
Continue?	Has to be tested		Has to be tested					
Attachment of the lid and nozzle	Screw		Sliders					
Characteristics	<ul style="list-style-type: none"> • Reliable • Good enclosure against pressure • Simple design 	<ul style="list-style-type: none"> • It can be a weak union depending on the material 	<ul style="list-style-type: none"> • Very secure fit • Easy to insert 	<ul style="list-style-type: none"> • More complex design • Is not as "sealed" • Could have 				
Continue?	Develop		No					

Figure 4.67: Extruder final combination decisions. Source: own

The options for the gearbox could go from a simple belt pulley transmission, a cycloidal or harmonical drive or a system of gears. Another thing to consider is the nozzle shape, which can be conical or have a sudden transversal area change. Also the entrance of clay should be on the side of the container so the least amount of clay gets stuck. The attachment mechanism will also be tested as a screw and some sort of sliders. In fig. 4.67 a final decision matrix of the last details is presented and then the final combinations are presented in the next picture (see fig. 4.68). At last, it was narrowed down to two possible combinations mostly focusing on the two gearboxes and the nozzles that are going to be further tested.

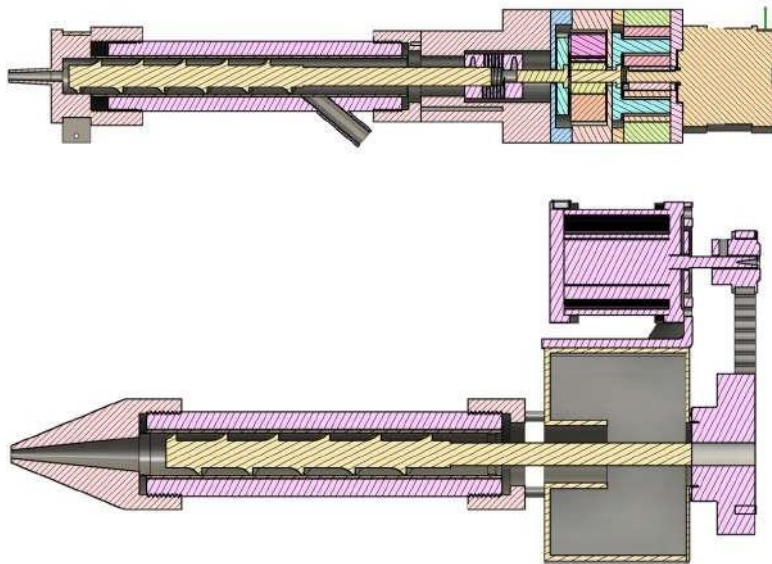


Figure 4.68: Extruder final configurations proposal. Source: own

Feeder and continuous workflow system preliminary design combination

For the feeder and the CWS there are three final decisions that need to be made, one regarding on how to switch between feeders, the other regarding to how the clay is going to be extruded, and also, deciding what has to be the sensor for the clay flow. So the final decision matrix for these components can be seen in the figure below fig. 4.69.

Component	Possible combinations					
Valve	Solenoid			Motorized		
Characteristics	<ul style="list-style-type: none"> • Easy control with Arduino • More precise • More durable 	<ul style="list-style-type: none"> • More expensive • Most are focused for water flow 	<ul style="list-style-type: none"> • Can be made • Cheaper • Easier to control 	<ul style="list-style-type: none"> • Could suffer a little more wear and tear 		
Continue?	No			Develop		
Flow meter	Magnetic			Differential		Ultrasonic
Characteristics	<ul style="list-style-type: none"> • It does not interrupt the flow • Better for control 	<ul style="list-style-type: none"> • Much more expensive • Hard to find one that is not industrial use 	<ul style="list-style-type: none"> • Easier to install • Easy to get • Easy to manufacture 	<ul style="list-style-type: none"> • Interrupts the flow • Hard to put in a smaller pipe 	<ul style="list-style-type: none"> • Very precise • Variants for higher viscosity 	<ul style="list-style-type: none"> • Very industrial type • Expensive • Not made for smaller tubes
Continue?	No			Develop		No
Extrusion mechanism	Plunger			Pressurized air		
Characteristics	<ul style="list-style-type: none"> • Control of the pressure • Easy to install • Requires less equipment 	<ul style="list-style-type: none"> • Involves more parts • There could be a void generation 	<ul style="list-style-type: none"> • Ensures a more consistent 	<ul style="list-style-type: none"> • Limitations on the control • Hard to switch in between feeder • More expensive 		
Continue?	Develop			No		

Figure 4.69: Feeder and CWS final configuration proposal. Source: own

The final configuration of the feeder and Continuous workflow system can be seen in fig. 4.70, and a motorized valve will be used instead of the solenoid one. The motorized valve will be constructed with a servo and controlled by Arduino making it easier to control. And a flow meter must be used, so a differential one is being considered to be the best option. Also, the mechanism that is going to be used is a plunger-like mechanism to ensure the switch between feeders can be done smoothly.

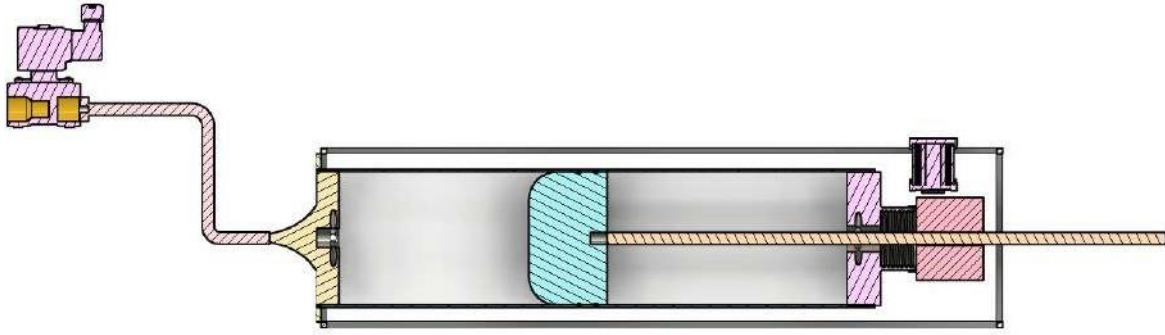


Figure 4.70: Feeder and CWS final configuration. Source: own

Pugmill and recycling system preliminary design combination

The Pugmill and recycling final preliminary configurations are going to be as shown in fig. 4.65 and fig. 4.66, because both systems are already decided on the components and the focus is rather going to be on the detailed design of such components.

4.5 Detailed design

4.5.1 Extruder detailed design

Motor, driver and micro controller selection

The motor selected for this endeavour is a stepper motor. More precisely a Nema 17, this is due to availability, since, the characteristics that this motor offers are great for this specific application. Since a stepper motor is almost the favorite option for applications that are related to numeric control. A stepper motor would offer great precision, since the movement of the shaft is based on small steps, which makes it great to control positioning and precise movement. The next figure shows a drawing of the motor.

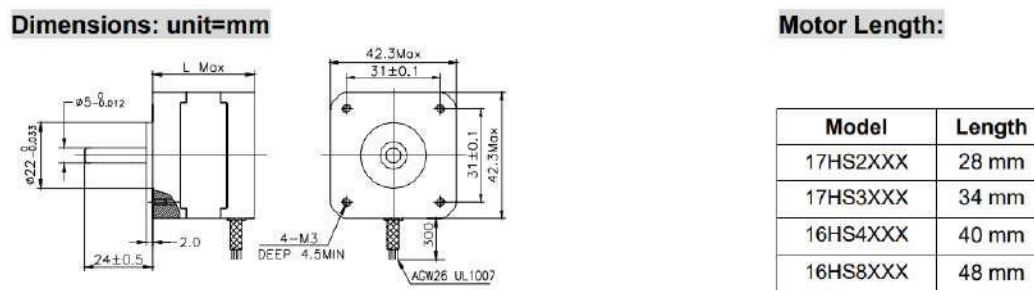


Figure 4.71: Stepper motor scheme. Source (DataSheet4U, n.d.)

And the main characteristics of the motor are presented on Table 4.8.

The torque curve for the motor can be seen in fig. 4.72

For controlling the motor the TB660 4A controller for stepper motors will be used fig. 4.73. This driver ensures a very smooth and easier control of the motor. An the micro controller will be an elegoo 2560 R3 ATmega2560 ATMEGA16U2 which is compatible with Arduino IDE, the reason is because Arduino is a very simple and intuitive system that can help make the coding a lot easier (see fig. 4.74).

Table 4.8: Stepper motor characteristics

Model	17HS4401S
Step	1.8°
Motor length	40 mm
Rated Current	1.7 A
Phase resistance	1.5 Ω
Phase inductance	2.8 mH
Holding torque	40 Ncm
Detent torque	2.2 Ncm
Rotor inertia	54 gcm^2
Lead wires	4
Motor weight	280 g

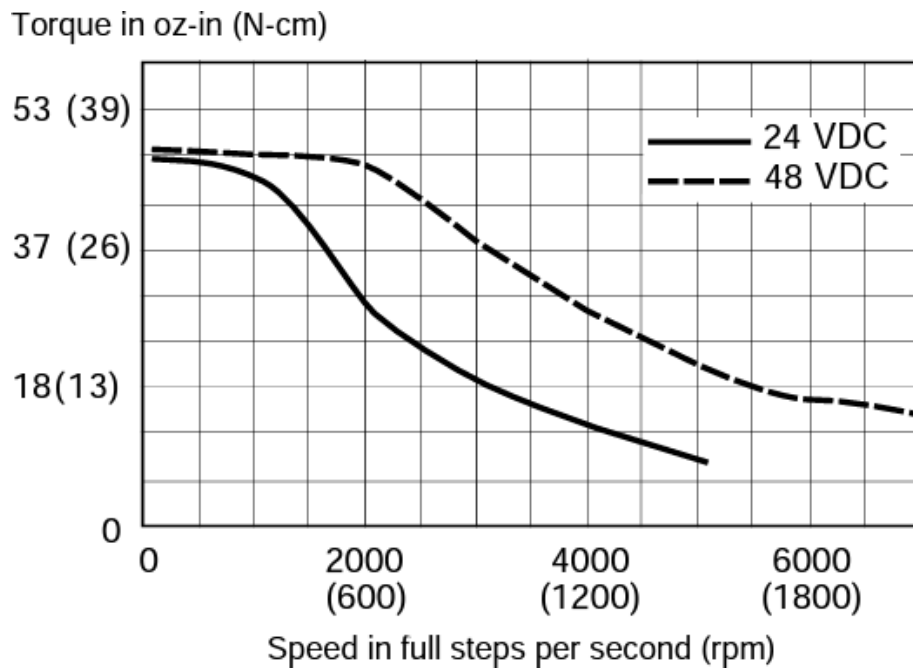


Figure 4.72: Torque curve for the motor nema 17



Figure 4.73: TB660 Driver for controlling stepper motor. Source: <https://articulo.mercadolibre.com.mx/>

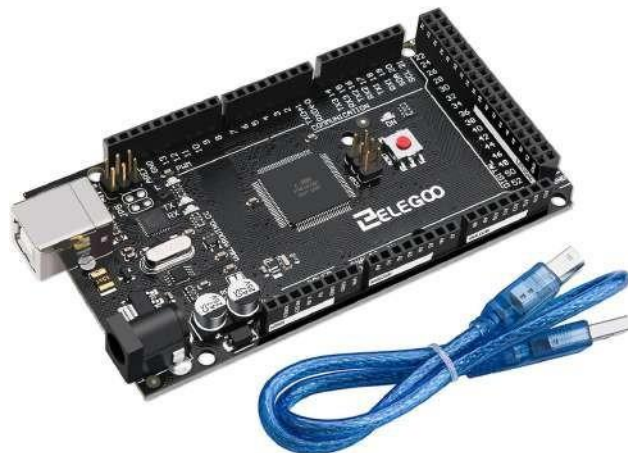


Figure 4.74: elegoo 2560 R3 ATmega2560. Source: <https://www.amazon.com.mx/>

Endless screw design

To design the endless screw first it is needed to set the parameters for which this screw has to work. As it can be seen on fig. 4.75 the design of the screw depends on the diameter of the container, the speed at which it turns, the length of the screw, and more. First, the dimensions and production of the screw will be calculated according to (Parra & Rodrigo, 2017) and the torque required for this screw will be calculated according to (Velilla Díaz et al., 2009).

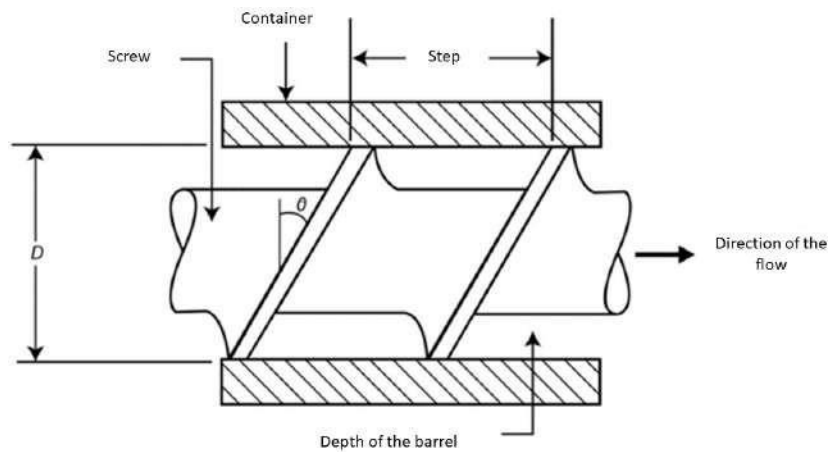


Figure 4.75: Screw parameters. Source: (Parra Rodrigo, 2017)

The initial parameters considered are shown in the following table (see Table 4.9).

Table 4.9: Design parameter for dimensioning the extruder

Parameter	value
Total screw length (L_t)	180 [mm]
Work screw length (L)	120 [mm]
Shaft length (l_s)	24 [mm]
Screw diameter (D)	15 [mm]

The first thing to know is the ratios L/D , which is a very important parameter, because it affects turn speed and the production. There is some typical ratios like 20:1 or 30:1, but these are more suitable for faster extrusions, since this extruder is not going to be necessarily

fast the ratio in 4.2 is acceptable.

$$\frac{L}{D} = \frac{120mm}{15mm} = 8 \quad (4.2)$$

This same relation is correlated to the number of turns for the helix. The compression degree, which is the relation between the feeding and dosage channels. This is found in between 2 and 4, when more pressure is required at the end of the extrusion the recommended number has to be low, for this extruder this number is going to be considered 3.

The screw step is recommended to be calculated with a factor between 0.8 and 1.2, in this case, the chosen factor is 1.

$$t = 1 * D = 1 * 15mm = 15mm \quad (4.3)$$

Thickness of the fillet

$$e = 0.1 * D = 0.1 * 15mm = 1.5mm \quad (4.4)$$

Depth of the feeding channel

$$h_1 = 0.2 * D = 0.2 * 15mm = 3mm \quad (4.5)$$

Depth of the dosage channel

$$h_2 = \frac{h_1}{i} = \frac{3mm}{3} = 1mm \quad (4.6)$$

Soul diameter

$$d = 0.6 * D = 9mm \quad (4.7)$$

Helix angle

$$\varphi = \arctan \frac{t}{\pi * D} = \arctan \frac{15mm}{\pi * 15mm} = 17.65 \quad (4.8)$$

Now, for the work length of the screw, there are three zones that must be calculated, the feeding zone, the measure zone and the compression zone. So (Parra & Rodrigo, 2017) recommends around 40% for the feeding zone, 35% for the measure zone and 25% for the compression zone:

For the length of the feeding zone, the parameter is:

$$L_f = 3.2 * D = 48mm \quad (4.9)$$

The length for the measure zone is:

$$L_f = 2.8 * D = 42mm \quad (4.10)$$

The length for the compression zone is:

$$L_f = 2 * D = 30mm \quad (4.11)$$

For the looseness of the screw and the cylinder or the tube (Parra & Rodrigo, 2017) recommends to use a relation of $0.005 * D$ for screws with small diameters.

$$\delta = 0.005 * D = 0.075mm \quad (4.12)$$

Now that the dimensions are known, the production of the screw can be calculated, understanding by production the flow rate that comes out of the extruder. This flow is composed by three other flows, the drag flow (α) caused by the turning of the screw, the pressure flow (β) which is the opposition flow, and the filtering flow (γ) which represents loss of material, and according to (V́ctor K. Savgorodny, 1978) the equation for the flow rate is as follows:

$$Q = \left(\frac{\alpha * K}{K + \beta + \gamma} \right) * N \quad (4.13)$$

Where,

Q: Unitary flow rate

K: Geometric shape constant of the extrusion nozzle

N: RPM of the screw

Each one of the flows required for equation 4.13 has to be calculated with the adequate parameters of the screw. To obtain the flow α te equation goes as follows.

$$\alpha = \frac{\pi * m * D * h_1 * \left(\frac{t}{m} - e \right) * \cos^2 \varphi}{2} \quad (4.14)$$

Where,

m: Number of channels of the screw

D: screw diameter

h_1 : Depth of the channel in the feeding zone

t: Screw step

e: Fillet thickness

φ : Helix angle

By replacing the known values of the screw:

$$\alpha = \frac{\pi * 1 * 15mm * 3mm * \left(\frac{15mm}{1} - 1.5mm \right) * \cos^2(17.65)}{2} = 866.53mm^3 \quad (4.15)$$

For β is a similar equation:

$$\beta = \frac{m * h^3 * \left(\frac{t}{m} - e \right) * \sin \varphi * \cos^2 \varphi}{12 * L} \quad (4.16)$$

Where,

L: Work length of the screw

Replacing the values:

$$\theta = \frac{1 * 3mm^3 * (\frac{15mm}{1} - 1.5mm) * \sin(17.65) * \cos^2(17.65)}{12 * 120mm} = 0.0232mm^3 \quad (4.17)$$

Finally, for γ the equation is as follows:

$$\gamma = \frac{\pi^3 * D^2 * \delta^3 * \tan\varphi}{10 * e * L} \quad (4.18)$$

Where,

δ : Looseness of the cylinder

Replacing the values:

$$\gamma = \frac{\pi^3 * 15mm^2 * 0.075mm^3 * \tan(17.65)}{10 * 1.5mm * 120mm} = 0.52 \times 10^{-3} mm^3 \quad (4.19)$$

The last thing needed is the constant of the shape for the extruding nozzle, this is going to depend on the geometry (which according to fig. 4.68 is going to be conical) and also depends on the diameter, which for this case, three are going to be computed in the equation 4.20, for 4 mm, for 6 mm and for 8 mm.

The equation for a conical channel goes as follows:

$$K_1 = \frac{3 * \pi * d_i^3 * d_o^3}{128 * L_{canal} * (d_i^2 + d_i * d_o + d_o^2)} \quad (4.20)$$

Where,

d_i : Entrance diameter of the material

d_o : Exit diameter of the material

For the first case of 15 mm and 4 mm

Table 4.10: Final dimensions of the screw

Geometry	Dimension [mm]
Screw diameter	15
Soul diameter	9
Stem diameter	12
Total length	180
Screw work length	120
Stem length	60
Channel's number	1
Fillet's number	8
Step	15
Fillet thickness	1.5
Feeding zone length	48
Compression zone length	42
Measure zone length	30
Depth of the feeding channel	3
Depth of the dosage channel	1

$$K_{4mm} = \frac{3 * \pi * 15mm^3 * 4mm^3}{128 * 35mm * (15mm^2 + 15mm * 4mm + 4mm^2)} = 1.51mm^3 \quad (4.21)$$

And similarly to this computation, for the other diameters the results are:

$$K_{6mm} = 4.37mm^3 \text{ and } K_{8mm} = 8.88mm^3$$

The following figure (see fig. 4.76) illustrates some of the dimensions a little better.

Now it is possible to obtain the flow rate for each nozzle at different RPM speeds, depending on what speed the print is needed this could vary. So, to obtain the flow rate the equation 4.13 has to be multiplied by the density of the material, in this case the clay, and, according to the units that all the flows were calculated, the density has to be transformed.

Considering the wet clay density to be 1.53 g/cm^3

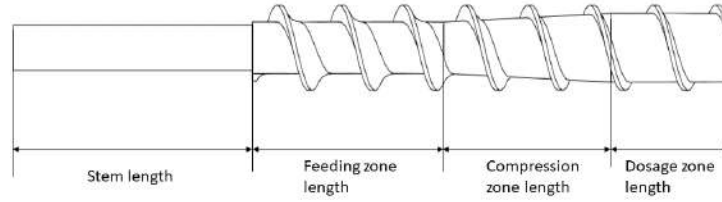


Figure 4.76: Screw extruder zones. Source: own

$$1.53g/cm^3 \left(\frac{1kg}{1000g} \right) \left(\frac{1cm}{10mm} \right)^3 = 1.53 \times 10^{-6} kg/mm^3 \quad (4.22)$$

On the following table different flow rates can be found for different RPM speeds.

Table 4.11: Flow rate for wet clay considering the 4 mm nozzle

RPM	Flow rate [kg/h]
10	0.7834
15	1.175
20	1.57

The same can be found for the other nozzle sizes

Table 4.12: Flow rate for wet clay considering the 6 mm nozzle

RPM	Flow rate [kg/h]
10	0.7912
15	1.19
20	1.582

The values on Table 4.11, Table 4.12 and Table 4.13 will be further tested on the prototype.

Table 4.13: Flow rate for wet clay considering the 8 mm nozzle

RPM	Flow rate [kg/h]
10	0.7934
15	1.19
20	1.587

There are two more calculations that need to be made to consider a good design for the extruder, one is for obtaining the torque and power required (this would be useful to help select a motor, but in this case, since there is already one selected because is the one available, would be necessary to determine if a gearbox is necessary to reach this specifications) and then, the pressures that the extruder experiments to select an adequate material.

The pressure calculation is based on the equation proposed by (Morton-Jones, 1989) which takes into consideration the maximum pressure occurring on the extruder. This happens when the screw has no movement. The equation goes as follows:

$$P_{max} = \frac{6 * \pi * D * L * \eta * \mu}{h^2 * \tan\varphi} \quad (4.23)$$

Where,

D: screw diameter

L: screw length

η : screw revolutions

μ : effective viscosity

h: dosage channel depth

φ : Helix angle

The effective viscosity must be determined (which will come in handy later) in terms of the shear rate. This shear rate depends on the geometric form of the screw and the channel by the following equation:

$$\epsilon = \frac{\pi * D * N}{\delta} \quad (4.24)$$

Where,

N: Screw speed at rps

δ : The screw looseness

The shear rate turns out to be:

$$\epsilon = \frac{\pi * 15mm * 0.166rps}{0.075mm} = 104.711/s \quad (4.25)$$

According to (Menchavez, Adavan, & Calgas, 2014) who investigates rheological properties of different clay slurries in terms of the shear rate, the viscosity is greatly affected by the rate. In fig. 4.77, and according to the value that was obtained in 4.25 the apparent viscosity for this calculation will be considered of 1.4 Pa-s. This probably will be the best approximation since is a study for ceramic slurries. So the maximum pressure will be:

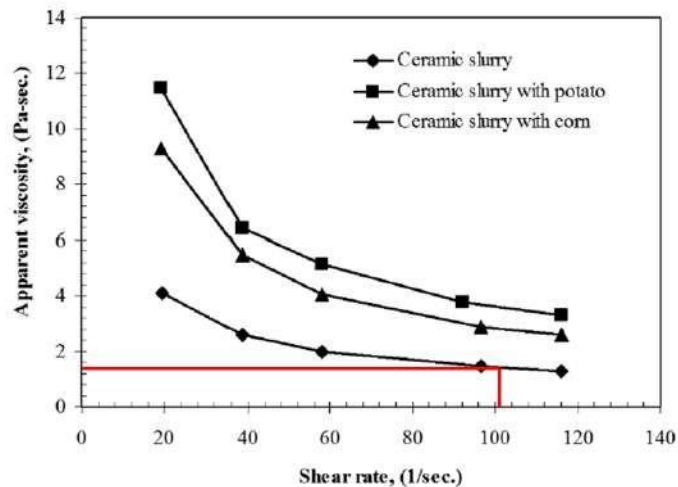


Figure 4.77: Apparent viscosity vs Shear rate. Source: (Menchavez et al., 2014)

$$P_{max} = \frac{6 * \pi * 0.015m * 0.12 * 0.1666rps * 1.4Pa - s}{0.001m^2 * \tan(17.65)} = 25.141kPa \quad (4.26)$$

To calculate the torque, there is a proposal in (V́ctor K. Savgorodny, 1978), however, this proposal is only good for polymers. So this calculation will be based on (Velilla D́az et al., 2009) who makes an approach based on the Navier-Stokes equations to obtain this

parameter (see the Appendix to see the full deduction of the equations used).

Radial component:

$$\rho \frac{\partial v_r}{\partial t} + v_r \frac{\partial v_r}{\partial r} + \frac{v_\theta}{r} \frac{\partial v_r}{\partial \theta} - \frac{v_\theta^2}{r} + v_z \frac{\partial v_r}{\partial z} = -\frac{\partial p}{\partial r} + \rho g_r$$

$$+ \mu \frac{\partial}{\partial r} \left(\frac{1}{r} \frac{\partial}{\partial r} r v_r \right) + \frac{1}{r^2} \frac{\partial^2 v_r}{\partial \theta^2} - \frac{2}{r^2} \frac{\partial v_\theta}{\partial \theta} + \frac{\partial^2 v_r}{\partial z^2} \quad (4.27)$$

Angular component:

$$\rho \frac{\partial v_\theta}{\partial t} + v_r \frac{\partial v_\theta}{\partial r} + \frac{v_\theta}{r} \frac{\partial v_\theta}{\partial \theta} - \frac{v_r v_\theta}{r} + v_z \frac{\partial v_\theta}{\partial z} = -\frac{1}{r} \frac{\partial p}{\partial \theta} + \rho g_\theta$$

$$+ \mu \frac{\partial}{\partial r} \left(\frac{1}{r} \frac{\partial}{\partial r} r v_\theta \right) + \frac{1}{r^2} \frac{\partial^2 v_\theta}{\partial \theta^2} - \frac{2}{r^2} \frac{\partial v_r}{\partial \theta} + \frac{\partial^2 v_\theta}{\partial z^2} \quad (4.28)$$

Axial component:

$$\rho \frac{\partial v_z}{\partial t} + v_r \frac{\partial v_z}{\partial r} + \frac{v_\theta}{r} \frac{\partial v_z}{\partial \theta} + v_z \frac{\partial v_z}{\partial z} = -\frac{\partial p}{\partial z} + \rho g_z$$

$$+ \mu \frac{1}{r} \frac{\partial}{\partial r} \left(r \frac{\partial v_z}{\partial r} \right) + \frac{1}{r^2} \frac{\partial^2 v_z}{\partial \theta^2} + \frac{\partial^2 v_z}{\partial z^2} \quad (4.29)$$

The flow regime that is going to be used is shown in the figure below.

Because of the complicated mathematics these equations represent, some assumptions are going to be made to make the problem much simpler.

1. Stable state

2. Laminar flow

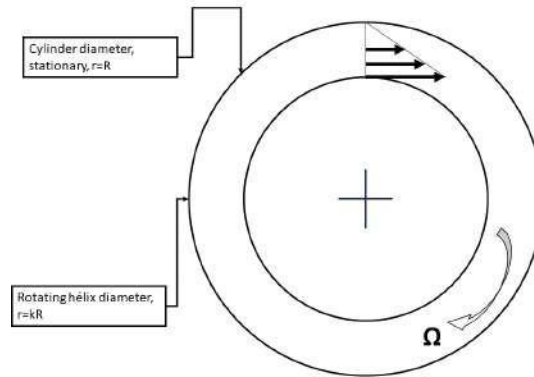


Figure 4.78: Scheme of the flow in the extruder. Source: own

3. Non compressible fluid

4. Newtonian fluid

5. Continuous system

6. Hydrodynamic flow

After making an order of magnitude analysis to eliminate partial derivatives that are not significant, the equations that are left are the following:

For the radial component

$$-\rho \frac{v^2}{r} = -\frac{\partial p}{\partial r} \quad (4.30)$$

For the angular component

$$\mu \frac{\partial}{\partial r} \left(\frac{1}{r} \frac{\partial}{\partial r} r v \right) \quad (4.31)$$

And for the axial component

$$-\frac{\partial p}{\partial z} + \mu \frac{1}{r} \frac{\partial}{\partial r} \left(r \frac{\partial v_z}{\partial r} \right) = 0 \quad (4.32)$$

To obtain the torque and power needed the selected equation to expand is the equation resulting from the angular component. To solve this, it is needed to use a method to solve the differential equation for the velocity, resulting on the following:

$$v_{\vartheta} = \Omega_{\vartheta} k R \frac{r}{kR - \frac{R}{k}} - \frac{R^2}{rkR - \frac{Rr}{k}} \quad \text{!} \quad (4.33)$$

With this equation, considering a Bingham type of flow and the law for Newtonian fluids, the shear stress can be obtained:

$$\tau_{r\vartheta} = -\mu \Omega_{\vartheta} k \frac{3R^2}{r^2 k - \frac{r^2}{k}} + \tau_0 \quad (4.34)$$

Having the behavior of the shear stress the force can be calculated as well to obtain the required motor torque. The force differential is the same as:

$$dF = \tau_{r\vartheta} dA_{contacto} \quad (4.35)$$

So what's needed is to calculate the differential for the contact area, since there is no clear contact area, the best course of action would be to calculate the contact surface. The following image illustrates this in a better way

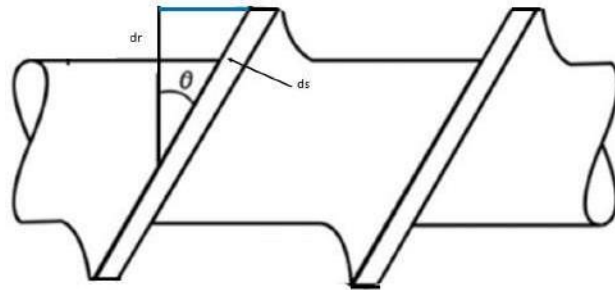


Figure 4.79: Differential surface area for the screw. Source: own

Since the total area is the sum of the total helices, the area differential must contemplate

the number of helices and both faces of each helix, as follows:

$$dA = 2n2\pi r ds \quad (4.36)$$

According to fig. 9.3 ds can be calculated as the projection of the radial differential, which would be:

$$ds = \frac{dr}{\cos\vartheta} \quad (4.37)$$

Now replacing dr on the original dA

$$dA = \frac{4n\pi r - r_{axis} dr}{\cos\vartheta} \quad (4.38)$$

Replacing dA on dF, the following is obtained:

$$dF = - \mu\Omega\vartheta k \frac{3R^2 - r^2}{r^2 k - \frac{r^2}{k}} + \tau_0 \frac{4n\pi r - r_{axis} dr}{\cos\vartheta} \quad (4.39)$$

The maximum shear stress is on r=R, so the resulting equation would be:

$$dF = - \frac{\mu\Omega\vartheta 3k}{k - \frac{1}{k}} + \tau_0 \frac{4n\pi r - r_{axis} dr}{\cos\vartheta} \quad (4.40)$$

All left to do is integrate to obtain the force

$$F = - \frac{\mu\Omega\vartheta 3k}{k - \frac{1}{k}} + \tau_0 \frac{4n\pi(\frac{R^2}{2} - r_{axis} r)|_{r=R}}{\cos\vartheta} \quad (4.41)$$

Now replacing r for the value of the maximum shear stress

$$F = - \frac{\mu\Omega\vartheta 3k}{k - \frac{1}{k}} + \tau_0 \frac{4n\pi(\frac{R^2}{2} - r_{axis} R)}{\cos\vartheta} \quad (4.42)$$

Now the required torque for the motor can be calculated by multiplying the helix radius.

$$T = F * r_{helix} = - \frac{\mu \Omega \vartheta 3k}{k - \frac{1}{k}} + \tau_0 \frac{4n\pi(\frac{R^2}{2} - r_{axis}R)}{\cos\vartheta} r_{helix} \quad (4.43)$$

Now, all the parameters are set to calculate the torque required for this particular case. Although, there are two values that are still unknown, the viscosity and the shear stress, the problem is that these values will vary according to the type of clay, the content of clay particles, moisture and other factors, making it really hard to really have an exact value. So, for the value of the clay viscosity, the best course of actions is to consider a slurry, rather than clay itself, this is because of the form clay is going to adopt when flowing through the system.

For the value of the viscosity, the value used in 4.26 of 1.4 Pa-s will be considered as it is the best approximation for ceramic clay slurries. As for the yield stress of clay, the value will be estimated by what (XianJun, Ying, WenHao, XiaoKang, & Peng, 2022) proposes and can be found on the following figure (see fig. 4.80) which illustrates a value of around 5000 Pa for a 40% solid slurry, considering that is the initial yield stress, then it can be considered as 100 Pa-s to keep units consistent.

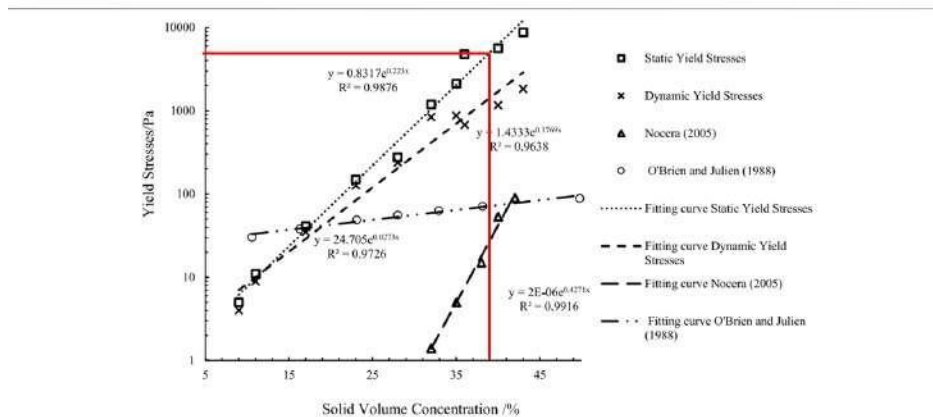


Figure 4.80: Initial yield stress according to solid concentration. Source: (XianJun et al., 2022)

Finally the table of values results in: (see Table 4.14)

Table 4.14: Values used to calculate torque

Parameter	Value
Rotational speed	0.1666 1/s
Initial shear stress	5000 Pa-s
Screw diameter	0.015 m
Cylinder diameter	0.01515 m
k	0.995
Viscosity	1.4 Pa-s
Number of helices	8
Axis radius	0.009 m
Helix angle	17.65°

$$T = - \frac{1.4Pa * s(0.16661/s)(3 * 0.995)}{0.995 - \frac{1}{0.995}} + 5000Pa * s$$

$$\frac{4 * 8\pi(\frac{0.015075m^2}{2} - 0.009m * 0.015075m)}{\cos(17.65)} * 0.015m = 0.172Nm(4.44)$$

Which in this case is a value that the motor can handle without any problem. A gearbox to increment its speed can even be considered to control better the flow of the clay.

Material selection for the extruder

Since this is a relatively low hydro static stress, and the maximum pressure of 25.141 kPa does not reach the yield stress of any metal or hard polymer, really a selection of material would be unnecessary, So, the material for the extruder could be any metal, but for testing it, PLA would be good enough since the yield stress is around 42 MPa (*Overview of materials for polyactic acid (PLA)*, n.d.), which is still way above the value of maximum pressure.

Nozzle design

The operation pressure on the nozzle also depends on the geometry of the nozzle, the revolutions and the effective viscosity. Since this is the point where the clay really has to go through a smaller diameter, the shear rate and viscosity must be calculated as well for each diameter of the nozzles. Almost the same way that the shear rate was calculated (V́ctor

K. Savgorodny, 1978) proposes an equation to calculate the shear rate for a conical nozzle.

$$V_c = \frac{32 * Q}{\pi * d^3} \quad (4.45)$$

Where,

Q: Production flow in it volumetric form (mm^3/s)

d: diameter of the nozzle

$$V_c = \frac{32 * 142.18mm^3/s}{\pi * 4mm^3} = 22.631/s \quad (4.46)$$

Similarly for the other two diameters

$$V_{c@6mm} = 6.77 \text{ and } V_{c@8mm} = 2.86$$

Now, the pressure will be calculated basing this on the more critical case, or, rather the case with the highest apparent viscosity which will be for the case of the 8mm nozzle. Extrapolating the graph of fig. 4.77, the resulting is around 10 Pa-s. So, the equation proposed by (Morton-Jones, 1989) results:

$$P_{op} = \frac{2 * \pi * \mu * D^2 * \eta * h * \text{sen}\varphi * \text{cos}\varphi}{\left(\frac{R^4}{2 * L_{nozzle}}\right) + \left(\frac{D * h^3 * \text{sen}^2\varphi}{2 * L_p}\right)} \quad (4.47)$$

Where,

D: screw diameter

η : screw revolutions per second

μ : Effective viscosity

h: Channel depth on the dosage zone

φ : Helix angle

R: nozzle radius

L_{nozzle} : Length of the nozzle

L_p : Work length of the extruder

So the operation pressure results as.

$$P_{op} = \frac{2 * \pi * 10Pas * 0.015m^2 * 0.166rps * 0.001m * \text{sen}(17.65) * \text{cos}(17.65)}{\left(\frac{0.004m^4}{2*0.018m}\right) + \left(\frac{0.015m*0.001m^3*\text{sen}^2(17.65)}{2*0.120m}\right)} = 6.37kPa \quad (4.48)$$

So to dimension the nozzle the only calculation left is to obtain the minimum thickness the walls must have to withstand the pressure. The critical case is at the entrance of the nozzle, which is around 15.15 mm, and the proposed equation is:

$$e_{min} = \frac{P_{op} * r}{\sigma_{adm}} \quad (4.49)$$

Where,

P: Pressure of operation

r: Nozzle entrance radius

σ_{adm} : admissible stress for the material

$$e_{min} = \frac{6.37kPa * 0.007575m}{42Mpa} = 1.15 \times 10^{-6}m \quad (4.50)$$

Which is 0.00115 mm, leaving the design with a big safety factor considering even a millimeter.

Cylinder design

For the cylinder final dimensions, the diameter is going to be 15.15, since the looseness is 0.075 mm. Now, since the prototype will be built with PVC, it will experiment a greater pressure as shown on the figure below. So, the only important thing is if that kind of tube will hold the pressure. if PVC holds well, then many materials will hold for a final.

The stress inside the tube can be found using the equation (Popov Egor, 1989).

$$\sigma = \frac{P * r_i}{t} \quad (4.51)$$

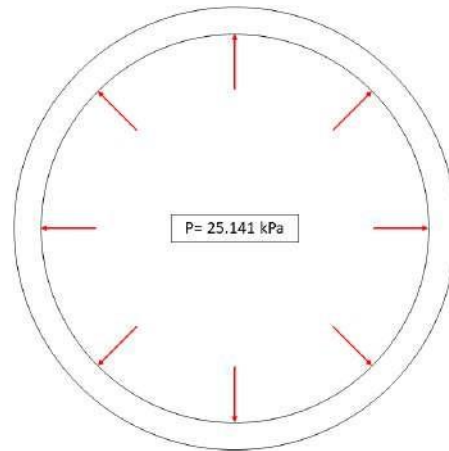


Figure 4.81: Internal pressure on the tube

Given the characteristics of the tube, the result of this stress will be:

$$\sigma = \frac{25.141kPa * 0.005m}{0.003m} = 41.901kPa \quad (4.52)$$

Considering that the tensile strength is 90 Mpa, the tube will hold well to the maximum pressure.

4.5.2 Feeder detailed design

Plunger design

Since the feeder will work, not through a screw extruder but rather a plunger style extruder, in this case probably the pressure will be more inside the tube and it will be harder to move along the clay. For this, a Hagen-Poiseuille type of flow will be considered to calculate the movement of the fluid. Consider a flow with a parabolic velocity profile depending on the radius of the pipe, a laminar flow and the flow is fully developed through the pipe (see fig. 4.82).

To solve, the equations of Navier-Stokes and the equations of motion for a cylindrical flow will be used (White, 1990). Consider the z-momentum equation:

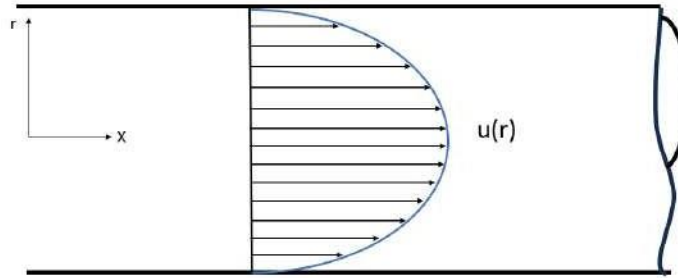


Figure 4.82: Fully developed flow on the feeder. Source: own

$$\frac{\partial v_z}{\partial t} + (\vec{v} \cdot \nabla)v_z = -\frac{1}{\rho} \frac{\partial p}{\partial z} + g_z + \nu \nabla^2 v_z \quad (4.53)$$

This equation reduces to 4.53 given the conditions of a fully developed laminar pipe flow.

$$\rho v_z \frac{\partial v_z}{\partial z} = -\frac{dp}{dz} + \frac{\mu}{r} \frac{d}{dr} \left(r \frac{dv_z}{dr} \right) \quad (4.54)$$

The term of convective acceleration vanishes since according to the equation of continuity, the change of velocity in z is zero.

$$\frac{\mu}{r} \frac{d}{dr} \left(r \frac{dv_z}{dr} \right) = \frac{dp}{dz} = \text{constant} \quad (4.55)$$

After solving the differential equation and considering the boundary conditions the solution for the velocity yields:

$$v_z = -\left(-\frac{dp}{dz}\right) \frac{1}{4\mu} (R^2 - r^2) \quad (4.56)$$

To solve this problem is necessary to know the flow in the pipe. Since this is easier to determine than the velocity of the fluid. Following the definition of flow rate

Table 4.15: Parameters of the feeders

Parameter	Value
Length	450 mm
Diameter	46.5 mm
Flow rate	1 kg/h (slightly above the necessary for the 4mm nozzle)
Viscosity	100000 Pa-s ((Velilla Díaz et al., 2009))

$$Q = \int v_z dA \quad (4.57)$$

After integrating equation 4.57 the result is:

$$Q = \frac{\pi R^4 \Delta p}{8 \mu L} \quad (4.58)$$

Now, setting some parameters and defining the flow rate needed for the clay, the pressure that needs to be input can be calculates, to calculate the necessary force to get the clay through the tubes into the extruder.

Now it is possible to get the pressure difference from 4.58

$$\Delta p = \frac{8 Q \mu L}{\pi R^4} \quad (4.59)$$

First, converting the flow rate to m^3/s :

$$Q = 1 \text{ kg/hr} \left(\frac{1 \text{ hr}}{3600 \text{ s}} \right) \left(\frac{1 \text{ m}^3}{1530 \text{ kg}} \right) = 1.82 \times 10^{-7} \text{ m}^3/\text{s} \quad (4.60)$$

Replacing with the parameters on Table 4.15 in the equation above the pressure difference we get is

$$\Delta p = \frac{8(1.82 \times 10^{-7} \text{ m}^3/\text{s})(100000 \text{ Pa} - \text{s})(0.45 \text{ m})}{\pi(0.02325 \text{ m})^4} = 79.30 \text{ kPa} \quad (4.61)$$

The force required to move the clay through the tube results from the definition of



Figure 4.83: Lead screw used for the feeder

Table 4.16: Lead Screw parameters

Parameter	Value
Length	300 mm
Thread pitch	2 mm
Lead of thread	8 mm
Angle of thread	14.5°
Type of shape	Trapezoidal
Material	Stainless steel

pressure:

$$F = PA \quad (4.62)$$

The area of the feeding tube is $A=0.001698 \text{ m}^2$, so the resulting force is:

$$F = 79.30 \text{ kPa} * 0.0017 \text{ m}^2 = 134.67 \text{ N} \quad (4.63)$$

Since a lead screw will be used to push the clay, it is a good idea to obtain the parameters of the lead screw that is going to be used:

The characteristics of the screw are shown in the Table 4.16.

To know the torque input for the required load the following equation can be used (Moore, 2023):

$$T_{req} = \frac{\sin\vartheta + \mu_k * \cos\vartheta}{\cos\vartheta - \mu_k * \sin\vartheta} * F_{load} * r_{screw} \quad (4.64)$$

Considering a friction coefficient of 0.15 between lubricated steels. The input torque for the required torque should be:

$$T_{req} = \frac{\sin(14.5) + 0.15 * \cos(14.5)}{\cos(14.5) - 0.15 * \sin(14.5)} * 134.67N * 0.008m = 0.458Nm \quad (4.65)$$

Which for the motor, a reduction of 15:1 will be more than enough. That reduction is more or less a value that has worked for other extruders. The viscosity was considered of about 100,000 Pa-s; it is higher value than before, but since this is considering the clay is not moving and also, getting a certain safety factor so the gearbox is enough for any kind of clay.

Design of the gearbox

Since the gearbox has to change the axis from the shaft of the motor to the direction of the power screw, there are two main options, right angle bevel gears, but, since the goal is to achieve a 30:1 reduction ratio, it would be very complex to fit such a gear drive inside an adequate space for the motor adapter. So, the better choice would be a worm gear type of gear box. Then again, the parameters of the motor considered are the ones on Table 4.8.

The geometry for a worm gear gearbox are as shown in the figure below (see fig. 4.84):

The main relation on a worm gear gearbox according to (Norton, Sánchez, Correa, Alvarado, & González, 2020) is:

$$P_x = \frac{L}{N_w} = p_c = \frac{\pi d_g}{N_g} \quad (4.66)$$

Considering an output of 20 RPM, the RPM of the motor according to fig. 4.72 must be 300 RPM and the approximate output torque of 30 Ncm. This will be an output of 450 Ncm

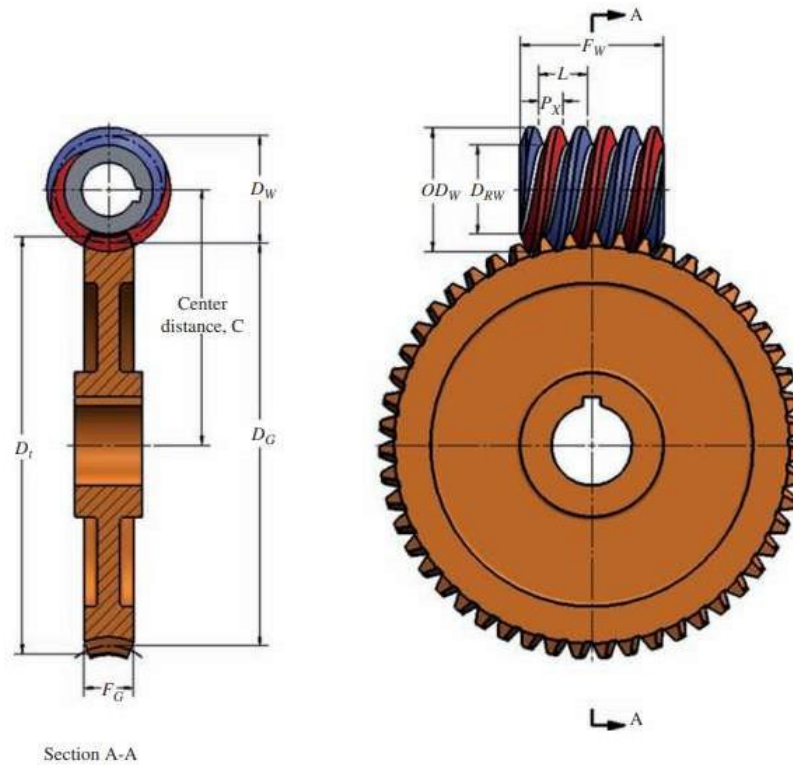


Figure 4.84: Worm gear geometry. Source. (Mott, 2004)

at 10 RPM and a power that can be seen on the next equation:

$$P = \frac{T * 2 * \pi * RPM}{60} = \frac{0.458Nm * 2 * \pi * 20}{60} = 0.959W \quad (4.67)$$

Space requirements ask for the main gear not to be greater than 60 mm. The number of teeth will be 30, since the reduction ratio is required to be 15:1, considering a double threaded worm.

The diametral pitch is:

$$P_d = \frac{30}{60mm} = 0.5[1/mm] \quad (4.68)$$

The circular pitch would result:

$$p = \frac{\pi}{0.5[1/mm]} = 6.2832mm \quad (4.69)$$

The distance between centers must be greater than 30 mm, so probably consider a distance of 37.5 mm, which would give the worm a diameter of 15 mm approximately.

The minimum worm diameter is given by:

$$D_w = \frac{C^{0.875}}{3} = 7.95mm \quad (4.70)$$

The maximum worm diameter is:

$$D_w = \frac{C^{0.875}}{1.6} = 14.9mm \quad (4.71)$$

A diameter in between would be the better answer, so the proposed worm diameter is 12 mm. This would make the distance between centers of:

$$C = \frac{(D_x + D_g)}{2} = 36mm \quad (4.72)$$

The worm outside diameter would be:

$$D_{ow} = D_w + 2a = 12mm + 2 * (1/0.5) = 16mm \quad (4.73)$$

The whole depth

$$h_t = \frac{2.157}{P_d} = 4.314mm \quad (4.74)$$

The face width for the gear would be:

$$F_g = \sqrt{D_{ow}^2 - D_w^2} = 10.58mm \quad (4.75)$$

The final face width will be specified in 11 mm. The addendum is:

$$a = \frac{1}{P_d} = \frac{1}{0.5} = 2mm \quad (4.76)$$

The throat diameter of the gear

$$D_t = D_g + 2a = 60 + (2 * 2mm) = 64mm \quad (4.77)$$

The recommended minimum face length of the worm:

$$F_w = 2 \sqrt{\left(\frac{D_t}{2}\right)^2 - \left(\frac{D_g}{2} - a\right)^2} = 30.98mm \quad (4.78)$$

The face length of the worm stays specified at 32 mm. For the testing the worm gear gearbox will be made out of 3D printed PLA, but, for the actual fabrication, the fabrication proposal will rather have a selected gearbox.

Design of the motorized valve

The motorized valve that is used to switch between feeders will be an array of a servo motor opening a sphere valve. For this, the only thing that is going to be important is if the motor is going to be capable of making the valve move. The available servo motor that will be used is the MG-995 Tower Pro Hi-Speed (see fig. 4.85); its characteristics are presented following:



Figure 4.85: Servo motor MG-995 Tower Pro Hi-Speed

The drawing of the servo motor is the following (see fig. 4.86).

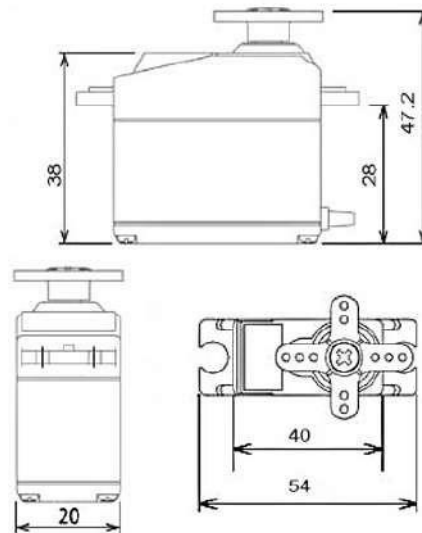


Figure 4.86: Servo motor MG-995 Tower Pro Hi-Speed

The specifications of the motor are show in section 4.5.2

Table 4.17: Specifications of the servo motor

Specification	Value
Weight	55 g
Dimensions	40.7 x 19.7 x 42.9 mm
Stall torque (4.8 V)	8.5 kgfcm
Stall torque (6 V)	10 kgfcm
Operating speed (4.8 V)	0.2s/60°
Operating speed (6 v)	0.16s/60°
Operating voltage	4.8 V a 7.2 V

The valve used is an Mueller spherical valve (see fig. 4.87), a 1/4" and a 1/2" will be considered, in case a change of hose is required due to the clay that is being used.

Since the motor reaches almost 10 kgfcm at a full current, and it takes approximately 5-7 kgfcm to close the valve (depending on the distance of the lever).



Figure 4.87: Mueller spherical valve. Source: <https://www.homedepot.com.mx>

4.5.3 Recycling system detailed design

For the recycling system a shredder-like system will be considered. The main scope is clay that has already been dried or fired, and so, because the recycling process of clay, requires dried clay in pieces, considering that whole structures will be recycled or at least compact structures will, it is necessary to accomplish certain size of piece to make a slurry again.

Motor selection and design of the cutting blades

Ceramics could vary in terms of tensile strength, and a lot, approximately from 0.69 MPa and up to 7000 MPa (Muñoz & Cuadros Bedoya, 2019). To set the tensile stress value, a need to set clay strength values is essential. Depending on the clay this values can be very different, but for this particular case the value will be set after clay bricks, since this product is probably the most common clay product produced in the world,

The study of (Afanador García, Guerrero Gómez, & Monroy Sepúlveda, 2012) goes through several tests for finding a bending resistance for clay bricks (see fig. 4.88). They go from 0.4 MPa up to 1.6 MPa, this is very likely to be the kind of stress the clay will be facing, but, in the study of (Muñoz & Cuadros Bedoya, 2019) they find material with a tensile strength up to 90 MPa, for this case, depends a lot on the clay used, but for this shredder, 15 MPa will be the set value to design the blades.



Figure 4.88: Bending strength study. Source: (Afanador García et al., 2012)

Also, another consideration that was made in the preliminary design and configurations proposals, is that, this shredder will be single shaft, this is with the objective of using less moving parts and having better direction of the scraps.

To define what is the minimum force that the blade needs to cut at, first a preliminary geometry has to be proposed, so, the figure below illustrates a proposed geometry. The diameter is 170 mm to cover for big pieces, its width is 8 mm. To obtain the area that the blade touches the ceramic, the projected area of the curvature of the blade is consider as a rectangle with the area of the width and approximately 35 mm of height.

To obtain the force that the blade has to put into the ceramic, the definition of stress is used:

$$F = \sigma_{obj}(A_{contact}) = 15\text{MPa} * 0.008\text{m} * 0.035\text{m} = 1800\text{N} \quad (4.79)$$

Now, since this is the minimum force, the torque required for the motor can be estimated as it follows:

$$T = F * \frac{d}{2} = 1800 * \frac{0.17\text{m}}{2} = 153\text{Nm} \quad (4.80)$$

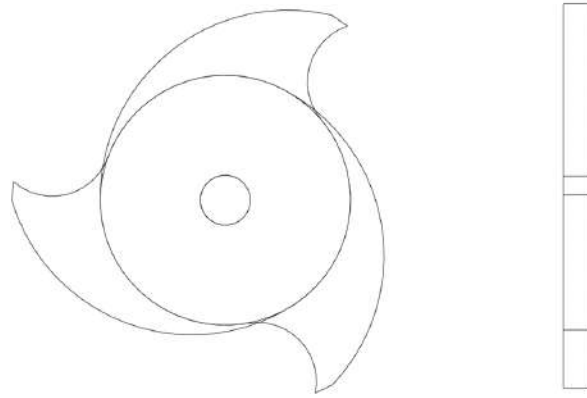


Figure 4.89: Blade geometry proposal. Source: own

To find a motor now the power required is calculated. For this, the capacity of the shredder must be determined. By capacity, this is how much quantity is going to be processed while working. So, for this, the size of this shredder is proposed to be around 30 cm by 40 cm, at least on the shredding area. So, assuming the scraps of clay are going to fall into a container of the same area and since this container has to be primarily water, the quantity can be estimated.

The height of the container is set at 20 cm, because the total volume would be around 24 liters. So, assuming a 65% water to 35% clay content, the available volume for clay would be 8.4 liters and given the density that has been considered, the approximate mass of clay for a full container is:

$$m_c = 0.0084m^3 * 1530kg/m^3 = 12.85kg \quad (4.81)$$

For each work cycle, the shredder should be capable of recycling up to 13 kg of clay. Given the assumption that the product is being recycled are bricks, and, assuming also these bricks have been 3D printing and improved in weight characteristics, they weight around 1.5 kg with the standard dimensions of a normal brick. So the machine would have to crush around 9 bricks for each cycle and it needs roughly 4 revolutions to bring a normal sized

brick into the desired size of the scraps, the total number of revolutions per cycle must be:

$$Revs = 4revs * 9 = 36Revs \quad (4.82)$$

Now, the operation time is expected to happen in around 15 seconds, so the revolutions per second are:

$$RPS = \frac{36Revs}{15s} = 2.4rps \quad (4.83)$$

So the angular velocity results:

$$\omega = 2\pi * RPS = 15.08rad/s \quad (4.84)$$

And the power the motor must have is:

$$P = T\omega = 152Nm * 15.08rad/s = 2.29kW \quad (4.85)$$

For selecting the motor, comparisons must be made. The search was mainly on three phase motors since the power requirement is somewhat high. The comparison can be found on the following image (see fig. 4.90):

The motor chosen is the WEG motor, since it meets the power requirement of at least 2.3 kW, but the nominal torque of the motor is not enough to cover the torque necessity, so design a gearbox is necessary. The ratio comes from the comparison of velocities.

The characteristics of the motor are shown in Table 4.18.

Design of the gearbox

$$RedutionRatio = \frac{3525RPM}{904.8RPM} = 3.89 \approx 4 : 1 \quad (4.86)$$

Which is a very reasonable gearbox ratio. Since this ratio is small enough (less than 10 according to (Mott, 2004)), the teeth ratio can be calculated. Considering the pinion number

Comparison of motors

Model	Company	Power	Torque	RPM
Multimontaje IE3 4 HP- 2P 100L 3F 230/460/380-415 V 60 Hz IC411 - TEFC - B3L(E)	WEG	3 kW (4 HP)	8.1 Nm	3525 RPM
5HP Electric Motor Three Phase 1480/1770 RPM,184T Frame,1-1/8Shaft Diameter CW/CCW Cast Iron Shell Air Compressor 50/60 HZ	Amazon	(3.68 kW) 5 HP	-	1770 RPM
Three-phase induction motors of two poles	Neri motors	3 kW (4 HP)	10.20 Nm	2800 RPM
CEBM3615T	ABB	3.68 kW (5 HP)	42.71 Nm	1800 RPM
IE2 - Aluminium Series	CR Motors	3.7 kW	-	2880 RPM

Figure 4.90: Motor comparison

of teeth at 12, which is the minimum that a pinion can have.

$$Gear\ teeth = Pinion\ teeth * Reduction\ Ratio = 12 * 4 = 48[teeth] \quad (4.87)$$

Calculating the geometries for both gears. The chosen pressure angle is 20° since it is very standard. First the diametral pitch is set to 0.2. Then the circular pitch is calculated by ((Norton et al., 2020) and (Mott, 2004)):



Figure 4.91: WEG motor. Source: <https://www.weg.net/catalog>

Table 4.18: Motor specifications

Specification	Value
Frecuency	60 Hz
Power	3 kW (4 HP)
Nominal speed	3525 RPM
Nominal voltage	230 V/460 V
Nominal current	10.4/5.19 A
Nominal torque	8.1 Nm (5.96 lbft)

$$p_c = \frac{\pi}{p_d} = 15.71mm \quad (4.88)$$

The base pitch is calculated as follows:

$$p_b = p_c \cos\phi = 15.71mm * \cos(20) = 14.76 \quad (4.89)$$

The diameters for both the pinion and the gear are:

$$D_p = \frac{N_p}{p_d} = \frac{12}{0.2} = 60mm; D_g = \frac{N_g}{p_d} = \frac{48}{0.2} = 240mm \quad (4.90)$$

The distance between centers is the sum of both pitch radius.

$$C = r_p + r_g = 30mm + 120mm = 150mm \quad (4.91)$$

The addendum and dedendum are obtained

$$a = \frac{2.54}{0.2} = 12.7mm; b = \frac{3.175}{0.2} = 15.875mm \quad (4.92)$$

The total depth is the sum of the addendum and dedendum

$$h_t = a + b = 12.7mm + 15.875mm = 28.575mm \quad (4.93)$$

The looseness is the difference between the dedendum and the addendum:

$$c = b - a = 15.875mm - 12.7mm = 3.175mm \quad (4.94)$$

The exterior diameter of both gears is the is the pitch diameter plus two time the addendum:

$$D_{op} = 60mm + 2 * (12.7mm) = 85.4mm \quad (4.95)$$

The exterior diameter of the gear

$$D_{og} = 240\text{mm} + 2 * (15.875\text{mm}) = 271.75\text{mm} \quad (4.96)$$

The torque over the pinion is the following:

$$T_p = \frac{P}{\omega_p} = \frac{3\text{kW}}{369.14\text{rad/s}} = 8.127\text{Nm} \quad (4.97)$$

And the output torque is:

$$T_g = m_g T_p = 4 * 8.127\text{Nm} = 32.508\text{Nm} \quad (4.98)$$

The transmitted load is equal for all of the gears. It is calculated as the ratio of the torque and the pitch diameter of that gear.

$$W_t = \frac{T_g}{d_p/2} = \frac{32.508\text{Nm}}{0.24\text{m}/2} = 270.9\text{N} \quad (4.99)$$

The radial component is:

$$W_r = W_t * \tan\phi = 270.9\text{N} * \tan(20) = 98.6\text{N} \quad (4.100)$$

And the total load is:

$$W = \frac{W_t}{\cos\phi} = \frac{270.9\text{N}}{\cos(20)} = 288.3\text{N} \quad (4.101)$$

Finally the loads over a single teeth, of both the pinion or gear are:

$$W_{t\text{alternative}} = \frac{W_t}{2} = 135.45\text{N} \quad (4.102)$$

The material picked for the gears is bronze, which is common material for gears. It will be further analysed through finite element on the chapter of the fabrication proposal (see

Chapter 6).

Design of the shaft

To design the shaft a combined stress has to be considered, both a bending stress due to the blades weight and a torsion stress due to the motor torque, according to the norm ANSI B106.IM-1985 the equation that contemplates this is defined as follows:

$$D = \frac{32N}{\pi} \sqrt[3]{\frac{K_f M}{s'_n} + \frac{3}{4} \left[\frac{T}{t S_y} \right]^2} \quad (4.103)$$

Where,

N: safety factor

K_f : Concentration factor due to fatigue stress

M: Bending moment of the shaft

s'_n : Fatigue strength

T: Torque around the shaft

S_y : Ultimate material strength

K_f ; Stress factor due to torsion fatigue

A common characteristic of shafts is that the process used to manufacture them is milling, so, considering that, a natural choice of material is some kind of carbon steel. So, a steel AISI 4340 is chosen to be the material, as seen on the following table:

Table 4.19: Properties of AISI 4340 steel. Source. <https://matweb.com/>

Density	7.85 g/cm ³
Ultimate Tensile strength	1282 MPa
Yield Tensile strength	862 MPa
Young's modulus	200 GPa
Poisson's ratio	0.29
Shear modulus	78 GPa
Brinell hardness	363

Since the ultimate tensile strength is less than 1.4 GPa (Mott, 2004) then the fatigue strength approximates to:

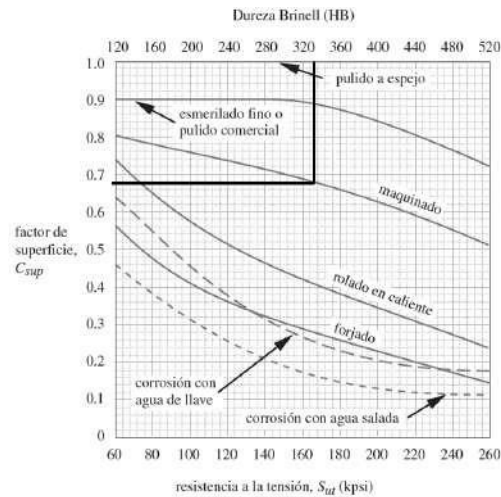


Figure 4.92: Correcting factor for surface. Source: (Norton et al., 2020)

$$S_n = 0.5S_{ut} = 0.5 * 1282MPa = 641MPa \quad (4.104)$$

Considering the correction factors as follows:

$C_{load} = 1$: Combined load

$C_{Temperature} = 1$: Work temperature below 400 °C

$C_{Surface} = 0.68$: According to the process considered (see fig. 4.92).

$C_{reliability} = 0.702$: Considering a reliability of 99.99

$C_{size} = 0.8125$: Considering the diameter 2 in maximum

The final fatigue strength corrected is:

$$s'_n = 284.62MPa \quad (4.105)$$

To obtain the stress concentration factor due to bending consider the equation:

$$K_f = 1 + q(K_t - 1) \quad (4.106)$$

Where:

K_t : Stress concentration factor due to torsion.

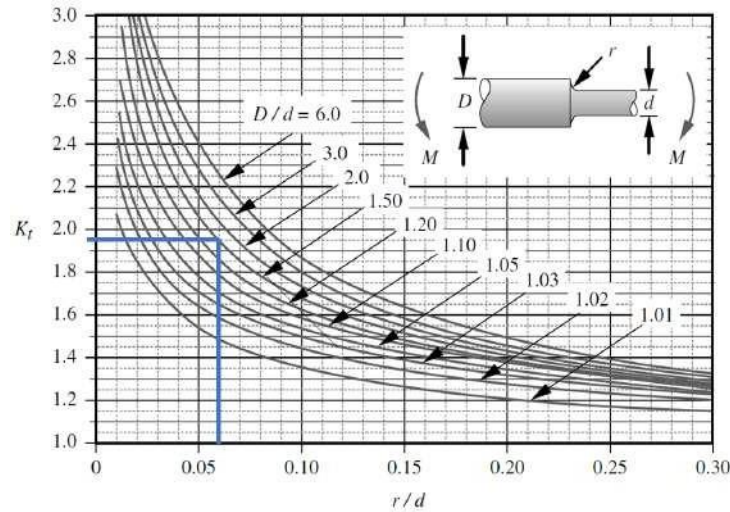


Figure 4.93: Concentration factor due to bending stress. Source: (Norton et al., 2020)

q : indent sensitivity

Indent sensitivity is calculated according to the following equation

$$q = \frac{1}{1 + \sqrt{\frac{a}{r}}} \quad (4.107)$$

Where,

\sqrt{a} : Neuber constant for steel

r : radius of the indent, considered at 2 mm

Replacing the values:

$$q = \frac{1}{1 + \frac{0.031}{\sqrt{0.0787in}}} \approx 0.9 \quad (4.108)$$

To obtain the concentration factor K_t the graph down below was used (see fig. 4.93):

The value of K_t was determined at 1.95 considering a 2 in main diameter and a 1.33 in sub diameter, to obtain a ration of 1.5.

Te value of the concentration factor K_f due to fatigue results:

$$K_f = 1 + 0.9(1.95 - 1) = 1.855 \quad (4.109)$$

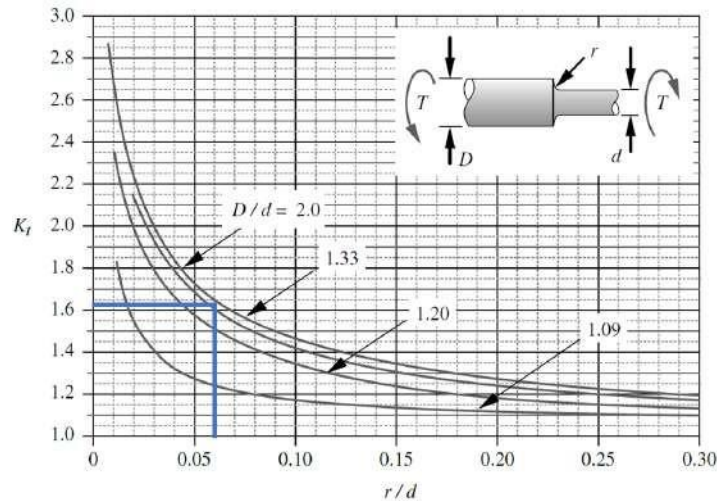


Figure 4.94: Concentration factor due to torsion stress. Source: (Norton et al., 2020)

A similar process is used to obtain the concentration factor due to torsion (see fig. 4.94).

Getting a geometric factor K_t of approximately 1.64.

Calculating the fatigue concentration factor due to torsion stress:

$$K_T = 1 + 0.9(1.64 - 1) = 1.576 \quad (4.110)$$

Calculating the torque over the shaft:

$$T = \frac{3kW}{94.6666rad/s} = 31.7Nm \quad (4.111)$$

Now to obtain the bending moment on the shaft, the weight of the blades is very important. The weight was obtained with Fusion 360 and using the material proposed (see fig. 4.95).

Considering the width of 8 mm, the 400 mm length of the long part of the shredder and also that every blade will be spaced by a piece of 12 mm, there are going to be around 20 blades on the shaft, and according to fig. 4.95 the blade is around 2.2 kg, so the shaft will have to support 44 kg.

The weight of the blade would result:

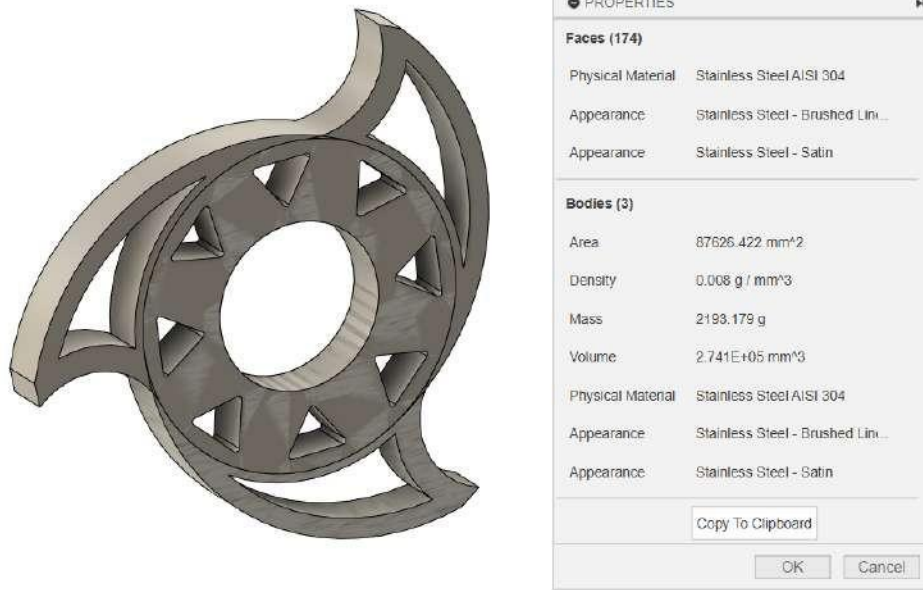


Figure 4.95: Physical properties of the blade. Source: own

$$W_b = m * g = 2.2kg * 9.8m/s^2 = 21.56N \quad (4.112)$$

To obtain the shear force and bending moment of the shaft, the shaft is going to be analyzed as if it were a beam with two supports with an evenly distributed load of 1078 Nm (the total weight of the blades). The analysis can be seen on fig. 4.96.

Finally, the values on the equation for the shaft diameter can be found:

$$D = \frac{32(3)}{\pi} \sqrt[3]{\left[\frac{1.855 * 8.624Nm}{284.62MPa}\right]^2 + \frac{3}{4} \left[\frac{1.576 * 31.7Nm}{862MPa}\right]^2} = 0.0132m \quad (4.113)$$

So the minimum diameter for the shaft is 13.2 mm, considering a shaft diameter of 17 mm to be able to put wedges and other indents (these were considered of about 2 mm). This way the shaft can be better manufactured.

Bearings selection

According to fig. 4.96 the reaction forces in the bearings, both A and B would be the

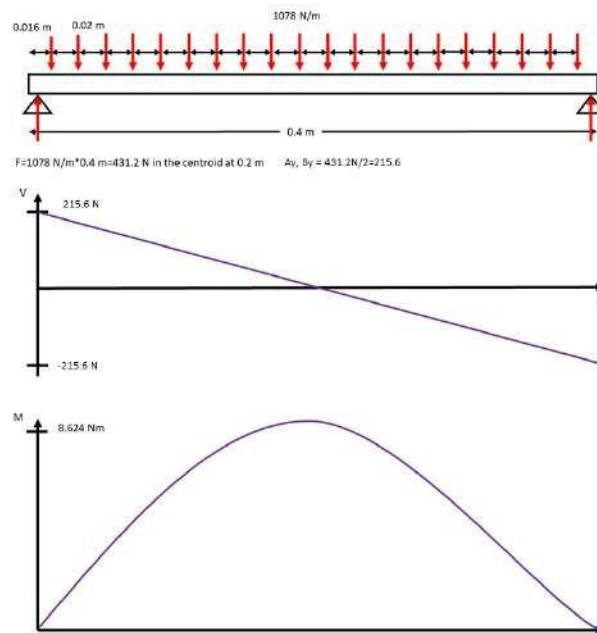


Figure 4.96: Analysis for the distributed load on the shaft. Source: own

same, 215.6 N, or 0.215 kN. Since the inside of the bearing is the radial load is the same to consider. The next step is to calculate the basic dynamic loading, so for this, 10^6 revolutions will be consider for this:

$$C = P_d \frac{L_d}{10^6}^{\frac{1}{k}} \quad (4.114)$$

According to the next figure (see fig. 4.97) the number of hours will be selected in agreement to the type of machine. Since this is for an electric motor the recommended hours are between 20000 and 30000, taking the middle point, the considered hours would be 25000.

To consider this selected life in revolutions:

$$L_d = (25000hr)(36RPM)\left(\frac{60min}{1hr}\right) = 54 \times 10^6 revs \quad (4.115)$$

Application	Design life L_{10} , h
Domestic appliances, instruments, medical apparatus	1000–2000
Aircraft engines	1000–4000
Automotive	1500–5000
Agricultural equipment, hoists, construction machines	3000–6000
Elevators, industrial fans, multipurpose gearing, rotary crushers, cranes	8000–15 000
Electric motors, industrial blowers, general industrial machines, conveyors	20 000–30 000
Pumps and compressors, textile machinery, rolling mill drives	40 000–60 000
Critical equipment in continuous, 24-h operation; power plants, ship drives	100 000–200 000

Figure 4.97: Recommended design life for bearings. Source: (Mott, 2004)

Taking $k=3$ since the selection is to have a ball bearing for equation eq. (4.114):

$$C = (215N) \frac{54 \times 10^6 \text{ revs}}{10^6}^{1/3} = 812.65N \quad (4.116)$$

According to the fig. 4.98, the 6000 bearing would be more than enough to accomplish the required conditions, the basic dynamic load is 4.62 kN, almost 6 times the minimum load calculate in eq. (4.116).

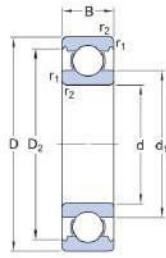
Bearing number	Nominal bearing dimensions						Basic load ratings				Maximum fillet radius r_{fillet}^1		Minimum shaft shoulder diameter, S		Maximum housing shoulder diameter, H		Bearing mass	
	Bore, d		Outside dia., D		Width, B		Static, C_0		Dynamic, C		mm	in	mm	in	mm	in	kg	lb _m
	mm	in	mm	in	mm	in	kN	lb _f	kN	lb _f								
6000	10	0.3937	26	1.0236	8	0.3150	1.96	441	4.62	1039	0.3	0.012	12	0.472	24	0.945	0.019	0.042
6200	10	0.3937	30	1.1811	9	0.3543	2.36	531	5.07	1140	0.6	0.024	14	0.551	26	1.024	0.032	0.071
6300	10	0.3937	35	1.3780	11	0.4331	3.06	687	6.40	1430	0.6	0.024	14	0.551	31	1.220	0.053	0.117

Figure 4.98: Single row ball bearings dimensions and specifications. Source: (Mott, 2004)

Now, selecting the bearing of the same series in SKF (*SKF*, n.d.), the inner and outer dimensions are the same, and the basic dynamic load is a bit more: 4.75 kN. The dimensions can be seen on the next figure (see fig. 4.99):

Design of the cutting blades

For the cutting blades, the only thing needed to design them are the dimension, which are set to fill size requirements and the material. This will be analysed in the Chapter 6, for the fabrication proposal. The material proposed is a stainless steel AISI 304L, this is a very common stainless steel and due to the abrasiveness of the material is a very good choice,



Dimensions

d	10 mm	Bore diameter
D	26 mm	Outside diameter
B	8 mm	Width
d ₁	≈ 14.8 mm	Shoulder diameter
D ₂	≈ 22.6 mm	Recess diameter
r _{1,2}	min. 0.3 mm	Chamfer dimension

Figure 4.99: Dimensions drawing for SKF bearing 6000 series. Source: (Mott, 2004)

besides, its yield strength is way below the necessary stress to crush the bricks.

4.5.4 Pug mill detailed design

A clay pug mill is widely used to mix and knead clay into the desired consistency, they can work as warmers, re-claimers and most of all, they can de-air the clay, which is one of the most important characteristics this system has to have for the clay to be considered ready to extrude, mostly because air bubbles in the process of firing can cause explosions or seriously affect the homogeneity of the print.

Since for this kind of system there is almost no information on how this product is designed, a selection can be considered, if the system meets the requirements shown on Table 4.20, if none of this commercial systems meet the complete specification then, design a pug mill could be considered an option.

Table 4.20: Parameters to select the pugmill

Size	Less than a cubic meter
Capacity	Around 13 kg
Size of the auger chamber	120 mm
Deairing pump	Yes
Desired screw	Kneading/extruding

Options

1. Peter pugger VPM-9 Vacuum power wedger (*Peter pugger*, n.d.)

2. Venco de-airing pug mill (*PUG MILLS* — *venco*, n.d.)

3. NIDEC NVS07 (*NVS-07*, 2019)

Peter pugger VPM-9 Vacuum power wedger



Figure 4.100: Peter pugger pug mill

- Batch capacity: 25 lb (11.34 kg)
- Dimensions: 91.44 cm x 35.56 cm x 35.56 cm
- Weight: 67.585 kg
- Material. Aluminum
- Hopper size: 13.35 cm x 13.35 cm
- Pug size: 7.62 cm
- Vacuum pump: 1/2 HP pump

This pug mill accomplished almost every characteristic, the only one that would probably be a problem is the pug size, since the extrusions are cylinders of around 7.62 cm, while the cartridge designed is 12 cm.

VENCO De-airing pug mill

- Batch capacity: Non specified



Figure 4.101: VENCO De airing pug mill

- Dimensions: 685 x 508 x 558 mm
- Weight: 40 kg
- Material. Stainless steel
- Pug size: 7.5 cm or 10 cm
- Vacuum pump: 1/2 HP pump

This is also a good option, the only thing is that the batch capacity is not specified, but it has a bigger pug to extrude cylinders.

NIDEC NVS07

- Batch capacity: 18.144 kg
- Dimensions: 88.9 cm x 43.18 cm x 83.82 cm
- Weight: 140.61 kg
- Hopper size: 21.59 cm x 29.21 cm
- Material. Stainless steel



Figure 4.102: NIDEC NVS07 pug mill

- Pug size: 8.89 cm
- Vacuum pump: yes (capacity non specified)

In terms of capability is a very good choice, the problem is that it would take a lot of space and is very heavy, and the pug is also not big enough.

So for the purposes of this project, the best option is probably to go with the Peter Puger since it is very similar to the pug mill proposed on the preliminary design, and make a modification to the pug so it can handle the bigger size of the feeder tube. To see the inside of the pug mill see the following image (see fig. 4.103)

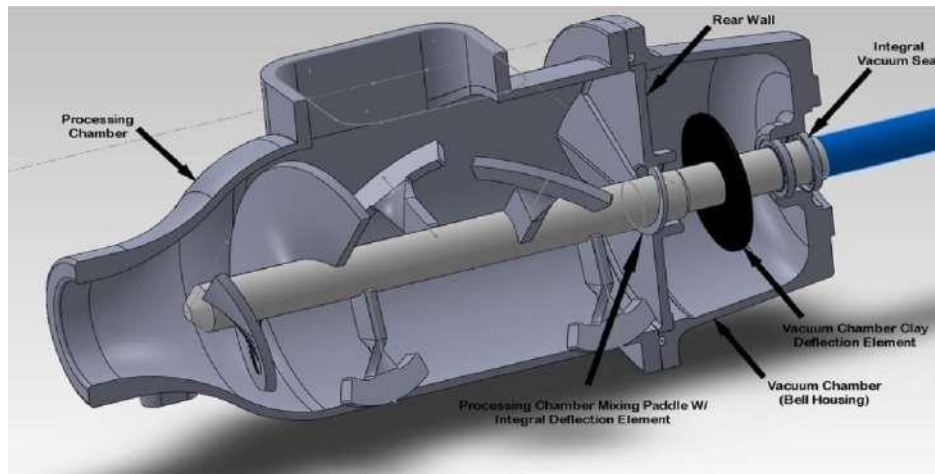


Figure 4.103: Peter pugger pug mill inside 3D model

5 Finite Element Analysis and fabrication Proposal

5.1 Finite element analysis

Finite Element Analysis will be performed on some critical elements of the system; the cutting blades of the shredder, the shaft for the two set of gears of the shredder, the extruding screw and the nozzle. For this analysis only static analysis will be performed, since the conditions are, either very slow so they are practically constant or, the case is critical to avoid the dynamic analysis. All the FEA analysis were made in the ANSYS Workbench software.

5.1.1 Blade analysis

For the blade analysis the material considered, as it was said in the detailed design, it is stainless steel 304. And the mesh used for the piece is tetrahedron shaped element, with an element size of 2 mm and the model for each element is quadratic. This resulted in 125211 nodes and 81087 elements, which is a very good approximation. The mesh can be seen on fig. 5.1.

To obtain the stresses on the blade, the boundary conditions are for the shaft hole to be fixed and the force applied is the force of 1800 N calculated in the detailed design as a normal force to one of the blades. This contemplates a situation where the machine gets stuck and the shaft is still forcing the blade. See the fig. 5.2.

As the figure of the results of the stress analysis captures it, the maximum stress on the



Figure 5.1: Mesh of the blade in ANSYS. Source: own

blade is about 49.9 MPa, which is way below the value of yield strength (215 MPa) for this material. However, this stress is not even present on the blade, rather on one of the cut triangles of the blade, this is a solvable problem by making an increment on the radius of this triangles, also, high stresses are on the shaft hole for the blade.

As for the blades, the stresses present of them (see fig. 5.3) are 35 MPa directly to the blade surface, and 44 MPa on the nearest corner of one of the cut blades arcs.

5.1.2 Shaft analysis

The shape is a much simpler geometry to mesh, again, the geometry chosen were tetrahedrons of 6 mm each element and the element order is quadratic. This resulted in 11303 nodes and 6396 elements. Also, to ensure better detail, the diameter reduction from 17 mm to 15 mm was refined to a 1 mm mesh to get more accurate results. See fig. 5.4

For the analysis, as explained in the detailed design, a bending load was contemplated simulating the weight of the blades. The fixed supports were simulated as cylindrical supports and a load of 431.2 N was applied in the center of the shaft producing the following results:

As it can be seen in fig. 5.5 the stresses were distributed as expected trough the shaft.

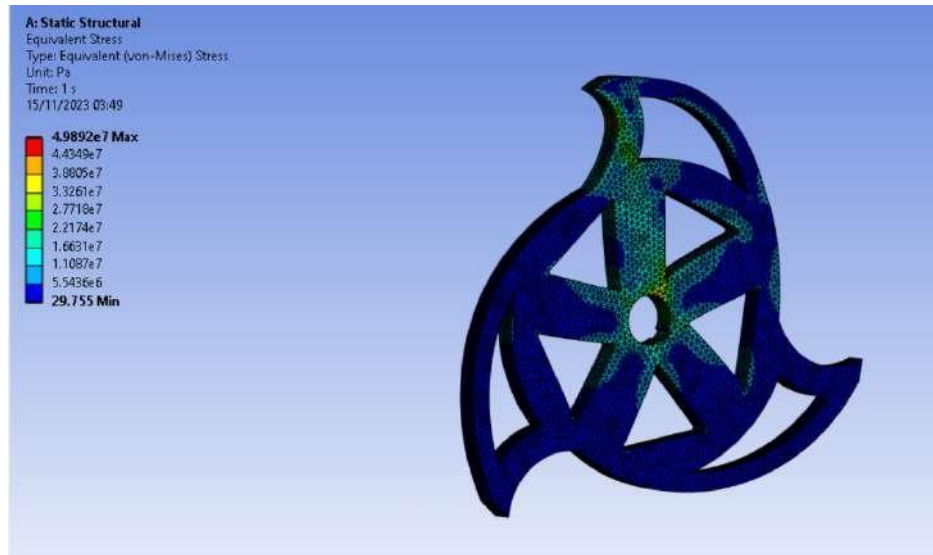


Figure 5.2: Von Misses equivalent stress in ANSYS. Source: own

The maximum stress is present in the diameter reduction, which was expected, and it is approximately 52.4 MPa, that for the purpose of this part is more than enough given that the calculated fatigue strength is around 284 MPa, this would result on a safety factor of around 5.5 ensuring the non-failure of this part.

5.1.3 Screw analysis

For the screw analysis the material considered was the AISI 8740 Steel (see the fabrication proposal for more details). The meshing (see fig. 5.6) was generated in the same way, tetrahedrons and a quadratic model, with an element size of 5 mm and was refined for the helices at 1.5 mm, resulting on 12803 nodes and 6795 elements.

The external forces acting is the pressure exerted by the clay in the helices. In this case the pressure considered was on the upper face of the helix, due to this is the direction of the flow, even tough the clay is going to pressure all the screw, the flow movement will generate more pressure. And in this case the pressure considered was the maximum pressure calculated in the design of 25.141 kPa. The boundary condition is for the shaft of the screw to be fixed, since this maximum pressure is calculated for the clay without movement.

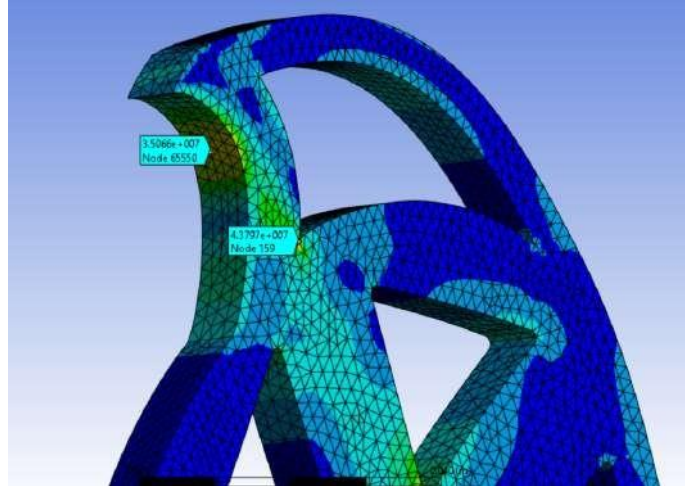


Figure 5.3: Stresses near the blade. Source: own

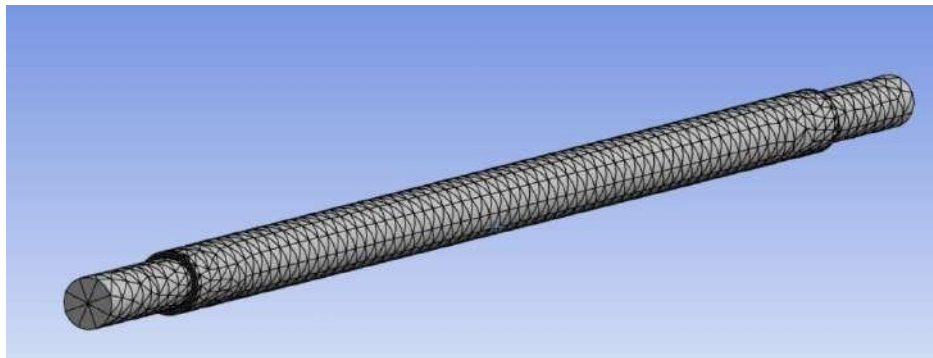


Figure 5.4: Mesh for the shaft in ANSYS. Source: own

In fig. 5.7 the equivalent stress distribution is presented. A maximum stress of 0.725 MPa is present on the union between the screw cylinder and the helix. And the distribution is decreasing as the radius of the helix increases, as it can be seen on the probes located on the helix. But, the stress generated by the clay flow is very small, even considering a plastic screw. Another case was considered, where the maximum pressure reaches a value of 1 MPa considering a way more viscous clay flowing through the system (see fig. 5.8).

In the case of the second consideration, which is probably the maximum pressure case for a brick clay, the stress values are way more significant, giving a result of 28.8 MPa in the same zones as the first analysis. But even with this case, stresses are not nearly as big to be considerable for the material of the screw to fail. Another thing that can be seen is that the stress reaches further through the length of the screw the more pressure there is.

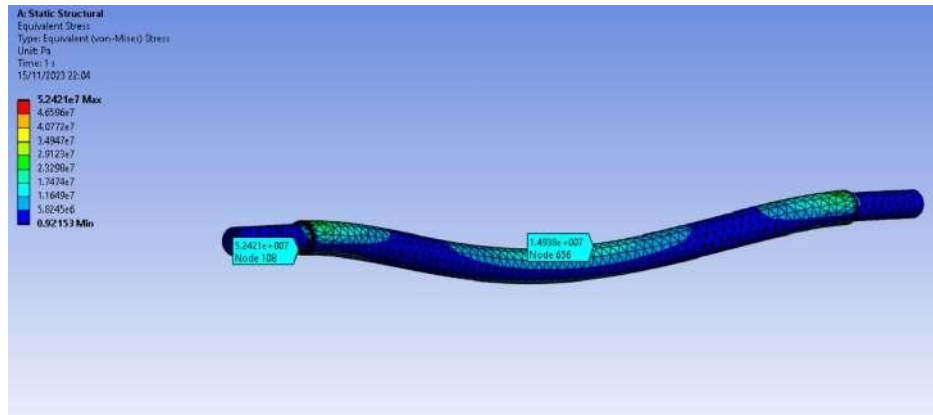


Figure 5.5: Shaft equivalent Von Mises stress results. Source: own

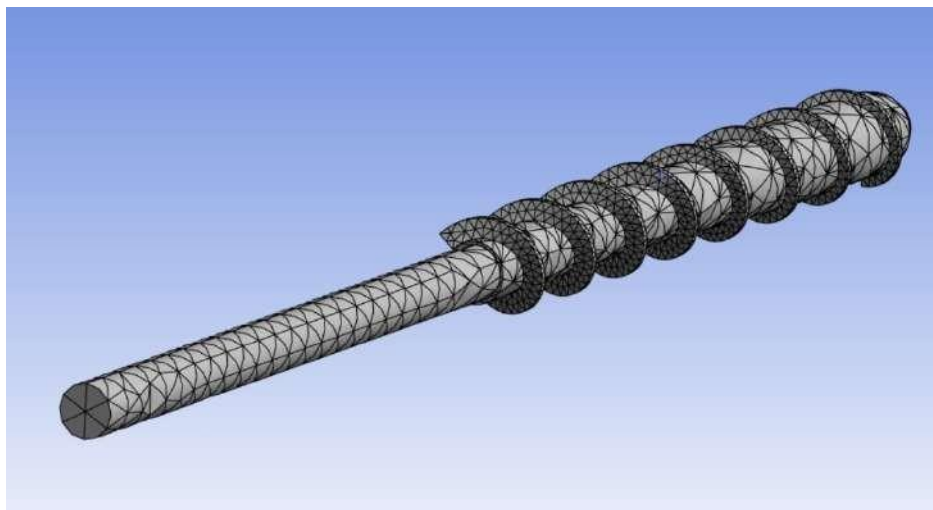


Figure 5.6: Screw meshing in ANSYS. Source: own

5.1.4 Nozzle analysis

For the three nozzle analysis that will be performed the considerations of the mesh and internal pressures are the same. For the overall model the element size is 4 mm with a quadratic model and tetrahedron shape. For the 4 mm nozzle, the meshing gives 35322 nodes and 20466 elements. In this case, the mesh was refined in the area changes close to the nozzle.

The pressure considered first is the operation pressure, which is 6.37 kPa and is being considered to be an internal pressure. The maximum pressure actually occurs on the base of the nozzle and it is around 82.5 kPa (see fig. 5.10) which is really not significant, considering

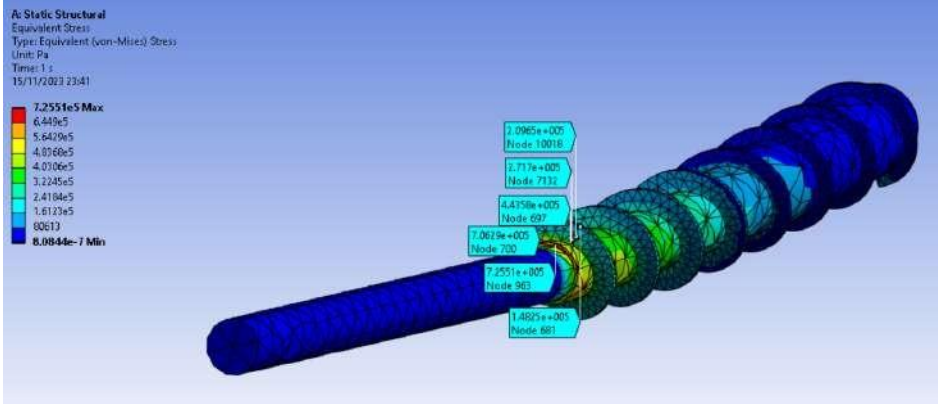


Figure 5.7: Stress analysis for the screw in ANSYS. Source: own

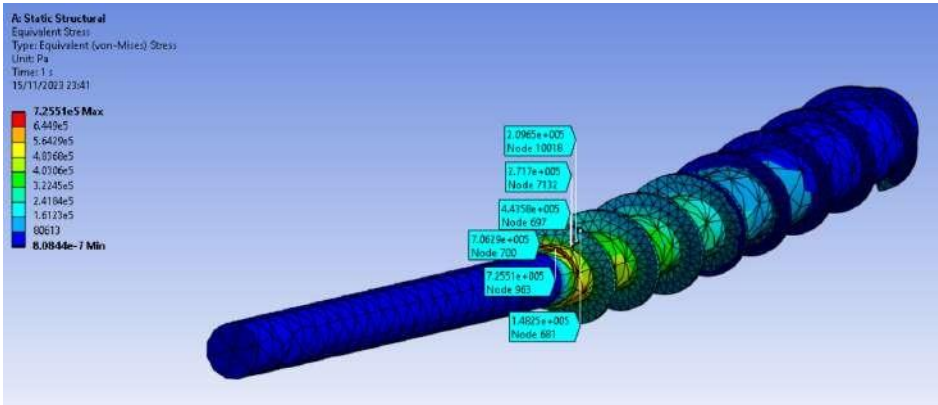


Figure 5.8: Screw stress analysis considering 1 MPa of external pressure. Source: own

even plastic material like ABS, which yield strength is around 43 MPa.

The pressure on the tip is around 30.88 kPa, which is even less than in the base of the nozzle. Also, the tip is of stainless steel so the pressure there is going to have less effect on the material. See fig. 5.11.

To account for tougher clay, another analysis was made considering 950 MPa, for the operating pressure. All the other considerations were the same. Again, the maximum pressure is on the bottom, which is about 12.6 MPa, and the pressure on the tip is around 4.42 MPa (see fig. 5.12), it has a more considerable effect, but still not enough to represent a significant effect on the materials of the nozzle.

For the other two nozzles (6mm and 8 mm) the stresses vary but by a very small amount, so, it is really not something to consider.

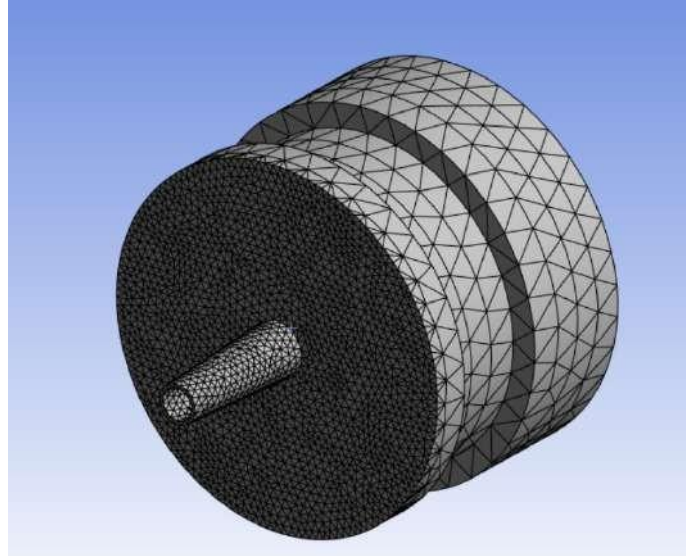


Figure 5.9: 4 mm nozzle meshing in ANSYS. Source: own

5.1.5 Pinion analysis

For the gears of the shredder, the mesh applied to the whole gear was of 5 mm and was refined in the surface where the force was considered to be acting, which was the face of one of the pinion's teeth. The mesh resulted of 8656 and 4568 elements. See fig. 5.13.

The analysis was simulating a completely fixed gear and receiving the surface load that was calculated in the detailed design, 135.45 N, It resulted on a maximum equivalent stress of 9.35 MPa. Which for the bronze C89320, whose yield stress is 124 MPa. So it is completely safe to say that the gear will hold the load well. As shown in fig. 5.14. The maximum stress zone is as expected on the fillet of the tooth.

For the gear, the same exact process was made, only this time the maximum stress was of 17.15 MPa, which is quite more considerable than the stress on the pinion, this was expected since the tooth is smaller relative to the gear. But, then again, in terms of material, the bronze is sufficient to meet the resistance requirements (see fig. 5.15).

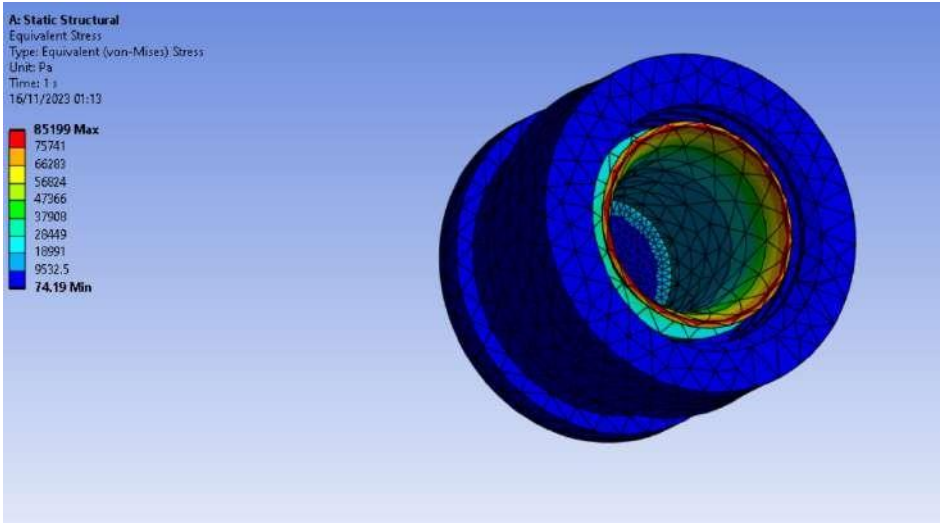


Figure 5.10: Nozzle 4mm stress analysis in ANSYS. Source: own

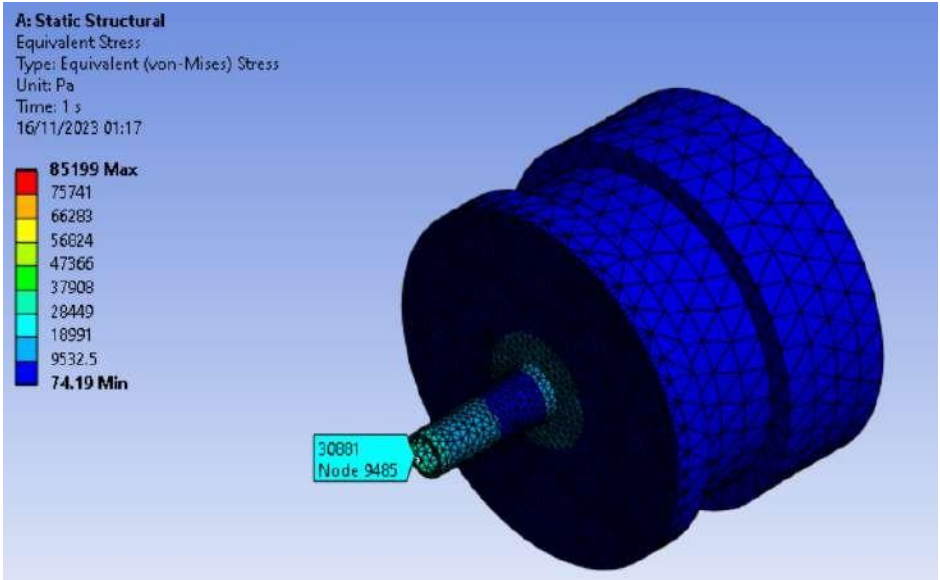


Figure 5.11: Nozzle 4mm stress analysis on the tip in ANSYS. Source: own

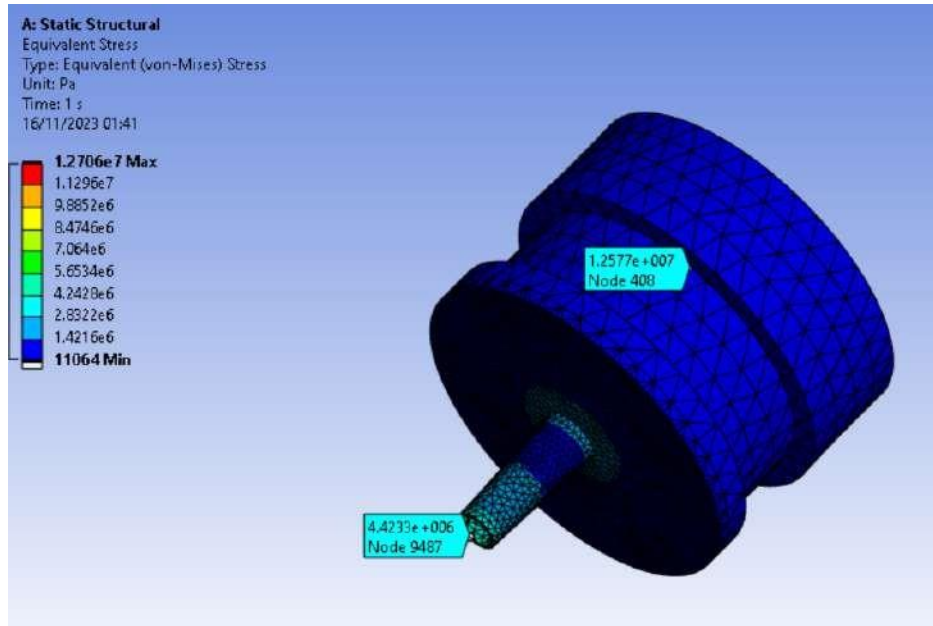


Figure 5.12: Nozzle 4mm stress analysis for 950 KPa. Source: own

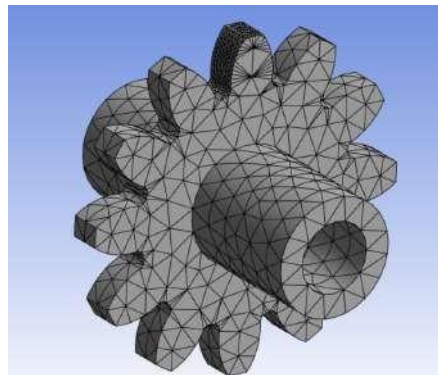


Figure 5.13: Mesh for the pinion in ANSYS. Source: own

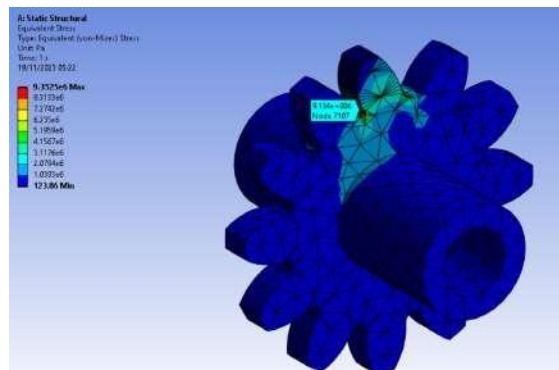


Figure 5.14: Pinion stress analysis. Source: own

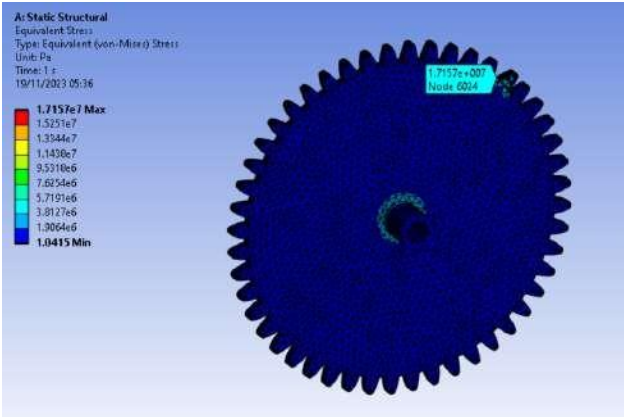


Figure 5.15: gear stress analysis in ANSYS. Source: own

5.2 Fabrication proposal

Since some of the systems such as the recycler or the pugmill will not be considered for the prototyping phase, and the extruder and feeder systems are going to be prototyped but not fabricated with more durable materials or other manufacturing processes, a fabrication proposal will be made for these systems, however, since some dimensions and specifications are going to probably change from a prototype to a final piece, this section will only propose materials and manufacturing processes (if needed) but will not delve into new dimensioning since this goes beyond the scope of the thesis.

For the fabrication proposal selection of materials, selection of manufacturing processes and tooling will be discussed in this section. Some of the principles of Design for Manufacturing (DFM) will be used but it is worth mentioning that not all the methodology will be applied.

The first proposal is for the extruder materials, more importantly, the central vessel, the nozzle and the extruder screw, which are the materials that are going to have more solicitations in terms of stress.

5.2.1 Extruder

Main vessel

For the main vessel the better selection would be to select a standard pipe so the manufacturing wouldn't be such a problem. For this task, the material would have to be able to withstand the inside pressure of the clay, obviously, some types of clay will be more tough than others and also it would have to be able to support the abrasiveness of the clay, the last one is probably the main worry.

One good example of the material necessary to extrude is in (Ji Chen, 2017)'s design, who proposes a Stainless steel AISI 316L, but in this case this material is contemplating the contact with food, thus have to be hygienic. In this case, since the PVC proved to be

sufficient to handle the inside pressure of the tube, the most likely case, even considering the worst case scenario, that is considering the viscosity value that (Velilla Díaz et al., 2009) proposes for brick-clay, the value of pressure does not even reach 1 MPa, so the resistance is not a problem.

The aspect that is going to be mainly taken into account is the resistance to abrasiveness, also considering the repeatability and structural integrity of the extruder. Going by this statement, toughness of the material is very important, if the material toughness is higher than the toughness of the abrasive material then the wear is not very high, just in this case is hard to consider a direct comparison between toughness since clay is a fluid.

In this case the main concern would be the comparison between the grain size of a certain clay and the roughness of the material. stainless steel has an approximate roughness of $Ra = 0.8\mu m$, considering the study of (Klinkenberg, Rickertsen, Kaufhold, Dohrmann, & Siegesmund, 2009) where they investigated the abrasiveness of bentonites, the most abrasive was a grain size of $63\mu m$. Which, is not very considerable. So it can be assumed that stainless steel will be sufficient to hold the abrasiveness without an extra process.

Hence the proposed material is a 304 stainless steel round tube. It is commonly used for construction, structural applications and plumbing (*304 stainless steel round tube*, n.d.). Since the dimensions that were chosen for the tube in the prototype are standard, then a 1" will be suggested for this is the closest dimension to the one proposed (see fig. 5.16).

More than likely, the tube will not require a thread since the outer container is the one actually connected to the lid and nozzle. So this tube will not require any sort of extra manufacturing process other than cutting the tube to fit inside the container.

Endless screw

For the endless screw stainless steel could be an option since it has a good resistance to abrasiveness but the machining of this type of steel could be somewhat complicated. So for this, the best option would be to first manufacture the screw with a carbon steel and then probably make an extra process to protect the material from the clay.

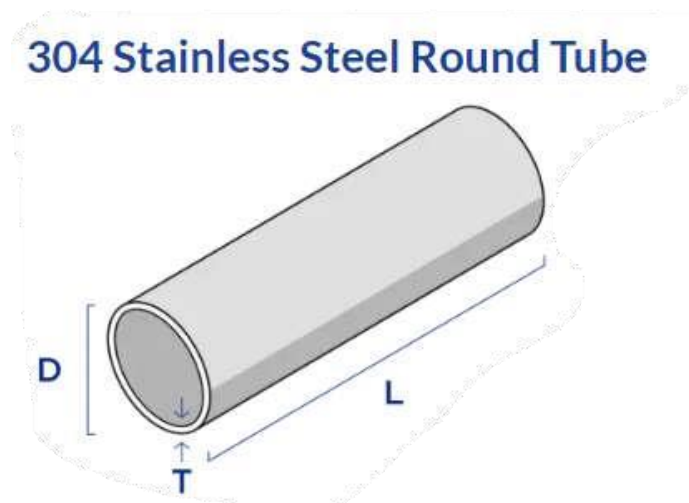


Figure 5.16: Stainless steel tube for the main vessel. Source (304 stainless steel round tube, n.d.)

The suggested material for the screw is AISI 8740 Steel, which is not only carbon steel but also has some extra elements such as Manganese, Nickel and Chromium (*MatWeb - the online materials information resource*, n.d.). This material has great mechanical properties such as fatigue resistance and resistance to corrosion, but also since it has been quenched and tempered it offers greater toughness and strength than most carbon steel. And, it is also fairly easy to manufacture (65% machinability according to (*MatWeb - the online materials information resource*, n.d.)), making an extra process not necessary.

Naturally, the chosen process for this piece is turning cutting because of the shape needed for the screw, a helix spiral. This process has to be carefully done because of the characteristics of the spiral itself. So probably a CNC cut would be the best option.

Nozzle

For the nozzle the idea keeps being the same, a material needs to resist the pressure and the corrosion and abrasiveness. But in this case, since it is a good idea that the outer container stays as a plastic material, is probably best to keep the structure that connects the nozzle with the container plastic as well, but, the tips would be the ones that are interchangeable. The selection of the materials would be the same as the main vessel, meaning the stainless steel.

Only this time, the better choice probably would be a metal sheet of a thickness bigger than the one calculated in the detailed design. So the manufacturing process would have to be cold extrusion to achieve the shape of a nozzle going from a hollow circle made out of sheet.

Outer container

The container best choice is to stay plastic, this will ensure cheaper production of this part and a better aesthetic. For this case, the best choice would be to use a harder plastic like nylon and manufacture the container by plastic molding. This technique is not suitable for a one time container production but very useful when it comes to making several of this, and in a much much faster way.

5.2.2 Feeder

Feeder cylinder

Depending on the length of this tube the pressure inside could increase by a large amount given the principle of movement, which is like a syringe plunger, creating an increased pressure. The proposal for this is the same as the main vessel of the extruder, the material proposed is Stainless steel 304L tube of about 2 inches, also another option would be to machine the tube in a turning cutter.

Worm gear drive

For the worm gear drive the decision of 3D printing it was merely because of budget reasons, commercial gearboxes like this one were too expensive for the scope of the project. The best thing, considering the reduction ratio needed is 30:1 would be to select an existing gearbox that achieves that requirement. So, for this, the Nema 23 worm gear drive would be the best option (see fig. 5.17).

Frame

For the frame a simple aluminium extrusion profile would be sufficient, considering that have to be adapted to the base of the 3D print (for this particular case the ABB robotic



Figure 5.17: Gearbox 30:1 for nema 23. Source: (<http://amazon.com>, n.d.)

arm). For this, an "L" extrusion aluminium profile (see fig. 5.18) is selected since, more than the mechanical properties, the easy adaptability to the frame of the robotic arm and also the easy union between profiles.



Figure 5.18: "L" aluminium extrusion profile. Source: (Extrusax, n.d.)

5.2.3 Recycling machine

Blades

First for the blades, the method used was the Ashby's map for selecting materials. In this case, the first reference the Young's modulus vs Density, which was set to be a minimum of 30 GPa and $2000\text{kg}/\text{m}^3$ respectively. This, for one to keep non-metals out of the picture and to set materials that have a decent strength-density ratio (see fig. 5.19).

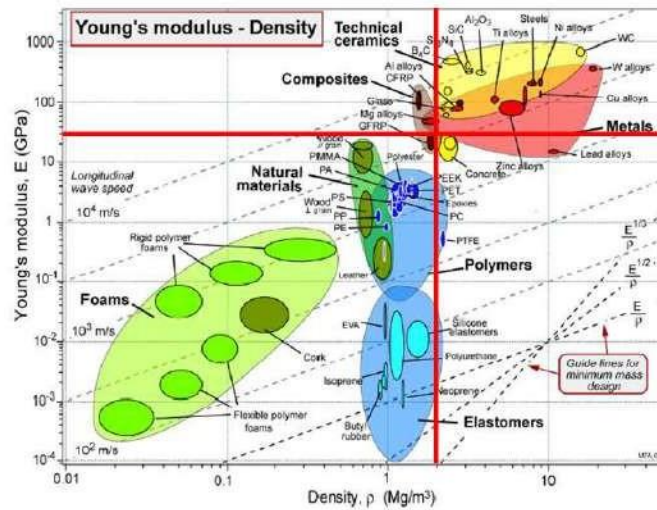


Figure 5.19: Young's modulus vs density graph. Source: (Solá Marcillo, 2009)

After this, the map of yield strength against young's modulus to further narrow the possible materials. In this case, the maximum yield strength allowed is 600 MPa, so some steels are considered, yet the heaviest ones are left out. This will yield a region of possible materials (see fig. 5.20).

Analysing the performance indexes regarding these two categories, the smallest result for the first one is the ideal, and since the material is not looking to outperform the needs of the blades, for the other index, it is sufficient that it does not surpasses a thousand. In reality the ratio of density is way more important since the values are way bigger.

Stainless steel 304

Density: $8000\text{ kg}/\text{m}^3$, Young's modulus: 193GPa and Yield strength: 215MPa

$$\frac{E}{\rho} = 24.125 \times 10^6 \quad (5.1)$$

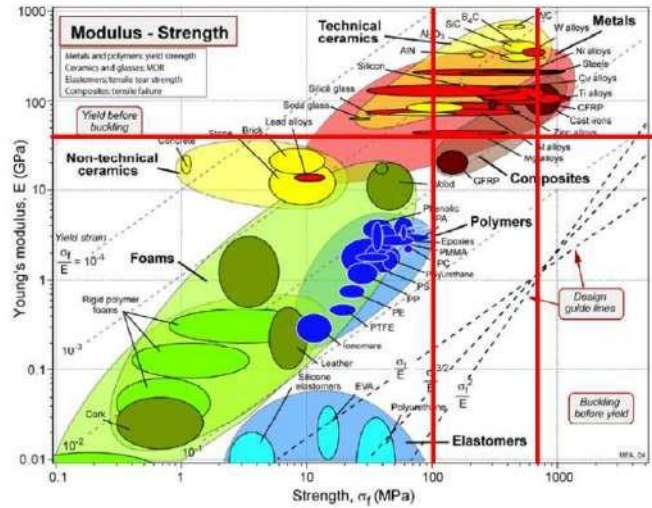


Figure 5.20: Young’s modulus vs Yield strength. Source: (Solá Marcillo, 2009)

$$\frac{E}{\sigma_y} = 897.67 \tag{5.2}$$

Steel AISI 4340

Density: 7850 kg/m³, Young’s modulus: 212GPa and Yield strength: 1475MPa

$$\frac{E}{\rho} = 27.006 \times 10^6 \tag{5.3}$$

$$\frac{E}{\sigma_y} = 143.728 \tag{5.4}$$

Steel AISI 8740

Density: 7850 kg/m³, Young’s modulus: 205GPa and Yield strength: 415MPa

$$\frac{E}{\rho} = 26.116 \times 10^6 \tag{5.5}$$

$$\frac{E}{\sigma_y} = 493.975 \tag{5.6}$$

Steel AISI 8740

Density: 7800 kg/m^3 , Young's modulus: 200 GPa and Yield strength: 1005 MPa

$$\frac{E}{\rho} = 25.64 \times 10^6 \quad (5.7)$$

$$\frac{E}{\sigma_y} = 199.004 \quad (5.8)$$

Aluminium 6061 T6

Density: 2700 kg/m^3 , Young's modulus: 68.9 GPa and Yield strength: 276 MPa

$$\frac{E}{\rho} = 25.519 \times 10^6 \quad (5.9)$$

$$\frac{E}{\sigma_y} = 249.64 \quad (5.10)$$

The chosen material out of this list is the AISI 304, since it gives the best performance between the elasticity modulus and the density by far, and, even though it has the greater ratio of the modulus and the yield stress, is decent enough, and additionally it has the quality of being stainless which makes it resistant to abrasion.

The proposed manufacturing method is milling a plaque of the same caliber as the design, which is 8 mm. A plaque of a 5/16 caliber will do just fine, since it is almost exactly 8 mm. And the milling technique is the best given the blades need to have some sort of sharpness, the cutting process will give this sharpness to them.

Shaft

For the shaft a similar analysis was conducted, the selected material is Steel AISI 4340, with a density of 7850 kg/m^3 , a yield strength of 862 MPa and a modulus of elasticity of 200 GPa , and according to the performance indexes gives the following value:

$$\frac{E}{\rho} = 25.477 \times 10^6 \quad (5.11)$$

$$\frac{E}{\sigma_y} = 232.02 \quad (5.12)$$

This is a very good performance overall, the properties change a little bit according to the first one because this is taking account of a round material to use a turning milling process. Again, the manufacture is considering a lathe process to mill the extra material, due to the 25 mm of original material.

Gears

For the gears of the shredder the material proposed is bronze C89320, which is a fairly standard for gears, the choice is mainly because the solicitations are met, in terms of the stresses and deformations, and also, because of the machinability that bronze has, which according to (*MatWeb - the online materials information resource*, n.d.), is around 80%, which is very good considering a proposed gear machining to make these parts.

6 Prototyping

6.1 Prototyping

For the prototyping the models were made to test certain important aspects of the system such as, size, flow, layer width and others. Mainly the extruder system and the feeding system are the ones that are going to be tested.

6.1.1 Extruder prototyping

For the extruder system prototyping the main body was 3D printed with PLA using software CURA Ultimaker. Since printing the whole container would really be a waste of material, the bottom and the top part will be printed separately since the things that need to be tested do not involve having the whole body available. The bottom and top part were printed as shown in fig. 6.1.

The parameters used to print the body top and bottom parts were the following (see Table 6.1). Worth mentioning that the infill percentage was zero since the walls were sufficient to fill the cylinder.

For the inside tube the material used was a 1 inch PVC tube with an inside diameter of 19 mm, which was the closest that could be found that met the requirements of inside diameter and thickness as well. The tube was cut at a 20 cm length to have some wiggle room in terms of the overall size, since the body was printed with a bottom and a top part, this allowed to play in between sizes fig. 6.2.

Also, the lid and the nozzle were printed to test the extrusion and fitting of the compo-

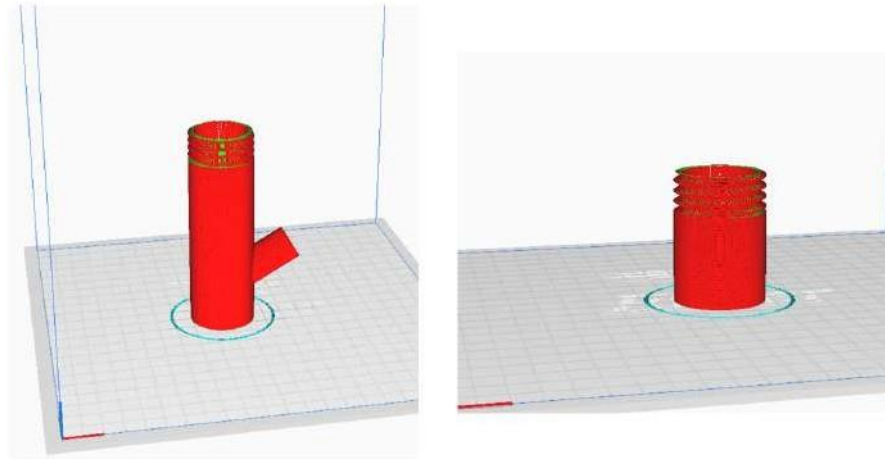


Figure 6.1: Main body print bottom and top part preview in CURA Ultimaker. Source: own

Table 6.1: Printing parameters for the body top and bottom parts. Source: own

Parameter	Value
Infill percentage	0%
Layer height	0.12 mm
Line width	0.4 mm
Wall lines	4
Horizontal expansion	-0.05 mm
Hole horizontal expansion	0.6 mm
Print speed	35 mm/s

nents. They were slightly modified to be installed in a test bank. The lid (see in fig. 6.3) has an additional flange to adapt it to the test bank.

The parameters used to print the lid were the following (see Table 6.2):

The printing for the nozzle was very similar (see fig. 6.4). Just in this case the width of the nozzle was edited to make sure more wall lines are printed. But basically the parameters are the same as Table 6.2.

Lastly, the endless screw for extruding the clay, will be also 3D printed. In this case, the screw will be printed separately, both the shaft and the screw are later going to be glued together. The test print can be seen on the next figure (see fig. 6.5).

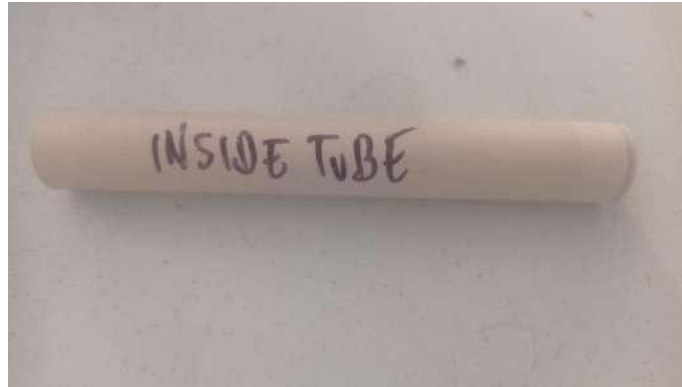


Figure 6.2: Inside PVC tube. Source: own

Table 6.2: Printing parameters for the Lid. Source: own

Parameter	Value
Infill percentage	45%
Layer height	0.12 mm
Line width	0.4 mm
Wall lines	4
Horizontal expansion	-0.05 mm
Hole horizontal expansion	0.6 mm
Print speed	35 mm/s
Supports	Normal and touching the build plate

The parameters used to print the screw can be seen on Table 6.3.

Also, to account for possible fails on the screw due to it being printed in two parts, an 11 mm drill bit was also bought to be tested as an endless screw. The length of the drill bit was 26 cm. and for the use of this drill bit an extra adapter had to be designed (see fig. 6.6).

The extra parts that had to be printed were an extra adapter for the drill bit because the screw did not fit the original flexible coupler that was being used. The complementary parts for this are the screws adapter for the motor to be standing, and the adjusters to ensure a tight fit on the screw. The print preview for this can be seen fig. 6.7.

And the parameters used were as seen on Table 6.5:

After printing this, a wooden test bank is manufactured to install the extruder and test it. The test bank can be seen in the following picture (see fig. 6.8).

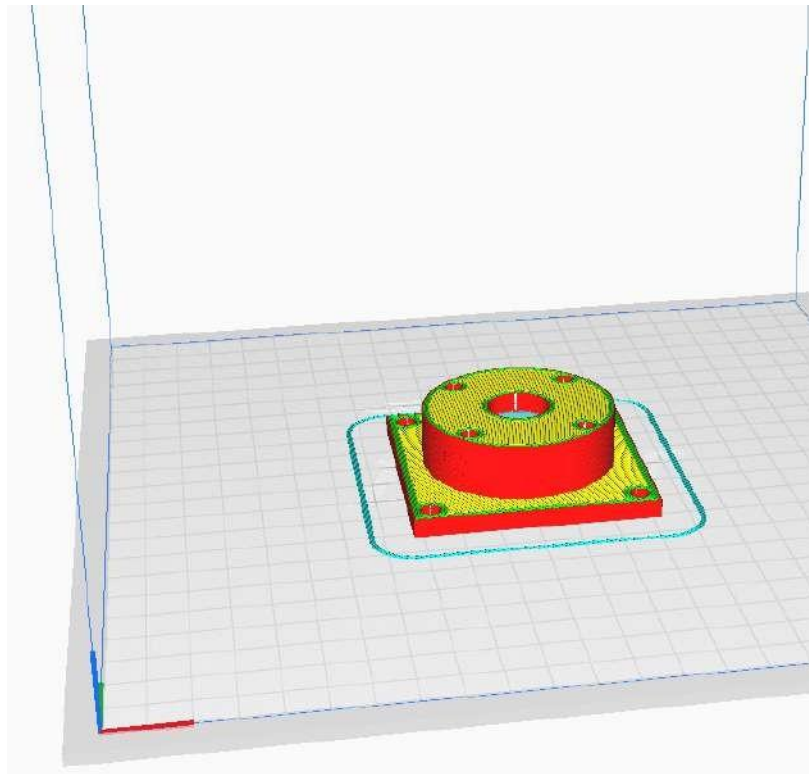


Figure 6.3: Lid print preview in CURA Ultimaker. Source: own

And the assembly to test the extruder model can be seen in fig. 6.9. As this goes, the structure will hold the extruder statically, with just the upper part and the bottom part of the main body joined to the rest, which is the lid and the nozzle.

The resulting printed pieces can be seen on the following pictures.

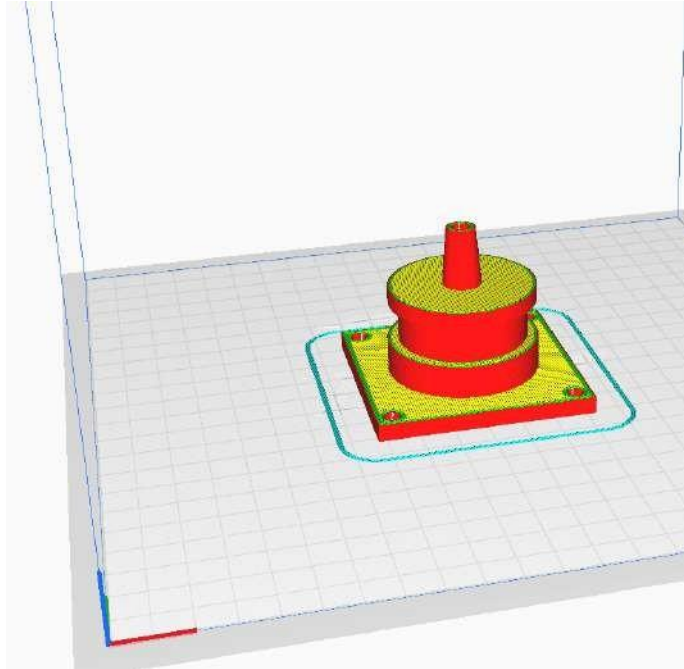


Figure 6.4: Nozzle print test preview on CURA Ultimaker. Source: own

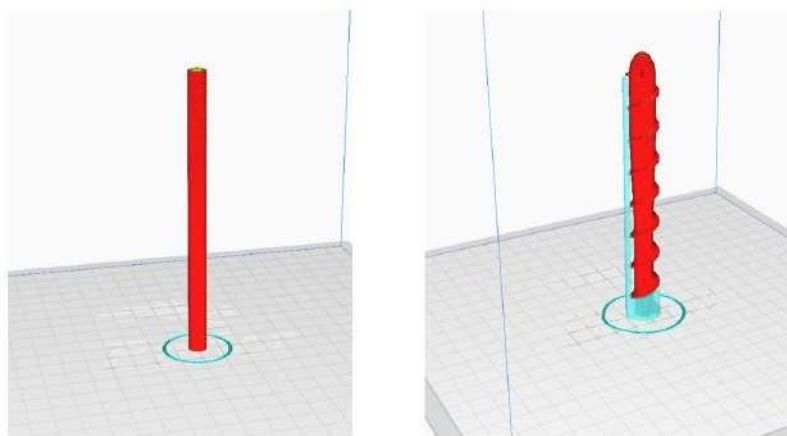


Figure 6.5: Endless screw print test preview on CURA Ultimaker. Source: own

Table 6.3: Printing parameters for the Screw. Source: own

Parameter	Value
Infill percentage	65%
Layer height	0.12 mm
Line width	0.4 mm
Wall lines	4
Horizontal expansion	-0.05 mm
Hole horizontal expansion	0.6 mm
Print speed	35 mm/s
Supports	Normal and touching the build plate



Figure 6.6: Drill bit used as a extruder. Source: own

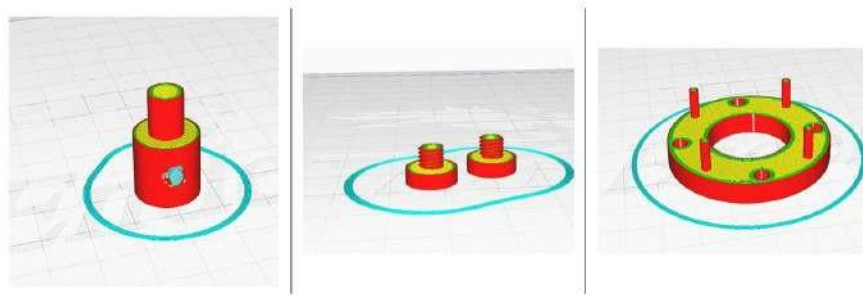


Figure 6.7: Parts for the screw adapter. Source: own

Table 6.4: Printing parameters for the Screw. Source: own

Parameter	Value
Infill percentage	45%
Layer height	0.12 mm
Line width	0.4 mm
Wall lines	3
Horizontal expansion	-0.05 mm
Hole horizontal expansion	0.4 mm
Print speed	40 mm/s
Supports	Normal and touching the build plate

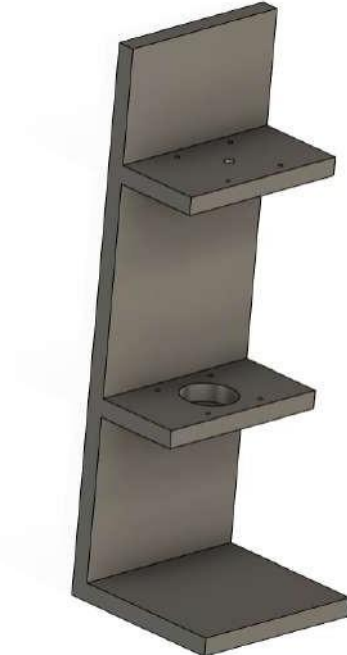


Figure 6.8: Test bank model. Source: own



Figure 6.9: Test bank configuration. Source: own



Figure 6.10: 3D printed lid. Source: own



Figure 6.11: 3D printed nozzle. Source: own



Figure 6.12: 3D printed bottom part. Source: own



Figure 6.13: 3D printed top part. Source. own



Figure 6.14: 3D printed motor support. Source: own



Figure 6.15: 3D printed screw adapter for the motor. Source: own



Figure 6.16: PVC with the adapted hole. Source. own



Figure 6.17: Wood bank test. Source: own

Additionally, to complete the prototype, a two way pneumatic fitting was used to connect the hose from the feeding system. Also, a set of screws sized 1/8 by 2 inches (3 mm by 52 mm) with its respective nuts (see fig. 6.18).



Figure 6.18: Pneumatic fitting for hose and screw-nut pair. Source: own



Figure 6.19: Motor and screw assembly. Source: own

The final prototype assembly resulted:

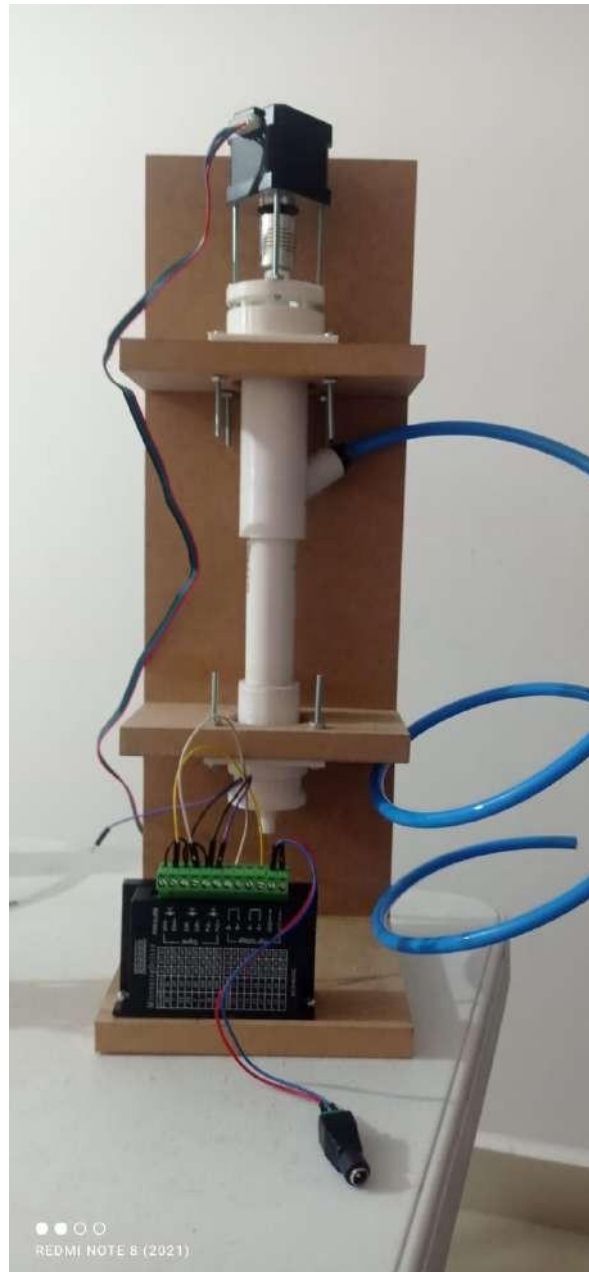


Figure 6.20: Final assembly of the prototype. Source: own

6.1.2 Feeder prototyping

Pusher system

For the feeder prototyping the main technique used was 3D printing as well. Also, to do this, the CURA Ultimaker software was the selected one. For the feeder nozzle two pieces were needed, the adapted to the tube, which is a cylinder with an outside screw and the nozzle itself with an inner screw. The previews for the process can be seen on fig. 6.21 and fig. 6.22.

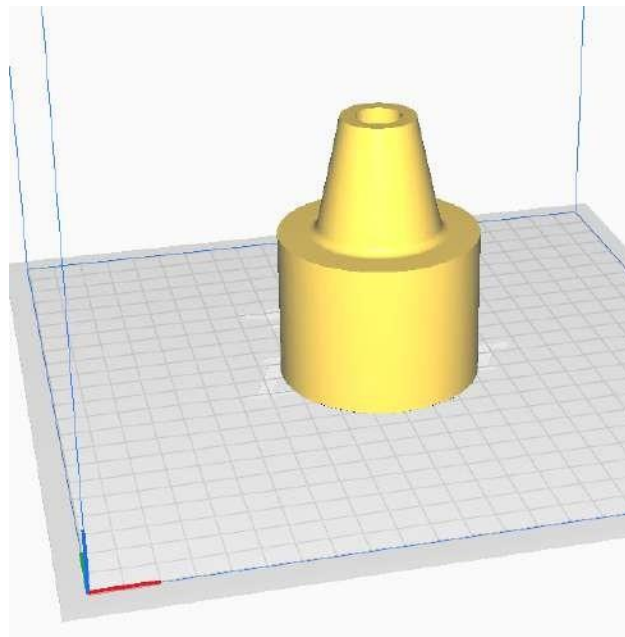


Figure 6.21: Nozzle of the feeder in cura Ultimaker. Source: own

For this, the lid for the entrance of the clay will also be 3D printed in the same way and with the same parameters as the nozzle, and since another adapter is needed, consider the adapter printing two times. For the lid see fig. 6.23 and the parameters used for these three prints are in

The plunger to push the clay through the feeder was 3D printed as well (see fig. 6.24), the parameters are almost identical to Table 6.5, except that the infill was of 75% to give this piece the needed toughness to push the clay through.

To finish printing the pushing system, a worm gear gearbox was also 3D printed (see

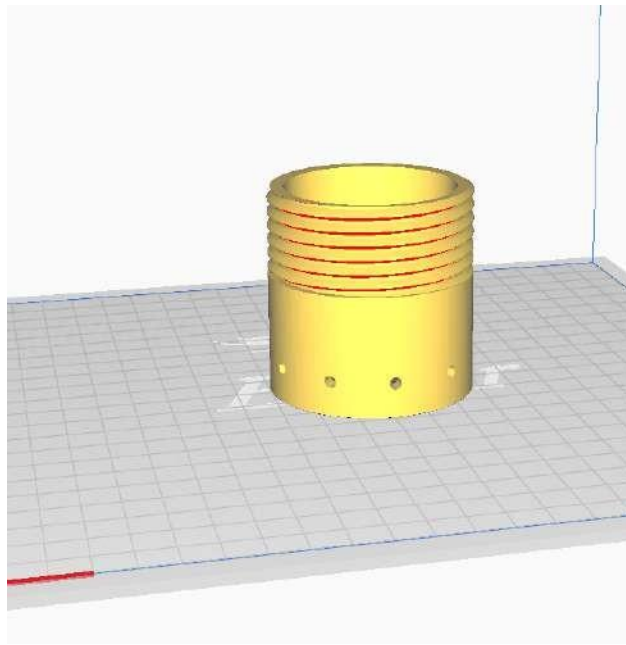


Figure 6.22: Tube-screw adapter to the feeder in cura Ultimaker. Source: own

fig. 6.25) to give the motor the torque reduction needed. In the case of the housing of the gearbox, the parameters were pretty similar, except that for this, the layer height was set to 0.16 and the infill was 45% to make it a little bit faster. For the worm and the crown gear, the layer height was restored at 0.12 mm and the infill was of 75% since they are going to be in constant contact.

Finally, finishing features, for this system, a PVC 50 mm of outside diameter and 46 mm of inside diameter (see) was cut to 25 cm length and was used to simulate the intended 2 inch tube proposed in the fabrication chapter (see fig. 6.26).

What is more, a T8 lead screw with two nuts (see fig. 6.27) to attach to the plunger and the gearbox, only for the gearbox, an extra adapter needed to be designed to be able to translate the movement from the crown gear to the lead screw (see fig. 6.28).

Finally, to join both parts of the gearbox, four 6 mm by 105 mm bolts were used as seen in fig. 6.29.

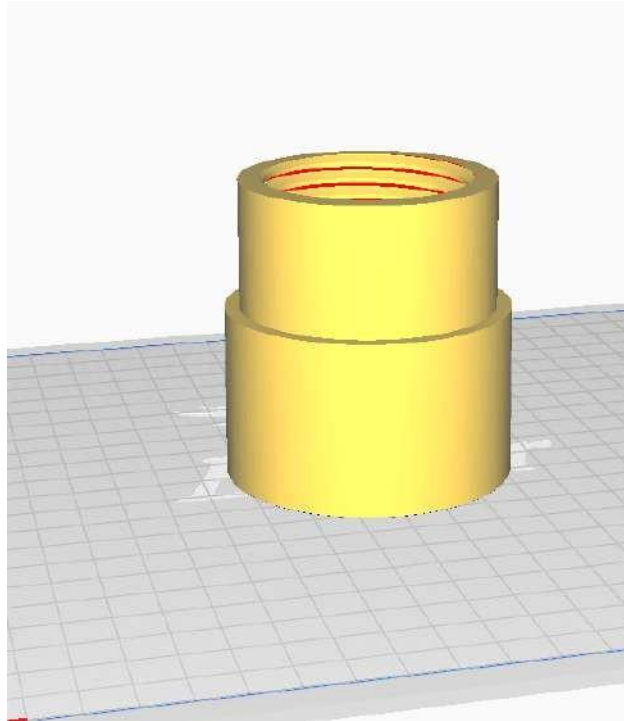


Figure 6.23: Feeder lid in cura Ultimaker. Source: own

Table 6.5: Printing parameters for the Screw. Source: own

Parameter	Value
Infill percentage	45%
Layer height	0.12 mm
Line width	0.4 mm
Wall lines	4
Horizontal expansion	-0.05 mm
Hole horizontal expansion	0.6 mm
Print speed	40 mm/s
Supports	Normal and touching the build plate

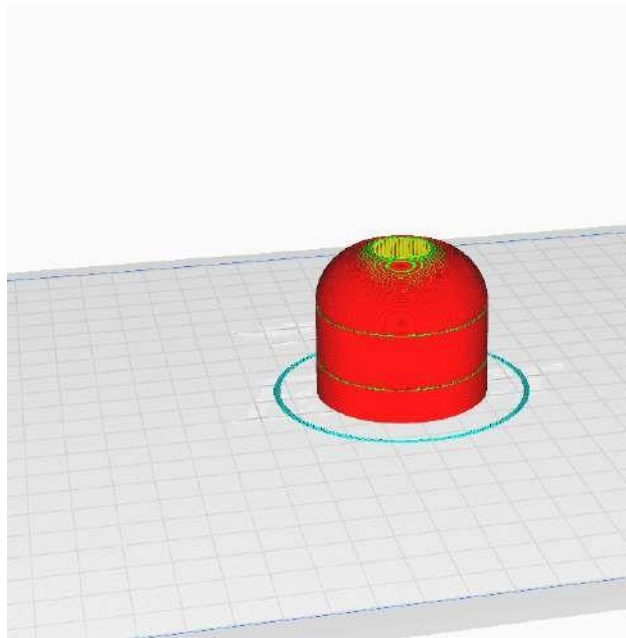


Figure 6.24: Plunger print preview in CURA Ultimaker. Source: own

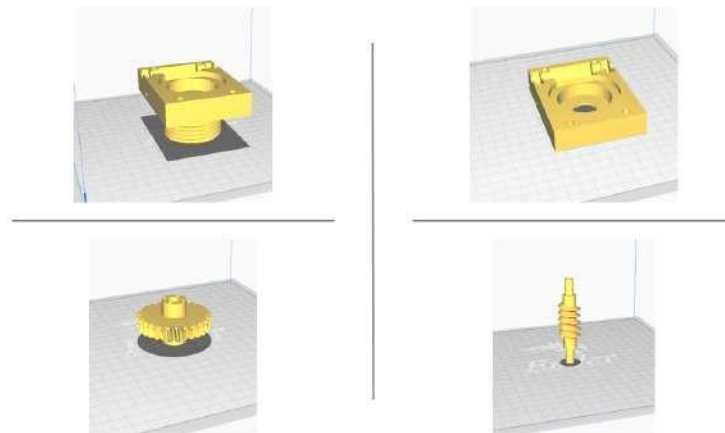


Figure 6.25: Gearbox set preview in CURA Ultimaker. Source: own



Figure 6.26: PVC feeder tube



Figure 6.27: 300 mm T8 Lead screw. Source: own

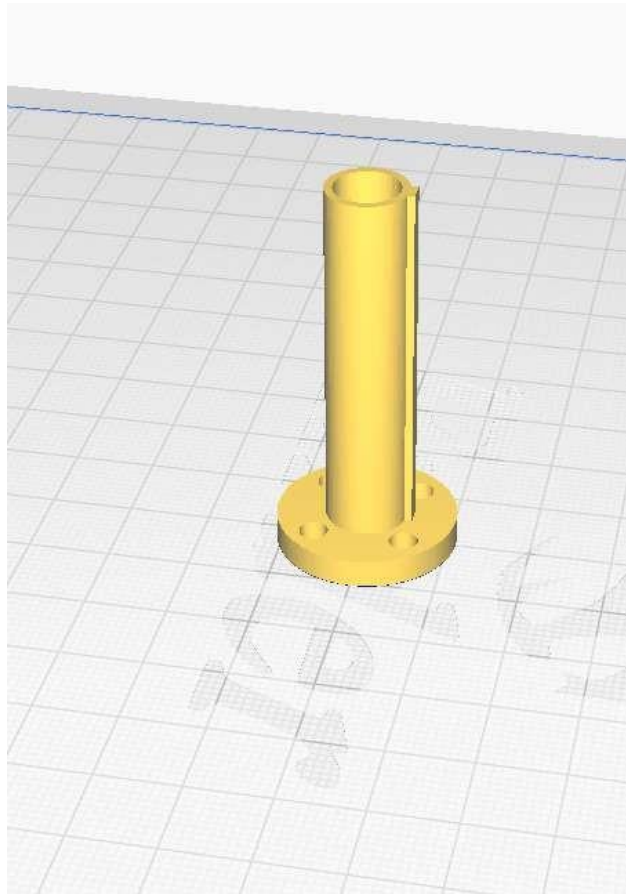


Figure 6.28: Adapter from gearbox to lead screw. Source: own



Figure 6.29: Bolts for attaching the gearbox. Source: own

Structural system

For the frame to hold the feeder, a wooden frame was made to hold all the feeder. A very simple hollow frame made out of ten bars. In the fabrication proposal chapter, the frame is suggested to be made out of aluminium profiles. But for a prototype, the use of wood will be enough (see fig. 6.30).

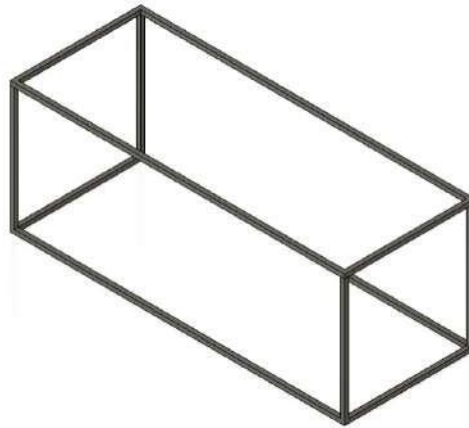


Figure 6.30: Model of the frame of the feeder. Source: own

To attach the feeder tube to the frame, two things were designed. one is a plaque with a hole in the middle to keep the nozzle in place and the other is an attachable clamp that can change position according to the length. The first one can be seen on fig. 6.31 and the clamp in fig. 6.32.

For this, the parameters were kept constant as the other prints, just changing the infill density to 35% since a lot of resistance is not needed.

Continuous workflow system

For the continuous workflow system, just a single structure had to be created to make the servo motor and the valve work together in order to automate the valve. The structure is basically to hold the motor over the valve. This structure can be seen on fig. 6.33.

In order to unite the shaft of the motor and the valve to be opened. This was adapted to the star shaped attachment of the servo motor for it to achieve more torque to open the

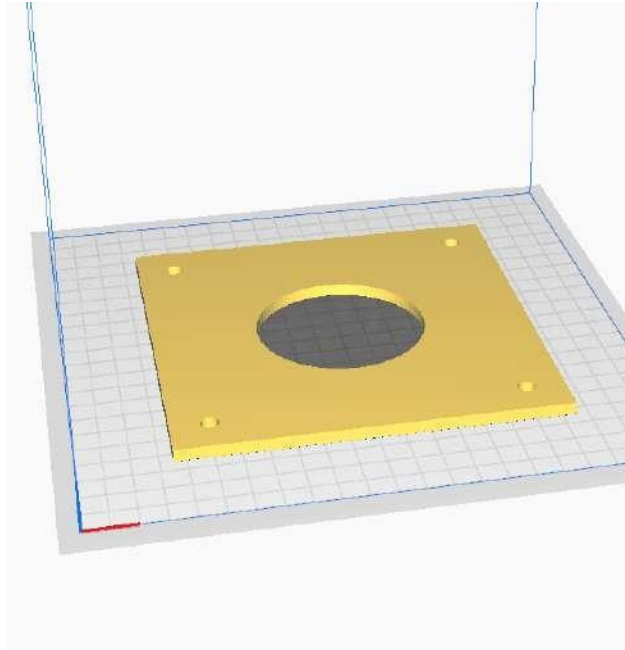


Figure 6.31: Plaque for attaching the nozzle to the frame. Source: own

valve (see fig. 6.34).

These two pieces were printed with very similar parameters to the rest of the printed pieces, except the shaft adapter which was printed with a 85% infill density so it does not break while turning with the servo and the valve. The final prototype would look a lot like what the final system should look once fabricated (see fig. 6.35).

The resulting 3D printed parts and the frame, the resulting can be seen in the following figures. The nozzle has already the two way pneumatic fitting with a rubber band used as a pack to avoid the spillage.

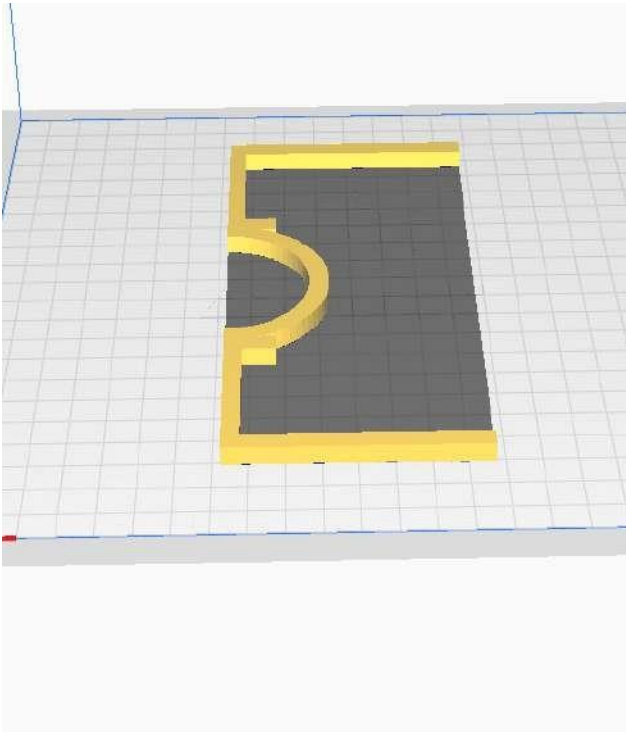


Figure 6.32: Clamp for attaching the body to the frame. Source. own

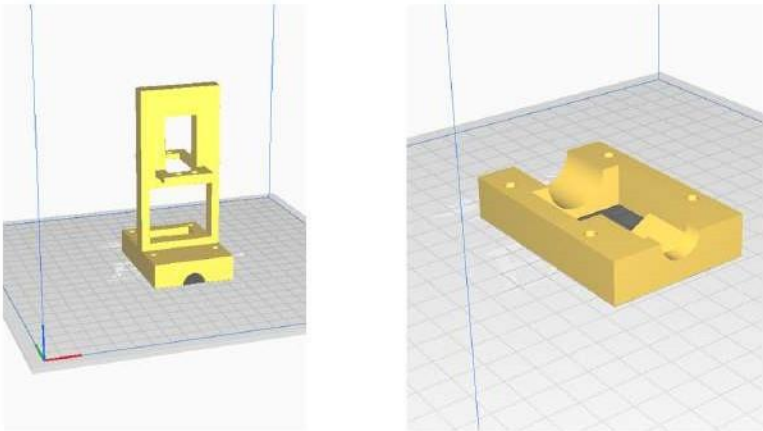


Figure 6.33: Adapter structure for the motor and the valve. Source: own

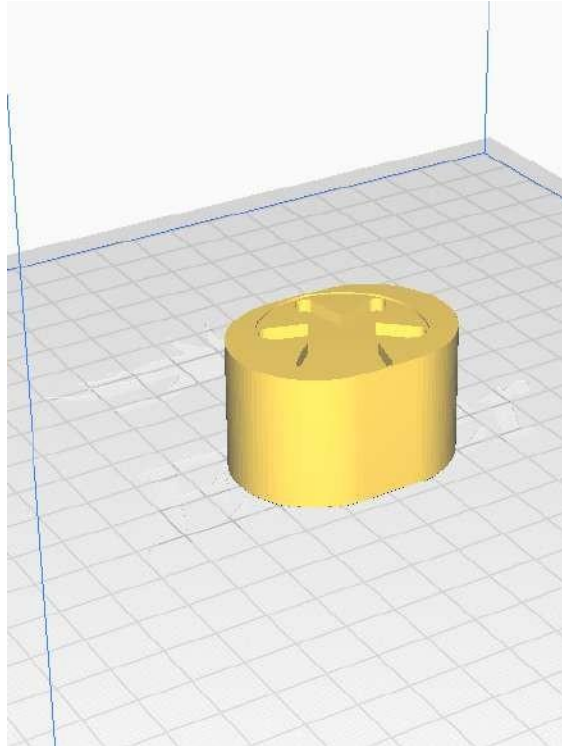


Figure 6.34: Shaft adapter between servo and valve. Source: own



Figure 6.35: Final look of the feeding system prototype. Source: own



Figure 6.36: Wooden frame. Source: own



Figure 6.37: Nozzle with two way fitting. Source: own



Figure 6.38: Adapter from the tube to the nozzle. Source: own



Figure 6.39: Printed plunger connected to the lead screw. Source: own

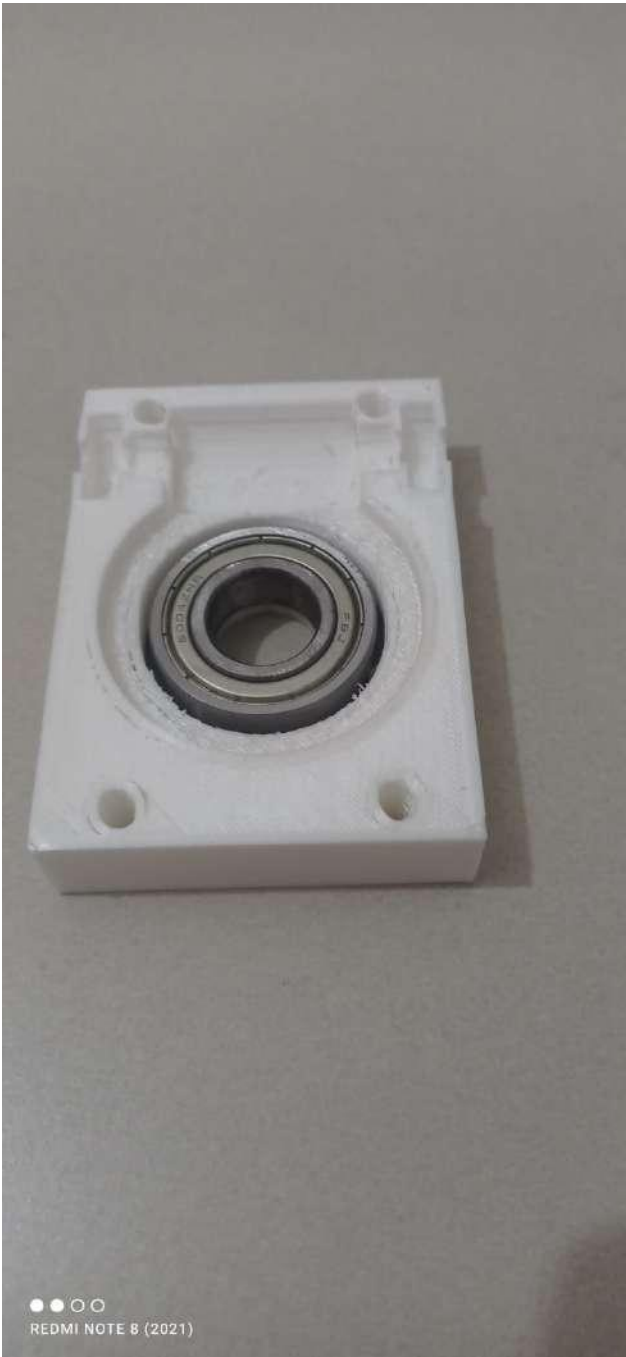


Figure 6.40: Half of the gearbox with its bearing. Source: own



Figure 6.41: Other half of the gearbox. Source: own



Figure 6.42: Crown gear for the worm-gear assembly. Source: own



Figure 6.43: Worm for the worm-gear assembly. Source: own



Figure 6.44: Ball bearings to hold the worm. Source: own

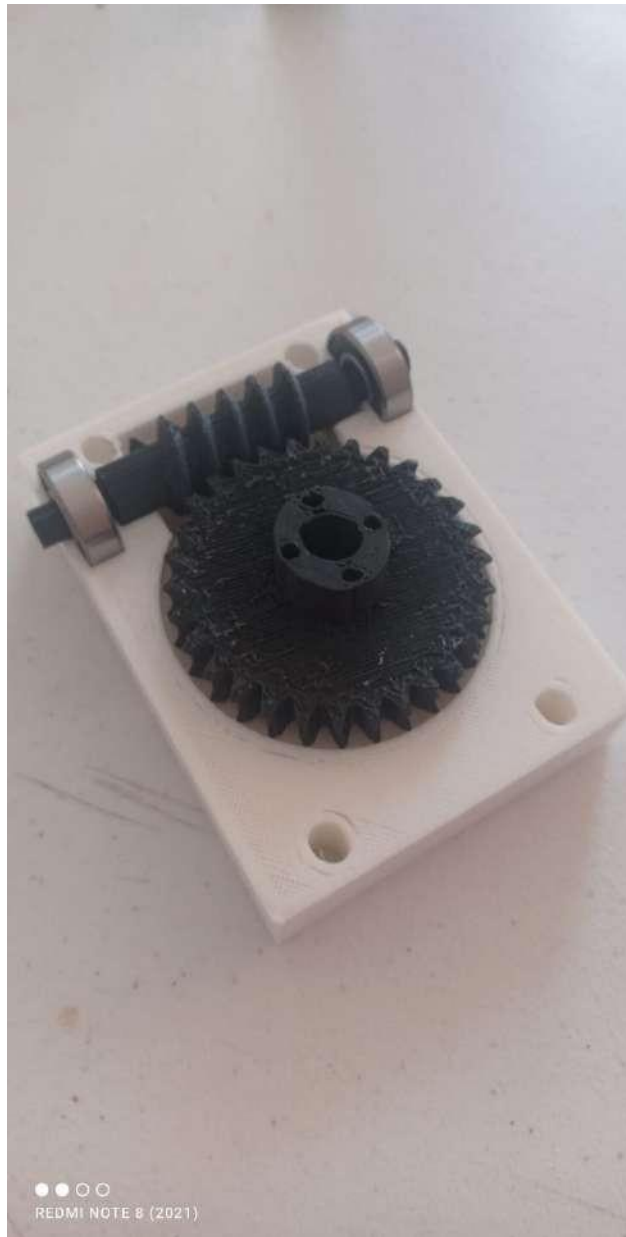


Figure 6.45: Worm-gear gearbox Assembly. Source: own

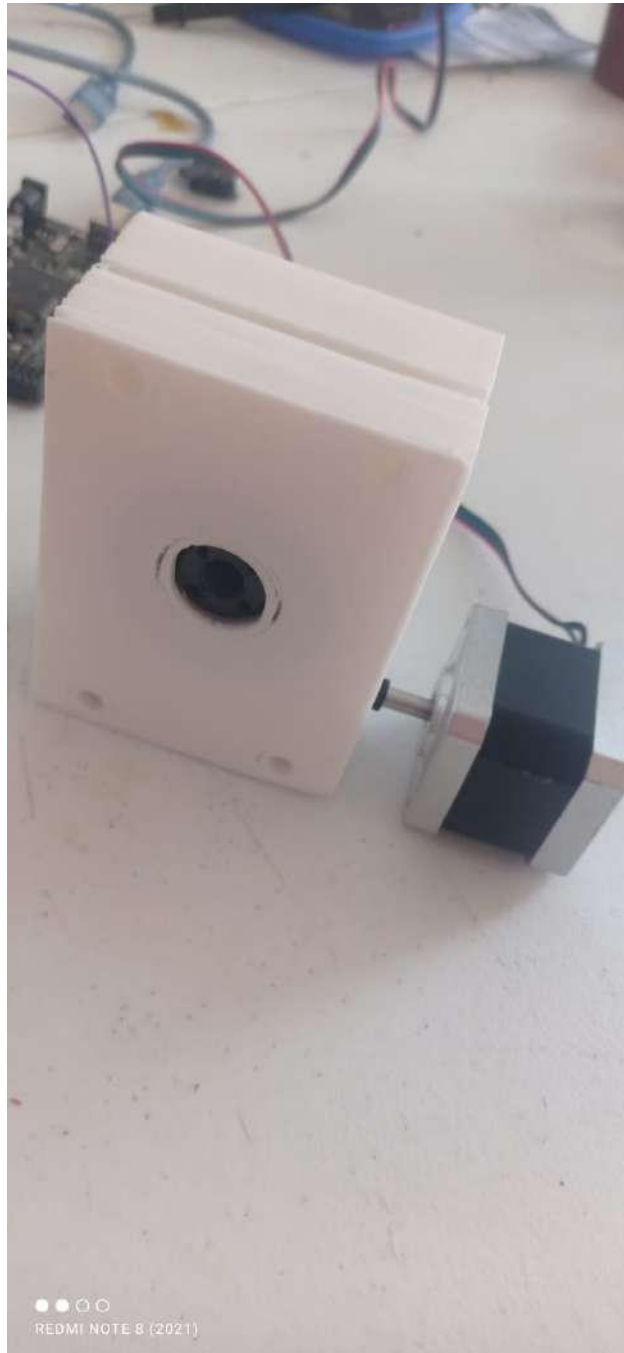


Figure 6.46: Final assembly of the worm-gear drive with stepper. Source: own

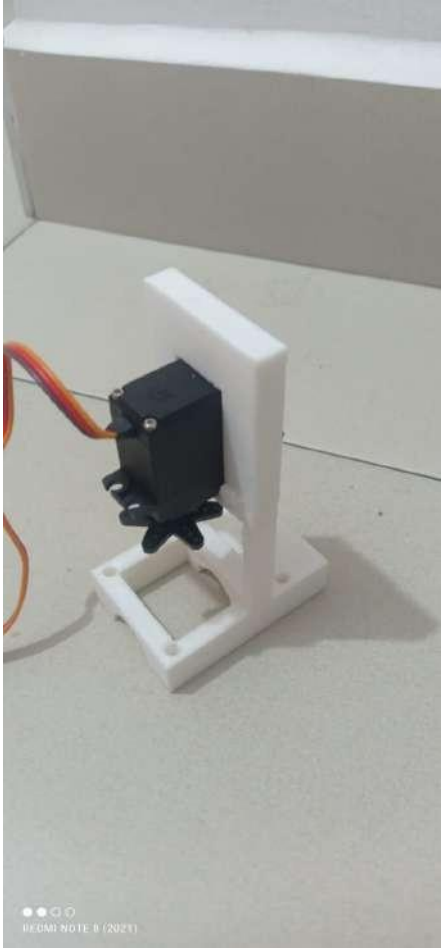


Figure 6.47: Top part of the servo and valve adapter. Source: own

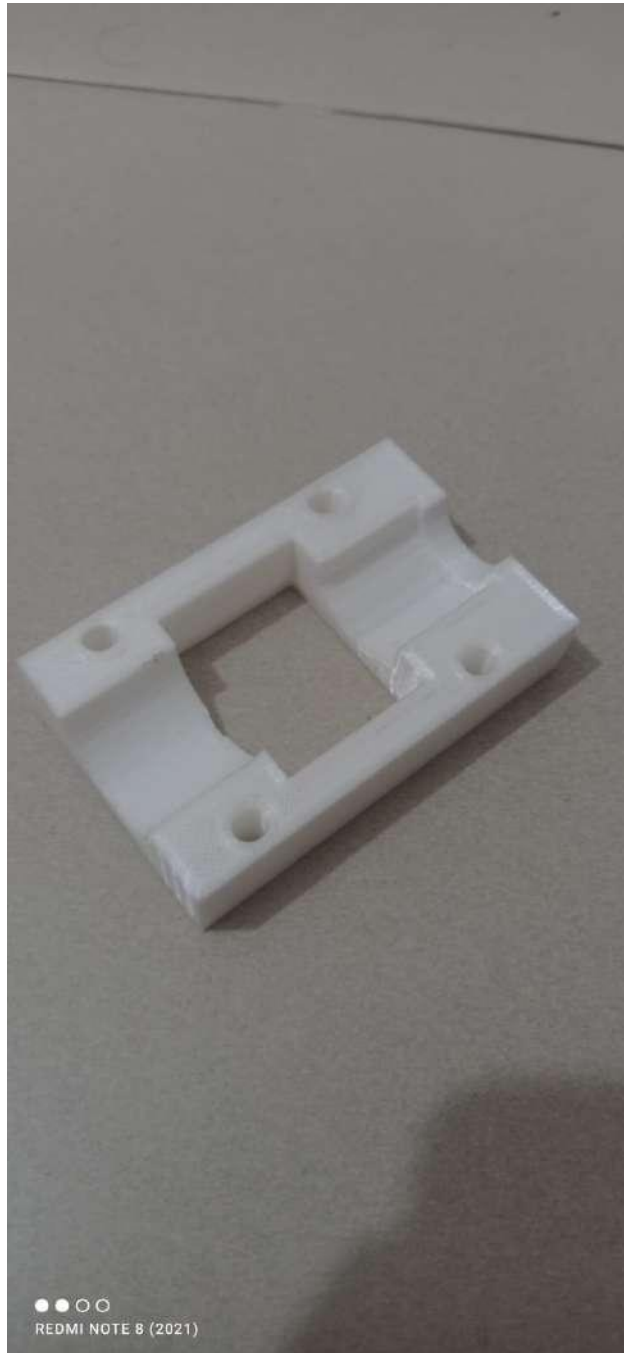


Figure 6.48: Bottom part of the servo and valve adapter. Source: own



Figure 6.49: Shaft adapter of the servo to the valve. Source: own



Figure 6.50: Modified valve to fit the shaft adapter. Source: own



Figure 6.51: Assembly of the CWS system. Source: own

Finally, the final prototype assembly is shown

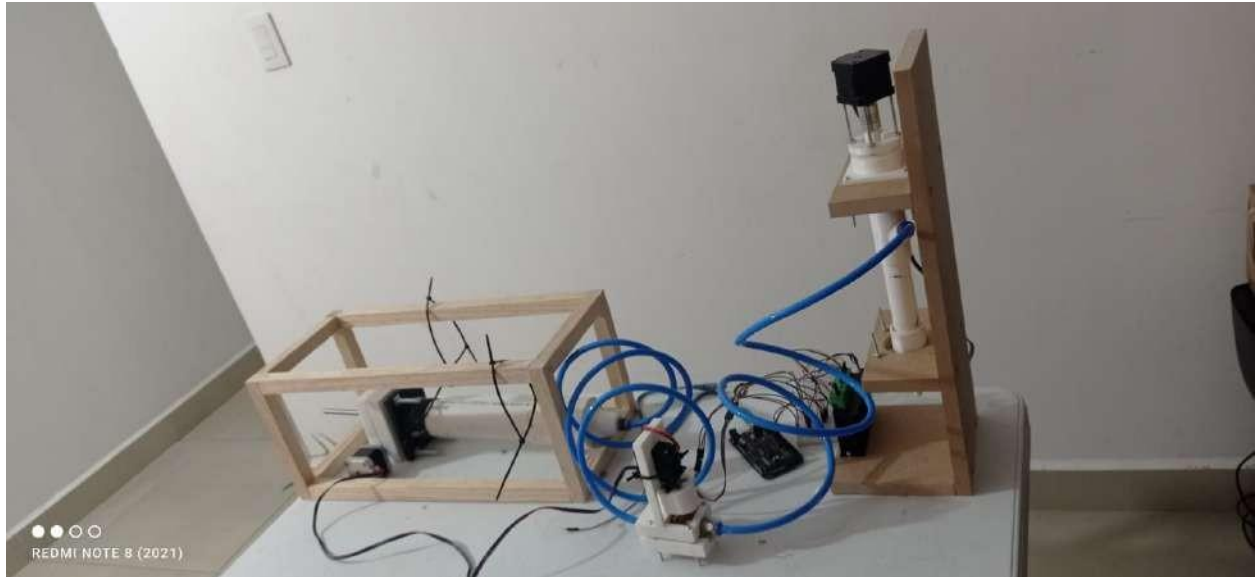


Figure 6.52: Final assembly prototype. Source: own

7Testing

For the testing, the tests performed were designed to test just core features of the system such as flow according to RPM of the motor, if the CWS system works, and use of the feeder with the extruder.

7.1Test of the CWS system

For the test of the CWS system, which is the system that combines the servo motor and the valve, the test was a simple turning of the servo by 90° to close and open the valve on a command in the serial monitor. The code used to test this is the following:

```
1 #include<Servo .h>
2
3 Servo servo 1;
4 intpinServo = 9;
5 intPULSOMIN= 300 ;
6 intPULSOMAX= 2400 ;
7
8 String inString ="";
9
10 voidsetup() {
11
12     Serial .begin( 9600 );
13
14     servo 1 .attach ( pinServo );
15
```

```
16 }
17
18 void loop() {
19
20   if( Serial.available() > 0){
21
22     int inChar = Serial.read();
23
24     if(inChar != '\n'){
25
26       inString += (char)inChar;
27
28     }else{
29
30       float angulo = inString.toFloat();
31
32       Serial.println(angulo);
33
34       servo1.write(angulo);
35
36       inString = "";
37
38     }
39
40   }
41
42 }
```

Listing 7.1: Control code for the servo

This code allows to command the servo to open or close the valve. As can be seen in the images below, both the open and close states of the shaft. How this would work is that basically whenever one feeder is empty, the servo would automatically close the valve and

open another valve for another feeder. Allowing for the workflow to be continuous.

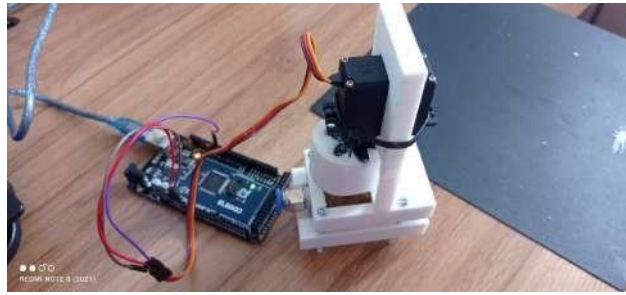


Figure 7.1: Valve opened state. Source: own



Figure 7.2: Valve closed state. Source: own

For the final configuration of the system, this would have to be related to the position of the steppers, more importantly to the position of the lead screw in the feeder, whenever the lead screw reaches the maximum position, one servo closes and the other opens.

7.2 Test of the extruder

For the extruder basically the test was to measure some relations between the flow and the revolutions of the motor. First, the clay was prepared, kneaded with approximately 25%



Figure 7.3: Preparation of the clay previous to the extruding. Source: own

of moisture content (see fig. 7.3)

Once the clay was inserted in the feeder (see fig. 7.4) this was connected directly to the extruder system. The control of the stepper was very simple, also just controlling the speed, by changing the amount of time the motor has to wait to take a step, This way the speed can be controlled very simply, just to test how this relates to the flow of the clay.

The code used to control the stepper motors is the following:

```
1  const int stepPin = 5;
2  const int dirPin = 2;
3  const int tenPin = 8;
4  int pasos = 90 * 32 / (1.8);
5  void setup() {
6    pinMode(stepPin, OUTPUT);
7    pinMode(dirPin, OUTPUT);
```



```
8  pinMode(enPin ,OUTPUT) ;
9  digitalWrite(enPin ,LOW) ;
10
11 }
12
13 voidloop() {
14  digitalWrite(dir Pin ,HIGH); //Enablesthemotortomoveinaparticular
    direction
15  for(intx = 0; x < 100 ; x++) {
16    digitalWrite(stepPin ,HIGH) ;
17    delayMicroseconds( 500 ) ;
18    digitalWrite(stepPin ,LOW) ;
19    delayMicroseconds( 500 ) ;
20  }
21  delay( 1000 ) ;
22  /* digitalWrite(dirPin,LOW); //Changesthedirectionofrotation
23  for(intx=0;x<800;x++){
24    digitalWrite(stepPin,HIGH);
25    delayMicroseconds( 500 );
26    digitalWrite(stepPin,LOW);
27    delayMicroseconds( 500 );
28  }
29  delay( 1000 ) */
30 }
```

Listing 7.2: Control code for the steppers

Once everything was assembled, the feeder was tested. The gearbox was lubricated with Grease (see fig. 7.5) to ensure a smooth movement and less wear on the gears.

The feeder was tested at a velocity of 200 rpm, expecting an output speed of 13.33 RPM and an output torque of about 4 Nm. The following image shows the extruded clay out of the feeder (see fig. 7.6).

Finally, once the feeder worked, the extruder was tested at different speeds to measure the flow of clay. Since the nozzle of 4 mm was the only one tested, the results were fed into the following table (see fig. 7.7).

In the following graph (see fig. 7.8) a trending curve was plotted to see the evolution of the flow while making the tests.

Some takeaways from this graph are:

- The more the flow stabilizes is the more the relative error minimizes in regard to expected value (see Table 4.11).
- There is an apparent trending of the flow tending to a similar value the more is let to stabilize. There is a notable difference between the extruded amount and the motor speed in the beginning, but as it goes on it seems to tend to a similar value for all speeds.
- The relative error minimizes as well, this is normal when it comes to a certain fluid flow.

Some further tests that need to be performed:

- Testing of the other nozzles to see the differences between flows.
- Trying to go into higher velocities to see if there is an asymptotic value or a limit when it comes to speed of extrusion.
- Testing the wall size, given the humidity of the clay. It has to be at least very approximate to the nozzle size.
- Calculating the necessary flow for a certain robotic arm velocity so it can develop a good wall size and a consistent flow.
- Testing retractions, to see up to what point the extruded clay can be retracted into the nozzle.



Figure 7.4: Clay inside the feeding tube. Source: own



Figure 7.5: Truper grease for lubing the worm gear. Source: own



Figure 7.6: Shape of the clay extrusion in the feeder. Source:own

	Motor speed	Time (s)	Amount of clay	Resulting flow (g/s)	Flow converted (kg/hr)	Expected value	Error	Relative error	Percentage
Test 1	10 RPM	10	4.1	0.41	1.476	0.7834	0.6926	0.884094971	88.409497
Test 2			3.2	0.32	1.152	0.7834	0.3686	0.470513148	47.051315
Test 3			2.7	0.27	0.972	0.7834	0.1886	0.240745468	24.074547
Test 4			3.3	0.33	1.188	0.7834	0.4046	0.516466684	51.646668
Test 5			3	0.3	1.08	0.7834	0.2966	0.378606076	37.860608
	Motor speed	Time (s)	Amount of clay	Resulting flow (g/s)	Flow converted (kg/hr)	Expected value	Error	Relative error	Percentage
Test 1	15 RPM	10	5.1	0.51	1.836	1.175	0.661	0.562553191	56.255319
Test 2			4	0.4	1.44	1.175	0.265	0.225531915	22.553191
Test 3			2.8	0.28	1.008	1.175	0.167	0.14212766	14.212766
Test 4			3	0.3	1.08	1.175	0.095	0.080851064	8.0851064
Test 5			2.9	0.29	1.044	1.175	0.131	0.111489362	11.148936
	Motor speed	Time (s)	Amount of clay	Resulting flow (g/s)	Flow converted (kg/hr)	Expected value	Error	Relative error	Percentage
Test 1	20 RPM	10	6	0.6	2.16	1.57	0.59	0.375796178	37.579618
Test 2			5.4	0.54	1.944	1.57	0.374	0.238216561	23.821656
Test 3			4.7	0.47	1.692	1.57	0.122	0.077707006	7.7707006
Test 4			3.9	0.39	1.404	1.57	0.166	0.105732484	10.573248
Test 5			4.2	0.42	1.512	1.57	0.058	0.036942675	3.6942675

Figure 7.7: Measurements for the tests in the extruder. Source: own

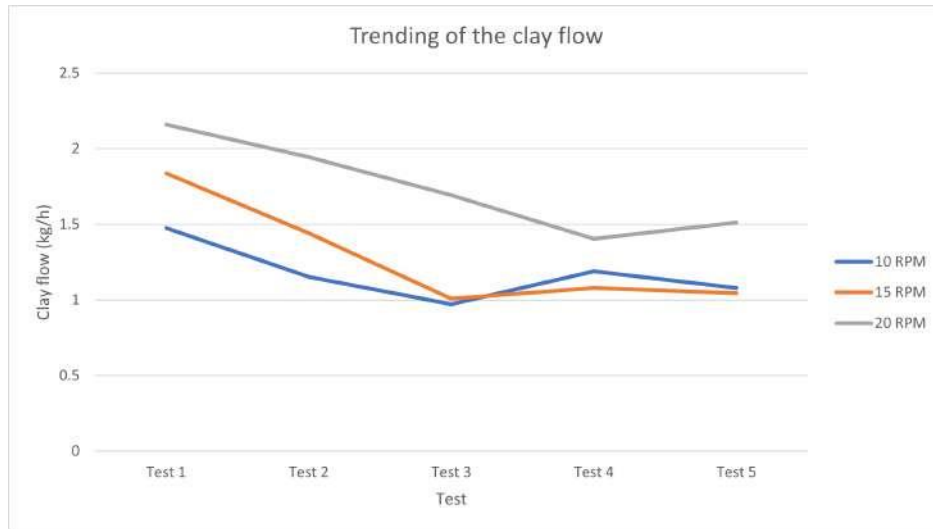


Figure 7.8: Trending curves of the evolution of the clay flow. Source: own

8 Conclusions and further studies

8.1 Conclusions

As a general conclusion, the main characteristics of the required system were met, the continuous workflow system was proposed as an arrangement of motorized valves that, with the right control system, would open and close according to the content of clay in the number of feeders that are being used. The system as a whole, contemplates four total sub systems, one for recycling in the form of a shredder, another for forming in the form of the selected pugmill and the transportation, feeding and extruding systems combination is the final stage to complete the whole machine.

For this thesis, many similar technologies were reviewed to construct the final concept of the design. Some of the best features, mostly regarding the extruding and the feeding system were used to create an extruding system that was not dependent on the amount of clay the cylinder could hold. With this in mind, a degree of innovation was achieved since there are almost no systems that achieve the continuity of the workflow this way.

Furthermore, the designs of every subsystem were achieved through calculation and space for improvement. Almost all the important parameters that these systems were based on, are free to be changed according to the conditions of the motors, the clay, and even the materials used. So, this system could be capable of be re-calculated for any given condition regardless of the current prototype.

Going further with the CWS, this was through several iterations of proposals that could achieve the status of continuous. From a pump that is constantly pumping clay into the

system, a system of cartridges, all the way to the current proposed solutions which is the feeder switch with motorized valves.

Some of the most critical parts were validated via a static finite element analysis simulation. Since some of the materials proposed were not available to use or to manufacture, this analysis gives a great insight on the behaviour of the parts, given the conditions and the final suggested materials to be used. This way a combination of 3D printed parts and machined parts work together as a final fabrication proposal. Developing a fatigue analysis will also be recommended.

After the detailed design was complete, a prototype made with 3D printing, wood and some other components was built. This prototype was used to measure some information on how it would work attached to a robotic arm. Naturally, most of the control was left out since it was beyond the scope of the thesis, so given some of the measured features and given that the error percentage was relatively small compared to the expected results (15%), what is left is to test it on the robotic arm.

Since this system is designed and calculated so the parameters of the fluid that it is extruding can be changed, many applications can be studied. Not only clay own applications like pottery, or brick-making or cockpit-like structures construction, but also, concrete, cement and some other materials considered more viscous could be also extruded with this system only changing its parameters.

8.2 Recommended improvements and further studies

Some improvements that can be proposed after the testings on the prototype. The first improvement proposed over the physical prototype is to change the materials to a more robust configuration, for example ABS to 3D print some parts like the servo-valve adapter and also consider some flexible materials mostly for the plunger, since this part really needs to cover the complete circle and also clear the clay from the walls of the cylinder.

The use of nema 23 instead of nema 17 is also recommended since this motor is more robust, offers better torque and more possibilities of adaptability, like the use of pre-fabricated worm gear gearbox to avoid the making of this part. Also, changing the couplings of the motor, from flexible to rigid would be a good idea to make a more rigid product.

Some further studies for this particular design are recommended as follows:

- 1.The development of a complete control system to test the system on the robotic arm.

This would include developing the control for the motors to ensure the flow is according to the speeds the robotic arm is moving, and also the system that monitors the content of clay in the feeders to control the motorized valves. This would include sensing, flow, pressure and positions on the motors to generate a good closed loop control.

- 2.Developments with specific types of clay, to study the torque and speeds necessary for the different properties. This would avoid the necessity of making rheological studies by working and testing directly on a specific type of clay.

- 3.Studying the properties, shapes and resistance of the products made with specific clays. For example, exploring the optimization of shape and geometry for bricks, aiming to save material with the same resistance. Other applications like the aforementioned can be investigated to test some of the results.

- 4.Finding how the design could work beyond clay. For instance exploring concrete, or exploring the possibility for it to be used in non.earth applications, like modifying it to work in a space or no gravity environment.

- 5.Developing further design optimizations such as implementing methodologies like design for manufacture, sustainability design, economical analysis for the fabrication of the system, etcétera.

9 Appendices

9.1 Appendix 1: Derivation of the Navier-Stokes equations

Deduction of the Navier-Stokes equations in the extruder cylinder.

This deduction of the equations will be inspired in (Velilla Díaz et al., 2009) who makes an approach based on the Navier-Stokes equations to obtain torque and power parameters. Using also the deduction of (Bird, Stewart, & Lightfoot, 2020).

Consider the following flow regime of a tangential flow for a fluid in between two concentric tubes.

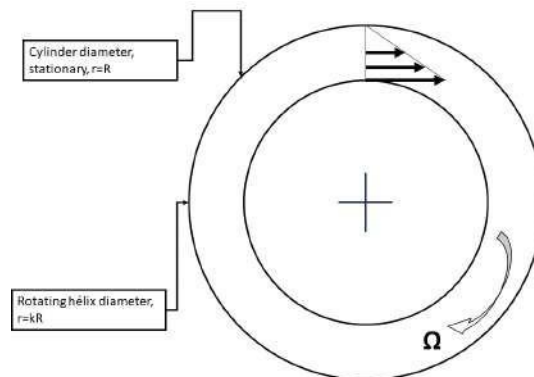


Figure 9.1: Scheme of the flow in the extruder. Source: own

Also, consider the Navier-Stokes equations for cylindrical coordinates.

Radial component:

$$\rho \frac{\partial v_r}{\partial t} + v_r \frac{\partial v_r}{\partial r} + \frac{v_\theta \partial v_r}{r \partial \theta} - \frac{v_\theta^2}{r} + v_z \frac{\partial v_r}{\partial z} = -\frac{\partial p}{\partial r} + \rho g_r$$

$$+ \mu \frac{\partial}{\partial r} \left(\frac{1}{r} \frac{\partial}{\partial r} r v_r \right) + \frac{1}{r^2} \frac{\partial^2 v_r}{\partial \theta^2} - \frac{2}{r^2} \frac{\partial v_\theta}{\partial \theta} + \frac{\partial^2 v_r}{\partial z^2} \quad (9.1)$$

Angular component:

$$\rho \frac{\partial v_\theta}{\partial t} + v_r \frac{\partial v_\theta}{\partial r} + \frac{v_\theta \partial v_\theta}{r \partial \theta} - \frac{v_r v_\theta}{r} + v_z \frac{\partial v_\theta}{\partial z} = -\frac{1}{r} \frac{\partial p}{\partial \theta} + \rho g_\theta$$

$$+ \mu \frac{\partial}{\partial r} \left(\frac{1}{r} \frac{\partial}{\partial r} r v_\theta \right) + \frac{1}{r^2} \frac{\partial^2 v_\theta}{\partial \theta^2} - \frac{2}{r^2} \frac{\partial v_r}{\partial \theta} + \frac{\partial^2 v_\theta}{\partial z^2} \quad (9.2)$$

Axial component:

$$\rho \frac{\partial v_z}{\partial t} + v_r \frac{\partial v_z}{\partial r} + \frac{v_\theta \partial v_z}{r \partial \theta} + v_z \frac{\partial v_z}{\partial z} = -\frac{\partial p}{\partial z} + \rho g_z$$

$$+ \mu \frac{1}{r} \frac{\partial}{\partial r} \left(r \frac{\partial v_z}{\partial r} \right) + \frac{1}{r^2} \frac{\partial^2 v_z}{\partial \theta^2} + \frac{\partial^2 v_z}{\partial z^2} \quad (9.3)$$

Assuming the following statements.

1. Stable state
2. Laminar flow
3. Non compressible fluid
4. Newtonian fluid
5. Continuous system

6. Hydrodynamic flow

According to (Bird et al., 2020), the radial and axial components of the velocity are zero, also there is no pressure gradient in the ϑ direction. With this, some components can disappear, but there is still the need to make a significance analysis by considering the order of magnitude each term has. Consider the following table (see fig. 9.2):

$v_r: \mathbf{O}$	$\partial v_r: \mathbf{O}$	$\partial v_r: \mathbf{I}$
$v_\theta: \mathbf{I}$	$\partial v_\theta: \mathbf{I}$	$\partial v_\theta: \mathbf{O}$
$v_z \approx \mathbf{I}$	$\partial v_z \approx \mathbf{I}$	$\partial v_z \approx \mathbf{I}$

$\frac{\partial v_r}{\partial r} \rightarrow \frac{\mathbf{O}}{\mathbf{O}} \rightarrow \mathbf{I}$	$\frac{\partial v_r}{\partial r} \rightarrow \frac{\mathbf{I}}{\mathbf{O}}$	$\frac{\partial v_r}{\partial r} \rightarrow \frac{\mathbf{I}}{\mathbf{O}}$
$\frac{\partial v_r}{\partial \theta} \rightarrow \frac{\mathbf{O}}{\mathbf{I}} \rightarrow \mathbf{O}$	$\frac{\partial v_r}{\partial \theta} \rightarrow \frac{\mathbf{I}}{\mathbf{I}} \rightarrow \mathbf{I}$	$\frac{\partial v_r}{\partial \theta} \rightarrow \frac{\mathbf{I}}{\mathbf{I}} \rightarrow \mathbf{I}$
$\frac{\partial v_r}{\partial z} \rightarrow \frac{\mathbf{O}}{\mathbf{I}} \rightarrow \mathbf{O}$	$\frac{\partial v_r}{\partial z} \rightarrow \frac{\mathbf{I}}{\mathbf{I}} \rightarrow \mathbf{I}$	$\frac{\partial v_r}{\partial z} \rightarrow \frac{\mathbf{I}}{\mathbf{I}} \rightarrow \mathbf{I}$

Figure 9.2: Significance table. Source: own

Each symbol has an established value. The **I** represents a high significance value, while the **O** represents a low significance value. This would make the partial derivatives to take into account the ones resulting **I/O**, for the following relation is true:

$$\frac{\mathbf{I}}{\mathbf{O}} \gg \mathbf{I} \gg \mathbf{O} \tag{9.4}$$

As said before the radial and axial components of the velocity are zero, but this is for the two dimensional case, since in this case the movement of the clay is advancing trough the cylinder, it cannot be considered completely zero. The component v_ϑ is still being considered of low significance. The value of ∂v_r is low significance since there is no acceleration if there is no velocity. Consider the same analysis for the partial derivatives of the other two components, giving the same values as the velocities. This results on the eliminations of the

following derivatives:

For the first equation the eliminated components are:

$$\frac{\partial v_r}{\partial t}, v_r \frac{\partial v_r}{\partial r}, \frac{v_\vartheta}{r} \frac{\partial v_r}{\partial \vartheta}, v_z \frac{\partial v_r}{\partial z}, \rho g_r, \frac{1}{r} \frac{\partial}{\partial r} r v_r, \frac{1}{r^2} \frac{\partial^2 v_r}{\partial \vartheta^2}, \frac{2}{r^2} \frac{\partial v_\vartheta}{\partial \vartheta}, \frac{\partial^2 v_r}{\partial z^2} \quad (9.5)$$

For the second equation the eliminated components are:

$$\frac{\partial v_\vartheta}{\partial t}, v_r \frac{\partial v_\vartheta}{\partial r}, \frac{v_\vartheta}{r} \frac{\partial v_\vartheta}{\partial \vartheta}, \frac{v_r v_\vartheta}{r}, v_z \frac{\partial v_\vartheta}{\partial z}, -\frac{1}{r} \frac{\partial p}{\partial \vartheta}, \rho g_\vartheta, \frac{1}{r^2} \frac{\partial^2 v_\vartheta}{\partial \vartheta^2}, \frac{2}{r^2} \frac{\partial v_r}{\partial \vartheta}, \frac{\partial^2 v_\vartheta}{\partial z^2} \quad (9.6)$$

For the third equation the eliminated components are:

$$\frac{\partial v_z}{\partial t}, v_r \frac{\partial v_z}{\partial r}, \frac{v_\vartheta}{r} \frac{\partial v_z}{\partial \vartheta}, v_z \frac{\partial v_z}{\partial z}, \rho g_z, \frac{1}{r^2} \frac{\partial^2 v_z}{\partial \vartheta^2}, \frac{\partial^2 v_z}{\partial z^2} \quad (9.7)$$

Yielding the following resulting equations for the three components:

For the radial component

$$-\rho \frac{v_\vartheta^2}{r} = -\frac{\partial p}{\partial r} \quad (9.8)$$

For the angular component

$$\mu \frac{\partial}{\partial r} \frac{1}{r} \frac{\partial}{\partial r} r v_\vartheta \quad (9.9)$$

And for the axial component

$$-\frac{\partial p}{\partial z} + \mu \frac{1}{r} \frac{\partial}{\partial r} r \frac{\partial v_z}{\partial r} = 0 \quad (9.10)$$

To obtain the torque and power needed the selected equation to expand is the equation resulting from the angular component. To solve this, it is needed to use a method to solve the differential equation for the velocity:

The differential equation can be integrated two times:

$$\frac{1}{r} \frac{\partial}{\partial r} r v_{\vartheta} = C_1 \quad (9.11)$$

$$r v_{\vartheta} = \frac{r^2}{2} C_1 + C_2 \quad (9.12)$$

$$v_{\vartheta} = \frac{r}{2} C_1 + \frac{1}{r} C_2 \quad (9.13)$$

The boundary conditions for the fluid are obtained by looking at the diagram in fig. 9.1.

The first boundary condition is when $r = R$, $V_{\theta} = 0$

The second one is when $r = kR$, $v_{\vartheta} = \Omega_{\vartheta} kR$

replacing the first boundary condition on the resulting equation for the velocity:

$$0 = \frac{R}{2} C_1 + \frac{1}{R} C_2 \quad (9.14)$$

$$C_2 = -\frac{R^2}{2} C_1 \quad (9.15)$$

Replacing the value of the second boundary condition and considering the result for C_2 :

$$\Omega_{\vartheta} kR = \frac{kR}{2} C_1 - \frac{1}{kR} \left(\frac{R^2}{2} C_1 \right) \quad (9.16)$$

$$C_1 = \frac{\Omega_{\vartheta} kR}{\left(\frac{kR}{2} - \frac{R}{2k} \right)} \quad (9.17)$$

replacing the values for the two constants in the original velocity equation:

$$v_{\vartheta} = \frac{r}{2 \left(\frac{kR}{2} - \frac{R}{2k} \right)} \Omega_{\vartheta} kR + \frac{1}{r} \left(-\frac{R^2}{2} \frac{\Omega_{\vartheta} kR}{\left(\frac{kR}{2} - \frac{R}{2k} \right)} \right) \quad (9.18)$$

Arranging the values:

$$v_{\vartheta} = \Omega_{\vartheta} k R \frac{r}{kR - \frac{R}{k}} - \frac{R^2}{rkR - \frac{Rr}{k}} \quad ! \quad (9.19)$$

With this equation, considering a Bingham type of flow and the law for Newtonian fluids, the shear stress can be obtained:

$$\tau_{r\vartheta} = -\mu \left(r \frac{\partial}{\partial r} \left(\frac{v_{\vartheta}}{r} \right) + \frac{1}{r} \frac{\partial v_r}{\partial \vartheta} \right) + \tau_0 \quad (9.20)$$

Neglecting the acceleration on the radial component, and replacing the value of the obtained angular velocity, the following is obtained:

$$\tau_{r\vartheta} = -\mu r \left(\frac{\partial}{\partial r} \left(\frac{\Omega_{\vartheta} k R \frac{r}{kR - \frac{R}{k}} - \frac{R^2}{rkR - \frac{Rr}{k}}}{r} \right) \right) + \tau_0 \quad (9.21)$$

The first term of the derivative is cancelled due to it being a constant:

$$\tau_{r\vartheta} = -\mu r \Omega_{\vartheta} k R \frac{3R^2}{r^2 k R - \frac{Rr^2}{k}} + \tau_0 \quad (9.22)$$

Shortening the equations this yields:

$$\tau_{r\vartheta} = -\mu \Omega_{\vartheta} k \frac{3R^2}{r^2 k - \frac{r^2}{k}} + \tau_0 \quad (9.23)$$

Having the behavior of the shear stress the force can be calculated as well to obtain the required motor torque. The force differential is the same as:

$$dF = \tau_{r\vartheta} dA_{\text{contact}} \quad (9.24)$$

So what's needed is to calculate the differential for the contact area, since there is no clear contact area, the best course of action would be to calculate the contact surface. The following image illustrates this in a better way

Since the total area is the sum of the total helices, the area differential must contemplate

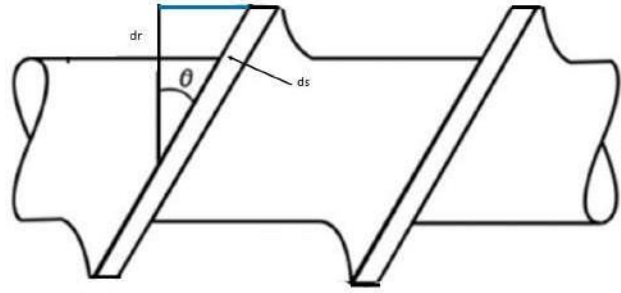


Figure 9.3: Differential surface area for the screw. Source: own

the number of helices and both faces of each helix, as follows:

$$dA = 2n2\pi r ds \tag{9.25}$$

According to fig. 9.3 ds can be calculated as the projection of the radial differential, which would be:

$$ds = \frac{dr}{\cos\vartheta} \tag{9.26}$$

Now replacing dr on the original dA

$$dA = \frac{4n\pi r - r_{axis} dr}{\cos\vartheta} \tag{9.27}$$

Replacing dA on dF, the following is obtained:

$$dF = - \mu\Omega\vartheta k \frac{3R^2 - r^2}{r^2 k - \frac{r^2}{k}} + \tau_0 \frac{4n\pi r - r_{axis} dr}{\cos\vartheta} \tag{9.28}$$

The maximum shear stress is on r=R, so the resulting equation would be:

$$dF = - \frac{\mu\Omega\vartheta 3k}{k - \frac{1}{k}} + \tau_0 \frac{4n\pi r - r_{axis} dr}{\cos\vartheta} \tag{9.29}$$

All left to do is integrate to obtain the force

$$F = - \frac{\mu \Omega_{\vartheta} 3k}{k - \frac{1}{k}} + \tau_0 \frac{4n\pi \left(\frac{r^2}{2} - r_{axis} r \right) \Big|_{r=R}}{\cos \vartheta} \quad (9.30)$$

Now replacing r for the value of the maximum shear stress

$$F = - \frac{\mu \Omega_{\vartheta} 3k}{k - \frac{1}{k}} + \tau_0 \frac{4n\pi \left(\frac{R^2}{2} - r_{axis} R \right)}{\cos \vartheta} \quad (9.31)$$

Now the required torque for the motor can be calculated by multiplying the helix radius.

$$T = F * r_{helix} = - \frac{\mu \Omega_{\vartheta} 3k}{k - \frac{1}{k}} + \tau_0 \frac{4n\pi \left(\frac{R^2}{2} - r_{axis} R \right)}{\cos \vartheta} r_{helix} \quad (9.32)$$

Finally obtained the power as well:

$$P = T * \Omega_{\vartheta} = -\Omega_{\vartheta} \frac{\mu \Omega_{\vartheta} 3k}{k - \frac{1}{k}} + \tau_0 \frac{4n\pi \left(\frac{R^2}{2} - r_{axis} R \right)}{\cos \vartheta} r_{helix} \quad (9.33)$$

9.2 Appendix 2: Stepper motor basics

Working principles of a stepper motor

A stepper motor is an electric motor which main characteristic is that it rotates a certain amount of degrees, this is called a step. The stepper motor is formed by an stator and a moving part which is the rotor. The stator is made out of some certain teeth, and on each tooth there are coils wired, the rotor is either a permanent magnet or an iron core. The following picture illustrates the stator and the rotor (see fig. 9.4).

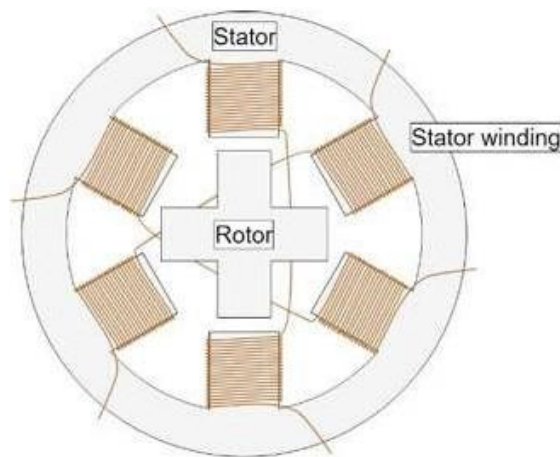


Figure 9.4: Cross section of a stepper motor. Source: (MPS, 2022)

This will rotate by energizing these coils mentioned before, by doing this a magnetic field is generated, and since the rotor is a magnet it aligns with the generated field. Naturally, by changing the energy through the coils this will make the rotor move a desired amount of degrees.

The different types of stepper motor depend on their construction. First, the different types of rotor are as follows:

1. Permanent magnet: a permanent magnet aligns naturally with the magnetic fields generated by the stator. The use of permanent magnets guarantee good torque and a detent torque (it can hold its position even when it is not energized). The setback is going to be a lower speed and a lower step resolution.

2. variable reluctance rotor: this is made out of an iron core that has a specific shape that aligns with the magnetic field. Almost contrary to the permanent magnet rotor, this option achieves better speeds and resolutions, but lower torques and no detent torque.
3. Hybrid: is the combination of both the permanent one and the variable reluctance one. In this case, the rotor is also shaped, but it is magnetized, this allows for the motor to have the advantages of the previous two. Since this requires a more complex construction, the cost for these type of motors is higher.

The different types of stator also affect the way the motor works. The stator can be define by the number of phases or independent coils. The number of phases is the number of independent coils and the pole pairs are the number of pair teeth that arein the motor. In this case, the are, two-phase, which is the most common one, also there are three-phase and five-phase, as can be seen on fig. 9.5.

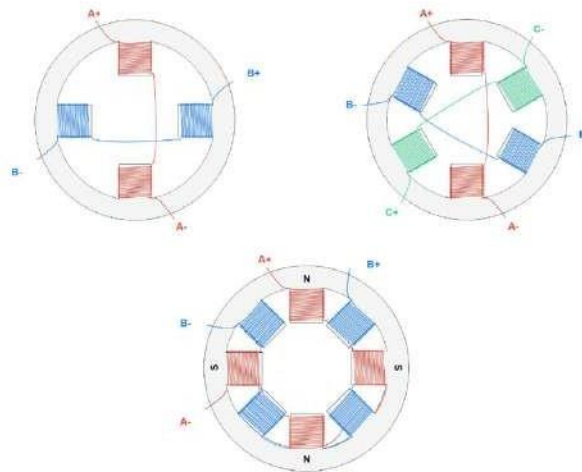


Figure 9.5: Two, three and five-phase stators. Source: (MPS, 2022)

Stepper motor control

As the motor needs the coils to be energized in a certain sequence, several devices are used to supply the necessary voltage to each coil. These devices are as follows:

- A transistor bridge which controls the electrical supply of each coil. Basically these bridges work as a switch interrupters, and for each coil one bridge is required.
- A pre-driver is also needed to activate the transistor.
- A micro controller is needed in turn to control the pre driver, this would be programmed by the user.

Drivers for the motor are also different for different features and applications. Some of these types are as follows:

- Step/direction: this works by sending a pulse to the step pin to perform a step, also controlling the direction.
- Phase/enable: for this, the phase determines the direction of the current and the activates enable if the phase is energized.
- PWM: controls the gate signals of the low-side and high-side FETs.

The drivers will also have to be able to control the voltage or the current. Depending of the control they offer, the torque and speed will be affected, being the control of the current a better choice over the control of this characteristics.

Some advantages and disadvantages

Advantages of these motors include:

- 1.They do not require a sensor to detect the motor position. Since the motor works by performing steps, the position can be know by just counting the number of steps in a given time.
- 2.The control is pretty simple, even though it requires a driver, it does not require calculations to work.
- 3.These motor offer good torque at low speeds and are great to hold position.

Disadvantages include:

- 1.If the torque is too high they could miss a step which could lead to unknown positions of the shaft and thus, inaccurate control.
- 2.The motors drain a lot of current, which could lead to efficiency loss and overheating.
- 3.Usually they offer low torques and are noisy at high speeds.

9.3 Appendix 3: Finite element method

Finite element method principles

The finite element method (FEM) is a tool for the numerical solution of the partial differential equations that are present in the analysis of a continuum (Papadopoulos, 2010). In 1941 R. Courant introduced the concept of discretization. Discretization, according to (Papadopoulos, 2010) and (Hsu, 2018), the process by which a continua or complex geometry is divided and fully defined by a finite number of degrees of freedom or elements.

These elements are interconnected at specific points the more notables called nodes, which are the intersections at corners. And for each of these elements an equation is derived, which then is going to be assembled into an overall structural equation.

Consider a deformable solid object subjected to loads in fig. 9.6. These loads can be anything from forces, pressure, heat, or others

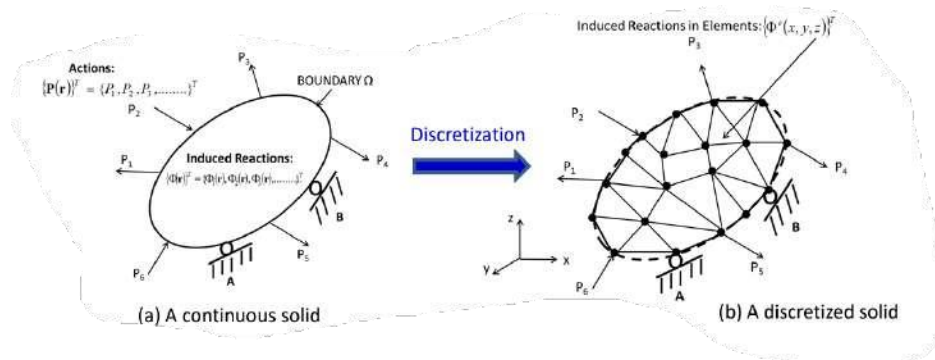


Figure 9.6: Continuous solid vs discretized object. Source: (Hsu, 2018)

Depending on the order of the geometry, if it is a 1D object, a 2D or 3D, there are some common geometric elements used to represent the object.

- 1.Bar elements: for 1D objects and beams.
- 2.Triangular or quadrilateral: for plane structures.
- 3.Torus elements: for axisymmetric geometries such as cylinders.

4. Tetrahedrons and hexahedrons: for 3D objects.

Once the object subjected to analysis is discretized, the next step is to identify the primary unknown quantities for the analysis, which have also common quantities according to the study (Hsu, 2018):

1. Stress analysis: displacements as vectors. Normally represented with $U^T = U_x, U_y, U_z$

2. Heat analysis: a temperature T in the object.

3. Fluid analysis: velocities as vectors. Normally represented with $V^T = V_x, V_y, V_z$

After defining the primary unknown quantity, a secondary unknown quantity can also be defined by using established relations with the primary ones. For example strain, for a stress analysis.

The third step is to derive interpolation functions. These functions relate to the primary quantities in the elements to those at the associated nodes of the same element (Hsu, 2018). The general form is as follows:

$$\Phi(\mathbf{r}) = [N(\mathbf{r})]\phi \quad (9.34)$$

Where,

$\Phi(\mathbf{r})$: is the primary unknown quantity of the element.

\mathbf{r} : is a position vector either in rectangular coordinates or cylindrical.

$[N(\mathbf{r})]$: is the interpolation function in a matrix form.

ϕ : the same primary quantities at the associate nodes of the same element.

A derivation of the interpolation function for simplex elements with scalar quantities at nodes. Take the fig. 9.7 and the following statements to define a simplex element.

1. The elements are connected to other elements at their nodes only.

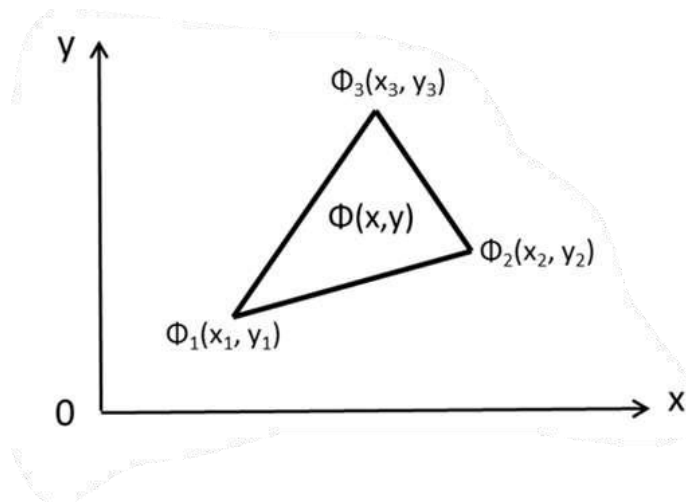


Figure 9.7: Simplex element. Source: (Hsu, 2018)

2.the primary quantity in each of these elements are related to their nodes by linear relationships.

In fig. 9.7 the primary quantity $\Phi(x, y)$ can be related by the following linear expression:

$$\Phi(x, y) = [N(x, y)] \begin{bmatrix} \phi_1 \\ \phi_2 \\ \phi_3 \end{bmatrix} \tag{9.35}$$

To derive the function $N(x, y)$ it needs to be assumed that the function is represented by a linear polynomial function (since this has three elements the polynomial function need to be of third grade and the function needs to give the most amount of information), with the following mathematical form:

$$\Phi(x, y) = \alpha_1 + \alpha_2x + \alpha_3y = [1, x, y] \begin{bmatrix} \alpha_1 \\ \alpha_2 \\ \alpha_3 \end{bmatrix} = [R]^T [\alpha] \tag{9.36}$$

The matrix $[R]^T$ and the coefficients $[\alpha_1, \alpha_2, \alpha_3]$ are constants that can be determined by substituting the specified coordinate of the nodal values ϕ_1, ϕ_2, ϕ_3 , which would yield:

$$\phi_1 = \alpha_1 + \alpha_2 x_1 + \alpha_3 y_1 \quad (9.37)$$

And so on and so forth for the other two elements of ϕ , which ins a matrix form is:

$$[\phi] = [A][\alpha] \dots \text{and} \dots [\alpha] = [A]^{-1} = [h][\phi] \quad (9.38)$$

The matrix [h] takes the form:

$$[h] = \frac{1}{|A|} \begin{bmatrix} x_2 y_3 - x_3 y_2 & x_3 y_1 - x_1 y_3 & x_1 y_2 - x_2 y_1 \\ y_2 - y_3 & y_3 - y_1 & y_1 - y_2 \\ x_3 - x_2 & x_1 - x_3 & x_2 - x_1 \end{bmatrix} \quad (9.39)$$

The determinant can be evaluated as:

$$|A| = (x_1 y_2 - x_2 y_1) + (x_2 y_3 - x_3 y_2) + (x_3 y_1 - x_1 y_3) = 2A \quad (9.40)$$

Where A is the plane area of the triangular element in fig. 9.7. By substituting all of this the function $\Phi(x, y)$ can be evaluated to:

$$\Phi(x, y) = [R]^T [h][\phi] \quad (9.41)$$

So, the interpolation form should have the following form:

$$[N(x, y)] = [R]^T [h] \quad (9.42)$$

For this method of course, there are a lot and more complex methods depending on the requirements, the bodies and the forces. For example, the Galerkin method, collocation method, point-collocation methods, subdomain-collocation method, least-squares method, composite method, and many more (Papadopoulos, 2010), but these all relate more to computation, since this is not the objective of this appendix, these methods are not going to be

investigated further.

Once the interpolation function is determined (which in the previous derivation is just one of the examples of the mentioned function), a relationship between the external actions needs to be set as reactions. For example, for stress analysis, the actions would be forces and the reactions would be displacements, strains and stresses. And, after this point is where the methods of deriving element equations are used to determine the relationship between the actions and reaction in the discrete continuum.

9.4 Appendix 4: Process for material selection

According to (Solá Marcillo, 2009) practically all products in the industry nowadays are made out of engineering materials, which is a material developed to fulfill a specific function or application. For engineering purposes materials can be subdivided into five categories; metals, ceramics, polymers, composites and naturals.

Depending on the conditions that the material could be subjected the properties can also be categorized in certain classes like general, where density or price come into place; mechanic, where properties like Young's modulus, shear modulus, yield stress, and other are the ones that are important; thermal, where properties like melting point, thermal conductivity or specific heat are important; electrical, where properties like resistance, dielectric constant and impedance are important; and other kinds of properties like optic, sound or environmental.

There are a series of factors that intervene in the material selection such as physical factors like shape, size, geometry, weight which may establish the first constraints like the number of pieces, posterior processes and cost. Then mechanical factors are taken into account to make sure the material resist any kind of external loads. Later, processing also needs to be considered as for how the parts are going to be made, and then, life cycle, cost and technology availability and even norms.

(Ashby & Cebon, 2005) proposes a general flow chart on how to proceed to the material selection:

1. Translating design requirements
2. Constraints establishment
3. Rank the material that can be useful
4. Seek for supporting information

In order to rank the materials indices can be derived to know quantitatively how they would perform according to the desired requirements. To derive a performance index let's call it P:

$$P = [(Functional - requirements, F), (Geometric - parameters, G), (Material - properties, M)] \quad (9.43)$$

or in another way

$$P = f(F, G, M) \quad (9.44)$$

P can be separated in three separate functions for each parameter

$$P = f_1(F) \cdot f_2(G) \cdot f_3(M) \quad (9.45)$$

Some common material indices are (Ashby & Cebon, 2005):

Table 9.1: Common material indices. Source: (Ashby Cebon, 2005)

Function, objective and constraint	Index
Tie, minimum weight, prescribed stiffness	$\frac{E}{\rho}$
Beam, minimum weight, prescribed stiffness	$\frac{E^{1/2}}{\rho}$
Beam, minimum weight, prescribed strength	$\frac{\sigma_y^{2/3}}{\rho}$
Beam, minimum cost, prescribed stiffness	$\frac{E^{1/2}}{C_m \rho}$
Beam, minimum cost, prescribed strength	$\frac{\sigma_y^{2/3}}{C_m \rho}$

A general process to follow when selecting materials, as (Ashby & Cebon, 2005) explains it:

1. Define design requirements

- Function: what does the component do?
- Constraints: essentials that MUST be met.

- Objective: what needs to be optimized.
 - Free variables: what can be "played" with.
2. Develop equations for constraints if necessary.
 3. Develop an equation for the objective to optimize.
 4. Identify free variables.
 5. Substitute these variable into the objective equation.
 6. Group the variables into the groups: functional geometry and material properties.
 7. Compare the performance to the functions that need to be optimized.

An example of the use of the property charts can be seen on fig. 9.8 where a limit of an elasticity modulus is set and a material index is set as well (the straight with a slope) after those are correlated through the map, a search region is born to look for the materials that achieve the requirements.

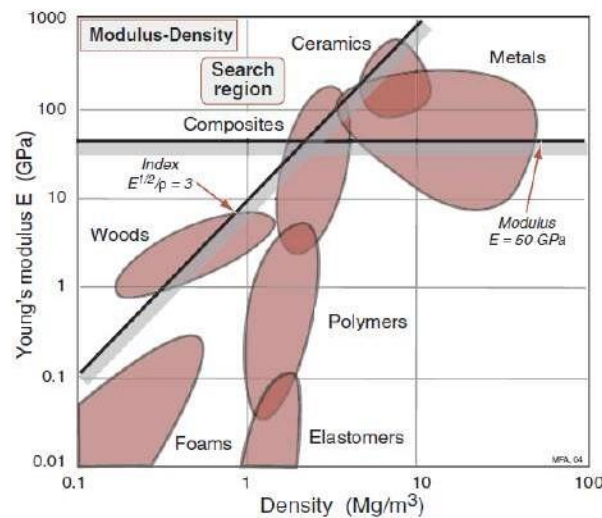
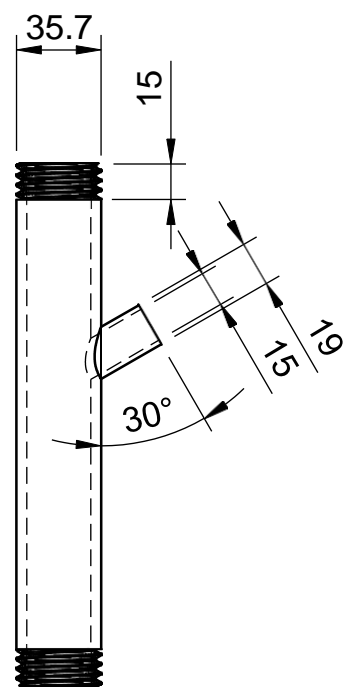
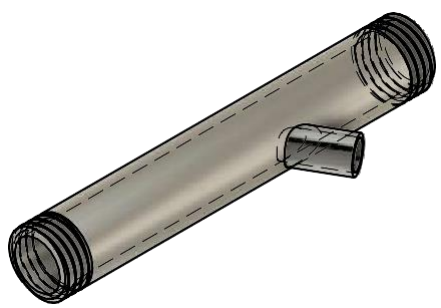
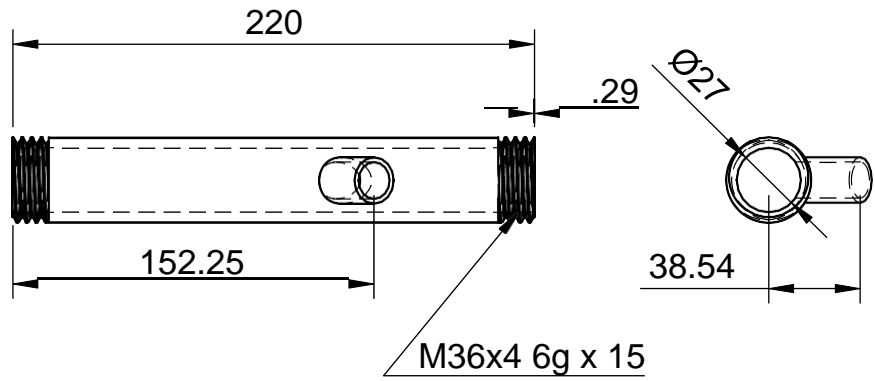


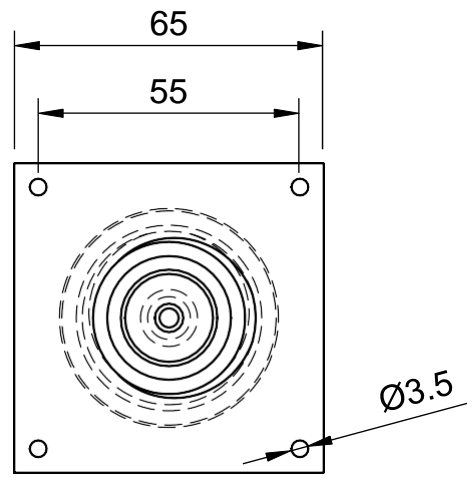
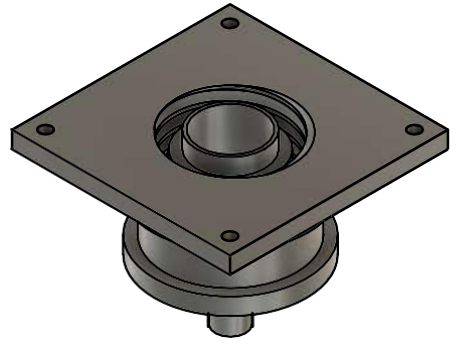
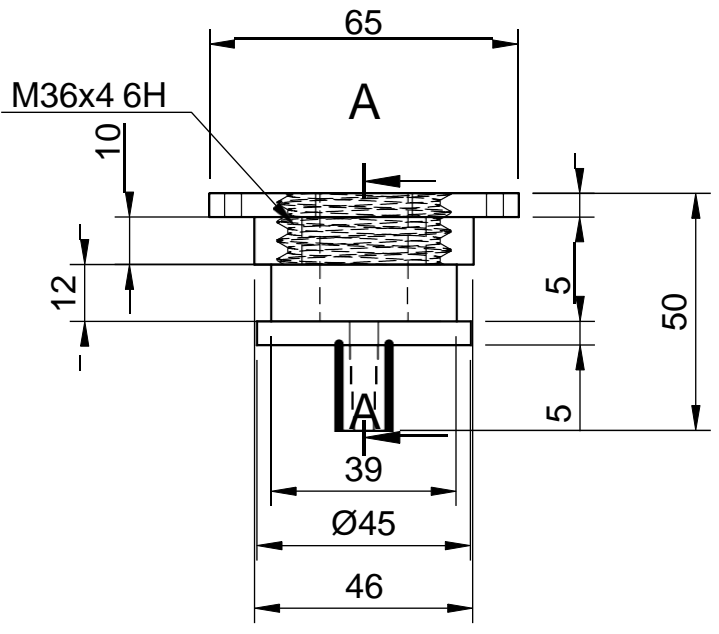
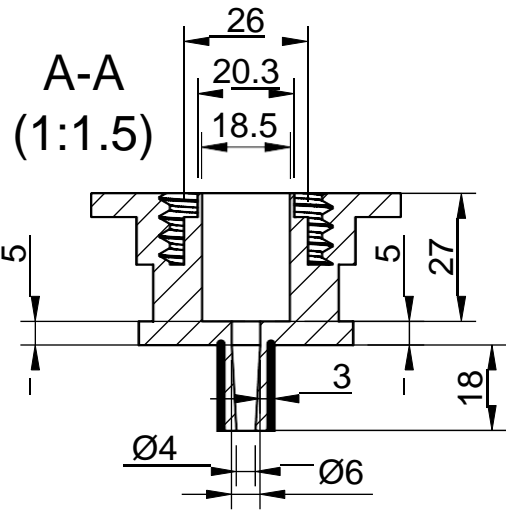
Figure 9.8: Example of an use of an Ashby chart given a set limit and a performance index. Source: (Ashby Cebon, 2005)

9.5 Appendix 5: Fabrication drawings

Note: for the fabrication planes the materials and manufacturing processes are related to the fabrication proposal and not to the prototype.

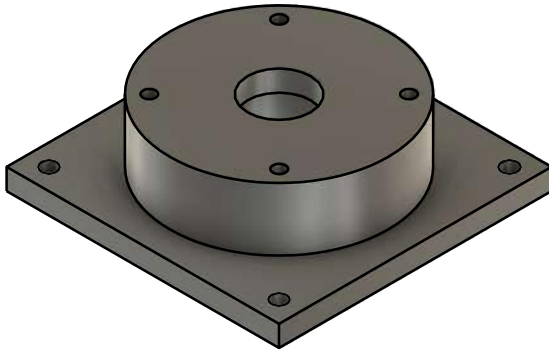
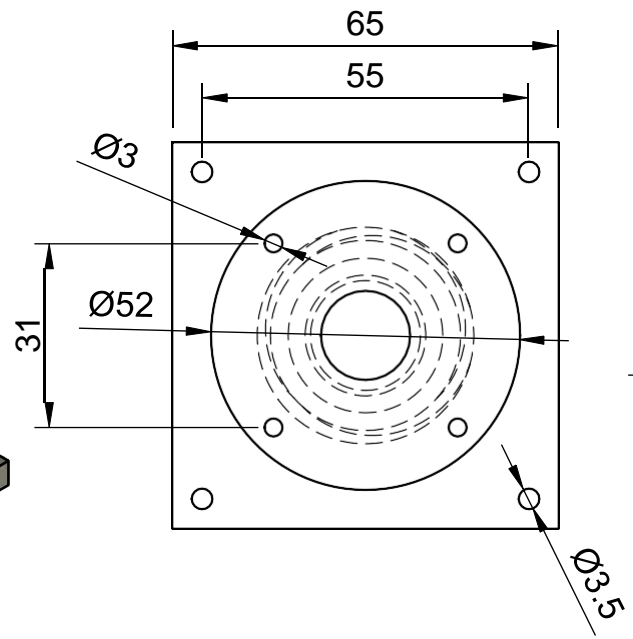
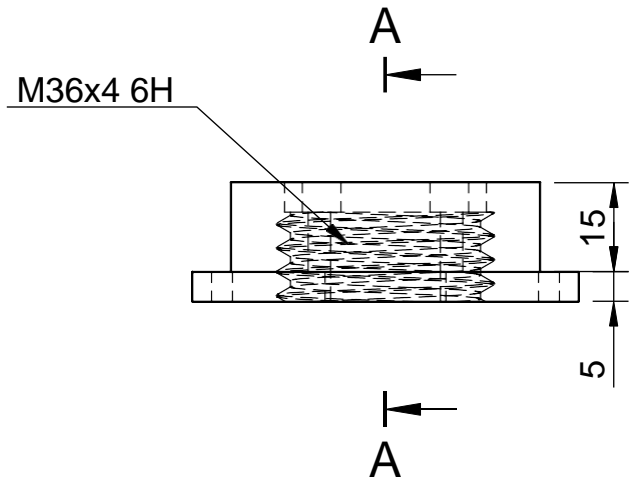
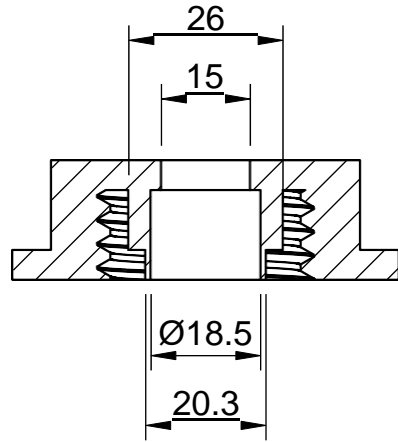


		Scale 1:3		Projection 	
		Manufacturing process Turning and welding		Material Stainless Steel AISI 304	
Dept. Facultad de Ingeniería	Technical reference Extr-1	Created by Giovanni Torres 24/11/2023		Mother part Extruder system	
		Document type Technical Drawing		Dimensions units mm	
		Title Main_Body_1		DWG No. Extr-01	
		Version V9	Date of issue 24-11-2023	Sheet 1/1	

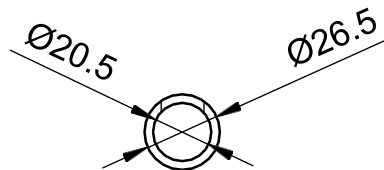
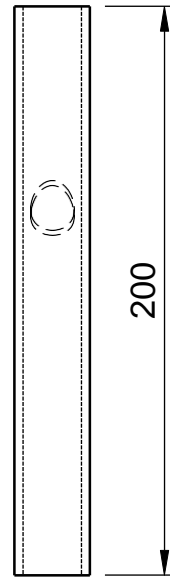
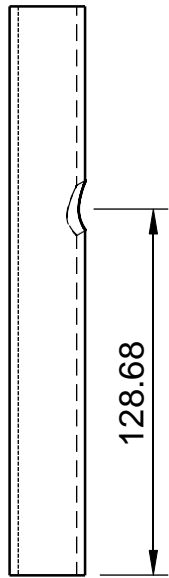


		Scale 1:1.5		Projection 	
		Manufacturing process Extrusion		Material ABS with stainless steel tip	
Dept. Facultad de Ingenieria	Technical reference Extr-2	Created by Giovanni Torres 25/11/2023		Mother part Extruder system	
		Document type Technical Drawing		Dimensions units mm	
		Title Nozzle_4 mm		DWG No. Extr-02	
		Version V1	Date of issue 24-11-2023	Sheet 1/1	

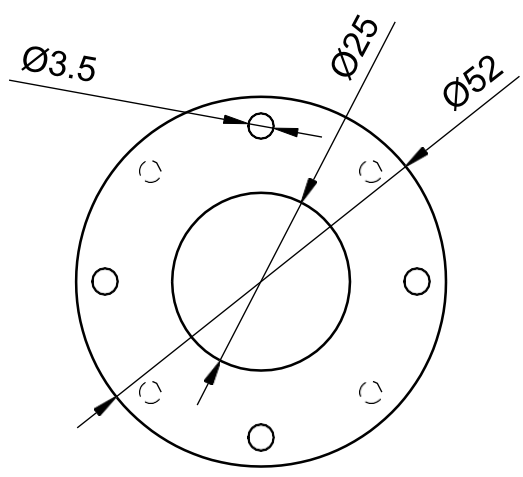
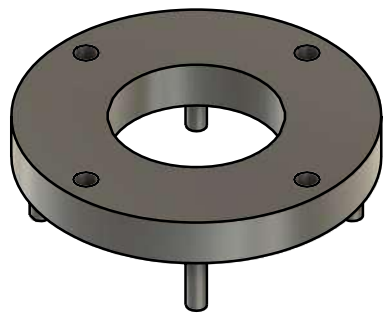
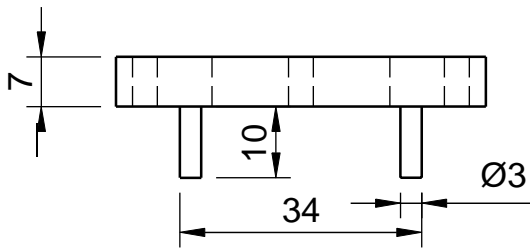
A-A (1:1.2)



		Scale 1:1.2		Projection 	
		Manufacturing process 3D Printing		Material ABS	
Dept. Facultad de Ingeniería	Technical reference Extr-3	Created by Giovanni Torres 25/11/2023		Mother part Extruder system	
		Document type Technical drawing		Dimensions units mm	
		Title Lid_1		DWG No. Extr-03	
		Version V1	Date of issue <25-11-2023>	Sheet 1/1	



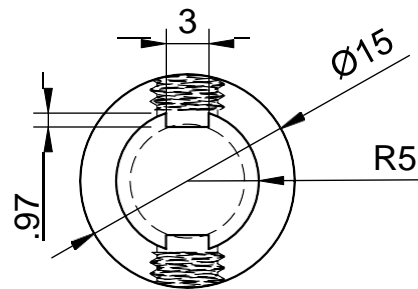
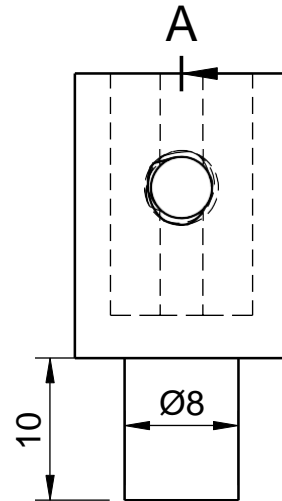
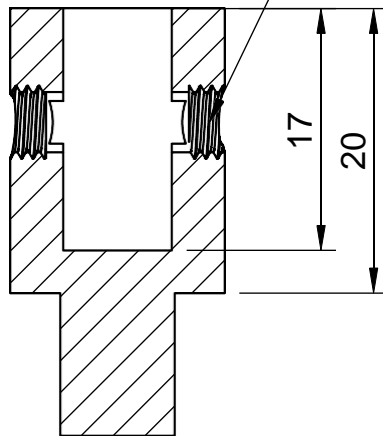
		Scale 1:2.5		Projection 	
		Manufacturing process		Material Stainless Steel AISI 304	
Dept. Facultad de Ingeniería	Technical reference Extr-4	Created by Giovanni Torres 25/11/2023		Mother part Extruder system	
		Document type Technical Drawing		Dimensions units mm	
		Title Tubo_PVC_26.5mm		DWG No. Extr-04	
		Version V4	Date of issue 24-11-2023	Sheet 1/1	



		Scale 1:1		Projection 	
		Manufacturing process		Material Nylon	
Dept. Facultad de Ingeniería	Technical reference Extr-5	Created by Giovanni Torres 25/11/2023		Mother part Extruder system	
		Document type Technical drawing		Dimensions units mm	
		Title Stepper motor mount		DWG No. Extr-05	
		Version V4	Date of issue 24-11-2023	Sheet 1/1	

A-A (2:1)

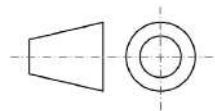
M5x0.8 6H x 2.5



Scale

2:1

Projection



Manufacturing process

Machining

Material

Steel

Dept.

Facultad de Ingeniería

Technical reference

Extr-6

Created by

Giovanni Torres 25/11/2023

Mother part

Extruder system

Document type

Technical Drawing

Dimensions units

mm

Title

Adapter for 10 mm screw

DWG No.

Extr-06

Version

V3

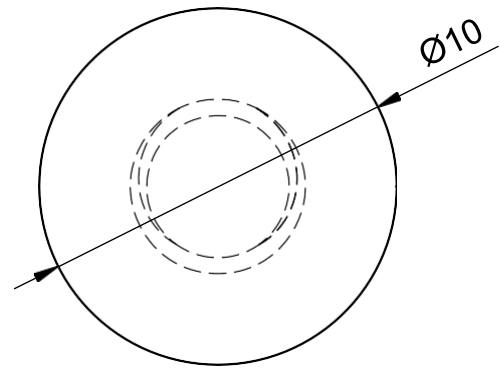
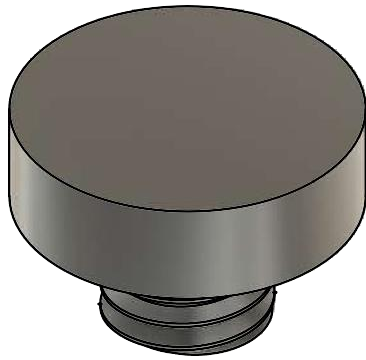
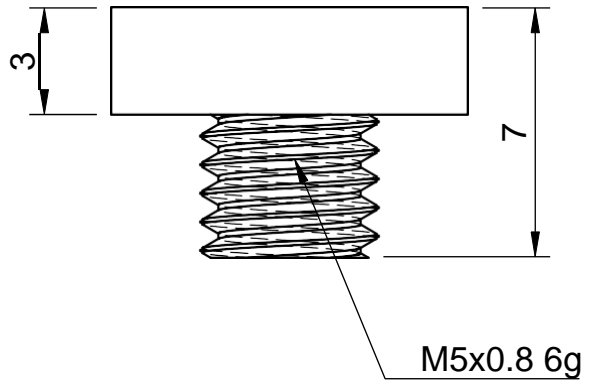
Date of issue

25-11-2023

Sheet

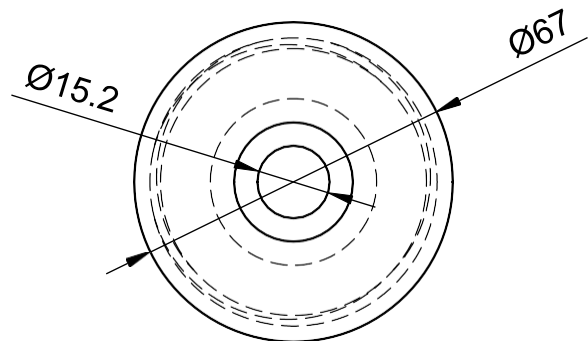
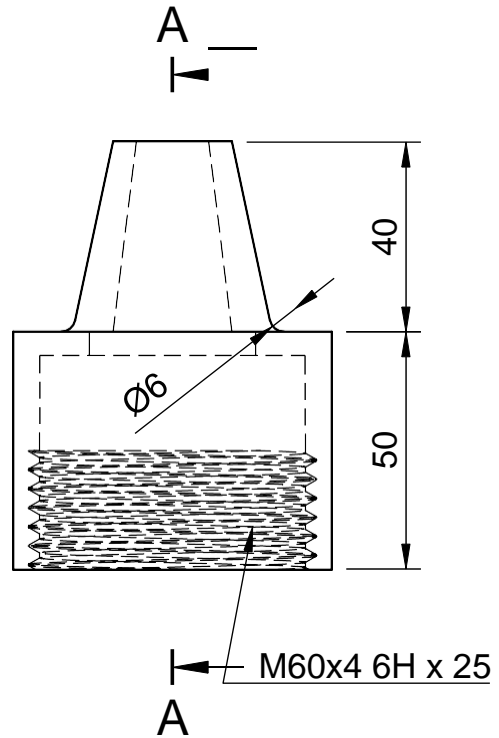
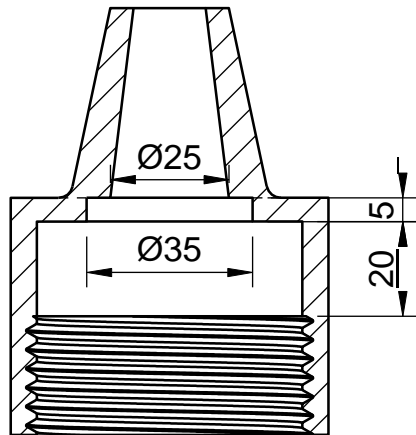
1/1



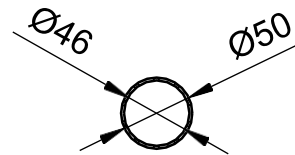
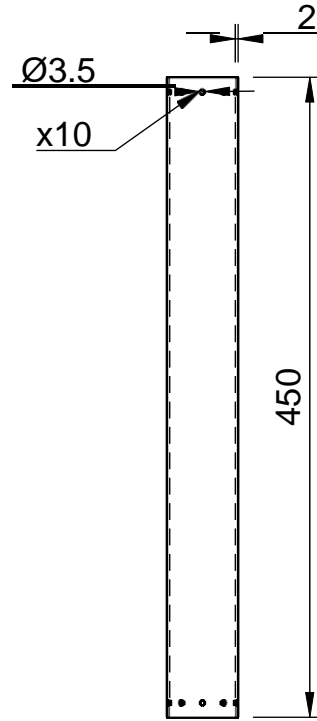


		Scale	5:1		Projection		
		Material	Steel				
		Manufacturing process	Machining				
Dept.	Technical reference	Created by	Mother part				
Facultad de Ingeniería	Extr-7	Giovanni Torres 25/11/2023	Extruder system				
		Document type	Dimensions units				
		Technical Drawing		mm			
		Title	DWG No.				
		Adjuster		Extr-07			
		Version	Date of issue	Sheet			
		V1	25-11-2023	1/1			

A-A (1:1.5)

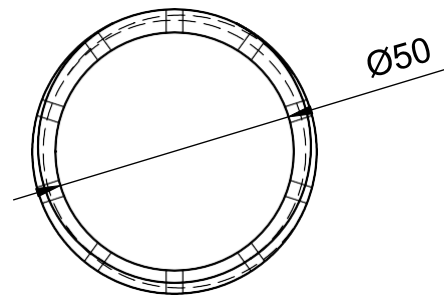
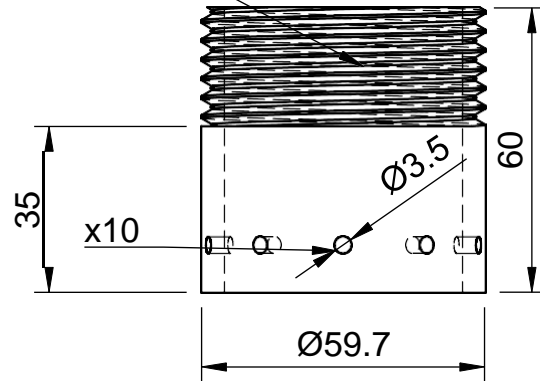


		Scale 1:1.5		Projection 	
		Manufacturing process Extrusion		Material ABS with steel tip	
Dept. Facultad de Ingeniería	Technical reference Fed-8	Created by Giovanni Torres 25/11/2023		Mother part Feeder system	
		Document type Technical Drawing		Dimensions units mm	
		Title Feeder_nozzle		DWG No. Fed-08	
		Version V7	Date of issue 25-11-2023	Sheet 1/1	



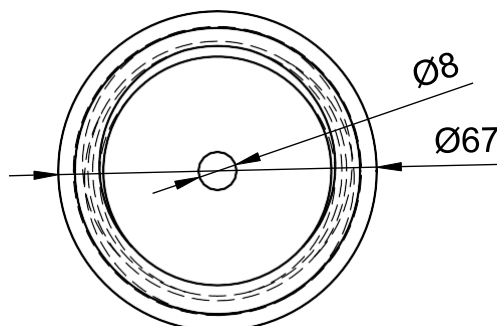
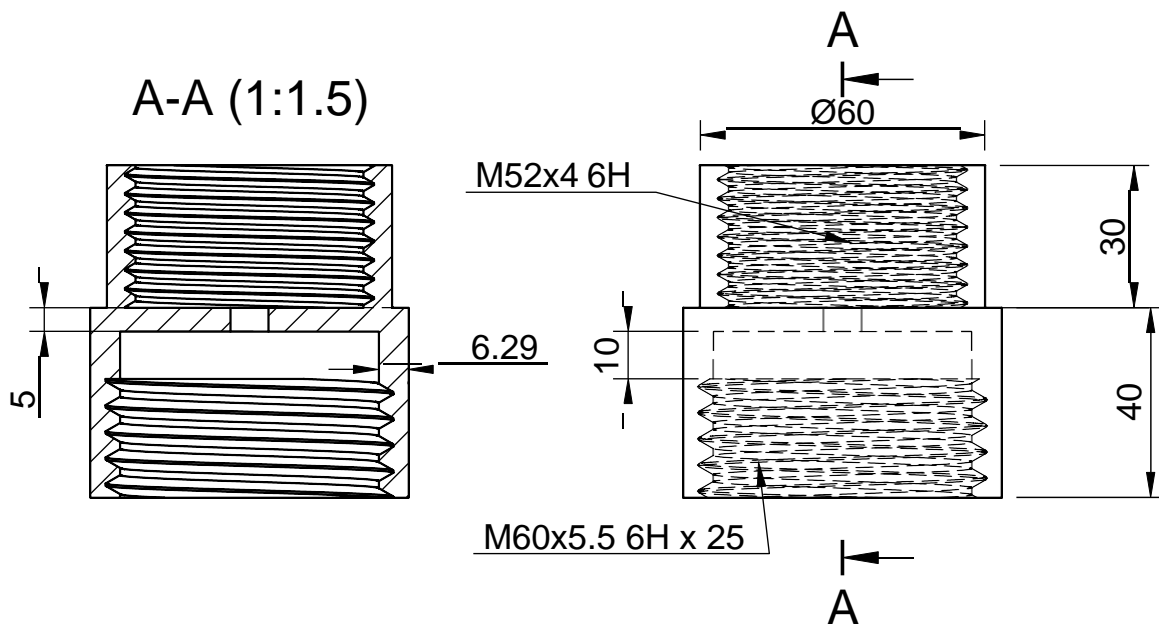
		Scale 1:5		Projection 	
		Manufacturing process		Material Acrylic	
Dept. Facultad de Ingeniería	Technical reference Fed-9	Created by Giovanni Torres 25/11/2023		Mother part Feeder system	
		Document type Technical Drawing		Dimensions units mm	
		Title Feeder_tube		DWG No. Fed-09	
		Version V8	Date of issue 25-11-2023	Sheet 1/1	

M60x4 6g x 25

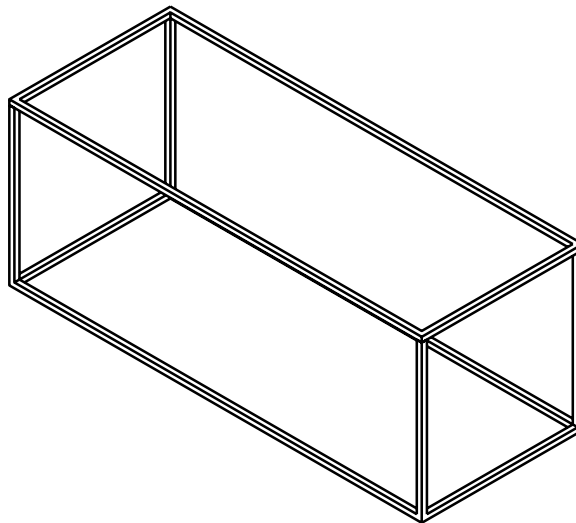
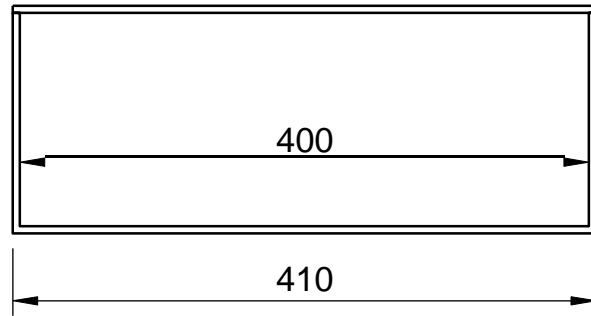
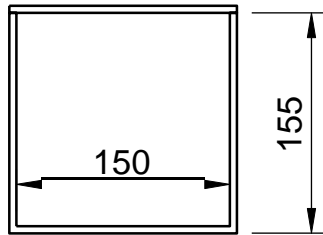


Scale	1:1.5	Projection
Manufacturing process	3D Printing	
Material	ABS	

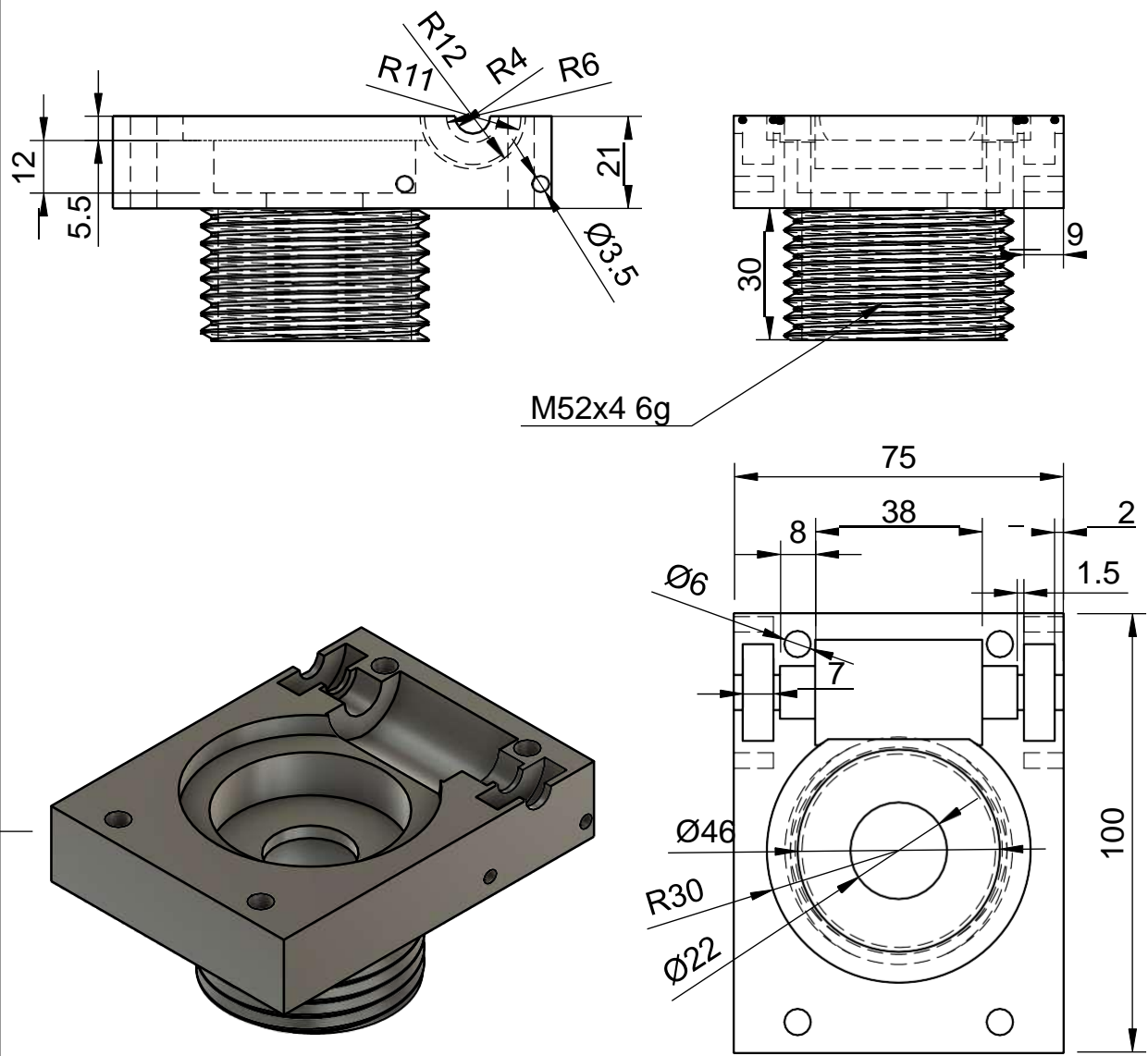
Dept. Facultad de Ingeniería	Technical reference Fed-10	Created by Giovanni Torres 25/11/2023	Mother part Feeder system
	Document type Technical Drawing	Dimensions units mm	
	Title Adapter_tube_nozzle	DWG No. Fed-10	
	Version V5	Date of issue 25-11-2023	Sheet 1/1



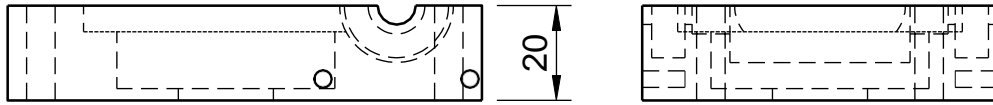
		Scale 1:1.5		Projection 	
		Manufacturing process 3D Printing		Material ABS	
Dept. Facultad de Ingeniería	Technical reference Fed-11	Created by Giovanni Torres 25/11/2023		Mother part Feeder system	
		Document type Technical Drawing		Dimensions units mm	
		Title Threaded_lid		DWG No. Fed-11	
		Version V2	Date of issue 25-11-2023	Sheet 1/1	



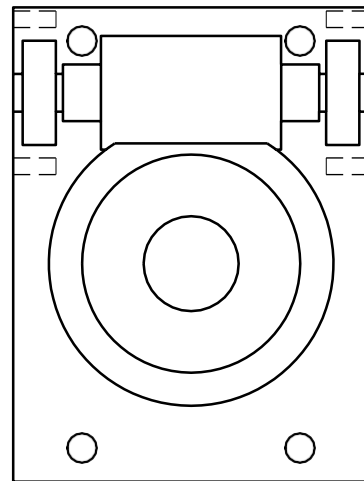
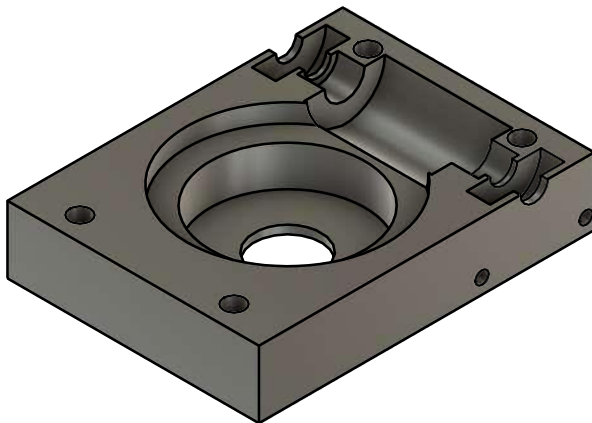
		Scale 1:5		Projection 	
		Manufacturing process		Material Aluminium	
Dept. Facultad de Ingeniería	Technical reference Fed-12	Created by Giovanni Torres 25/11/2023		Mother part Feeder system	
		Document type Technical Drawing		Dimensions units mm	
		Title Frame		DWG No. Fed-12	
		Version V2	Date of issue 25-11-2023	Sheet 1/1	



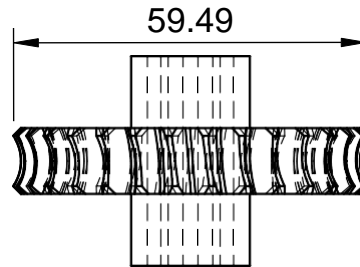
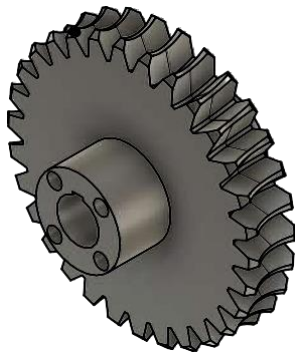
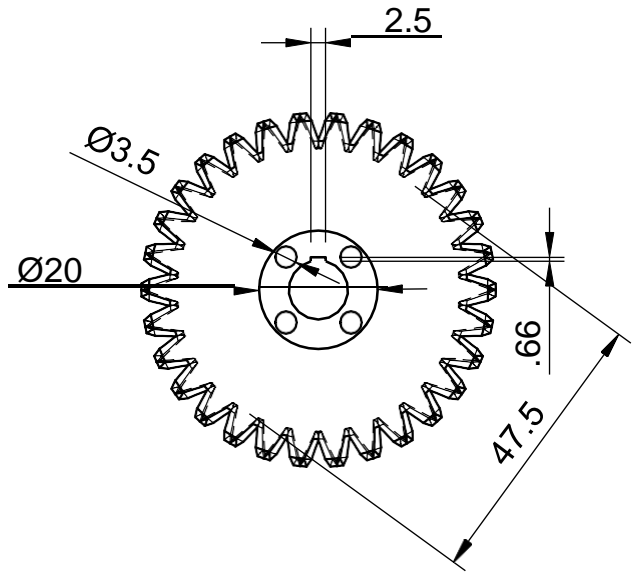
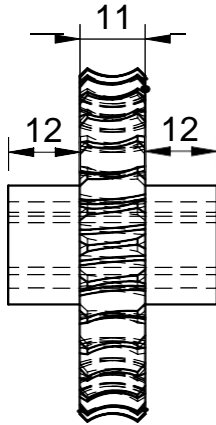
		Scale 1:1.5		Projection 	
		Manufacturing process 3D printing		Material ABS	
Dept. Facultad de Ingeniería	Technical reference Fed-13	Created by Giovanni Torres 25/11/2023		Mother part Feeder system	
		Document type Technical Drawing		Dimensions units mm	
		Title Gearbox_male		DWG No. Fed-13	
		Version V5	Date of issue 25-11-2023	Sheet 1/1	



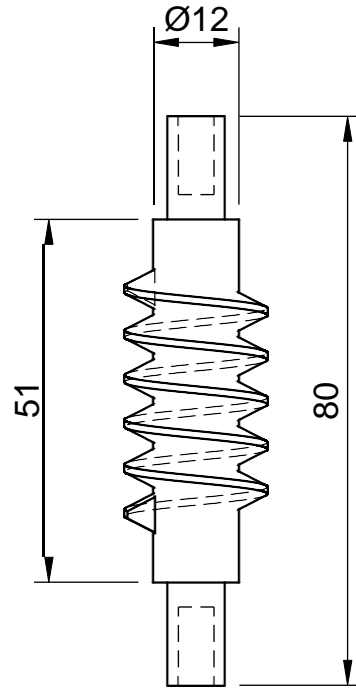
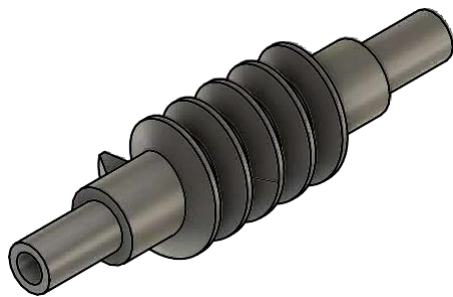
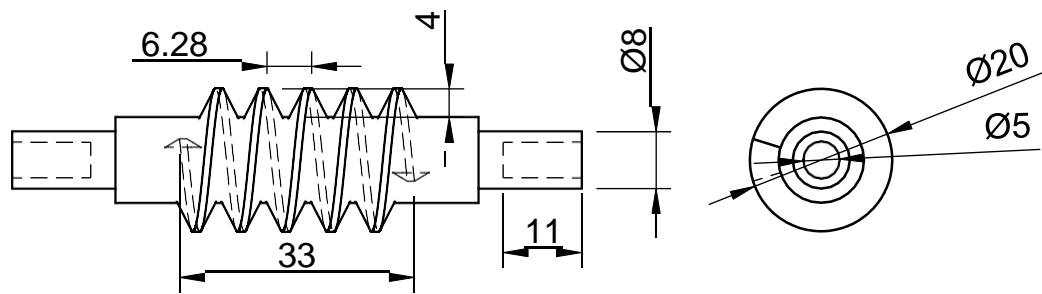
The dimensions are the same for this piece as the Gearbox_male, except for the depth.



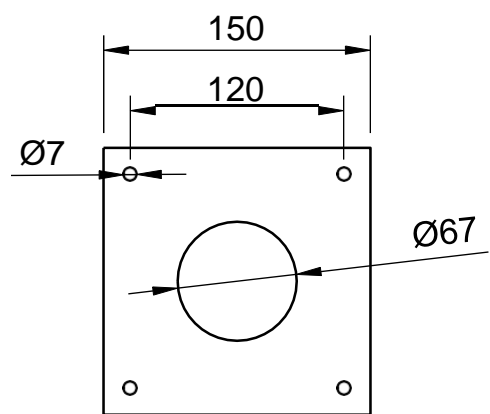
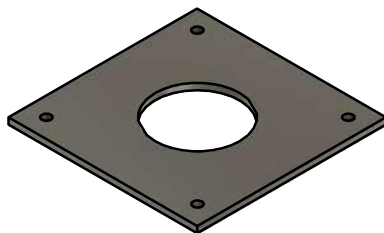
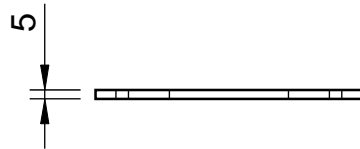
		Scale 1:1.5		Projection 	
		Manufacturing process 3D printing		Material ABS	
Dept. Facultad de Ingeniería	Technical reference Fed-14	Created by Giovanni Torres 25/11/2023		Mother part Feeder system	
		Document type Technical Drawing		Dimensions units mm	
		Title Gearbox_female		DWG No. Fed-14	
		Version V3	Date of issue 25-11-2023	Sheet 1/1	

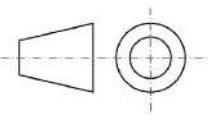



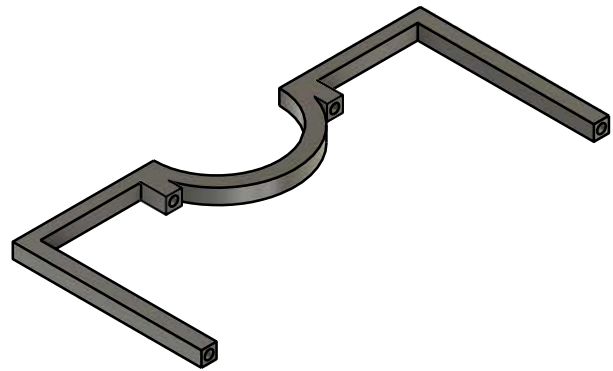
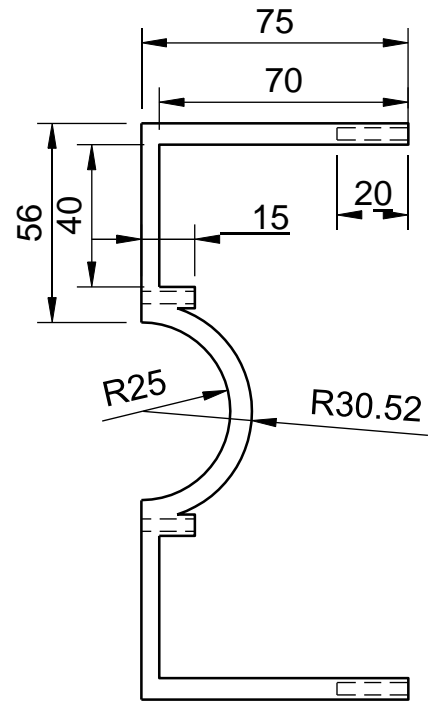
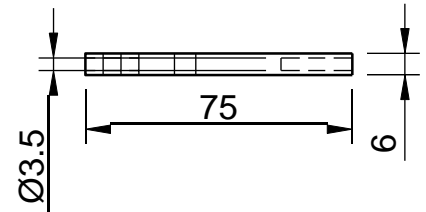
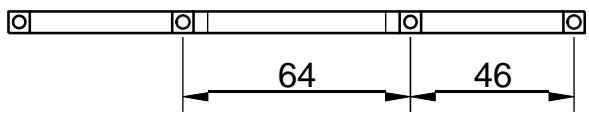
		Scale 1:1.2		Projection 	
		Manufacturing process 3D Printing		Material ABS	
Dept. Facultad de Ingeniería	Technical reference Fed-15	Created by Giovanni Torres 25/11/2023		Mother part Feeder system	
		Document type Technical Drawing		Dimensions units mm	
		Title Crown gear 15-1		DWG No. Fed-15	
		Version V2	Date of issue 25-11-2023	Sheet 1/1	



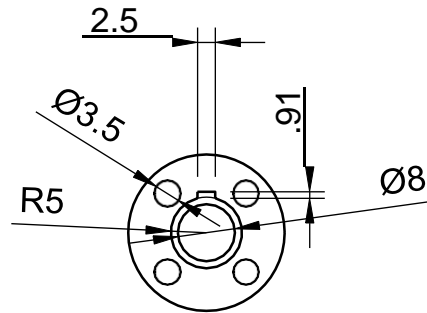
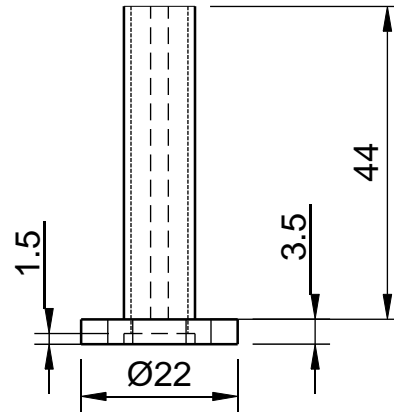
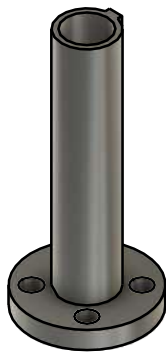
		Scale 1:1		Projection 	
		Manufacturing process 3D Printing		Material ABS	
Dept. Facultad de Ingeniería	Technical reference Fed-16	Created by Giovanni Torres 25/11/2023		Mother part Feeder system	
		Document type Technical Drawing		Dimensions units mm	
		Title Worm 15-1		DWG No. Fed-16	
		Version V7	Date of issue 25-11-2023	Sheet 1/1	



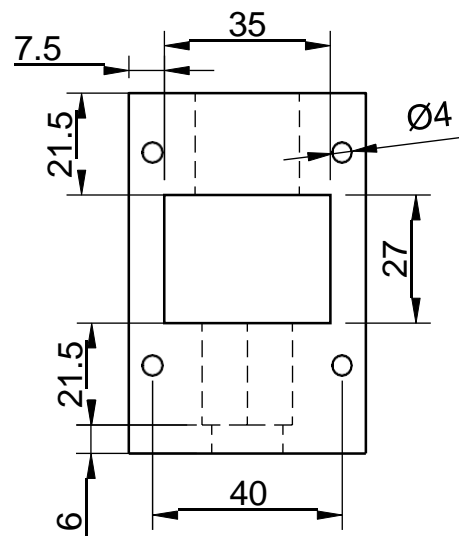
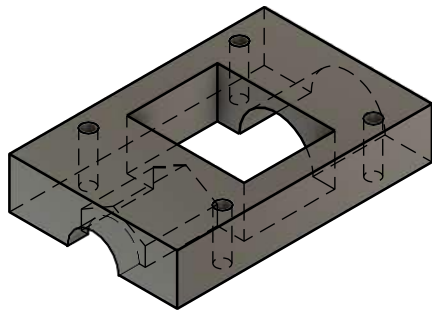
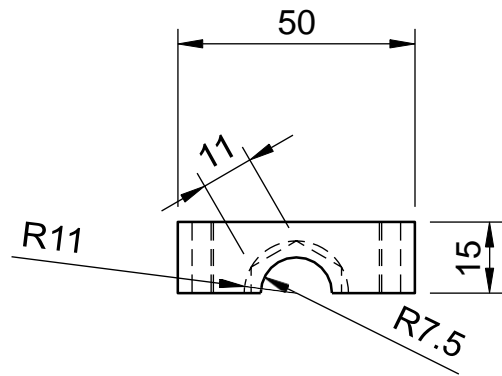
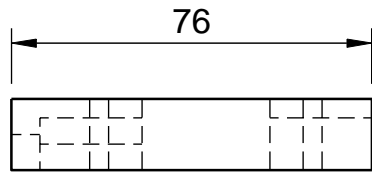
		Scale 1:4		Projection 	
		Manufacturing process Machining		Material Steel	
Dept. Facultad de Ingeniería	Technical reference Fed-17	Created by Giovanni Torres 25/11/2023		Mother part Feeder system	
		Document type Technical Drawing		Dimensions units mm	
		Title Plaque		DWG No. Fed-17	
		Version V4	Date of issue 25-11-2023	Sheet 1/1	



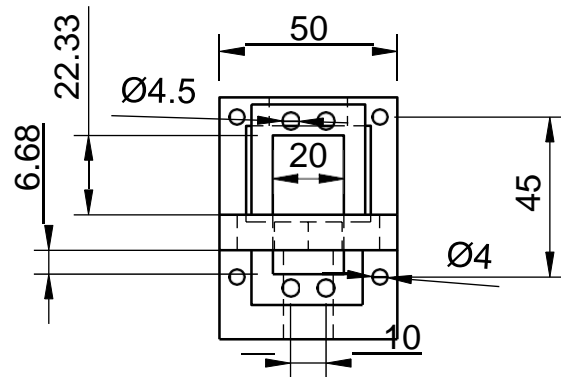
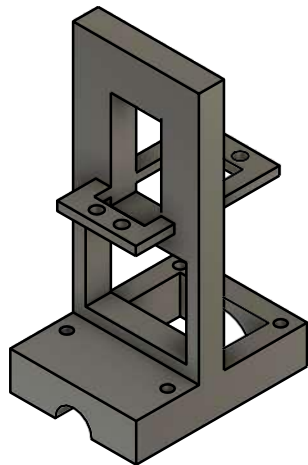
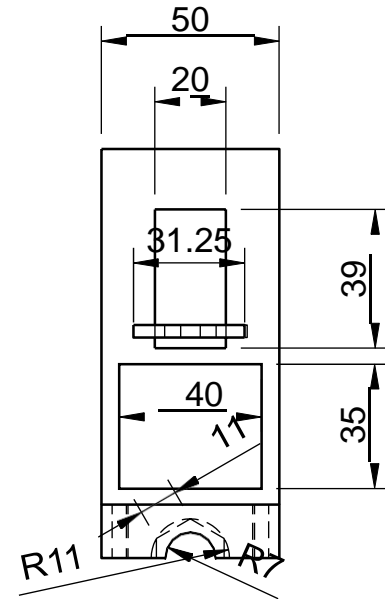
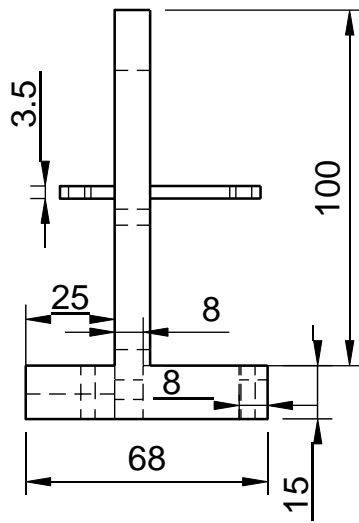
		Scale 1:1.5		Projection 	
		Manufacturing process Machining		Material Steel	
Dept. Facultad de Ingeniería	Technical reference Fed-18	Created by Giovanni Torres 25/11/2023		Mother part Feeder system	
		Document type Technical Drawing		Dimensions units mm	
		Title Clamp		DWG No. Fed-18	
		Version V4	Date of issue 25-11-2023	Sheet 1/1	



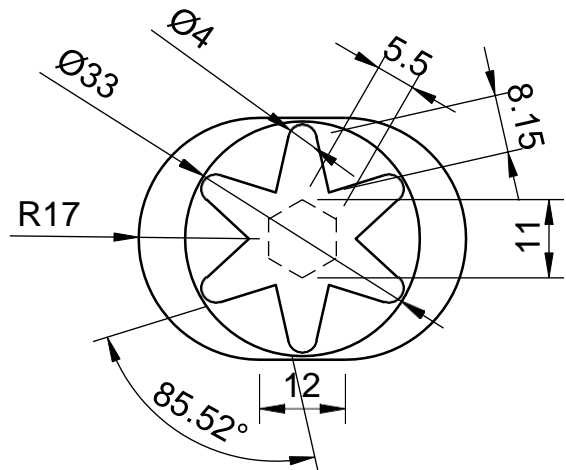
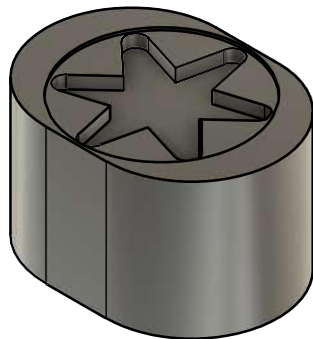
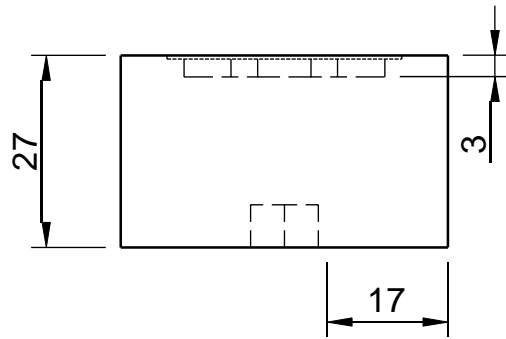
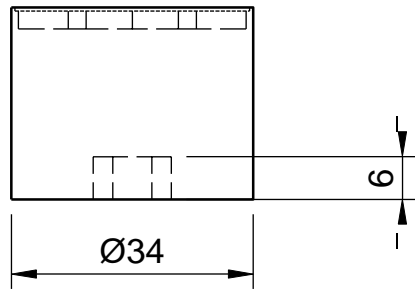
		Scale 1:1		Projection 	
		Manufacturing process Machining		Material Aluminium	
Dept. Facultad de Ingeniería	Technical reference Fed-19	Created by Giovanni Torres 25/11/2023		Mother part Feeder system	
		Document type Technical Drawing		Dimensions units mm	
		Title Crown adapter lead screw		DWG No. Fed-19	
		Version V2	Date of issue 25-11-2023	Sheet 1/1	



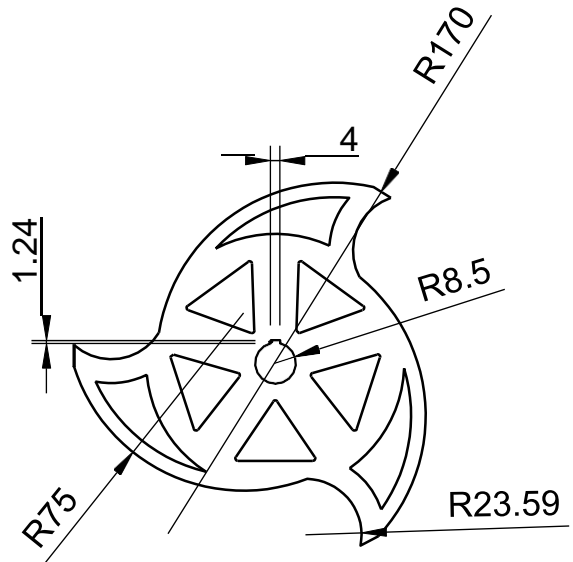
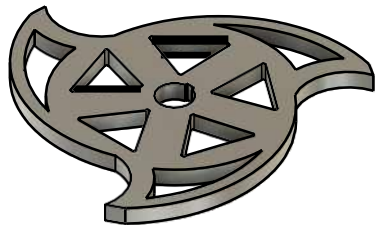
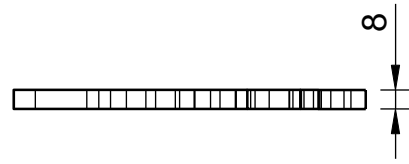
		Scale 1:1.5		Projection 	
		Manufacturing process 3D printing		Material ABS	
Dept. Facultad de Ingeniería	Technical reference Fed-20	Created by Giovanni Torres 25/11/2023		Mother part Feeding system	
		Document type Technical Drawing		Dimensions units mm	
		Title Motor_valve_bottom_adapter		DWG No. Fed-20	
		Version V5	Date of issue 25-11-2023	Sheet 1/1	



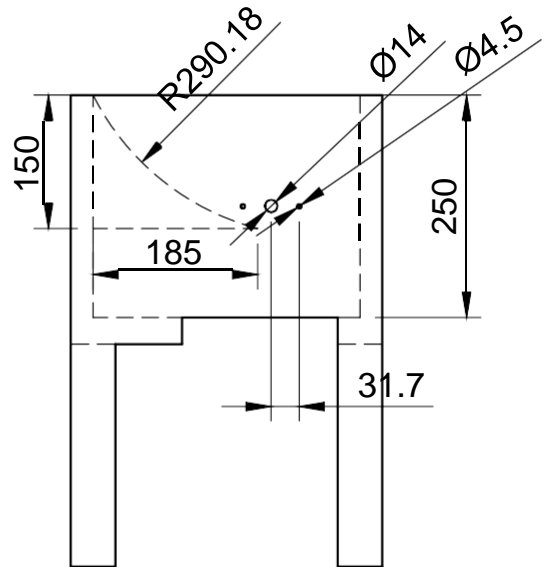
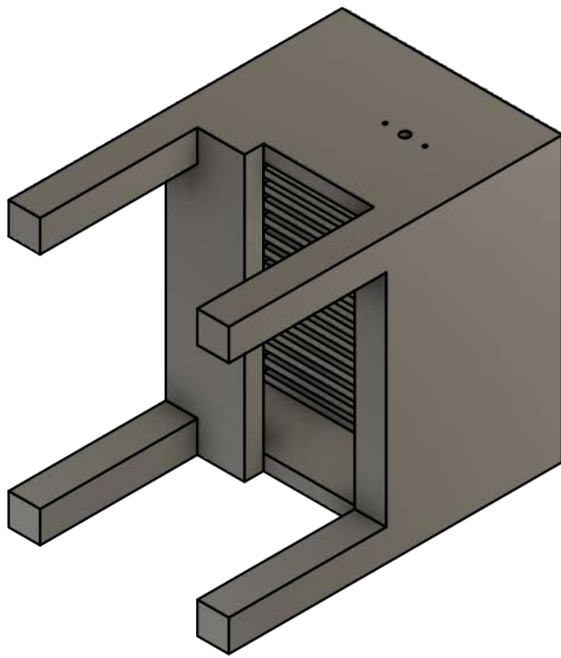
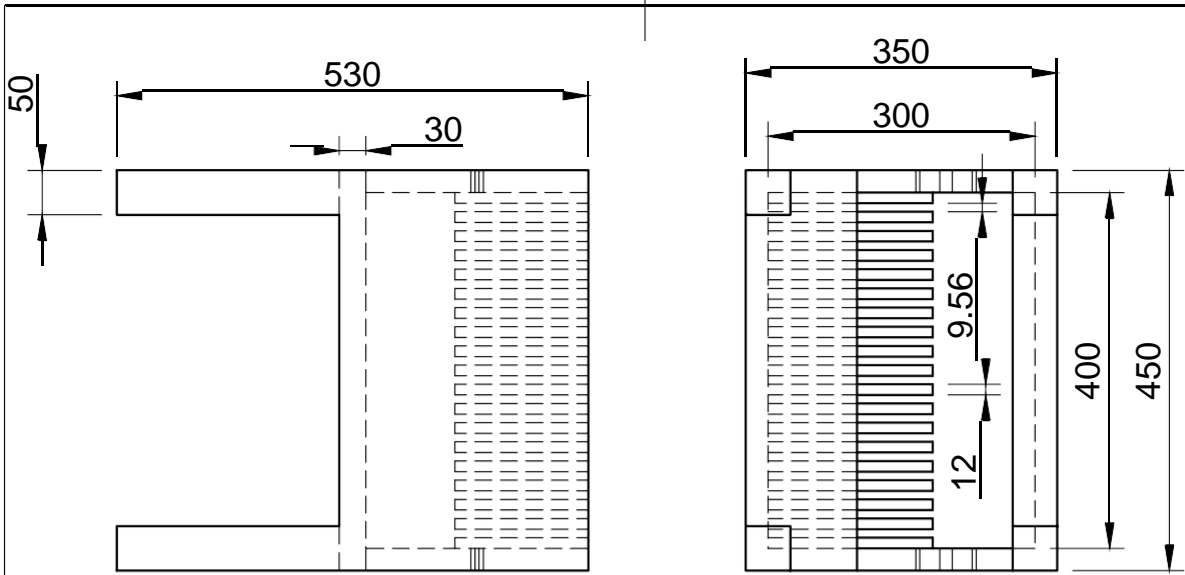
		Scale 1:2		Projection 	
		Manufacturing process 3D printing		Material ABS	
Dept. Facultad de Ingeniería	Technical reference Fed-21	Created by Giovanni Torres 25/11/2023		Mother part Feeder system	
		Document type Technical Drawing		Dimensions units mm	
		Title Adaptador motor valvula		DWG No. Fed-21	
		Version V6	Date of issue 25-11-2023	Sheet 1/1	

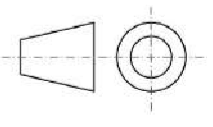



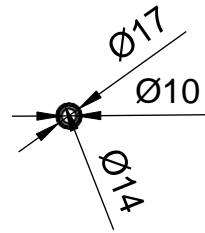
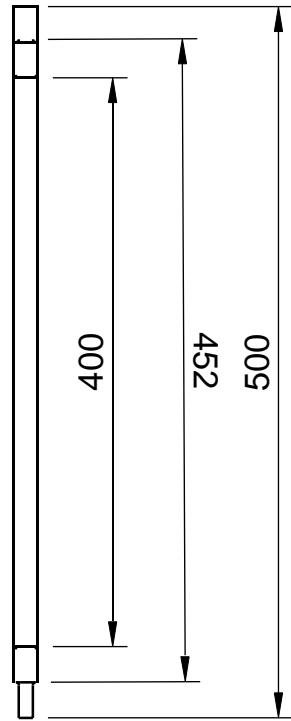
		Scale 1:1		Projection 	
		Manufacturing process 3D printing		Material ABS	
Dept. Facultad de Ingeniería	Technical reference Fed-22	Created by Giovanni Torres 25/11/2023		Mother part Feeder system	
		Document type Technical Drawing		Dimensions units mm	
		Title Servo_Valve_Adapter		DWG No. Fed-22	
				Version V10	Date of issue 25-11-2023



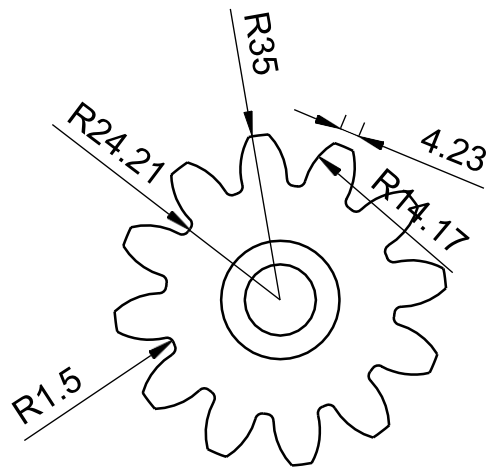
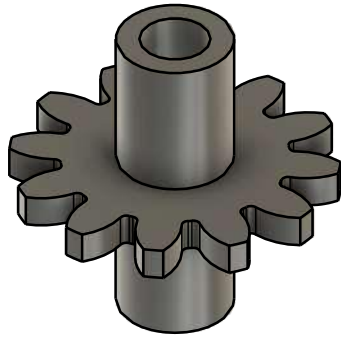
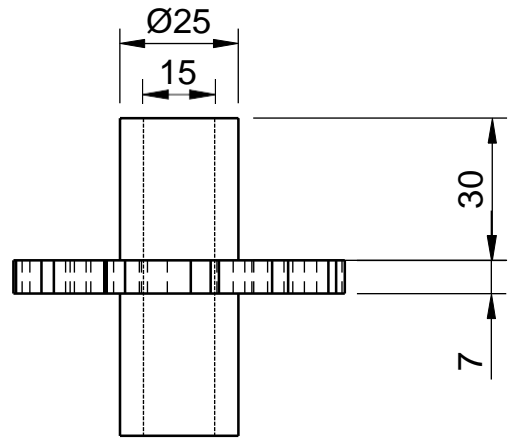
		Scale 1:3		Projection 	
		Manufacturing process Machining		Material Stainless Steel AISI 304	
Dept. Facultad de Ingeniería	Technical reference Fed-23	Created by Giovanni Torres 25/11/2023		Mother part Feeder system	
		Document type Technical Drawing		Dimensions units mm	
		Title Blade		DWG No. Fed-23	
		Version V11	Date of issue 25-11-2023	Sheet 1/1	



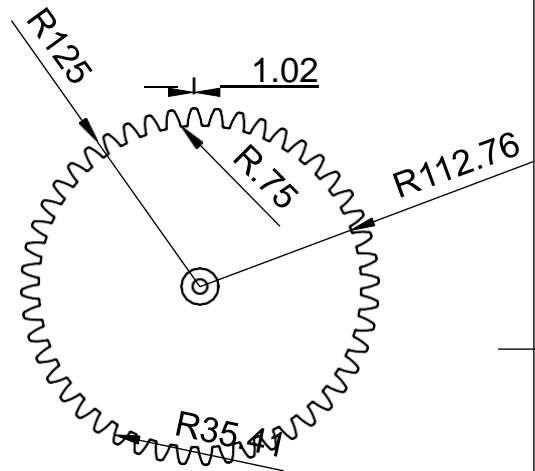
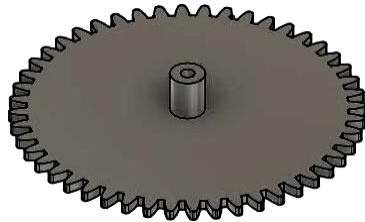
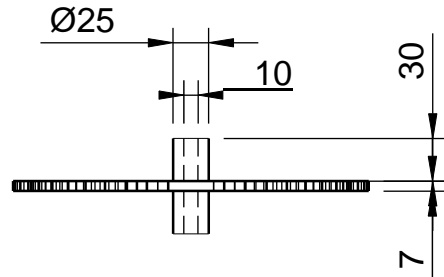
		Scale 1:8	Projection 	
Manufacturing process		Material Steel		
Dept. Facultad de Ingeniería	Technical reference Fed-24	Created by Giovanni Torres 25/11/2023	Mother part Feeder system	
	Document type Technical Drawing	Dimensions units mm		
	Title Shredder_box	DWG No. Fed-24		
	Version V12	Date of issue 25-11-2023	Sheet 1/1	



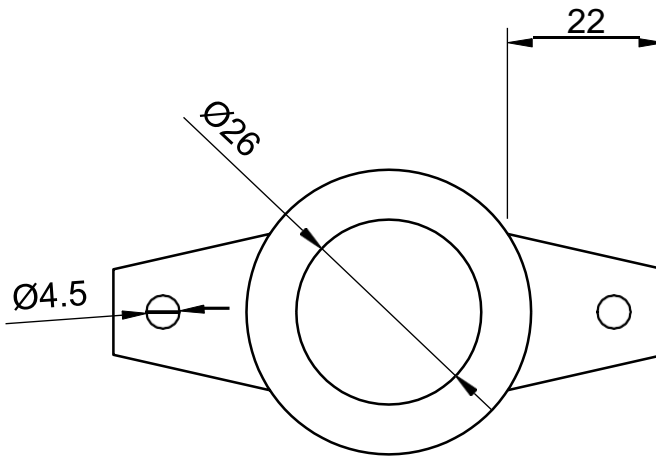
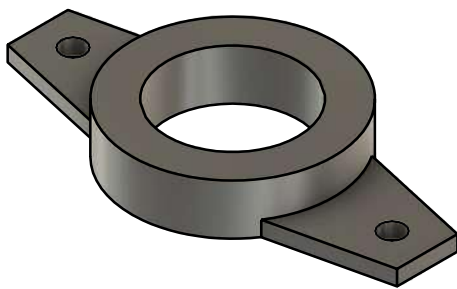
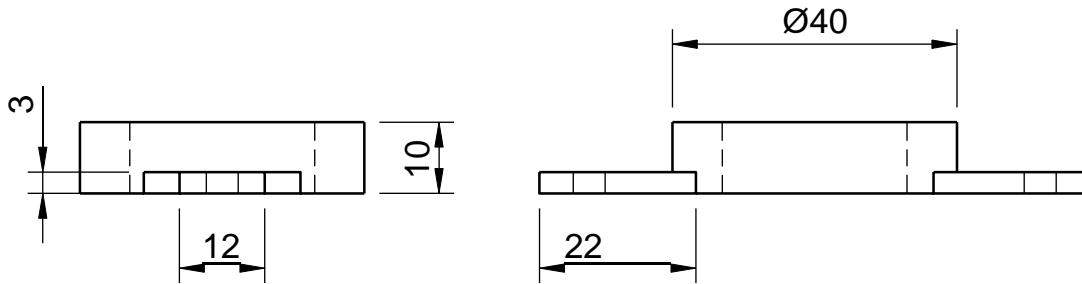
		Scale 1:10		Projection 	
		Manufacturing process Machining		Material Steel AISI 4340	
Dept. Facultad de Ingeniería	Technical reference Fed-25	Created by Giovanni Torres 25/11/2023		Mother part Feeding system	
		Document type Technical Drawing		Dimensions units mm	
		Title Shaft		DWG No. Fed-25	
				Version V10	Date of issue 25-11-2023

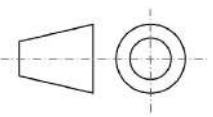



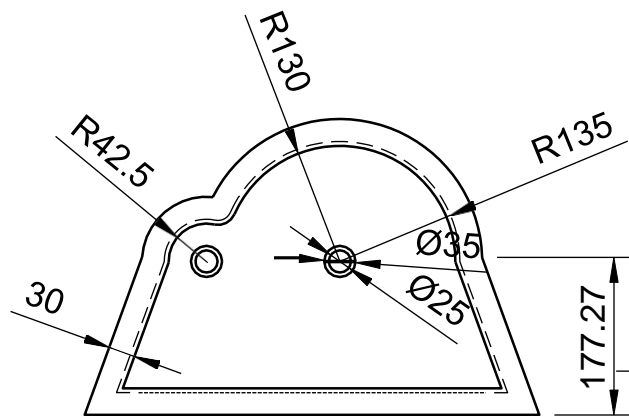
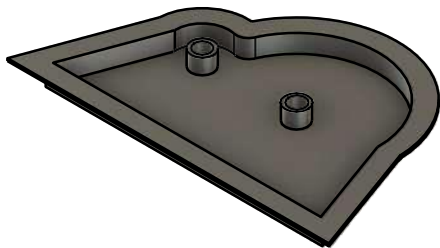
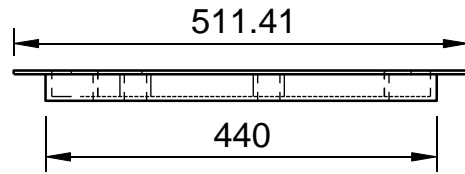
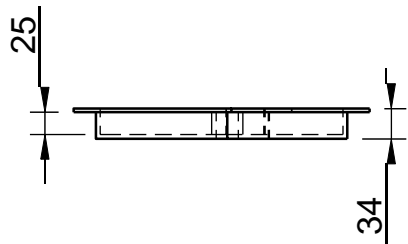
		Scale 1:1.5		Projection 	
		Manufacturing process Machining		Material Bronze C89320	
Dept. Facultad de Ingeniería	Technical reference Fed-26	Created by Giovanni Torres 25/11/2023		Mother part Feeding system	
		Document type Technical Drawing		Dimensions units mm	
		Title Pinion 12 teeth		DWG No. Fed-25	
		Version V4	Date of issue 25-11-2023	Sheet 1/1	



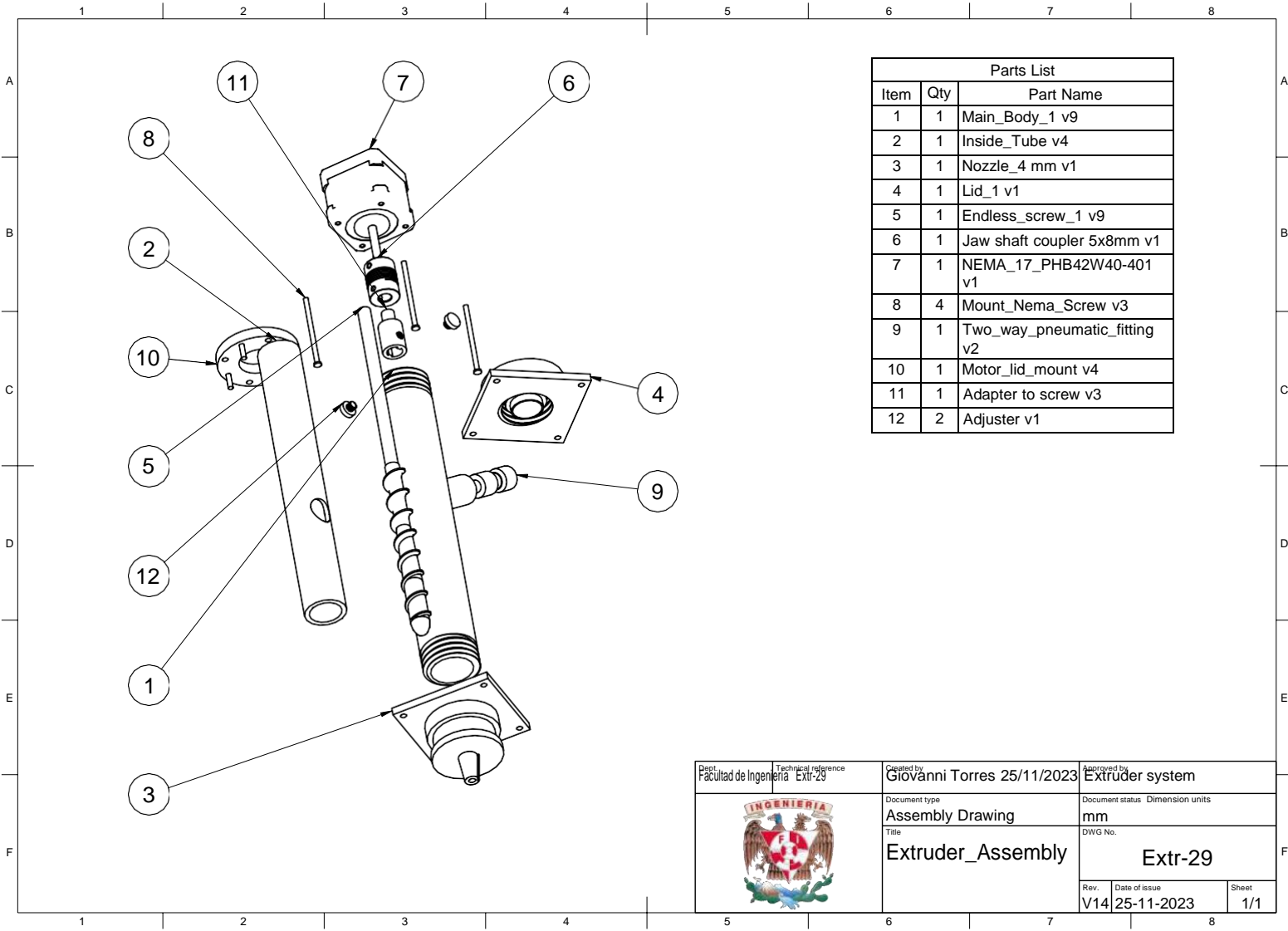
		Scale 1:5		Projection 	
		Manufacturing process Machining		Material Bronze C89230	
Dept. Facultad de Ingeniería	Technical reference Fed-26	Created by Giovanni Torres 25/11/2023		Mother part Feeding system	
		Document type Technical Drawing		Dimensions units mm	
		Title Gear 48 teeth		DWG No. Fed-26	
		Version V6	Date of issue 25-11-2023	Sheet 1/1	




		Scale 1:1		Projection 	
		Manufacturing process Machining		Material Steel	
Dept. Facultad de Ingeniería	Technical reference Fed-27	Created by Giovanni Torres 25/11/2023		Mother part Feeding system	
		Document type Technical Drawing		Dimensions units mm	
		Title Bearing_mount		DWG No. Fed-27	
		Version V1	Date of issue 25-11-2023	Sheet 1/1	



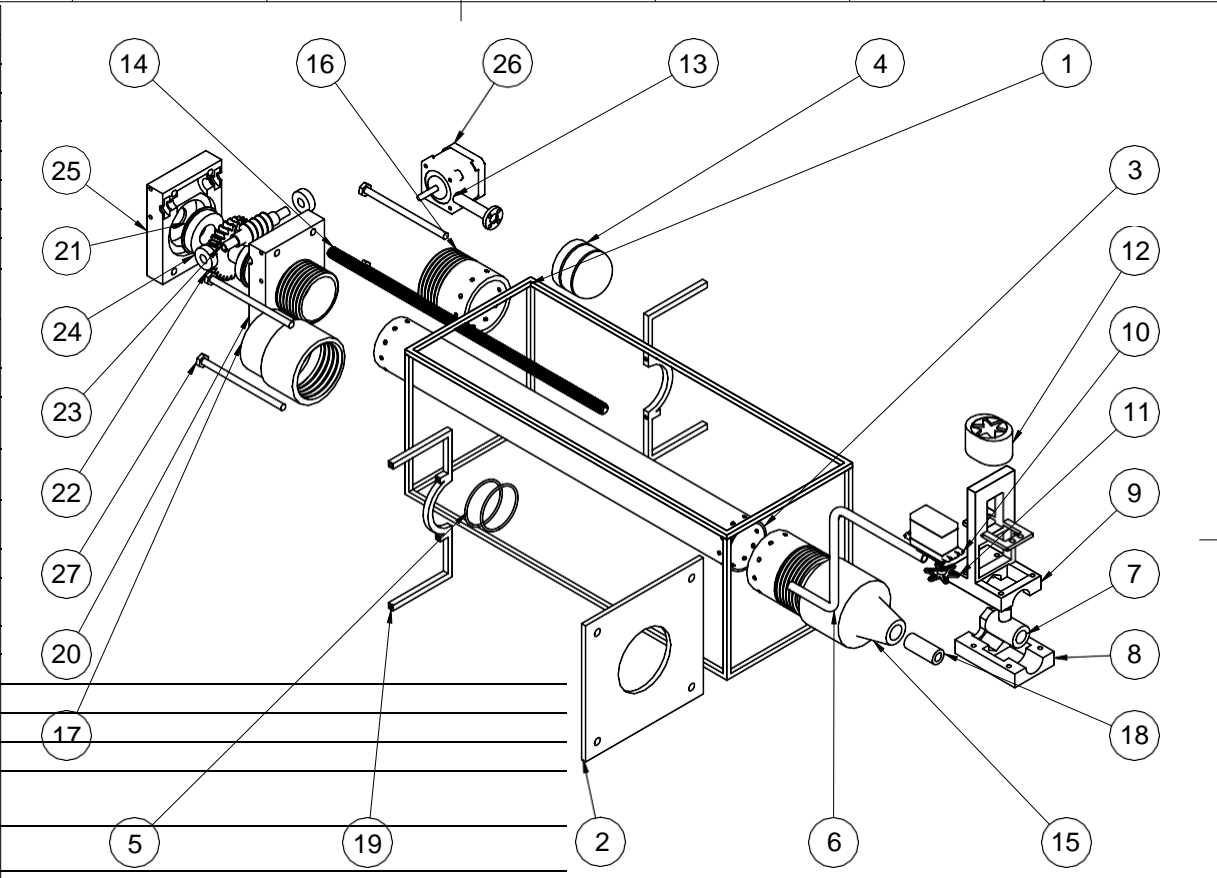
		Scale 1:8		Projection 	
		Manufacturing process		Material Steel	
Dept. Facultad de Ingeniería	Technical reference Fed-28	Created by Giovanni Torres 25/11/2023		Mother part Feeding system	
		Document type Technical Document		Dimensions units mm	
		Title Gearbox		DWG No. Fed-28	
		Version V1	Date of issue 25-11-2023	Sheet 1/1	




Parts List		
Item	Qty	Part Name
1	1	Main_Body_1 v9
2	1	Inside_Tube v4
3	1	Nozzle_4 mm v1
4	1	Lid_1 v1
5	1	Endless_screw_1 v9
6	1	Jaw shaft coupler 5x8mm v1
7	1	NEMA_17_PHB42W40-401 v1
8	4	Mount_Nema_Screw v3
9	1	Two_way_pneumatic_fitting v2
10	1	Motor_lid_mount v4
11	1	Adapter to screw v3
12	2	Adjuster v1

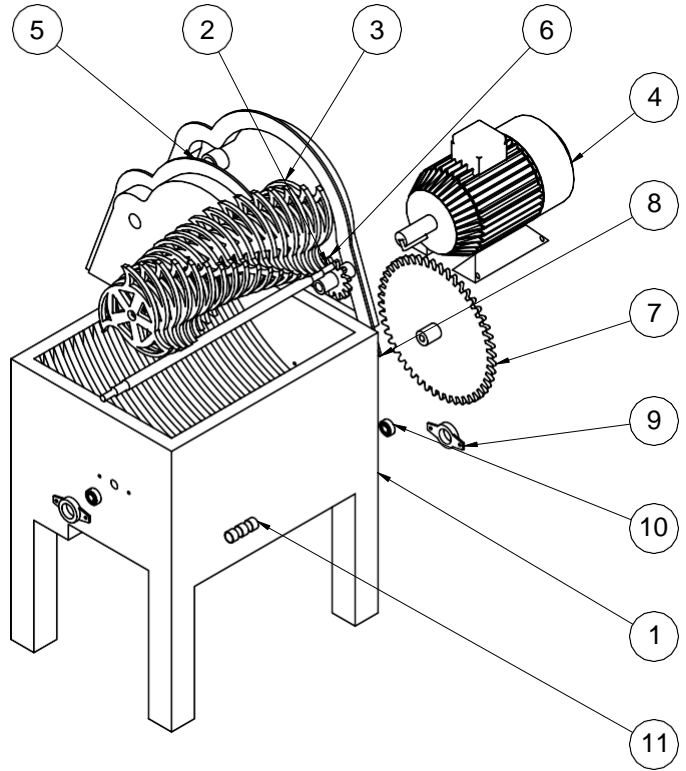
Dept. Facultad de Ingeniería	Technical reference Extr-29	Created by Giovanni Torres 25/11/2023	Approved by Extruder system
	Document type Assembly Drawing	Document status Dimension units mm	
	Title Extruder_Assembly	DWG No. Extr-29	
Rev. V14	Date of issue 25-11-2023	Sheet 1/1	


Parts List		
Item	Qty	Part Name
1	1	Main Frame v2
2	1	Plaque v4
3	1	Main tube v6
4	1	Plunger v5
5	2	Rubber v3
6	1	Pipe adapter v2
7	1	Valve dummy v1
8	1	Servo_valve_support_bottom v5
9	1	Servo_valve_support_top v6
10	1	Mg995 v1
11	1	Servo_MG995_Starhorn v1
12	1	Servo Valve Shaft Adapter v10
13	2	Crown adapter lead screw v2
14	1	Lead Screw v1
15	1	Nozzle with screw v7
16	2	Tube to screw v5
17	1	Lid with screw v2
18	1	Adapter to hose v1
19	2	Clamp v4
20	1	Gearbox bottom v5
21	2	Big bearing v1
22	1	Crown gear 15-1 v2
23	1	Worm 15-1 v7
24	2	Small bearing v2
25	1	Gearbox top v3
26	1	NEMA_17_PHB42 W40-401 v1
27	4	Screw v1



Dept. Facultad de Ingeniería	Technical reference Fed-30	Created by Giovanni Torres 25/11/2023	Approved by Extruder system
		Document type Assembly Drawing	Document status/ Dimension units mm
		Title Feeder_Assembly	DWG No. Fed-30
Rev. V11	Date of issue 25-11-2023	Sheet 1/1	

Parts List		
Item	Qty	Part Name
1	1	Box v12
2	1	Shaft v10
3	18	Blade_3 v11
4	1	AC Motor v2
5	1	Gearbox opposite v3
6	1	Pinion 12 teeth v4
7	1	Gear 48 teeth v6
8	1	Gearbox v1
9	2	Bearing mount v1
10	2	Skf_bearing_6000_2 v1
11	3	Separator v1



Dept. Facultad de Ingeniería	Technical reference Shr-31	Created by Giovanni Torres 25/11/2023	Approved by Shredder system
		Document type Assembly drawing	Document status mm
		Title Shredder_Assembly	DWG No. Shr-31
Rev. V10	Date of issue 25-11-2023	Sheet 1/1	

9.6 Appendix 6: Data sheets

The data sheets for all the commercial components used and proposed are presented next.

DATA SHEET



Three Phase Induction Motor - Squirrel Cage

Customer : _____

Product line : Multimounting IE3 Three-Phase
 Product code : 13984023
 Catalog # : 00318ET3WAL100L-W22

Frame	: L100L	Locked rotor time	: 23s (cold) 13s (hot)
Output	: 4 HP (3 kW)	Temperature rise	: 80 K
Poles	: 4	Duty cycle	: S1
Frequency	: 50 Hz	Ambient temperature	: -20°C to +40°C
Rated voltage	: 220/380 V	Altitude	: 1000 m.a.s.l.
Rated current	: 10.8/6.26 A	Protection degree	: IP55
L. R. Amperes	: 84.3/48.8 A	Cooling method	: IC411 - TEFC
LRC	: 7.8	Mounting	: B3L(E)
No load current	: 5.53/3.20 A	Rotation ¹	: Both (CW and CCW)
Rated speed	: 1430 rpm	Noise level ²	: 53.0 dB(A)
Slip	: 4.67 %	Starting method	: Direct On Line
Rated torque	: 2.03 kgfm	Approx. weight ³	: 34.8 kg
Locked rotor torque	: 310 %		
Breakdown torque	: 330 %		
Insulation class	: F		
Service factor	: 1.25		
Moment of inertia (J)	: 0.0120 kgm ²		
Design	: N		

Output	25%	50%	75%	100%	Foundation loads	
Efficiency (%)	87.6	87.7	88.0	87.7	Max. traction	: 182 kgf
Power Factor	0.38	0.65	0.77	0.83	Max. compression	: 217 kgf

		<u>Drive end</u>	<u>Non drive end</u>
Bearing type	:	6206 ZZ	6206 ZZ
Sealing	:	V'Ring	V'Ring
Lubrication interval	:	-	-
Lubricant amount	:	-	-
Lubricant type	:	Mobil Polyrex EM	

Notes

This revision replaces and cancel the previous one, which must be eliminated.
 (1) Looking the motor from the shaft end.
 (2) Measured at 1m and with tolerance of +3dB(A).
 (3) Approximate weight subject to changes after manufacturing process.
 (4) At 100% of full load.

These are average values based on tests with sinusoidal power supply, subject to the tolerances stipulated in NEMA MG-1.

Rev.	Changes Summary	Performed	Checked	Date
Performed by		Page		Revision
Checked by		1 / 2		
Date	26/11/2023			

TORQUE AND CURRENT VS SPEED CURVE

Three Phase Induction Motor - Squirrel Cage



Customer : _____

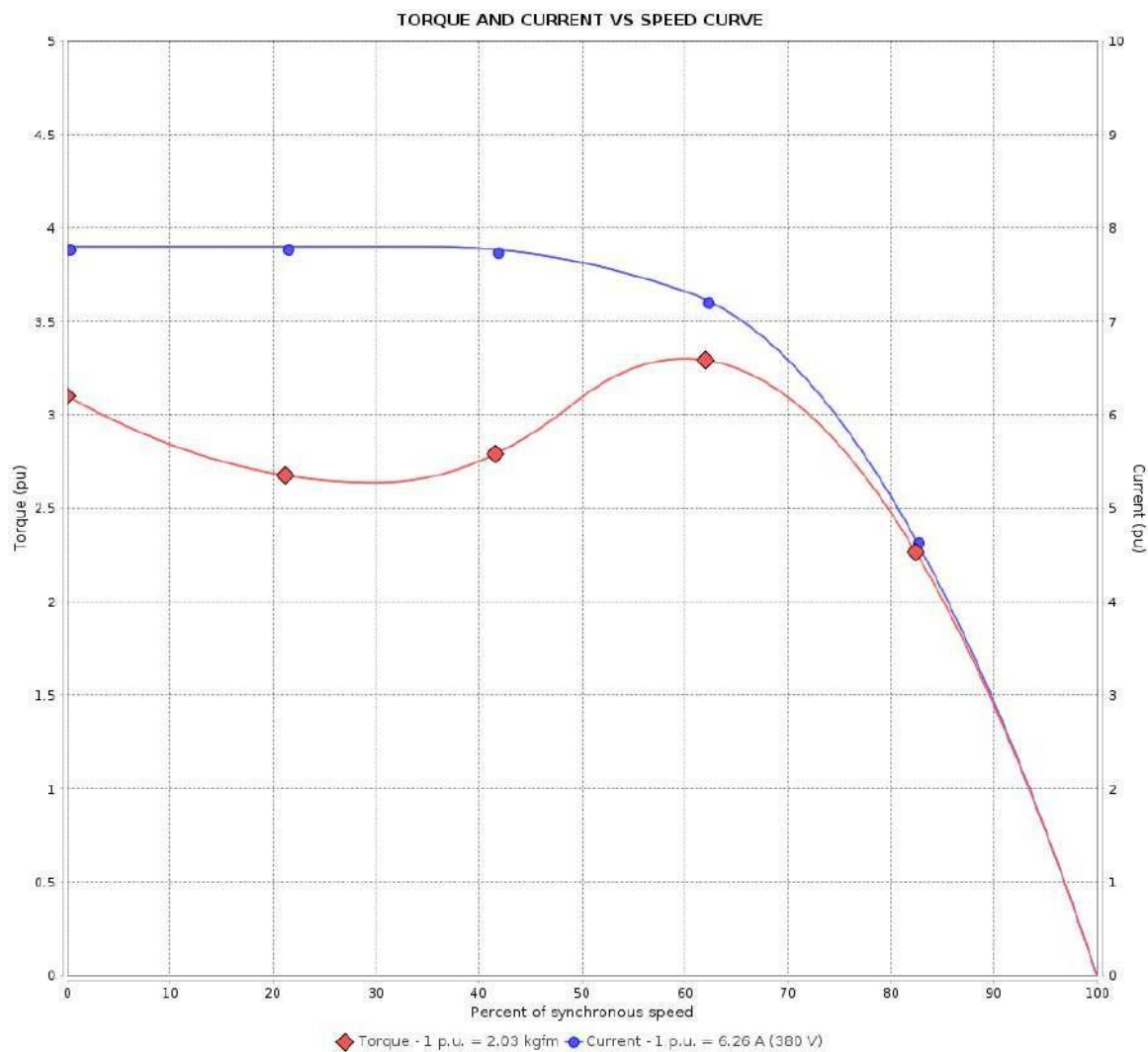
Product line : Multimounting IE3 Three-Phase

Product code :

13984023

Catalog # :

00318ET3WAL100L-W22



Performance : 220/380 V 50 Hz 4P

Rated current : 10.8/6.26 A

LRC : 7.8

Rated torque : 2.03 kgfm

Locked rotor torque : 310 %

Breakdown torque : 330 %

Rated speed : 1430 rpm

Moment of inertia (J) : 0.0120 kgm²

Duty cycle : S1

Insulation class : F

Service factor : 1.25

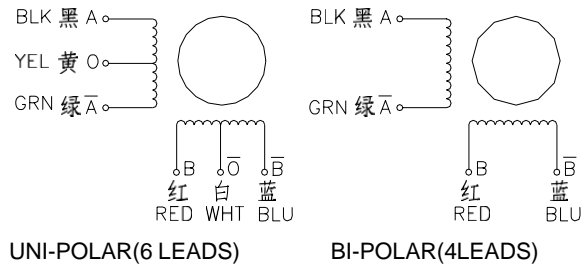
Temperature rise : 80 K

Design : N

Locked rotor time : 23s (cold) 13s (hot)

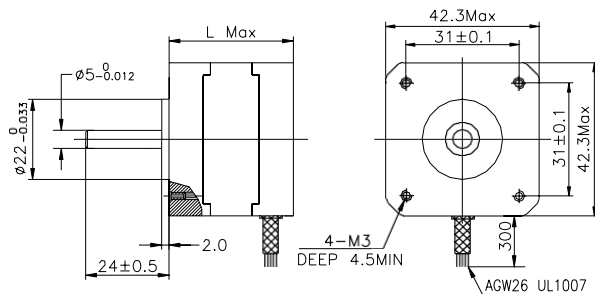
Rev.	Changes Summary	Performed	Checked	Date
Performed by		Page		Revision
Checked by		2 / 2		
Date	26/11/2023			

2 Phase Hybrid Stepper Motor 17HS series-Size 42mm(1.8 degree)


Wiring Diagram:

Electrical Specifications:

Series Model	Step Angle (deg)	Motor Length (mm)	Rated Current (A)	Phase Resistance (ohm)	Phase Inductance (mH)	Holding Torque (N.cm Min)	Detent Torque (N.cm Max)	Rotor Inertia (g.cm ²)	Lead Wire (No.)	Motor Weight (g)
17HS2408	1.8	28	0.6	8	10	12	1.6	34	4	150
17HS3401	1.8	34	1.3	2.4	2.8	28	1.6	34	4	220
17HS3410	1.8	34	1.7	1.2	1.8	28	1.6	34	4	220
17HS3430	1.8	34	0.4	30	35	28	1.6	34	4	220
17HS3630	1.8	34	0.4	30	18	21	1.6	34	6	220
17HS3616	1.8	34	0.16	75	40	14	1.6	34	6	220
17HS4401	1.8	40	1.7	1.5	2.8	40	2.2	54	4	280
17HS4402	1.8	40	1.3	2.5	5.0	40	2.2	54	4	280
17HS4602	1.8	40	1.2	3.2	2.8	28	2.2	54	6	280
17HS4630	1.8	40	0.4	30	28	28	2.2	54	6	280
17HS8401	1.8	48	1.7	1.8	3.2	52	2.6	68	4	350
17HS8402	1.8	48	1.3	3.2	5.5	52	2.6	68	4	350
17HS8403	1.8	48	2.3	1.2	1.6	46	2.6	68	4	350
17HS8630	1.8	48	0.4	30	38	34	2.6	68	6	350

*Note: We can manufacture products according to customer's requirements.

Dimensions: unit=mm

Motor Length:

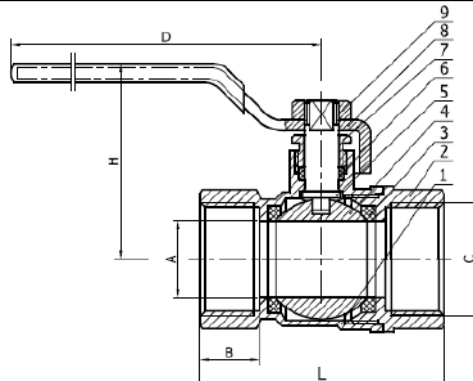
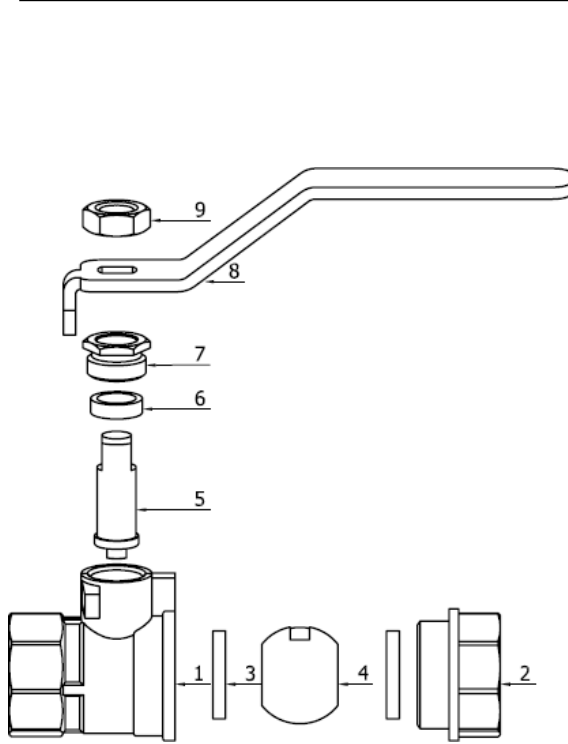
Model	Length
17HS2XXX	28 mm
17HS3XXX	34 mm
16HS4XXX	40 mm
16HS8XXX	48 mm

LATÓN

VÁLVULA DE ESFERA

Características:

- 400 PSI WOG
- Servicio de agua y aire
- Paso estándar
- Esfera de latón cromado
- Asiento de PTFE
- Temperatura de trabajo de -10°C a 90°C



Especificaciones de materiales

No.	Descripción	Material
1	Cuerpo	LATÓN
2	Tapa	LATÓN
3	Asiento	PTFE
4	Esfera	LATÓN
5	Vástago	LATÓN
6	Empaque	PTFE
7	Tuerca de Presión	LATÓN
8	Maneral	ACERO
9	Tuerca	ACERO

Dimensiones en pulgadas

No. Parte	SKU	Tamaño	A	B	C	L	H	D	Peso (lbs)
ES65152	107861	1/2"	0.49	0.43	NPT 1/2	1.75	1.97	4.02	0.44

Presión de trabajo

Presión de trabajo Non-Shock (psi)
Agua, Aire
400



No. Parte.
ES65152
1/2"
Roscada
HD-SKU:107861

- Extremo roscado cumple con ANSI/ASME B1.20.1

TB6600

Stepper Motor Driver

Analog Driver Model TB6600

Analog Technology, max. 40 VDC / 4.0 A (PEAK)



Product Description:

The TB6600 single axis drive is a low cost microstepping drive. It is suitable for driving 2-phase and 4-phase hybrid stepper motors. Not for professional applications.

Features:

- Cost-effective
- Supply voltage up to +40 VDC, Output current up to 4.0 A (PEAK)
- Output current selectable in 8 steps via DIP-switch
- Automatic idle-current reduction (in standstill mode) to reduce motor heating
- Pulse input frequency up to 20 kHz
- Input suitable for 5 V signals
- Inputs are optically isolated
- 6 selectable microstep resolutions, up to 6400 steps/rev with standard 1.8° motors
- Suitable for 2-phase and 4-phase motors
- Supports PUL/DIR mode
- Over current and overheat protection

Electrical Specifications:

Parameters	Min	Typ.	Max	Unit
Output current	0.7	-	4.0 (3.5 RMS)	A
Supply voltage	+9	+36	+40	VDC
Logic signal current	8	10	15	mA
Puls input frequency	0	-	20 when duty cycle is 25 high / 75 low 13 when duty cycle is 50 / 50	kHz
Insulation resistance	500			MΩ

Further Specifications:

Microsteps / 1,8 °	200		6400
PUL / DIR		yes	
NEMA sizes	17		24
Motor type Mecheltron	42BYGH-XXXX		60BYGH-XXX

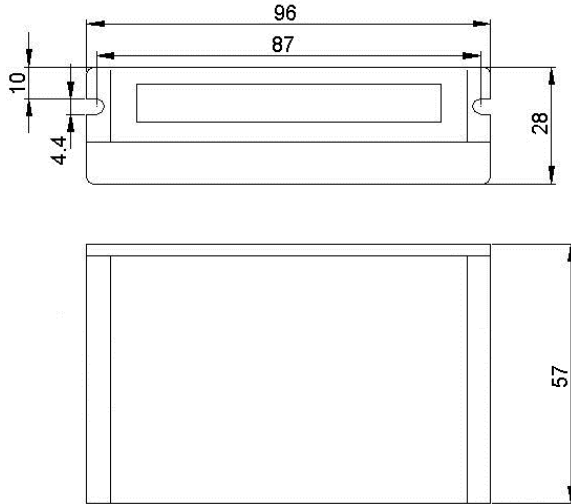
22.01.18

TB6600

Stepper motor driver

Analog Driver
Model TB6600

Mechanical Specifications: (Unit: mm)

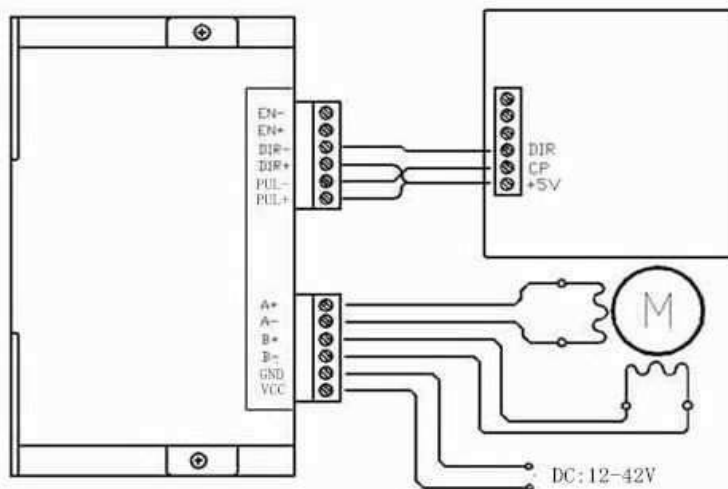


Applications:

Suitable for a wide range of stepping motors of NEMA sizes 17, 23 and 24 (42x42 mm to 60x60 mm). It can be used in various kinds of machines, such as X-Y tables, engraving machines, labeling machines, laser cutters, pick-place devices, and so on. Particularly well suited for applications where low noise levels, less heat development, high speed and high precision are desired.

Typical Connection Schematic:

A typical system consists of stepper motor, stepper motor driver, power supply and controller. The following image shows a typical connection schematic:



Logic control signals which have 5 V can be connected directly;

R 1kΩ must be connected in line when control signal is 12V;

R 2kΩ must be connected in line when control signal is 24V to ensure control signal current is 8mA to 15mA.

22.01.18



1 The Board

Arduino® Mega 2560 is a successor board of Arduino Mega, it is dedicated to applications and projects that require large number of input output pins and the use cases which need high processing power. The Arduino® Mega 2560 comes with a much larger set of IOs when we compare it with traditional Uno board considering the form factor of both the boards.

1.1 Application Examples

- **Robotics:** Featuring the high processing capacity, the Arduino Mega 2560 can handle the extensive robotic applications. It is compatible with the motor controller shield that enables it to control multiple motors at an instance, thus making it perfect of robotic applications. The large number of I/O pins can accommodate many robotic sensors as well.
- **3D Printing:** Algorithms play a significant role in implementation of 3D printers. Arduino Mega 2560 has the power to process these complex algorithms required for 3D printing. Additionally, the slight changes to the code is easily possible with the Arduino IDE and thus 3D printing programs can be customized according to user requirements.
- **Wi-Fi:** Integrating wireless functionality enhances the utility of the applications. Arduino Mega 2560 is compatible with WiFi shields hence allowing the wireless features for the applications in 3D printing and Robotics.

1.2 Accessories

1.3 Related Products

- Arduino® Uno Rev 3
- Arduino® Nano
- Arduino® DUE without headers



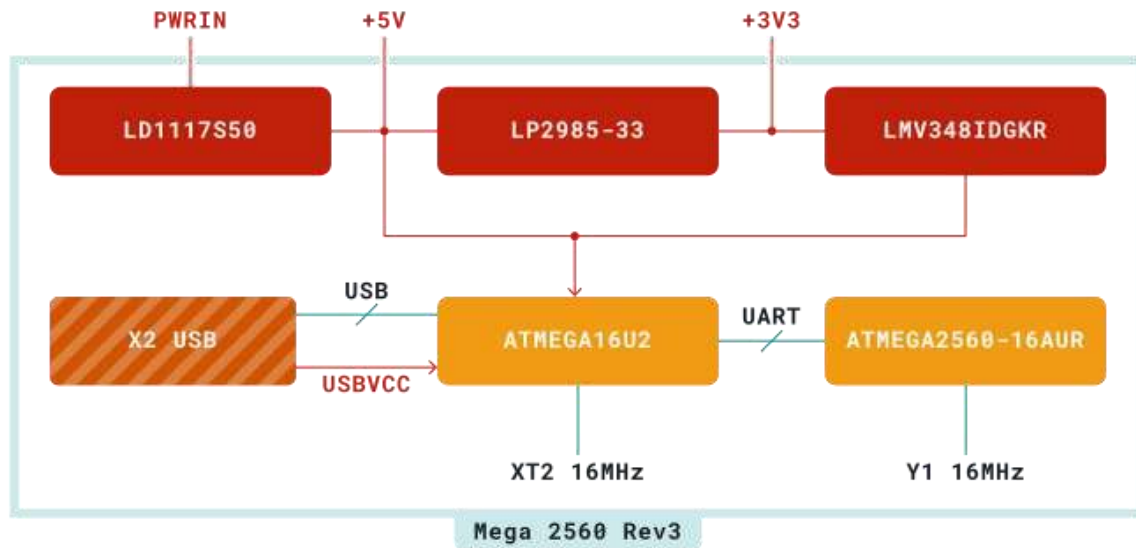
2 Ratings

2.1 Recommended Operating Conditions

Symbol	Description	Min	Typ	Max	Unit
V_{IN}	Input voltage from VIN pad / DC Jack	7	7.0	12	V
V_{USB}	Input voltage from USB connector	4.8	5.0	5.5	V
T_{OP}	Operating Temperature	-40	25	85	°C

3 Functional Overview

3.1 Block Diagram



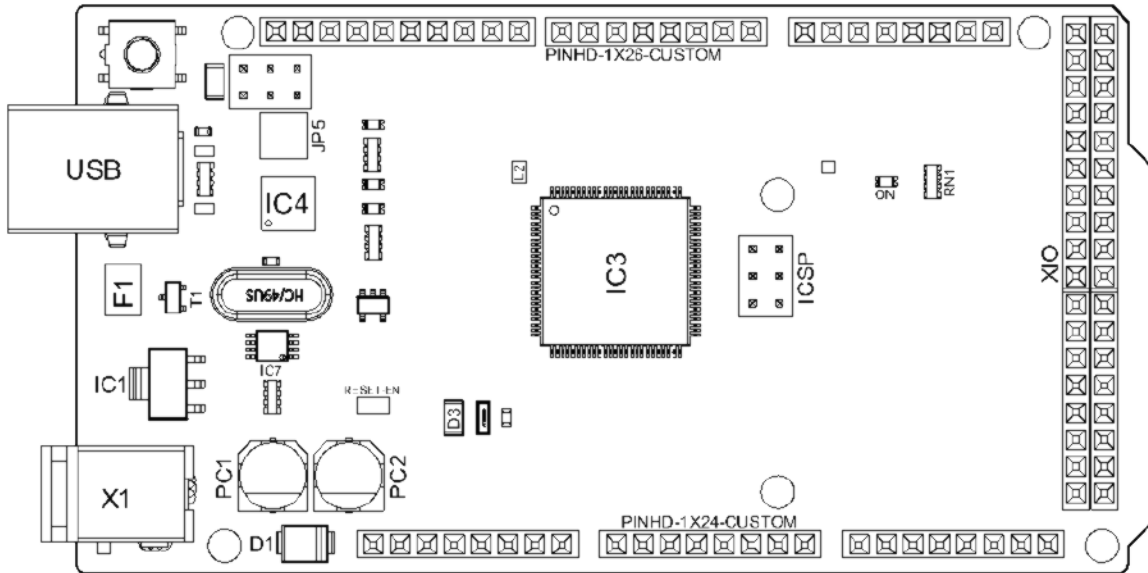
- Power
- LED
- Internal Parts
- Microcontroller
- Data Communication
- Connectors

Arduino MEGA Block Diagram



3.2 Board Topology

Front View



Arduino MEGA Top View

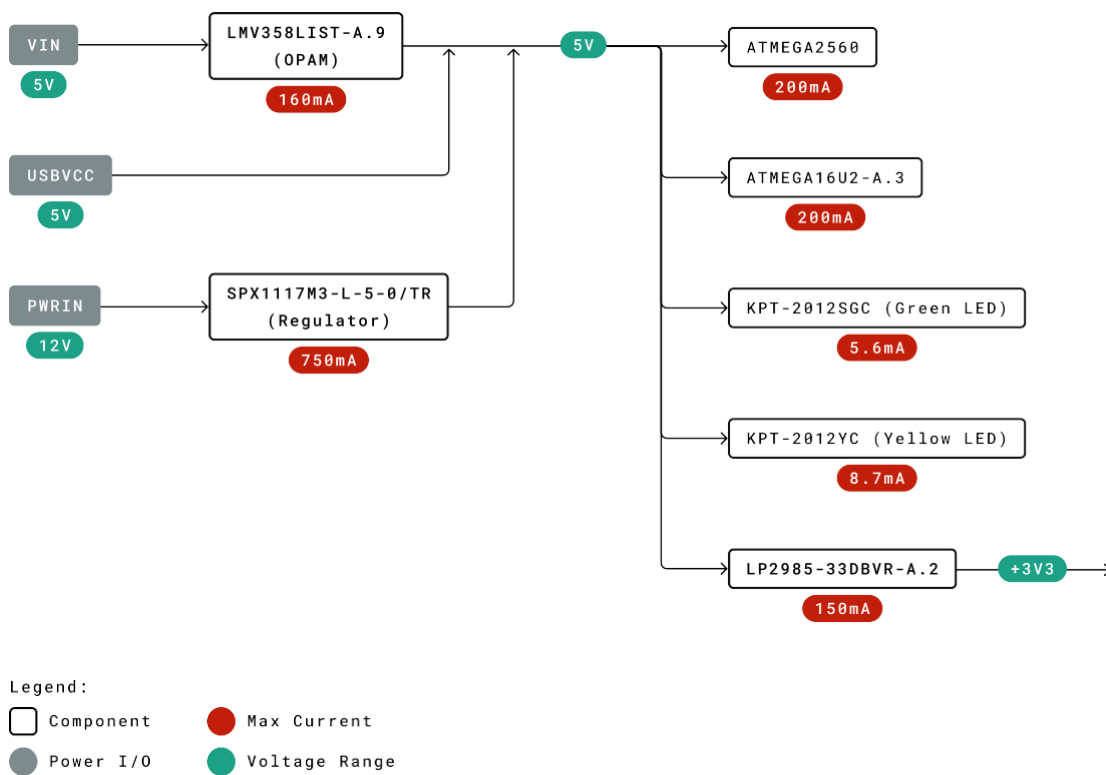
Ref.	Description	Ref.	Description
USB	USB B Connector	F1	Chip Capacitor
IC1	5V Linear Regulator	X1	Power Jack Connector
JP5	Plated Holes	IC4	ATmega16U2 chip
PC1	Electrolytic Aluminum Capacitor	PC2	Electrolytic Aluminum Capacitor
D1	General Purpose Rectifier	D3	General Purpose Diode
L2	Fixed Inductor	IC3	ATmega2560 chip
ICSP	Connector Header	ON	Green LED
RN1	Resistor Array	XIO	Connector



3.3 Processor

Primary processor of Arduino Mega 2560 Rev3 board is ATmega2560 chip which operates at a frequency of 16 MHz. It accommodates a large number of input and output lines which gives the provision of interfacing many external devices. At the same time the operations and processing is not slowed due to its significantly larger RAM than the other processors. The board also features a USB serial processor ATmega16U2 which acts an interface between the USB input signals and the main processor. This increases the flexibility of interfacing and connecting peripherals to the Arduino Mega 2560 Rev 3 board.

3.4 Power Tree



Power Tree



4 Board Operation

4.1 Getting Started - IDE

If you want to program your Arduino® MEGA 2560 while offline you need to install the Arduino® Desktop IDE [1] To connect the Arduino® MEGA 2560 to your computer, you'll need a Type-B USB cable. This also provides power to the board, as indicated by the LED.

4.2 Getting Started - Arduino Web Editor

All Arduino® boards, including this one, work out-of-the-box on the Arduino® Web Editor [2], by just installing a simple plugin.

The Arduino® Web Editor is hosted online, therefore it will always be up-to-date with the latest features and support for all boards. Follow [3] to start coding on the browser and upload your sketches onto your board.

4.3 Sample Sketches

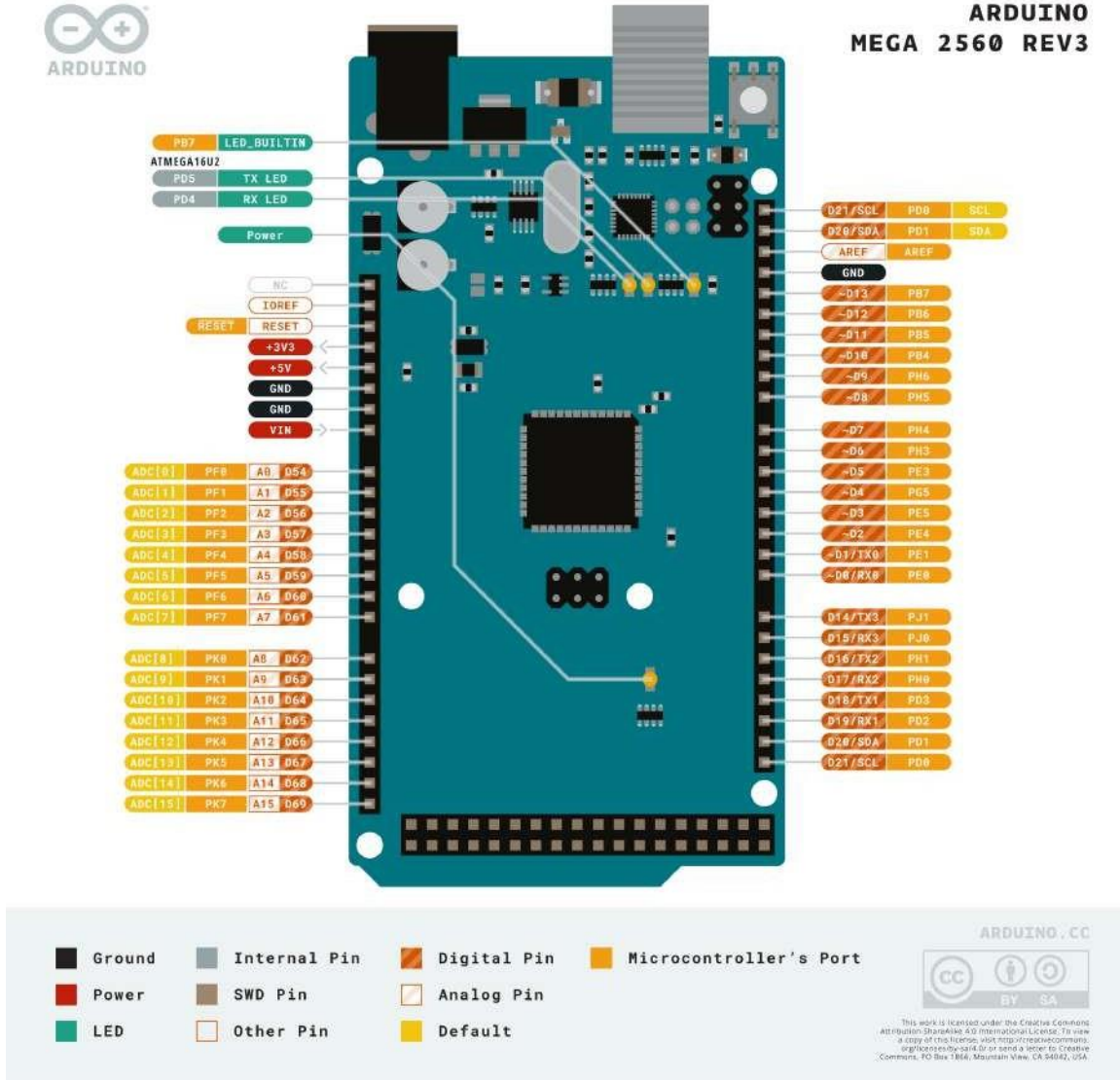
Sample sketches for the Arduino® MEGA 2560 can be found either in the "Examples" menu in the Arduino® IDE

4.4 Online Resources

Now that you have gone through the basics of what you can do with the board you can explore the endless possibilities it provides by checking exciting projects on ProjectHub [5], the Arduino® Library Reference [6] and the online store [7] where you will be able to complement your board with sensors, actuators and more.



5 Connector Pinouts



Arduino Mega Pinout

6000 Deep groove ball bearing



Deep groove ball bearing

Single row deep groove ball bearings are particularly versatile, have low friction and are optimized for low noise and low vibration, which enables high rotational speeds. They accommodate radial and axial loads in both directions, are easy to mount, and require less maintenance than many other bearing types.

- Simple, versatile and robust design
- Low friction
- High-speed capability
- Accommodate radial and axial loads in both directions
- Require little maintenance

Overview

Dimensions

Bore diameter	10 mm
Outside diameter	26 mm
Width	8 mm

Performance

Basic dynamic load rating	4.75 kN
Basic static load rating	1.96 kN
Reference speed	67 000 r/min
Limiting speed	40 000 r/min
SKF performance class	SKF Explorer

Properties

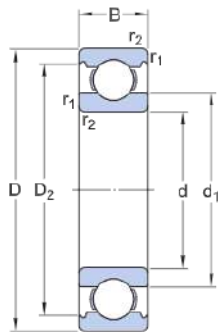
Filling slots	Without
Number of rows	1
Locating feature, bearing outer ring	None
Bore type	Cylindrical
Cage	Sheet metal
Matched arrangement	No
Radial internal clearance	CN
Tolerance class	Class P6 (P6)
Material, bearing	Bearing steel
Coating	Without
Sealing	Without
Lubricant	None
Relubrication feature	Without

Technical Specification

SKF performance class

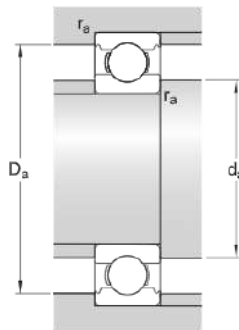
SKF Explorer

Dimensions



d	10 mm	Bore diameter
D	26 mm	Outside diameter
B	8 mm	Width
d ₁	≈ 14.8 mm	Shoulder diameter
D ₂	≈ 22.6 mm	Recess diameter
r _{1,2}	min. 0.3 mm	Chamfer dimension

Abutment dimensions



d _a min.	12 mm	Diameter of shaft abutment
D _ε max.	24 mm	Diameter of housing abutment
r _a max.	0.3 mm	Radius of shaft or housing fillet

Calculation data

Basic dynamic load rating	C	4.75 kN
Basic static load rating	C ₀	1.96 kN
Fatigue load limit	P _u	0.083 kN
Reference speed		67 000 r/min

Limiting speed		40 000 r/min
Minimum load factor	k_r	0.025
Calculation factor	f_0	12

Mass

Mass bearing		0.019 kg
--------------	--	----------

Tolerance class

Dimensional tolerances		P6
Radial run-out		P5

608 Deep groove ball bearing



Deep groove ball bearing

Single row deep groove ball bearings are particularly versatile, have low friction and are optimized for low noise and low vibration, which enables high rotational speeds. They accommodate radial and axial loads in both directions, are easy to mount, and require less maintenance than many other bearing types.

- Simple, versatile and robust design
- Low friction
- High-speed capability
- Accommodate radial and axial loads in both directions
- Require little maintenance

Overview

Dimensions

Bore diameter	8 mm
Outside diameter	22 mm
Width	7 mm

Performance

Basic dynamic load rating	3.45 kN
Basic static load rating	1.37 kN
Reference speed	75 000 r/min
Limiting speed	48 000 r/min
SKF performance class	SKF Explorer

Properties

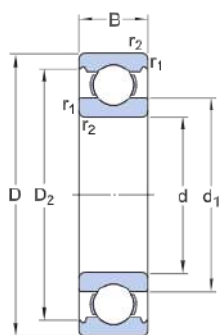
Filling slots	Without
Number of rows	1
Locating feature, bearing outer ring	None
Bore type	Cylindrical
Cage	Sheet metal
Matched arrangement	No
Radial internal clearance	CN
Tolerance class	Class P6 (P6)
Material, bearing	Bearing steel
Coating	Without
Sealing	Without
Lubricant	None
Relubrication feature	Without

Technical Specification

SKF performance class

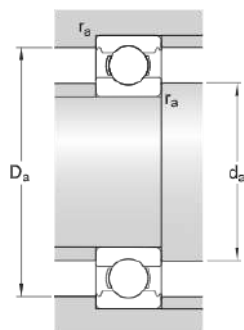
SKF Explorer

Dimensions



d	8 mm	Bore diameter
D	22 mm	Outside diameter
B	7 mm	Width
d ₁	≈ 12.15 mm	Shoulder diameter
D ₂	≈ 19.2 mm	Recess diameter
r _{1,2}	min. 0.3 mm	Chamfer dimension

Abutment dimensions



d _a	min. 10 mm	Diameter of shaft abutment
D _ε	max. 20 mm	Diameter of housing abutment
r _a	max. 0.3 mm	Radius of shaft or housing fillet

Calculation data

Basic dynamic load rating	C	3.45 kN
Basic static load rating	C ₀	1.37 kN
Fatigue load limit	P _u	0.057 kN
Reference speed		75 000 r/min

Limiting speed		48 000 r/min
Minimum load factor	k_r	0.025
Calculation factor	f_0	12

Mass

Mass bearing		0.012 kg
--------------	--	----------

Tolerance class

Dimensional tolerances		P6
Radial run-out		P5

6004 Deep groove ball bearing



Deep groove ball bearing

Single row deep groove ball bearings are particularly versatile, have low friction and are optimized for low noise and low vibration, which enables high rotational speeds. They accommodate radial and axial loads in both directions, are easy to mount, and require less maintenance than many other bearing types.

- Simple, versatile and robust design
- Low friction
- High-speed capability
- Accommodate radial and axial loads in both directions
- Require little maintenance

Overview

Dimensions

Bore diameter	20 mm
Outside diameter	42 mm
Width	12 mm

Performance

Basic dynamic load rating	9.95 kN
Basic static load rating	5 kN
Reference speed	38 000 r/min
Limiting speed	24 000 r/min
SKF performance class	SKF Explorer

Properties

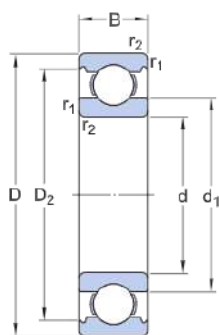
Filling slots	Without
Number of rows	1
Locating feature, bearing outer ring	None
Bore type	Cylindrical
Cage	Sheet metal
Matched arrangement	No
Radial internal clearance	CN
Tolerance class	Class P6 (P6)
Material, bearing	Bearing steel
Coating	Without
Sealing	Without
Lubricant	None
Relubrication feature	Without

Technical Specification

SKF performance class

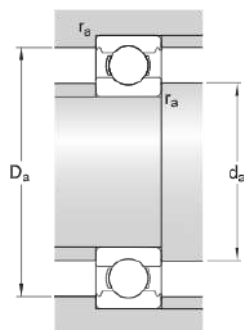
SKF Explorer

Dimensions



d	20 mm	Bore diameter
D	42 mm	Outside diameter
B	12 mm	Width
d ₁	≈ 27.2 mm	Shoulder diameter
D ₂	≈ 37.19 mm	Recess diameter
r _{1,2}	min. 0.6 mm	Chamfer dimension

Abutment dimensions



d _a min.	23.2 mm	Diameter of shaft abutment
D _ε max.	38.8 mm	Diameter of housing abutment
r _a max.	0.6 mm	Radius of shaft or housing fillet

Calculation data

Basic dynamic load rating	C	9.95 kN
Basic static load rating	C ₀	5 kN
Fatigue load limit	P _u	0.212 kN
Reference speed		38 000 r/min

Limiting speed		24 000 r/min
Minimum load factor	k_r	0.025
Calculation factor	f_0	14

Mass

Mass bearing		0.067 kg
--------------	--	----------

Tolerance class

Dimensional tolerances		P6
Radial run-out		P5



Tornillos tipo estufa

- Fabricados en acero con recubrimiento galvanizado
- Cabeza de gota
- Entrada para desarmador plano



Especificaciones

Individuales

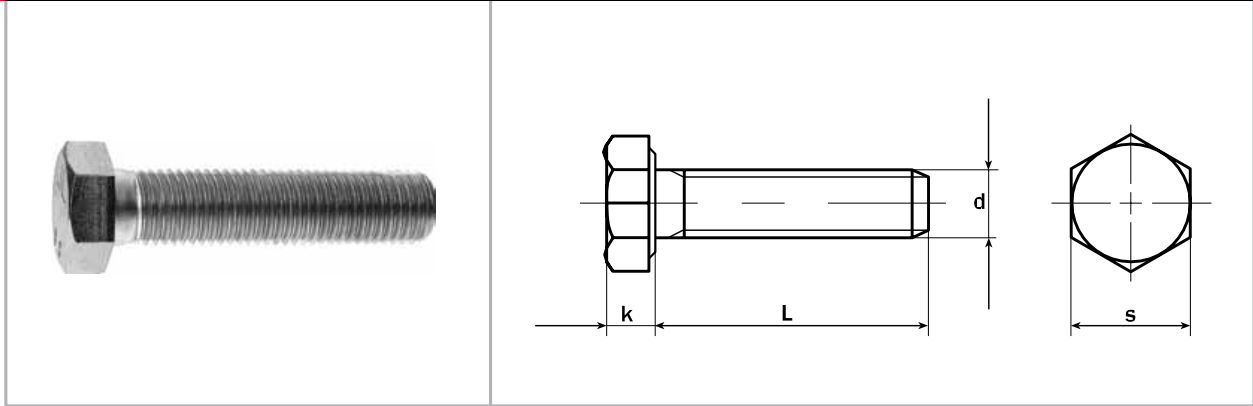
Código	Clave	Diámetro de cuerda	Largo	Piezas por bolsa
44599	TORE-1/8X1/2	1/8" (3 mm)	1/2" (13 mm)	700
44600	TORE-1/8X5/8	1/8" (3 mm)	5/8" (16 mm)	600
44601	TORE-1/8X3/4	1/8" (3 mm)	3/4" (19 mm)	500
44602	TORE-1/8X1	1/8" (3 mm)	1" (25 mm)	400
44603	TORE-1/8X1-1/4	1/8" (3 mm)	1-1/4" (32 mm)	350
44604	TORE-1/8X1-1/2	1/8" (3 mm)	1-1/2" (38 mm)	300
44605	TORE-1/8X2	1/8" (3 mm)	2" (50 mm)	250
44606	TORE-5/32X1/2	5/32" (4 mm)	1/2" (13 mm)	450
44607	TORE-5/32X5/8	5/32" (4 mm)	5/8" (16 mm)	400
44608	TORE-5/32X3/4	5/32" (4 mm)	3/4" (19 mm)	350
44609	TORE-5/32X1	5/32" (4 mm)	1" (25 mm)	300
44610	TORE-5/32X1-1/4	5/32" (4 mm)	1-1/4" (32 mm)	250
44611	TORE-5/32X1-1/2	5/32" (4 mm)	1-1/2" (38 mm)	200
44612	TORE-5/32X2	5/32" (4 mm)	2" (50 mm)	150
44613	TORE-5/32X2-1/2	5/32" (4 mm)	2-1/2" (65 mm)	150
44614	TORE-3/16X1/2	3/16" (5 mm)	1/2" (13 mm)	300
44615	TORE-3/16X5/8	3/16" (5 mm)	5/8" (16 mm)	250
44616	TORE-3/16X3/4	3/16" (5 mm)	3/4" (19 mm)	250
44617	TORE-3/16X1	3/16" (5 mm)	1" (25 mm)	200

Individuales

Código	Clave	Diámetro de cuerda	Largo	Piezas por bolsa
44618	TORE-3/16X1-1/4	3/16" (5 mm)	1-1/4" (32 mm)	150
44619	TORE-3/16X1-1/2	3/16" (5 mm)	1 1/2" (38 mm)	150
44620	TORE-3/16X2	3/16" (5 mm)	2" (50 mm)	100
44621	TORE-3/16X2-1/2	3/16" (5 mm)	2 1/2" (65 mm)	100
44622	TORE-3/16X3	3/16" (5 mm)	3" (75 mm)	100
44623	TORE-1/4X1/2	1/4" (6.5 mm)	1/2" (13 mm)	150
44624	TORE-1/4X5/8	1/4" (6.5 mm)	5/8" (16 mm)	150
44625	TORE-1/4X3/4	1/4" (6.5 mm)	3/4" (19 mm)	150
44626	TORE-1/4X1	1/4" (6.5 mm)	1" (25 mm)	100
44627	TORE-1/4X1-1/4	1/4" (6.5 mm)	1 1/4" (32 mm)	100
44628	TORE-1/4X1-1/2	1/4" (6.5 mm)	1 1/2" (38 mm)	80
44629	TORE-1/4X2	1/4" (6.5 mm)	2" (50 mm)	50
44630	TORE-1/4X2-1/2	1/4" (6.5 mm)	2 1/2" (65 mm)	50
44631	TORE-1/4X3	1/4" (6.5 mm)	3" (75 mm)	50

Generales

Tipo de cuerda	Standard
Empaque individual	Bolsa



Hexagon head bolts - Metric fine pitch thread
 Boulon à tête hexagonale - Filetage métrique à pas fin

Tornillos de cabeza hexagonal - Rosca métrica fina

dxP	M8x1	M10x1 M10x1,25	M12x1,25 M12x1,5	M14x1,5	M16x1,5	M18x1,5 M18x2	M20x1,5 M20x2
k	5,3	6,4	7,5	8,8	10	11,5	12,5
s	13	17/16*	19/18*	22/21*	24	27	30

L/d: Peso/Weight 1000 ud. kg

8	8,600	16,70					
10	9,300	17,80	25,50	38,80			
12	9,900	18,90	27,00	40,90	55,10		
14	10,60	19,90	28,50	43,00	57,90		
16	11,30	21,00	30,00	45,10	60,70		
18	11,90	22,10	31,50	47,20	63,40	86,60	115,00
20	12,60	23,20	33,00	49,30	66,20	90,00	119,00
22	13,20	24,20	34,50	51,30	69,00	93,40	124,00
25	14,20	25,80	36,70	54,40	73,20	98,60	131,00
28	15,20	27,40	39,00	57,60	77,30	104,00	137,00
30	15,90	28,50	40,50	59,70	80,10	107,00	141,00
35	17,60	31,20	44,20	64,90	87,10	116,00	152,00
40	19,20	33,90	48,00	70,20	94,00	124,00	163,00
45	20,90	36,60	51,70	75,40	101,00	133,00	174,00
50	22,60	39,30	55,50	80,60	108,00	141,00	186,00
55	24,20	42,00	59,20	85,80	115,00	150,00	197,00
60	25,90	44,70	63,00	91,10	122,00	159,00	208,00
65	27,60	47,40	66,70	96,30	129,00	167,00	219,00
70	29,20	50,00	70,50	102,00	136,00	176,00	230,00
75	30,90	52,70	74,20	107,00	143,00	184,00	241,00
80	32,50	55,40	78,00	112,00	150,00	193,00	253,00
85	34,20	58,10	81,70	117,00	157,00	202,00	264,00
90	35,90	60,80	85,40	122,00	164,00	210,00	275,00
95	37,50	63,50	89,20	128,00	171,00	219,00	286,00
100	39,20	66,20	92,90	133,00	177,00	227,00	297,00
110	42,50	71,60	100,00	143,00	191,00	244,00	319,00
120	45,90	77,00	108,00	154,00	205,00	261,00	342,00
130		82,40	115,00	164,00	219,00	279,00	364,00
140		87,70	123,00	175,00	233,00	296,00	386,00
150		93,10	130,00	185,00	247,00	313,00	409,00
160			138,00	196,00	260,00	330,00	431,00
170			145,00	206,00	274,00	347,00	453,00
180			153,00	217,00	288,00	365,00	475,00
190				227,00	302,00	382,00	498,00
200				238,00	316,00	399,00	520,00

CALIDADES/GRADES: *Tamaño según norma ISO/Size as per ISO standard

4.6	4.8	5.6	5.8	6.8	8.8	10.9	12.9	A2	A4
-----	-----	-----	-----	-----	-----	------	------	----	----



VPM-7 Vacuum Power Wedger

(14 lb. Max. Batch Size)

"The Vacuum Deairing Pugger-Mixer"

Comes equipped with 110V electrical for standard service. 220V operation (\$100 additional) also available for overseas operation.

\$4,449.USD

Description

Features

Capabilities

Safety

Vacuum Pump

Cleaning

Options

Question: "When is Peter Pugger going to come up with something small for us single potter studios?"

Answer: The VPM-7 has arrived. With all the bells and whistles, and a price that competes with the standard "offshore" pugmills, the compact VPM-7 does it all. Any clay that has not been fired can be reclaimed in the VPM-7. With the fastest mixing times in the industry, broken green ware, slop, powder and water can be thrown into the pugmill and reclaimed in minutes. With the latest advancements in mixing, deairing and extruding technology, the VPM-7 outshines the competition. Quality, durability and proven performance...Why settle for anything else?

Specifications

- **Maximum Batch Capacity*:** 14 pounds
- **Pugging Rate:** 350 lbs. per hour
- **Mixing Rate:** 100 lbs. per hour
- **Dimensions:** 33.5"L x 12"W x 13.75"H
- **Crated Weight:** Aluminum Version - 133 lbs. (Ships FED EX Ground)
- **Hopper Door Size:** 4.5" x 4/5"
- **Pug Size:** 3" round
- **Electrical:** 1/2 HP 1-phase, 6 amps at 120 volts, 4 amps at 240V
- **Vacuum Pump:** 1/3 HP, (Included; operates off main electrical)

*Max Batch Capacity may vary depending on material density and moisture content

References

- 304 stainless steel round tube. (n.d.). <https://www.industrialmetalsupply.com/304-and-316-stainless-round-tube>. (Accessed: 2023-11-14)
- 3D potterbot scara V4 ceramic 3D clay printer — real clay 3D ceramic printer. (n.d.). <https://3dpotter.com/printers/scara>. (Accessed: 2023-11-8)
- Abdallah, Y. K., & Estévez, A. T. (2021). 3d-printed biodigital clay bricks. *Biomimetics*, 6(4), 59.
- Afanador García, N., Guerrero Gómez, G., & Monroy Sepúlveda, R. (2012). Propiedades físicas y mecánicas de ladrillos macizos cerámicos para mampostería. *Ciencia e ingeniería neogranadina*, 22(1), 43–58.
- Ali, S. (2019). Design and development of extrusion machine. Retrieved from <https://www.researchgate.net/publication/342699251> doi: 10.13140/RG.2.2.13040.07687
- Ashby, M. F., & Cebon, D. (2005). Materials selection in mechanical design. *MRS Bull*, 30(12), 995.
- Bedarf, P., Dutto, A., Zanini, M., & Dillenburger, B. (2021). Foam 3d printing for construction: A review of applications, materials, and processes. *Automation in Construction*, 130, 103861.
- Bird, R. B., Stewart, W. E., & Lightfoot, E. N. (2020). *Fenómenos de transporte*. Reverté.
- BRANDT, G. W., & E, H. E. (n.d.). *On-site wall structure formation* (Granted Patent No. US 3966533 A). Retrieved from <https://lens.org/190-157-577-853-506>
- Camacho, D. D., Clayton, P., O'Brien, W. J., Seepersad, C., Juenger, M., Ferron, R., & Salamone, S. (2018). Applications of additive manufacturing in the construction industry—a forward-looking review. *Automation in construction*, 89, 110–119.
- Carbon. (n.d.). *The 7 types of additive manufacturing*. Retrieved from <https://www.carbon3d.com/resources/blog/the-7-types-of-additive-manufacturing>
- Carmona Reverte, V. J. (2016). Diseño y prototipado de extrusor para impresora 3d de alimentos.
- Castillo-Rodríguez, C., García-Lara, A. M., Castruita-Ávila, L. G., Saucedo-Zendejo, F. R., Para, C., & Rodríguez, C. C. (2022). Additive manufacturing: applications and methods. *CienciAcierta*, 71.
- CeraStruder. (n.d.). <https://www.bryancera.com/cerastruder>. (Accessed: 2023-11-8)
- Charles, A., Hofer, A., Elkaseer, A., & Scholz, S. G. (2021). Additive manufacturing in the automotive industry and the potential for driving the green and electric transition. In *Proceedings of the international conference on sustainable design and manufacturing* (pp. 339–346).
- Cherdo, L. (2019, 3). *The 13 best construction 3d printers in 2023*. Retrieved from <https://www.aniwaa.com/buyers-guide/3d-printers/house-3d-printer-construction/> (Accessed: 2023-5-9)
- Chiu, B. W. (2020). *Additive manufacturing applications and implementation in aerospace* (Unpublished doctoral dissertation). Massachusetts Institute of Technology.
- Clay 3D printers. add-ons for clay, porcelain, concrete, suspensions. (n.d.). <https://www.stoneflower3d.com/>. (Accessed: 2023-11-8)
- Clay products and refractories global market share, key emerging players 2032.

- (2023). <https://www.thebusinessresearchcompany.com/report/clay-products-and-refractories-global-market-report>. (Accessed: 2023-10-13)
- Dehghanghadikolaei, A., Namdari, N., Mohammadian, B., & Fotovvati, B. (2018). Additive manufacturing methods: A brief overview. *Journal of Scientific and Engineering Research*, 5.
- Díaz, D. T. (2016). Tecnologías de fabricación digital aditiva , ventajas para la construcción de modelos , prototipos y series cortas en el proceso de diseño de productos. *Iconofacto*, 12.
- el Mesbahi, J., Buj, I., & el Mesbahi, A. (2021, 11). Design of an innovative new extrusion system for a printing machine for ceramics. *The International Journal of Advanced Manufacturing Technology*, 117. doi: 10.1007/s00170-021-07431-6
- EPMA. (2015). Introduction to additive manufacturing technology: A guide for designers and engineers. *European Powder Metallurgy Association*.
- Extruders. (n.d.). <https://www.3dwasps.shop/en/category/extruders/>. WASP. (Accessed: 2023-11-8)
- Extrusion system for 3D printing ceramics*. (2021, December). <https://jetclay.com/project/open-source-clay-extrusion-system>. (Accessed: 2023-11-8)
- Fortune Business Insights. (n.d.). *Ceramics market size, share, growth | industry statistics, 2028*.
- Gibson, I., Rosen, D. W., & Stucker, B. (2010). *Additive manufacturing technologies: Rapid prototyping to direct digital manufacturing*. doi: 10.1007/978-1-4419-1120-9
- Group, A. M. R. (2018). *The 7 categories of additive manufacturing*. Retrieved from <https://www.lboro.ac.uk/research/amrg/about/the7categoriesofadditivemanufacturing/>
- Guía, P., Larrondo, J., De, P. M., Comisión, L. A., Ruiz, R., Benjamin, G., & Cárdenas, B. (2018). *César ignacio salazar ibÁÑez*.
- Hsu, T.-R. (2018). *Applied engineering analysis*. John Wiley & Sons.
- HUBS. (2022). *Market changes and technological shifts in the 3d printing market*. Retrieved from www.hubs.com
- Issa, M., et al. (2021). *Additive manufacturing in the engineering and construction industry: Development and potentiality* (Unpublished master's thesis). Universitat Politècnica de Catalunya.
- J, L. F. (n.d.). *Apparatus for the preparation of elliptical structures* (Granted Patent No. US 3376602 A). Retrieved from <https://lens.org/039-502-310-962-199>
- Ji Chen, W. (2017). *Diseño de un extrusor para imprimir chocolate* (B.S. thesis). Universitat Politècnica de Catalunya.
- Jimenez, M. C., & Galán, J. P. (2013). La fabricación aditiva. la evidencia de una necesidad. *Interempresas Industria Metalmecánica*, 235.
- Jo, J. H., Jo, B. W., Cho, W., & Kim, J.-H. (2020). Development of a 3d printer for concrete structures: laboratory testing of cementitious materials. *International Journal of Concrete Structures and Materials*, 14(1), 1–11.
- Kalender, M., Kılıç, S. E., Ersoy, S., Bozkurt, Y., & Salman, S. (2019). Additive manufacturing and 3d printer technology in aerospace industry. In *2019 9th international conference on recent advances in space technologies (rast)* (pp. 689–694).
- Khajavi, S. H., Tetik, M., Mohite, A., Peltokorpi, A., Li, M., Weng, Y., & Holmström,

- J. (2021). Additive manufacturing in the construction industry: The comparative competitiveness of 3d concrete printing. *Applied Sciences*, 11 (9), 3865.
- Khandelwal, R. (2020). Additive manufacturing in the automotive industry. *Int Res J Eng Technol*, 7(8).
- Khoshnevis, B. (2004). Automated construction by contour crafting—related robotics and information technologies. *Automation in construction*, 13(1), 5–19.
- Klinkenberg, M., Rickertsen, N., Kaufhold, S., Dohrmann, R., & Siegesmund, S. (2009). Abrasivity by bentonite dispersions. *Applied Clay Science*, 46(1), 37–42.
- Kloft, H., Gehlen, C., Dörfler, K., Hack, N., Henke, K., Lowke, D., . . . Raatz, A. (2021). Tr 277: Additive manufacturing in construction. *Civil Engineering Design*, 3 (4), 113–122.
- Kumari, N., & Mohan, C. (2021). Basics of clay minerals and their characteristic properties. *Clay Clay Miner*, 24, 1–29.
- Laboratory of architecture + design and technological experimentation [LATE]*. (2023). <https://arquitectura.unam.mx/late.html>. (Accessed: 2023-13-10)
- Lee, T. (2022, November). *DIY ceramic 3D printer 015 - test printing a vase*. Youtube.
- Leinster, M. (1945). Things pass by,. *Thrilling Wonder Stories*, 27, 20.
- Makery, J. (2020, July). *Building a clay mixing pug mill - part 1*. Youtube.
- MatWeb - the online materials information resource*. (n.d.). <https://matweb.com/search/DataSheet.aspx?MatGUID=fc6556e04950495d8e015b1d856f5f05&ckck=1>. (Accessed: 2023-11-14)
- Menchavez, R. L., Adavan, C. R. M., & Calgas, J. M. (2014). Starch consolidation of red clay-based ceramic slurry inside a pressure-cooking system. *Materials Research*, 17, 157–167.
- Moore, J. (2023). *Mechanics map*. Retrieved from <https://LibreTexts.org>
- Morton-Jones, D. H. (1989). Polymer processing. (*No Title*).
- Mott, R. L. (2004). *Machine elements in mechanical design*. Pearson Educación.
- Murali, K., Sambath, K., & Mohammed Hashir, S. (2018). A review on clay and its engineering significance. *International Journal of Scientific and Research Publications*, 8(2), 8–11.
- Muñoz, E. F., & Cuadros Bedoya, E. (2019). Diseño de equipo triturador para residuos cerámicos que permite la reutilización del material en nuevos procesos.
- Norton, R. L., Sánchez, M. R., Correa, C. O., Alvarado, M. A., & González, M. P. (2020). *Diseño de maquinaria*. McGraw-Hill Interamericana de España.
- NVS-07. (2019, April). <https://www2.ceramics.nidec-shimpo.com/nvs-07/>. NIDEC-SHIMPO - Ceramics Equipment. (Accessed: 2023-11-7)
- Overview of materials for polyactic acid (pla)*. (n.d.). Retrieved from <https://matweb.com/search/DataSheet.aspx?MatGUID=ab96a4c0655c4018a8785ac4031b9278&ckck=1> (Accessed: 2023-3-11)
- Pacillo, G. A., Ranocchiali, G., Loccarini, F., & Fagone, M. (2021). Additive manufacturing in construction: A review on technologies, processes, materials, and their applications of 3d and 4d printing. *Material Design & Processing Communications*, 3(5), e253.
- Paolini, A., Kollmannsberger, S., & Rank, E. (2019). Additive manufacturing in construction: A review on processes, applications, and digital planning methods. *Additive manufacturing*, 30, 100894.

- Papadopoulos, P. (2010). Introduction to the finite element method. *California: Berkeley University of California*.
- Parra, B., & Rodrigo, N. (2017). *Diseño de extrusora de filamento para impresión 3d a partir de plásticos reciclados*.
- Peter pugger. (n.d.). <https://peterpugger.com/>. (Accessed: 2023-11-7)
- Popov Egor, P. (1989). *Mecánica de sólidos*. Limusa.
- PUG MILLS — venco. (n.d.). <https://www.venco.com.au/pug-mills/>. (Accessed: 2023-11-7)
- R, U. J. (n.d.). *Machine for building walls of hardenable plastic material* (Granted Patent No. US 2607100 A). Retrieved from <https://lens.org/163-178-868-443-439>
- Ramírez, E. R., Andrés, S., Moreno, H., Díaz, E. T., Burgos, N. P., & Moreno-Contreras, G. G. (2021). Design of a clay extrusion system for low cost 3d printing. , 16. Retrieved from www.arpnjournals.com
- Reinforced clay printing -. (n.d.). <https://www.iaacblog.com/programs/reinforced-clay-printing-3d-printing-pla-printing/>. (Accessed: 2023-11-8)
- Repinskiy, O., Romaneskul, N., & Studenkova, N. (2021). Using of additive manufacturing (am) in construction economics—shortcomings, advantages, prospects. In *Iop conference series: Earth and environmental science* (Vol. 751, p. 012170).
- SHUTER, E. (n.d.). *Concrete wall machine* (Granted Patent No. US 2532246 A). Retrieved from <https://lens.org/000-276-187-347-570>
- SKF. (n.d.). <https://www.skf.com/group/products/rolling-bearings/ball-bearings/deep-groove-ball-bearings/productid-6000>. (Accessed: 2023-11-24)
- Solá Marcillo, A. R. (2009). *Elaboración de un manual para la selección y control de materiales* (B.S. thesis). QUITO/EPN/2008.
- Standard, A. (2012). Iso/astm 52900: 2015 additive manufacturing-general principles-terminology. *ASTM F2792-10e1*.
- Sánchez, F., & Rivera2, A. B. (2008). "mejoramiento y tecnificación de máquina extrusora para la elaboración de ladrillos artesanales".
- T, M. P. (n.d.). *Machine for building a dome or sphere* (Granted Patent No. US 4734021 A). Retrieved from <https://lens.org/028-882-128-139-620>
- theLUTUM® eco clay extruder. (2020, April). <https://vormvrij.nl/blog/the-lutum-eco-extruder-fro-clay-printing/>. (Accessed: 2023-11-8)
- Ullman, D. G. (2003). *The mechanical design process*.
- Ulrich, K. T., Eppinger, S. D., & Yang, M. C. (2008). *Product design and development* (Vol. 4). McGraw-Hill higher education Boston.
- Urschel, W. E. (1943, March 23). *Molding and depositing machine for solidifiable plastic materials*. Google Patents. (US Patent 2,314,468)
- Vafadar, A., Guzzomi, F., Rassau, A., & Hayward, K. (2021). Advances in metal additive manufacturing: a review of common processes, industrial applications, and current challenges. *Applied Sciences*, 11(3), 1213.
- Velilla Díaz, W., et al. (2009). *Diseño y validación de un modelo de extrusora de arcilla*. (Unpublished master's thesis). Maestría en Ingeniería Mecánica.
- Víctor K. Savgorodny, L. U. (1978). *Transformación de plásticos*. Gustavo Gil.
- White, F. M. (1990). *Fluid mechanics*. New York.

- WillysGarageNorway. (2020, January). *DIY ceramics 3D printer (part 2b) - extruder experiments / THE EXTRUDER / CAD*. Youtube.
- Wohlers, T., & Gornet, T. (2014). History of additive manufacturing 2014. *Wohlers Report 2014 - 3D Printing and Additive Manufacturing State of the Industry*.
- Wolf, A., Rosendahl, P. L., & Knaack, U. (2022). Additive manufacturing of clay and ceramic building components. *Automation in Construction*, 133, 103956.
- XianJun, J., Ying, L., WenHao, C., XiaoKang, S., & Peng, S. (2022). Determination of static and dynamic yield stress of chengdu clay slurry. *Frontiers in Physics*, 663.